DISSERTATION

NA^+-ACTIVATED K^+ CHANNELS PROTECT AGAINST OVEREXCITATION AND SEIZURE-LIKE BEHAVIOR IN DROSOPHILA

Submitted by

Nathan S. Byers

Department of Biomedical Sciences

In partial fulfillment of the requirements

For the Degree of Doctor of Philosophy

Colorado State University

Fort Collins, Colorado

Spring 2021

Doctoral Committee:

Advisor: Susan Tsunoda

Deborah Garrity
Shane Hentges
Frederic Hoerndli
Michael Tamkun

ABSTRACT

NA$^+$-ACTIVATED K$^+$ CHANNELS PROTECT AGAINST OVEREXCITATION AND SEIZURE-LIKE BEHAVIOR IN DROSOPHILA

Na^+-activated K^+ channels (K_{Na}) encode K^+ channels that are activated by internal Na^+ and are widely expressed throughout the mammalian central nervous system. Based on the biophysical properties of the channels, it has long been postulated that they act as a reserve mechanism to combat neuronal overexcitation. Specifically, early electrophysiological recordings suggested that only when intracellular Na^+ levels rise significantly, for instance in neuropathological conditions, do K_{Na} channels become active. More recent evidence suggests that they may function under normal physiological circumstances by means of binding cytoplasmic factors and via the persistent Na^+ current. However, to date it is unclear if K_{Na} channels function to prevent overexcitation *in vivo*. Therefore, research in my dissertation sets out to test the hypothesis that K_{Na} channels protect against overexcitation in *Drosophila* models of epilepsy.

Drosophila contain one gene encoding a K_{Na} channel, *dSlo2*. In the third chapter of this dissertation, I examine expression of dSlo2 channels throughout the nervous system. Findings from this chapter show that dSlo2 channels are expressed in cholinergic neurons, the main excitatory neuron of the *Drosophila* brain. Furthermore, dSlo2 channels were excluded from GABAergic neurons. I additionally found that dSlo2 channels are localized to axonal regions of multiple neuronal subtypes in the nervous system. Thus, these results suggest that as K^+ channels widely and preferentially expressed in excitatory neurons in the brain, dSlo2 channels may function to dampen neuronal, and perhaps behavioral, excitability.

In Chapter 4, I test the hypothesis that dSlo2 channels protect against behavioral abnormalities caused by cholinergic overexcitation. I first show that the loss of *dSlo2* exacerbates behavioral deficits and death associated with prolonged exposure to a cholinergic agonist, Imidacloprid. Furthermore, I found that

adult flies lacking *dSlo2* exhibit mechanically induced seizure-like behavior following feeding of Imidacloprid, which does not occur in wild-type flies. Combined, these results suggest that dSlo2 channels do indeed protect against cholinergic overexcitation.

It has previously been shown that mammalian K_{Na} channels are activated by a persistent Na^+ current (I_{NaP}) in neurons, suggesting that these channels may ameliorate behavioral consequences of an increased I_{NaP} *in vivo*. In Chapter 5, I test the hypothesis that dSlo2 channels protect against *Drosophila* seizure-like behavior induced by an increased I_{NaP}. I find that the loss of *dSlo2* significantly exacerbates seizure-like behavior in multiple *Drosophila* epileptic models, including a model for human generalized epilepsy with febrile seizures plus (GEFS+). Additionally, the absence of *dSlo2* worsens seizure-like behavior when flies are exposed to Veratridine, a pharmacological agent known to increase I_{NaP}. Interestingly, the loss of *dSlo2* also revealed a spontaneous seizure phenotype in I_{NaP}-affected seizure models that was otherwise absent. Altogether, these results are consistent with the model that K_{Na} channels are activated by I_{NaP}, and protect against seizure-like behavior actuated by increased I_{NaP}.

Overall, the work in my dissertation expands our understanding of the role of K_{Na} channels. These findings suggest that K_{Na} channels may play a protective role for many neuropathological diseases associated with an increased I_{NaP}, such as epilepsy, amyotrophic lateral sclerosis, neuropathic pain, and ischemia.

ACKNOWLEDGEMENTS

First, I would like to thank my adviser, Dr. Susan Tsunoda. From the very beginning, I knew we clicked. Our shared interests in neuroscience, and the desire to understand how genes can influence behavior, made me very excited at the prospect of having you as a mentor. I cannot express how much I appreciate you accepting me into your lab. While my research project required a lot of exploration and tool design, you always supported my endeavors. You provided great insights, and helped me keep my eye on the ball. You have always been extremely optimistic, which I must admit is very admirable in a scientist. I have learned so much from you over the years, Susan, and am extremely grateful. Also, thanks for always being willing to figure out the most relevant analogy to fit whatever situation I was facing. We came up with some great ones.

Next, I would like to thank all of my lab mates. You all provided great company and support over the years. I could always rely on help with a new technique, good scientific discussions, and a valuable resource to complain about experiments that were not working for one reason or another. I also would like to thank you all for exposing me to completely different life experiences from my own. Having shared what it is like to grow up in different cultures around the world has vastly expanded my appreciation for what growing up outside of the US is like. Girma, I would like to specifically thank you for everything over the years; For teaching me, and re-teaching me, molecular biology techniques and good fly keeping practices; For telling me over and over that I'm trying to get things done too quickly; For always intently listening to my struggles and successes; And for our many discussions about world politics. I greatly cherish the friendship we have built over these years.

I would like to also acknowledge the members of my committee. You were always available to meet with me, either formally or informally. You have all provided invaluable feedback, whether it was related to science, writing, or just generally about life. I really appreciate the time you each took over the years to help me grow as a scientist.

I would next like to thank my family, especially my parents, for your constant love and support. You've always been there to help me through any problems and to celebrate any victories. You've always been excited about any career avenue I've explored, and never once told me that I shouldn't pursue something. You both lead by example, and I've always looked up to you for that. Thank you for everything.

Lastly, I would like to thank you, Sarah. When we moved out to Colorado together, with no social network, no job, and little money, I don't think either of us fully grasped the journey we were embarking on. You have always been there to support me, whether that entailed telling me that an experiment failing wasn't actually "failure", or celebrating the successes throughout my PhD. You are a constant inspiration to improve myself. I couldn't have done it without you. Thank you.

DEDICATION

To Preston, for everything

TABLE OF CONTENTS

LIST OF TABLES

LIST OF FIGURES

CHAPTER 1. INTRODUCTION

1.1 Neuronal excitability

Over millennia, humans have sought to understand the brain and how this extremely complex organ provides the ability for thought and consciousness. Hippocrates, roughly 2500 years ago, first suggested that the brain is responsible for thought, sensation, and cognition[1]. While this is the first record of this idea, it has taken many years to test this hypothesis. In the late 19th and early 20th centuries, Ramón y Cajal, considered by many to be the father of neuroscience, proposed a groundbreaking model later termed the neuron doctrine. In this model, he suggested that neurons were contiguous, not continuous as other scientists believed at the time. His theories postulated that neuronal communication occurred across small gaps between cells, termed synapses. It would be another 30 some years before the significant discoveries of Hodgkin and Huxley identified the action potential[2]. Using a giant squid axon, these researchers were able to identify that ionic gradients separated by a plasma membrane are what give rise to electrical signaling within a neuron. This was further expanded upon by the identification of the Goldman-Hodgkin-Katz equation, which calculates the membrane voltage based on the concentration gradient and permeability of Na^+, K^+, and Cl^- across the plasma membrane[3,4]. Hodgkin and Huxley later identified these currents as being affected by voltage, and therefore proposed a model in which channels must regulate ion permeability[5,6]. The Na^+ channel protein complex was purified from an electric eel roughly 20 years later using tetrodotoxin (TTX), which selectively blocks Na^+ conductance[7]. In an artificial phospholipid bilayer, the largest protein subunit of this complex was shown to sufficiently carry a Na^+ current[8–10], and was therefore postulated to be the sodium channel. In addition to the Na^+ channel, K^+ channels were beginning to be identified in *Drosophila melanogaster*. Mutations in a fly that exhibited a shaking phenotype were mapped to a gene encoding a K^+ channel, and was therefore named *Shaker*[11,12]. Other voltage-gated K^+ channels were also identified in *Drosophila*, such as *Shab*, *Shaw*, and *Shal*[13–16]. Not long after this, the crystal structure of both prokaryotic and mammalian K^+ channels was uncovered by Dr. Robert Mackinnon's lab[17–19]. These

monumental findings laid the groundwork for further exploration of how neurons regulate excitability by altering ion channel function.

These developments identified neuronal excitability, or rather the ability to alter ionic gradients along the plasma membrane, as a central determinant of neuronal communication. Expanding on Hippocrates early hypothesis, neuronal excitability is therefore thought to underlie the brain's capacity for learning, memory, sensation, emotion, and consciousness. With such an important role, maintaining the proper range of excitation within each neuron is extremely important. Large fluctuations in neuronal excitability can be detrimental to the neurons themselves, and therefore the larger circuit as a whole. These can manifest as many different pathologies in the organism. The aim of my research was to test the hypothesis that a specific ion channel, the Na^+-activated K^+ (K_{Na}) channel, protects against overexcitation.

1.2 Pathological hyperexcitability

The delicate balance between excitation and inhibition is extremely important for proper functioning of an organism. This is true for both the survival of individual neurons as well as entire neuronal circuits guiding behavior. When this balance becomes destabilized, it can lead to detrimental outcomes at the cellular, network, and organismal levels. These disruptions in neural networks, when left unchecked, are often pathogenic. Many times, these pathologies are closely associated with an increase in excitability, or hyperexcitability. This can be defined as a decreased threshold for excitation of a neuron or increased activity of a neuron or circuit which would normally be quiescent. Consequential behavioral phenotypes include uncontrolled motor behavior, altered social interactions, dementia, neuronal cell death, and organismal death. Pathologies associated with hyperexcitability fall into categories of autism spectrum disorders, pain, injury or insult, neurodegenerative, and epilepsy. While these pathologies are very complex and by no means fully understood, animal models and human studies suggest that an underlying theme is increased neuronal activity. This is manifested by an imbalance in excitation-inhibition ratio, either occurring by an increase in excitatory drive, a decrease in inhibitory drive, or a combination of both. In many of these pathologies, neuronal hyperexcitability is found to precede some of the more permanent

damage and neuronal death. In some cases, increases in network activity have even been suggested as an early indicator of some pathologies. Below, I will describe studies suggesting that hyperexcitability is a common factor underlying multiple pathological conditions.

1.2.1 Autism spectrum disorders

Autism spectrum disorders (ASD) are a broad category of neurodevelopmental disorders in which the individual displays altered social interactions, impaired communicative abilities, repetitive behaviors, restricted interests, and heightened sensory responses[20]. There are a large number of genetic risk factors that have been found to correlate with these disorders. Similarly, the broad spectrum of phenotypes make it hard to associate any one specific mutation with one disorder. For example, two individuals with two completely separate mutations may both be diagnosed with Asperger's, however, the prevalence of certain behaviors associated with Asperger's differs. This has led to a push to understand common themes behind ASD with the hope of finding a better treatment for all. To work towards this, a few different mouse models have been generated to better understand the underlying causes. One of these is a model for Fragile X Syndrome (FXS). Roughly one third of patients with FXS show signs of ASD[21,22]. FXS is caused by the transcriptional silencing of *Fmr1*, the gene that encodes for the protein Fragile X Mental Retardation Protein (FMRP)[23]. FMRP is an RNA binding protein that acts as a negative regulator of translation. A knock-out mouse, *Fmr1*$^{-/y}$, has been generated and similar to humans with FXS, displays an enhanced sensitivity to sensory stimuli[24]. In these mice, it has been shown that there's an overall increase in neuronal and circuit excitability in the barrel cortex caused by a decreased inhibitory tone[25]. Furthermore, is has been found that this increased activity is associated with alterations in glutamatergic ion channel expression and function[21,26,27]. These changes in channel function were found to be associated with altered intrinsic homeostatic plasticity[28]. In this study, they found that *Fmr1* knock-out mice exhibited enhanced Na^+ channel activity which likely led to alterations in homeostatic plasticity. These alterations were associated with an increase in firing of multi-spike cortical neurons. Beyond the FXS mouse model, other papers have examined other mouse models of ASD, and similarly found an increased excitation to inhibition ratio

common to all models[29–31]. One of these studies examined multiple mouse models for ASD, including the *Fmr1* knock-out mouse. They found that in each model, there was a common decrease in inhibitory feedforward signaling, while the excitatory signaling was only slightly increased. This led to an overall increase in the excitatory to inhibitory ratio[31]. Taken together, while many different factors have been found to contribute to ASDs, one common theme seems to be hyperexcitability. Therapies to combat this overexcitation through development may be able to combat this spectrum of disorders leading to better outcomes for the individuals.

1.2.2 Neuropathic pain

Neuropathic pain is caused by an alteration or disease of the somatosensory system. Many different etiologies can lead to neuropathic pain, such as mutations in ion channels, diabetes, age, spinal cord injury, or cancer treatments[32]. In general, the sensation of neuropathic pain is due to hyperexcitability of the peripheral nervous system. While the increased sensation of pain is a common factor associated with the etiologies listed above, the underlying physiological mechanisms are very broad[33]. For example, a recent meta-analysis of genetic relationship to neuropathic pain found mutations in genes that regulate everything from neurotransmission, immune response, and metabolism[34]. Perhaps the most studied gene associated with altered pain transmission is the voltage-gated Na^+ channel $Na_V1.7$. Gain-of-function mutations in $Na_V1.7$ cause paroxysmal extreme pain disorder (PEPD)[35], inherited erythromelalgia (IEM)[36], and painful diabetic peripheral neuropathy (PDPN)[37]. These mutations, while all found in $Na_V1.7$, alter different properties of the channel, thereby affecting Na^+ currents. Summarized well by Calvo and colleagues, IEM is due to a lower threshold for activation of the channel, PEPD is caused by an enhanced persistent Na^+ current (I_{NaP}), and PDPN is caused by impaired inactivation of the channel[33]. While each mutation alters differing components of $Na_V1.7$ activity, they all lead to an increase in Na^+ current. Understanding these differing underlying etiologies greatly helps when considering pharmacological treatment of each disorder individually. While $Na_V1.7$ has been the most extensively studied, mutations in other voltage-gated Na^+ channels, such as $Na_V1.1$, $Na_V1.6$, $Na_V1.8$, and $Na_V1.9$ have also been found to be associated with the

sensation of pain[38]. Unfortunately, current pharmacological treatments for neuropathic pain are ineffective because of low efficacy and negative side effects[39]. The drugs most effective at preventing pain, opioids, have caused an addiction crisis leading to a large push to find effective, non-addictive alternatives[40]. These new treatments must include ways to stave off the underlying hyperexcitability that is the root cause of neuropathic pain.

1.2.3 Injury or insult

Neuronal injury, either physically induced such as in traumatic brain injury (TBI) or caused by energy deprivation such as in the case of ischemic conditions, can lead to a host of issues in humans. Recent studies suggest that in both instances, neurons become hyperexcitable following the transient event which is hypothesized to lead to longer lasting detrimental effects and neuronal loss.

It has been well characterized over the years that an ischemic injury or insult results in increased neuronal excitability[41,42]. The loss of oxygen supply to the neurons reduces cellular ATP levels, thereby inhibiting the Na^+/K^+ ATPase. This causes an increase in intracellular Na^+ which depolarizes the neuron. Upon depolarization, voltage-gated Na^+ and Ca^{2+} channels open, resulting in further depolarization and release of neurotransmitters, notably glutamate. Excessive glutamate release, and in turn stimulation of nearby neurons, results in a depolarization cascade. This overexcitation, if left unchecked, results in excitotoxicity and neuronal death due to activation of apoptotic pathways via excessive increases in intracellular Ca^{2+},[43]. Additionally, other alterations in ion channel function caused by oxygen deprivation further exacerbate the overexcitation. This include increases in I_{NaP}[44,45] and simultaneously decreasing the transient Na^+ current (I_{NaT}), both of which were associated with a shortened action potential duration[46]. Increased depolarization also has been found to cause an increase in outward K^+ current[47]. Increased extracellular K^+ is believed to further cause neuronal damage. Indeed, voltage-gated K^+ channel blockers, tetraethylammonium (TEA) and clofilium, were found to be neuroprotective in a mouse model of ischemia[48,49]. This excessive K^+ efflux occurring in ischemic conditions has been suggested to be caused by a specific voltage-gated K^+ channel, $K_V2.1$[50,51]. Interestingly, non-conducting clusters of these channels

on the soma have been shown to decluster in response to oxygen deprivation or glutamate exposure, suggesting a role in ischemic response[52]. Declustering of $K_V2.1$ channels has been shown to disrupt endoplasmic reticulum and plasma membrane junctions[53]. While the function of this coupling and uncoupling is still under active study[54], recent data suggests that disruption of $K_V2.1$ clustering is neuroprotective following stroke in mice[55]. Taken together, these results suggest that increased neuronal excitability following an ischemic insult, such as a stroke or heart attack, is what leads to neuronal damage and death. As such, preventing this overexcitation could be neuroprotective, which would decrease the damage following the insult.

Another neuropathological disability, which has recently gained notoriety in the United States, is TBI. TBI is a result of extensive and direct blows to the head causing alternate head-brain movement[56]. Common situations causing TBI include, but are not limited to, bicycle accidents, car accidents, sports such as football and soccer, and military conflicts. There is a large body of evidence which suggest that TBI events often lead to hyperexcitability and downstream issues associated with the increased excitability. Indeed, humans suffering from a TBI have a 20-50% likelihood of developing epilepsy depending on the setting and cause[57]. The events of a TBI can generally be broken into the primary insult, which is the blunt physical trauma itself, and secondary insults, which are cellular responses to the blunt trauma that include increased glutamate release[58], oxidative stress[59], mitochondrial dysfunction[60], and cortical and hippocampal neurodegeneration[61,62]. Combined, these cellular responses along with epileptogenic phenotypes are consistent with the idea that TBI induces general hyperexcitability. To this point, multiple groups have examined TBI mouse models that lead to neuronal hyperexcitability seen by glutamate imaging, evoked field potentials[58], and functional magnetic resonance imaging (fMRI)[63]. Interestingly, single-unit and multiunit recordings suggest that there is an initial phase with decreased activity, followed by an increase in excitability in mouse cortical neurons following injury[64,65]. This would suggest that homeostatic responses during the initial dampening of signaling may be causing the downstream cellular responses and increased excitability.

While both types of neuronal injury listed here are caused by different means, the downstream consequences are similar. Both functionally lead to alterations in mitochondrial function thereby causing dysfunctional release of glutamate. Increased extracellular glutamate can lead to disruptions to the intrinsic excitability of neurons, and if left unchecked can cause apoptosis. Therefore, preventing the increased excitability may offer a therapeutic approach to protect against subsequent neuronal death and the detrimental outcomes associated with neuron loss.

1.2.4 Neurodegenerative diseases

Neurodegenerative diseases are debilitating pathologies caused by the progressive degradation of the nervous system. These disorders are associated with dysfunctional neuronal activity, and both increases[66–68] and decreases[69,70] in activity have been reported. Interestingly, our lab has recently proposed a model in which early increases in activity can lead to homeostatic responses which subsequently decrease neuronal activity[71]. Alterations in either direction can be detrimental to neurons and eventually lead to neuronal cell death. In the case of overexcitation, this can lead to neuronal cell death via the glutamate induced apoptotic pathway described above. Neurodegenerative pathologies associated with overexcitation include Amyotrophic Lateral Sclerosis (ALS), Parkinson's Disease (PD), and Alzheimer's Disease (AD). Most of these are associated with age, such that as the individual gets older they are either more likely to get the disease or more likely to suffer severe consequences of the disease. I will focus on the common underlying mechanism of hyperexcitability associated with each of these neurodegenerative diseases.

ALS is a progressive neurodegenerative disease that often manifests in defective motor control such as falling, muscle twitching, and slurred or altered speech. These alterations are associated with a decrease in corticospinal neurons, brainstem neurons, and spinal motor neurons[68]. ALS can progress to more severe prognoses such as altered behavioral responses, difficulty breathing, and dementia. The cause for this disease is generally unknown, as only 5-10% of cases are inherited. While the causes for ALS are still not well understood, the common indicators and early factors have been studied using mammalian models of the disease and by examining humans diagnosed with ALS. One common feature is cortical

hyperexcitability, which can be seen early in the prognosis[72–74]. Using transcranial magnetic stimulation (TMS), researchers have identified cortical hyperexcitability in familial ALS patients[75]. Furthermore, cortical hyperexcitability was found to precede clinical symptoms of the disease[73]. Additionally, researchers have reported a strong correlation between the level of cortical hyperexcitability and disease prognosis. These findings emphasize the detrimental effects could be caused by overexcitation[76]. It has been proposed that this early cortical hyperexcitability leads to glutamate induced excitotoxicity and neuronal cell death of the downstream spinal motor neurons[77], which would explain the behavioral symptoms observed in the later stages of ALS. Beyond cortical hyperexcitability, increased excitation in downstream motor neurons has also been observed and reviewed[78]. These phenotypes have been found mainly in embryonic or early *SOD1* mutant mouse models of ALS[79–81]. Interestingly, in these studies, an increased action potential firing rate of cultured and *ex vivo* motor neurons from mutant *SOD1* mice corresponded with increases in the I_{NaP}[79,81]. Additionally, postmortem in humans with ALS, a decrease in delayed rectifier K^+ channel expression was observed in the spinal cord[82]. While the etiology of this disease is still not well understood, the general increase in excitability suggests that early interventions decreasing excitation, either in the cortex or motor neurons, might slow the progression of the disease. To this end, Riluzole, an inhibitor of I_{NaP}, has been used to treat ALS since 1995[83]. This is of interest in relation to results of this dissertation, which suggest that K_{Na} channels may be able to protect against increases in I_{NaP}.

PD is another neurodegenerative disease that causes symptoms associated with motor dysfunction, such as bradykinesia, akinesia, tremors, and postural instability[84]. This disease is generally characterized by degeneration of nigrostriatal dopaminergic neurons. This is why drugs mimicking dopamine action, such as L-3,4-dihydroxyphenyalanine (L-DOPA), are the current standard therapy[84]. In addition to decreased dopaminergic signaling, an increase in cholinergic signaling within the striatum has also been observed and reviewed[85]. Decreases in K^+ currents have been associated with increased action potential firing rates in both dopaminergic and cholinergic interneurons of animal models of PD[67,85]. In addition to treatment with L-DOPA, another accepted treatment for PD is with anticholinergics[86]. Interestingly, both the striatal

cholinergic interneurons and dopaminergic neurons display tonic, pacemaker activity[87,88]. A major component regulating activity of these pacemaking neurons is the after-hyperpolarization (AHP). As such, it has been suggested that alterations in K^+ currents regulating the AHP might be causing the hyperexcitability. Indeed, the voltage-gated delayed rectifier K^+ channel $K_V1.3$ and the Ca^{2+} activated K^+ channel, SK, have been implicated in cholinergic and dopaminergic overexcitation, respectively[67,85]. Other ionic currents affecting the pacemaking activity and AHP of these neurons may also play a role in altered excitability in PD models. To my knowledge, these have not yet been explored. Pertaining to this dissertation, a system like the Ca^{2+}-activated K^+ channels may exist in K_{Na} channels. Indeed, it has been suggested that K_{Na} channels may regulate neuronal pacemaking and bursting patterns which will be further discussed in Section 1.6.4.

AD is the most common neurodegenerative disease, characterized by cognitive impairment and memory loss. It is directly correlated with age, and mostly occurs sporadically, although there are some known familial mutations causing early-onset AD[89]. AD is associated with altered amyloid precursor protein (APP) processing, leading to aberrant amyloid-β (Aβ) plaque formation[90]. These plaques were initially found to be associated with neuronal cell death, which led to "the amyloid cascade" hypothesis of AD progression[91]. It was later suggested that in addition to Aβ plaque toxicity, oligomeric forms of Aβ were also neurotoxic, inhibiting LTP and causing cell death [92]. Since then, these Aβ oligomers have been shown to be toxic in several ways, reviewed by Ferreira et al. 2015[93]. One intriguing finding is that these oligomers can disrupt excitatory neuronal functioning, leading to hyperexcitability[66,71,94–103]. This overexcitation has been a common theme in invertebrate models of AD[71,94,98] and mammalian models[95,97,99–102]. While the underlying physiological mechanisms that cause increased neuronal activity differ between each study, hyperexcitability remains a common theme. Our lab has found in a *Drosophila* AD model, flies exhibit a decrease in the A-type K^+ channel *Shal*. Decreases in this channel were associated with increased action potential firing along with learning and locomotion defects as well as neurodegeneration. Importantly, these defects were attenuated by restoring *Shal* function[94]. These findings strongly suggest that

attenuating Aβ-induced hyperexcitability can prevent downstream prognosis. Additionally, our lab recently found that *in vitro* neurons expressing Aβ initially exhibit an increase in spontaneous synaptic activity at DIV 5, followed by a decrease in spontaneous synaptic activity at DIV 9[71]. This study suggests that as neurons encounter Aβ-induced hyperexcitability, homeostatic mechanisms respond, thereby decreasing neuronal activity to a level lower than that of the control neurons. One possibility is that these homeostatic responses cause long-term damage, facilitating neurodegeneration and cognitive decline[104]. Additionally, a recent study suggests that overexpression of the inward rectifier K^+ channel, $K_{ir}2.1$, prevents Aβ-induced neuronal apoptosis[98], suggesting that hyperactivity could be causing cell death. This evidence, combined with previous studies in our lab, suggest that by preventing hyperexcitability caused by oligomeric Aβ, the detrimental homeostatic responses and pathogenesis of AD may be attenuated.

1.2.5 Epilepsy

Affecting 65 million people worldwide, epilepsy is one of the most common neurological diseases[105]. It is defined by the International League Against Epilepsy (ILAE) as "transient occurrence of signs and/or symptoms due to abnormal excessive or synchronous neuronal activity in the brain"[106] and is associated with the regular occurrence of seizures that affect the individual's cognitive, psychological, social, and financial well-being[106]. Increased brain activity causing a seizure can either occur in one region of the brain, called focal seizures, occur in both hemispheres with a wide distribution, called generalized, or does not fall into these classifications and would be labeled as unknown[107]. The causes of epilepsy are vast, and are broken down into six etiologies: structural, genetic, infectious, metabolic, immune, and unknown[107]. With advances in genomic and exonic sequencing, genetic etiologies of epilepsy have become an attractive target for study[108]. Of the genetic etiologies identified, many mutations fall into ion channels responsible for regulating neuronal excitability[109–111]. These include mutations in ion channels, such as K^+ channels, Ca^{2+} channels, Cl^- channels, HCN channels, γ-aminobutyric acid (GABA) receptors, nicotinic acetylcholine receptors (nAChRs), and others (reviewed by Deng et al. 2014[109]). Most prevalent of epileptogenic ion channel mutations are in either voltage-gated Na^+ or K^+ channels[108,110,112,113]. I will focus

on mutations in the voltage-gated Na^+ channel as this most closely relates to my studies on the K_{Na} channel. Some voltage-gated Na^+ channel mutations have been recapitulated in model organisms to examine the electrophysiological consequences of the mutations. Of these, Dravet Syndrome (DS) and Generalized Epilepsy with Febrile Seizures Plus (GEFS+) are notable due to their recapitulation in model organisms[114–118]. DS and GEFS+ are associated with roughly 600 different mutations in the *SCN1A* gene, which codes for $Na_V1.1$[118]. GEFS+ is associated with febrile seizures that occur early on in childhood and persist past 6 years of age[119]. DS individuals, previously called Severe Myoclonic Epilepsy in Infancy (SMEI)[120], exhibit both febrile and afebrile seizures throughout their first year, which are commonly associated with developmental delays in their second year[120]. DS is the more severe of the two disorders. In both cases, initial seizures are often associated with an increase in body temperature, such as a fever, vaccination, or a hot water bath[119,120]. Several mouse models have examined the effects of mutations in $Na_V1.1$ similar to those found in DS and GEFS+ patients. Truncation mutations, such as those found in some DS cases, were the first models examined in mice. These researchers found, upon deletion of the last exon of *Scn1a*, there was a decrease in Na^+ current in GABAergic neurons that corresponded with a decrease in action potential firing[121,122], suggesting that a decrease in GABAergic input may lead to overall overexcitation. Consistent with these results, another group found that targeted deletion of $Na_V1.1$ in GABAergic interneurons was sufficient to induce spontaneous epileptic seizures and ataxia in mice[114]. Additionally, two mouse models based on mutations causing DS[123] (Sugawara et al. 2002) and GEFS+[124] have been generated using homologous recombination. Their results were again consistent with previous models, showing that these mutations decreased excitability in GABAergic interneurons. Combined, these results have led to an interneuron hypothesis, the underlying idea being that decreases in inhibitory tone lead to an overall increase in excitability, otherwise known as disinhibition, which could trigger seizures. Expanding on these findings, point mutations found to cause GEFS+[125] and DS[123] in humans were recapitulated in *Drosophila*. Importantly, *Drosophila* contain only one gene encoding for a voltage-gated Na^+ channel, *para*. Unlike mammalian models, this prevents potential compensatory mechanisms from other voltage-gated Na^+ channels when examining mutations in *para*. Consistent with the mammalian findings, these mutations led

to a decrease in inhibitory neuron spikelet frequency upon an increase in temperature[116–118]. Interestingly, it was found that the GEFS+ and DS mutations led to gain-of-function and loss-of-function phenotypes in the Na^+ current, respectively[116,117], which will be discussed in greater detail in Section 1.4.1. Regardless of their alterations in ion channel function, both caused temperature induced seizure-like behavior in the flies. Similar to humans, the DS phenotype was significantly worse than the GEFS+ phenotype[118]. I have chosen to highlight these two epileptic disorders as they are relevant to my studies. Additionally, it emphasizes the need to understand the biophysical properties causing each individual type of epilepsy, as pharmacological or genetic treatments would need to be differentially targeted depending on the underlying cause.

In addition to the genetic causes of epilepsy, it is worth noting that many of the pathological diseases discussed in this section are also associated with epilepsy. For instance, ASD and epilepsy are often comorbid, with 9% of individuals with ASD also having epilepsy and 12% of people with epilepsy also diagnosed with ASD[126]. While the mechanisms of this are still unclear, it has been noted that both diseases share similar biological pathways[127]. Additionally, injury and insults of the brain, such as ischemic stroke and TBI, have been associated with the development of post-traumatic epilepsy (PTE). Following ischemic stroke, chances of developing post-stroke epilepsy range anywhere from 3 to 30%[128–131]. Similarly, TBI events can lead to PTE between 4% in milder cases to up to 50% in more severe cases[132–136]. Lastly, AD has been found to increase the likelihood of seizure by 87-fold in an age-matched, non-AD group[137]. Whether the comorbidity was coincidence or causative is still elusive, however a couple studies suggest that Aβ can induce seizures in mice. This was initially suggested when researchers found nonconvulsive seizure-like activity in the hippocampus and cortices of three separate APP transgenic mouse lines[103]. This was expanded upon by another study that found that both endogenously overexpressed Aβ as well as exogenously applied Aβ aggregates cause enhanced cortical excitability that is associated with epileptic seizures recorded by EEG in transgenic mice[102].

The prevalence of comorbidity between neuropathological conditions discussed in this chapter and epilepsy further suggests that hyperexcitability is a common etiology. Additionally, previous therapeutic

approaches have suggested that prevention of overexcitation early in the disease prognosis may attenuate detrimental pathologies later on. Therefore, further exploration of neuronal processes that protect against overexcitation would provide valuable insight into potential therapeutic approaches. My research explores the possibility that K_{Na} channels act to prevent overexcitation. There has been significant research into the ways in which cells attempt to prevent overexcitation themselves. Many of these involve homeostatic mechanisms, in which the cell attempts to maintain a certain degree of excitability. These types of homeostatic responses will be outlined in the following section.

1.3 Homeostatic responses

It has long been postulated that in order for complex biological systems to store information, changes in individual neuronal excitability would be required to stabilize network connections. First proposed by Donald Hebb[138], Hebbian plasticity postulated that coincidence patterns of pre- and postsynaptic activity can lead to strengthening of the synapse. This theory provided an outline of how learning, memory, development, and recovery in the brain could occur. Since its inception, this theory has been expanded on and indeed shown to play a role in classical learning paradigms of long-term potentiation (LTP)[139–144] and long-term depression (LTD)[145–147]. While this has been shown to be essential for learning and memory, it also generates a positive feedback mechanism, and if left unchecked could lead to excitotoxicity in some neurons and alternatively no activity in other neurons. In theory, this could cause extreme network destabilization, to the point where the organism could no longer learn from experiences. Instead, homeostatic plasticity acts as a negative feedback mechanism, attempting to bring the neuronal activity back to an earlier set point. It is thought that these two mechanisms work together, where Hebbian plasticity leads to synaptic strengthening, while homeostatic plasticity works to bring the neurons back to their original state[148,149]. Mechanisms that induce homeostatic plasticity include: increases or decreases in inhibitory signaling, strengthening or weakening of synaptic connections, and alterations in intrinsic neuronal excitability. Below, I will discuss what is currently known regarding synaptic and intrinsic mechanisms of homeostatic plasticity.

1.3.1 Synaptic homeostasis

Neurons in the CNS are integrated into a complex network, of which both excitatory and inhibitory inputs play a critical role in relaying information. To maintain a precise level of excitability, neurons can effectively increase or decrease activity at individual synapses, called synaptic scaling. To accomplish this, neurons can adjust both presynaptic release of neurotransmitters as well as postsynaptic receptors. Some of the earlier studies examining synaptic scaling were done in cultured mammalian neurons in which activity was blocked using the voltage-gated Na^+ channel blocker tetrodotoxin (TTX). Upon washing out of TTX, miniature excitatory postsynaptic current (mEPSC) amplitudes were significantly increased, suggesting an alteration in postsynaptic receptor number or function[150]. These experiments sparked the idea that synaptic scaling, acting as a negative feedback mechanism, could protect neurons from disturbances in network activity. These *in vitro* experiments have been further expanded upon *in vivo*. In young rats reared in complete darkness, the amplitude of the mEPSC was significantly increased in the visual cortex[151]. This evidence suggested an increase in postsynaptic receptor activity. Indeed, later data using similar visual deprivation protocols on 4-week old mice, found that levels of the ionotropic glutamate receptor, GluR1, increased in the visual cortex in response to dark rearing[152]. Increases in GluR1 levels corresponded with increased inward rectification through α-amino-3-hydroxy-5-methyl-4-isoxazolepropionic acid (AMPA) receptors. Similar synaptic scaling and increased levels of AMPA receptors in the visual cortex was observed in aged mice, suggesting these responses aren't specific to certain developmental windows[153]. In addition to synaptic scaling in sensory systems, similar inactivity-induced alterations have been observed in hippocampal neurons[154]. As an alternative to inactivity-induced increases in activity, there appears to be a mechanism to dampen activity in response to increased activity. Using optogenetic approaches, Goold and Nicoll 2010 found that prolonged stimulation led to a depression in AMPA and *N*-Methyl-D-aspartic acid (NMDA) receptor function[155]. This reduction relied upon increased Ca^{2+} influx thereby activating Ca^{2+}/calmodulin-dependent protein kinase kinase (CaMKK) and Ca^{2+}/calmodulin-dependent protein

kinase-IV (CaMKIV). Therefore, bidirectional synaptic scaling mechanisms are present at excitatory synapses to protect against both increases and decreases in activity.

In complex networks, global synaptic scaling of both excitatory and inhibitory synapses in the same direction would be counterproductive, thereby not protecting the overall system activity. Therefore, separate regulation of excitatory and inhibitory synapses would be advantageous for the network. Indeed, in comparison to the described excitatory mechanisms described above, regulation of inhibitory synapses has been observed. Visual deprivation, either by darkness rearing or inhibition of retinal activity, was shown to decrease GABA staining in cortical areas[156–159], which was thought to be regulated by brain-derived neurotrophic factor (BDNF) signaling. Interestingly, exposing cortical cultures to BDNF prevented an inactivity-induced decrease in GABAergic signaling[160,161]. Similarly, activity deprivation in neuronal cultures has been found to induce changes in postsynaptic $GABA_A$ receptors and reductions the in presynaptic protein glutamate decarboxylase-65 (GAD65), which produces the inhibitory neurotransmitter GABA[162,163]. Combined, these results suggest that synaptic scaling at inhibitory synapses can work alongside changes at excitatory synapses, thereby causing similar alterations to excitability throughout the network.

While glutamatergic synaptic scaling has been extensively studied and reviewed, scaling at other synapses is less understood. Research of synaptic homeostasis at other synapses will not only elucidate common mechanisms but can also shed light on disease states associated with non-glutamatergic synapses. Indeed, alterations in cholinergic synapse activity has been associated with a number of pathological conditions, including epilepsy, nicotine addiction, and AD[71,164,165]. Similar to glutamatergic receptors, some cholinergic nicotinic acetylcholine receptors (nAChRs) are permeable to Ca^{2+}, suggesting they could also be involved in Ca^{2+}-dependent synaptic scaling mechanisms. Indeed, using excitatory cholinergic neurons from *Drosophila*, it was found that inactivity induced by curare, which blocks nAChRs, led to an increase in Dα7 nAChR levels[166]. Furthermore, downstream changes in neuronal activity were mediated by Ca^{2+} influx through nAChRs and Ca^{2+}/calmodulin-dependent protein kinase-II (CaMKII) activation. Relevant to

AD, nAChRs have also been found to mediate early increases in activity induced by amyloid beta 42 (Aβ42), a peptide strongly associated with AD. Increased nAChR activity drove compensatory synaptic mechanisms that led to a later decrease in neuronal activity[71]. Results in cholinergic synaptic scaling suggest not only that similar mechanisms could be occurring at glutamatergic and cholinergic synapses, but also that cholinergic synaptic scaling is relevant to human diseases.

1.3.2 Intrinsic homeostasis

Activity-dependent alterations in intrinsic neuronal properties were first shown in invertebrate central pattern generators[167]. In these experiments, isolated Lobster stomatogastric ganglion neurons were subjected to stimulating pulses and found to alter their intrinsic tonic firing. This was found to be dependent upon increases in intracellular Ca^{2+}. Experimental and modeling assays have further suggested that these neurons are able to alter intrinsic properties to maintain a basal level of firing[168–170]. Following these invertebrate studies, it was found that depriving cultured vertebrate cortical neurons of activity using TTX lead to a significant increase in voltage response to a current injection[171]. These researchers also found that this increased excitability was associated with an enhanced Na^+ current as well as a decreased K^+ current. Together, these studies laid the foundation to suggest that individual neurons in both invertebrates and vertebrates could alter their intrinsic activity to respond to external stimuli and maintain a basal level of activity.

Following this *in vitro* data, many experiments have examined the ability of neurons to alter intrinsic excitability *ex vivo*. Vertebrate *ex vivo* intrinsic homeostatic responses have been seen in hippocampal[172–174], visual[175], and somatosensory[176] neurons. In all of these cases, alterations in neuronal activity led to activity-dependent changes in conductance of K^+. Further analysis using *Drosophila* have shown that these changes also occur *in vivo*. These studies found homeostatic responses in the larval motor neurons in response to deletion of the delayed rectifying K^+ channel *Shab*[177] as well as in the adult mushroom body neurons in response to altered action of the input neurons[178]. Recently, our lab has also shown that upon inhibition of cholinergic activity *in vivo*, nAChR levels were increased as a synaptic

homeostatic response. This subsequently led to an increase in levels of the A-type voltage-gated K^+ channel, *Shal*, to compensate for the increase in activity caused by the increased nAChR levels[179].

In addition to altering ion channel levels, neuronal structural changes also occur in response to altering external stimulation. One structural region that strongly regulates neuronal excitability is the axon initial segment (AIS). AIS remodeling occurs to both reduce and increase excitability of the neuron. To reduce excitability, the AIS moves down the axon away from the soma in response to increased input[180]. Contrastingly, the AIS will increase in length in response to neuronal activity deprivation, thereby enhancing activity[181].

In all of these instances, altered neuronal input led to a change in intrinsic excitability, which in turn brought the neuron back to a basal level of activity. Intrinsic homeostasis, in conjunction with synaptic plasticity, seem to be acting to preserve network activity. This preservation of activity is what simultaneously prevents overexcitation while still allowing enough activity to respond properly to external stimuli. It is remarkable that with all of this remodeling occurring simultaneously throughout the nervous system that more pathological conditions are not seen in which runaway hyperexcitability occurs. The use of genetically tractable model organisms with well characterized behavior, such as *Drosophila*, can be used to better understand how organisms prevent overexcitation.

1.4 *Drosophila melanogaster* models of overexcitation

Flies have long been identified as a model for seizure-like behavior. Examples of early seizure-like behavior dates back roughly 80 years[182,183]. A shaking phenotype in a *Drosophila* line was originally described by Catsch 1944, and this line was subsequently referred to as *Shaker*. In this line, a spontaneous mutation was found localized to the X-chromosome[182]. Additionally, two other lines were reported that displayed a similar shaking phenotype upon exposure to ether, which was used to anesthetize the flies[183]. Mutations in these lines were later mapped and genes in which they were found were labeled based on the shaking phenotype, *Shaker*, *ether á go-go,* and *Hyperkinetic*[184]. In later experiments, these mutations were

found to alter K^+ currents that affected seizure threshold[185]. Additionally, a temperature induced hyperexcitable phenotype was identified in early mutagenic screens[186–189]. In these flies, elevated temperatures would cause paralysis, whereas wild-type flies would continue behaving normally. Worth noting, these experiments led to the discovery of the fly line *paralyzed*[186], whose mutation was later mapped to the gene *para* which encodes a voltage-gated Na^+ channel[190]. Early electrophysiological experiments on a few of these mutants showed failure of action potential firing and excitatory post-synaptic currents at elevated temperatures between 32-34˚C[187,191]. These initial studies laid the groundwork for *Drosophila* to be studied as a model for overexcitation. Below, I discuss two models of seizure-like behavior induced by either increased temperature or mechanical stimulation. I also discuss the similarities between these *Drosophila* models and human epilepsy, suggesting that these models help to uncover the underlying physiological mechanisms causing epilepsy and potential genetic and pharmacological methods to protect against seizures.

1.4.1 Temperature-sensitive flies

Neuronal hyperexcitability is thought to be the main cause of epileptic disorders. As the excitability of neurons is heavily regulated by Na^+ currents, the voltage-gated Na^+ channel is of particular interest in causing epilepsy. Indeed, many different mutations in human voltage-gated Na^+ channels lead to epilepsy[192]. Model organisms are being used to better understand the mechanisms underlying these epileptogenic mutations[118]. This is particularly true for *Drosophila*, which are a genetically tractable organism and contain only one gene encoding a voltage-gated Na^+ channel, *para*. The O'Dowd lab has generated two separate knock-in *Drosophila* lines containing the mutations S1231R and K1270T in *para*. These mutations are homologous to mutations in humans that cause Dravet Syndrome (DS)[123] and Generalized Epilepsy and Febrile Seizures plus (GEFS+)[125], respectively. Humans with DS or GEFS+ exhibit seizures upon an increase in body heat, such as when they have a fever, are vaccinated, or placed in a hot bath[119,120]. Similar to the human phenotype, *Drosophila* containing homologous mutations also exhibit seizure-like behavior when subjected to elevated temperatures[116,117]. Generating these mutants provided a

unique opportunity that revealed different physiological mechanisms that lead to the temperature-induced seizure-like behavior. They found the DS mutation, S1231R, causes a loss-of-function in *para* in which elevated temperatures decreased the amplitude of I_{NaT}, increased the threshold for Na^+ channel activation, and caused a depolarizing shift in the deactivation of I_{NaP} (Fig. 1.1)[117]. In contrast, the GEFS+ mutation, K1270T, leads to a gain-of-function mutation in which elevated temperatures cause a decrease in Na^+ channel activation threshold and an increase in I_{NaP} (Fig. 1.1)[116]. Recapitulation of two separate human epileptic models in *Drosophila*, leading to similar behavioral outcomes, suggests they could be used to further explore the genetic basis of human epilepsy. Additionally, these flies could be used to screen for potential pharmacological or genetic means of attenuating the seizure-like behavior. In Chapter 5, I examine the ability of the *Drosophila* K_{Na} channel, dSlo2, to prevent seizure-like behavior in these flies.

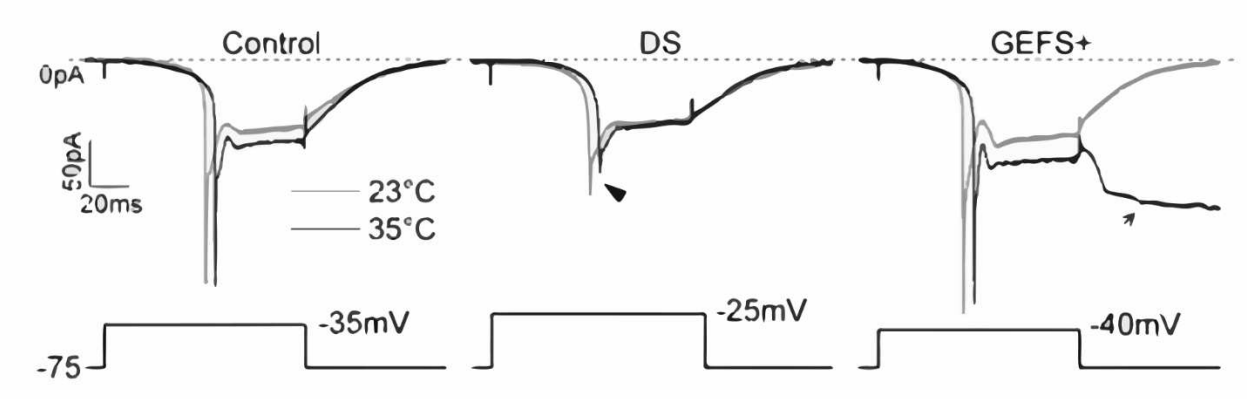

Figure 1.1: DS and GEFS+ mutations differentially affect the Na^+ current. Data combined in Schutte et al. 2014 shows the decreased transient Na^+ current caused by the DS mutation (arrowhead, middle). The GEFS+ mutation led to an increased persistent Na^+ current (arrow, right).

1.4.2 Bang-sensitive flies

In addition to the ether-induced shaking phenotype, mutagenic screens identified a seizure-like phenotype that was induced by a "bang", such as a tap of the vial onto the benchtop or brief vortexing, and these flies were therefore called "bang-sensitive"[193]. Following the bang, flies exhibit seizure-like behavior that is characterized by an initial seizure of 2 seconds, temporary paralysis of 20-300 seconds, and a recovery seizure of 2 seconds[193,194]. Since these earlier experiments, at least 14 different bang-sensitive mutant lines have been identified[195]. These flies contain mutations in different genes but exhibit a similar

phenotype, albeit to differing degrees of severity. It has also been documented that upon brain stimulation, researchers can elicit electroconvulsive behavior in *Drosophila*[196]. This behavior has been linked to a specific circuit, the giant fiber (GF) pathway[197], which normally initiates jump-and-flight escape reflexes[198]. Electrical stimulation of the GF pathway elicits a response in one of the downstream targets of the GF fiber, the dorsal longitudinal muscles (DLMs) (Fig. 1.2.A). Recordings from the DLMs can be used as a physiological readout for seizure-like behavior. Indeed, electrical recordings from the DLMs mimics seizure-like behavior, in which there is an initial burst of activity, followed by a period of synaptic failure, and finally by another burst of activity (Fig. 1.2.B)[197,199]. In addition to the behavioral phenotype, electrophysiological experiments have shown that bang-sensitive flies have a lowered seizure threshold induced by an electrical shock[200]. In this case, homozygous bang-sensitive mutants had a seizure threshold of 3-7V, whereas wild-type fly seizure threshold was between 45-49V. Mutations underlying these bang-sensitive flies have been shown to affect Na^+ or K^+ channel dynamics. Three lines (*bang-senseless* (*bss*), *slamdance* (*sda*), and *easily-shocked* (*eas*)) have been shown to increase the persistent component of the voltage-gated Na^+ channel[201,202]. Interestingly, each of these three mutant lines affects a different gene. The *bss* mutation was mapped to *para*, the only gene coding for a voltage-gated Na^+ channel in *Drosophila*[201]. *sda* and *eas* mutations were found in genes coding for aminopeptidase N[203] and an ethanolamine kinase[204],

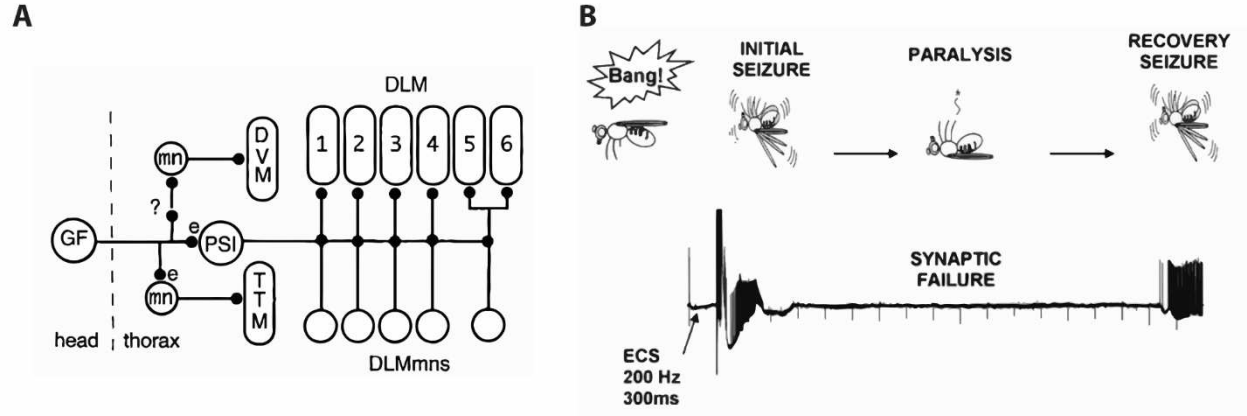

Figure 1.2: Giant fiber stimulation mimics seizure-like behavior. A) The GF pathway begins in the head of the fly and synapses onto downstream targets in the thorax, eventually terminating in the dorsal longitudinal muscles (DLMs). Modified from Pavlidis and Tanouye 1995. B) Stereotypic bang-sensitive fly behavior shown on top matches the timing of GF stimulation and synaptic failure recorded from the DLMs (bottom). Modified from Song and Tanouye 2008.

respectively. All three mutants exhibit increases in I_{NaP} and seizure-like behavior that differs in severity. *bss* is the most severe, *eas* is moderate between the *bss* and *sda*, and *sda* shows the least severe phenotype[195,200]. Additionally, it was found that the *bss* mutation caused a missense mutation in *para*[201], while the *sda* and *eas* mutations lead to changes in alternative splicing of *para*. In *sda* and *eas*, incorporation of exon *L*, instead of exon *K*, enhances I_{NaP}[205,206]. Pharmacological or genetic methods to revert this alternative splicing reduced the severity of the seizure-like behavior[205,206]. In an effort to induce seizure-like behavior with more spatially and temporally precise mechanisms, optogenetic approaches have recently been developed and shown to similarly induce seizure-like behavior and physiology in bang-sensitive flies[207].

1.4.3 Similarities between *Drosophila* and human epilepsy

While flies cannot be considered miniature humans, many similarities exist between these organisms that suggest *Drosophila* can be used to study the underlying molecular mechanisms that induce seizure-like behavior. First, similar to humans, all flies have a threshold for seizure behavior induced by electrical shock[200]. These shocks trigger uncontrollable muscle spasms and paralysis reminiscent of seizures in humans. Second, genetic mutations can render both species more susceptible to seizure-like behaviors[200]. Third, seizure-like activity travels throughout the fly nervous system, relying on functional synaptic connections to transmit the activity[196,198,200,207]. Fourth, seizure-like behavior can spawn from specific regions of the *Drosophila* CNS[207,208]. Fifth, *Drosophila* seizure-like behavior can be ameliorated by antiepileptic drugs (AEDs) shown to similarly prevent seizures in humans. These drugs include valproate[209], phenytoin[210], gabapentin[210], and Potassium Bromide[211]. Sixth, mutations affecting *Drosophila* voltage-gated Na^+ and Ca^{2+} channels convey protective properties against seizure-like behavior[207,212]. Seventh, mutations in humans that cause the epileptic disorders DS and GEFS+ have been recapitulated in *Drosophila* and similarly shown to cause temperature-induced seizures[116,117]. Lastly, the underlying mechanisms associated with epilepsy are similar between *Drosophila* models and humans. This includes increases in I_{NaP}[116,201,202,213] and increases in synchronicity thought to underlie many human epilepsies[214,215].

These similarities combined suggest that *Drosophila melanogaster* make an attractive model organism for studying the underlying mechanisms leading to seizure-like behavior, and additionally potential ways to prevent seizures from occurring.

1.5 The persistent Na^+ current

1.5.1 Molecular identity of the persistent Na^+ current

The persistent Na^+ current (I_{NaP}) is characterized by a voltage-dependent, non-inactivating component of the voltage-gated Na^+ channel that follows the well-known transient Na^+ current (I_{NaT}). This persistent component is usually between 0.5-5% of the transient component and has been reviewed previously[216]. While it was initially observed in 1979 in hippocampal neurons[217], the underlying causes are still not well understood. As both the transient and persistent components are blocked by extracellular application of TTX, it has been suggested that they both come from similar voltage-gated Na^+ channels. It has been difficult to directly test this hypothesis in mammals, which have nine genes that encode the α-subunits for Na^+ channels. *Drosophila* offer a particularly good model organism to test this hypothesis as they contain only one gene coding for a voltage-gated Na^+ channel, *paralytic* (*para*)[190]. While there is only one coding gene, *para* has been shown to express as many as 27 different splice forms[218]. Research out of Dr. Richard Baine's lab has linked alterations in the I_{NaP} to specific splice forms of *para*[205,206,218]. Furthermore, specific point mutations in *para* were found to directly alter the I_{NaP}[116,219]. Combined, this research suggests that voltage-gated Na^+ channels are at least one source of I_{NaP}. As for other potential sources, it has been found that the Na^+ leak channel, non-selective (NALCN) can contribute to a persistent depolarizing current that regulates resting membrane potential and is necessary for respiration[220]. The *Drosophila* ortholog of this channel, *narrow abdomen* (*na*), has been shown to promote behavioral rhythmicity and regulate circadian pacemaker neurons[221,222]. While this presents another I_{NaP} source, I will mainly focus on the I_{NaP} produced by the voltage-gated Na^+ channel for this dissertation.

1.5.2 Physiological role of the persistent Na^+ current

While the I_{NaP} is relatively small in relation to the transient component responsible for action potential firing, its contribution to neuronal excitability can be rather large due to its activation at subthreshold voltages. Since the input resistance of neurons is high at these voltages, it has been estimated that a I_{NaP} could depolarize the neuron as much as 26 mV[223]. Having this much influence over neuronal excitability at subthreshold levels suggests it could play a crucial role in regulating neuronal firing properties.

Neurons in the CNS exhibit many different types of firing patterns that define their role in the network. One specific type of firing pattern seen in neurons is bursting activity. Bursting activity is a crucial component of many different central pattern generating networks, which regulate stereotypic behaviors including locomotion, respiration, and mastication[224–229]. Burst patterns can vary widely among neuronal populations and are the result of both synaptic activity as well as intrinsic excitability. Many neurons located within central pattern generating networks have been found to exhibit intrinsic bursting activity independent of synaptic input[230]. I_{NaP} has been found to regulate this intrinsic bursting activity in some neuronal populations of the CNS, including mesencephalic V neurons[231], dorsal column nuclei[232], hippocampus[233], neocortex[234], and spinal cord[235]. Regulation of intrinsic burst firing, that is essential for stereotypic motor behaviors, suggests that the I_{NaP} could alter these behaviors. Indeed, it has been shown that changes in the I_{NaP} alter locomotor rhythm in isolated rat spinal cords[228] as well as fictive locomotion in mouse spinal cord[236].

Given that the I_{NaP} has been found to regulate burst firing, synaptic amplification, and subthreshold oscillations, it has been predicted that it may also regulate network oscillations throughout the brain. Network oscillations are due to synchronous neuronal discharges that are the sum of rapid membrane potential changes in excitatory and inhibitory neurons[237,238]. These oscillations, measured by electroencephalogram (EEG), have been broken down into subcategories that are associated with different cognitive states[239]. Gamma oscillations, of which are fast (30-90 Hz), are thought to be responsible for memory retrieval and attentional selection[240,241]. Impaired gamma oscillations have been associated with

multiple pathologies, including FXS, AD, and epilepsy[242–244]. Recently, these gamma oscillations have been found to be regulated by I_{NaP}. In two papers out of Dr. Sang-Hun Lee's lab, the investigators report that riluzole, a I_{NaP} blocker, inhibited oscillations in five different cell subtypes in mouse hippocampus[245]. They additionally found that phenytoin, another I_{NaP} blocker, decreased gamma oscillations in the hippocampus which was associated with decreased excitability of CA1 pyramidal neurons[246]. This recent evidence suggests that the relatively small I_{NaP} plays a major role in network synchronization and could greatly affect organismal function and behavior.

1.5.3 Pathologies caused by altered persistent Na^+ current

The physiological properties of I_{NaP} enable it to play a major role in regulating neuronal excitability. As such, I_{NaP} may be a common factor in different pathologies associated with hyperexcitability. Indeed, this current is associated with multiple nervous system disorders, including ischemia[247], FXS[248], neuropathic pain[249], ALS[80,250], and epilepsy (reviewed in Stafstrom 2007[213]). Of particular interest to my dissertation is the capacity for increased I_{NaP} to cause epilepsy, and how K_{Na} channels might be able to protect against this.

Multiple human mutations in the voltage-gated Na^+ channel which lead to different forms of epilepsy have been recapitulated in heterologous expression systems and knock-in models to study the root causes of the disease. Early on, these mutations were made in *SCN1A* and expressed in tsA201 cells. The researchers found that three point mutations, R1648H, W1204R, and T1875M all led to an increase in I_{NaP}[251,252]. Additionally, investigators have found that pilocarpine-induced status epilepticus in mice is associated with an increase in I_{NaP}[253]. Another group found that exposing rat hippocampal slices to thrombin caused a significant increase in I_{NaP}. This finding is interesting because neurons are exposed to thrombin, a common protein in the blood, following intracerebral hemorrhage (ICH). ICH regularly occurs alongside head and brain injury as well as stroke. This led the authors to hypothesize that following an ischemic attack, neurons are exposed to thrombin, causing neuronal hyperexcitability by increasing I_{NaP}, thereby leading to post-ischemic epilepsy[254]. Knock-in models have also been generated to examine the pathogenic

nature these mutations. Originally, researchers generated transgenic mice containing a mutation in *Scn2a* which caused incomplete inactivation of the channel. These investigators found that an increase in I_{NaP} could lead to seizures[255]. However, more recent transgenic and knock-in mouse models did not uncover an increase in I_{NaP} caused by the R1648H mutation[115,124]. In humans, these mutations lead to seizures upon an increase in temperature. These experiments, however, did not investigate whether increased temperatures alter I_{NaP} in these mice. This concept was further explored in Sun et al. 2012[116], in which a separate GEFS+ mutation (K1270T) was recapitulated in the *Drosophila* voltage-gated Na^+ channel *para*. The authors found that an increase in temperature caused a significant increase in I_{NaP}. As previously stated, these flies exhibited seizure-like behavior upon introduction to an elevated temperature. In this GEFS+ *Drosophila* model, as well as another model, *bss*, which also enhances I_{NaP}, anti-epileptic drugs known to decrease I_{NaP} were found to attenuate seizure-like behavior[202,209,210,214,256]. Additionally, researchers found that increased I_{NaP} in these *Drosophila* models led to increased synchronicity between motor neurons. Using genetically encoded Ca^{2+} reporters, the authors showed that increased synchronicity was correlated with seizure-like activity. Furthermore, anti-epileptic drugs which decrease I_{NaP}, decreased the synchronicity of firing between motor neurons[214]. These results suggest there could be multiple ways in which increased I_{NaP} could be leading to seizure-like behavior.

In addition to animal models, humans with these disorders have also provided insight into the causes of these diseases. First, multiple anti-epileptic drugs which have been shown to decrease the I_{NaP} are efficacious in treating epileptic patients with gain-of-function mutations[257,258]. Second, a study examined pyramidal neurons posthumously from drug-resistant patients with temporal lobe epilepsy. The researchers found a significant increase in I_{NaP} in a subset of neurons, hypothesizing that this could be the reason for the disorder[259].

Overall, these findings suggest a major role of I_{NaP} in setting membrane excitability and neuronal firing patterns, thereby affecting overall network activity. It is therefore not surprising that an increase in the I_{NaP} is a common etiology among different forms of epilepsy. One intriguing possibility is that a negative

regulator of this current, such as the K_{Na} channel, might be able to protect against increases in I_{NaP}. However, this possibility has not yet been examined in an *in vivo* model. Therefore, my dissertation mainly revolves around the ability of K_{Na} channels to protect against global overexcitation, and more specifically examines its ability to protect against hyperexcitability induced by increases in I_{NaP}.

1.6 Na^+-activated K^+ (K_{Na}) channels

1.6.1 History of K_{Na} channels

A Na^+-activated K^+ (K_{Na}) current was first identified in cardiomyocytes in 1984[260]. Na^+-dependent K^+ currents were further recorded in multiple species and cell types before identifying the gene responsible for the currents[261–270]. In 1998, the first K_{Na} channel was cloned from the rat. In these initial experiments, function was only observed when co-expressed with Slo1 which encodes a Ca^+-dependent K^+ current. Due to this observation, combined with similar sequence at the pore domain and C-terminus of the Slo1 Ca^+-activated K^+ (BK) channel, it was given the name *Slack*, for "Sequence Like A Ca^{2+} activated K^+ channel"[271]. Then, in 2003, researchers realized that when expressed without Slo1, Slack was regulated by internal Na^+, not by Ca^{2+} (Fig. 1.3.A)[272]. This Na^+-dependent current has been described in multiple organisms, including *Xenopus* spinal neurons, *C. elegans*, lamprey, *Drosophila*, and rat[266,269,272–274]. It has also been identified in non-neuronal cells such as the kidney[275]. Two mammalian genes have since been identified that encode K_{Na} channels, *Slack* and *Slick*; their human orthologs are termed *KCNT1* and *KCNT2*, respectively. For purposes of clarity, a new nomenclature has been proposed for K_{Na} channels, as their identification in multiple species has led to different names for the same genes[276]. Following this guidance, I will use the terminology *K_{Na}1.1* (*Slack/KCNT1*) and *K_{Na}1.2* (*Slick/KCNT2*) when referring to specific mammalian channels for the rest of this dissertation.

K_{Na} channels are tetrameric 6-transmembrane domain K^+ channels with a large C-terminal domain containing multiple regulatory sites (Fig. 1.3.B)[271,277–281]. Two main regions of regulation within the C-terminus have been identified as the Regulators of Conductance of K^+ (RCK) domains[272]. Later, a Na^+-

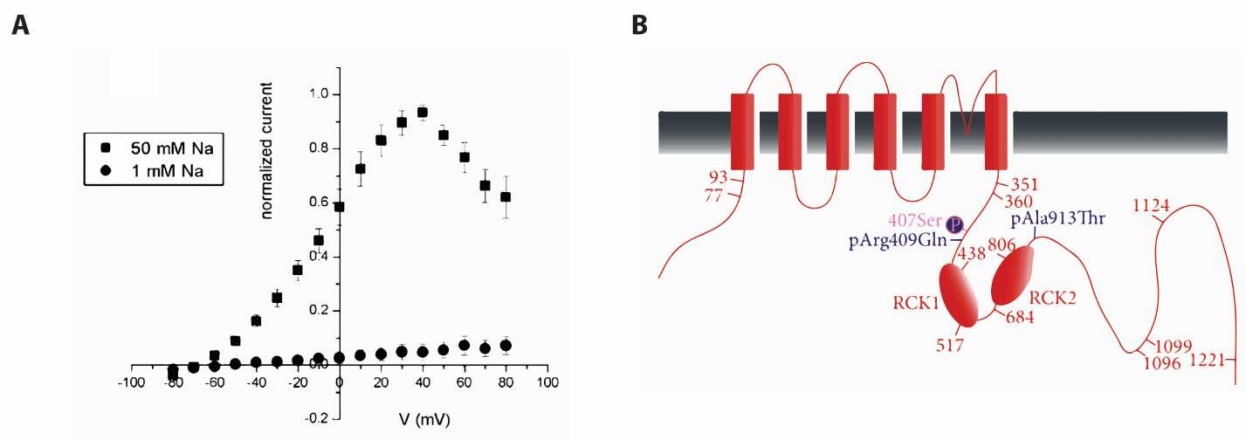

Figure 1.3: K_{Na} channels are activated by internal Na^+. A) Rat $K_{Na}1.1$ expressed in *Xenopus* oocytes is activated by internal Na^+. Modified from Yuan et al. 2003. B) K_{Na} subunit showing the two Regulators of Conductance of K^+ (RCK) domains. Also identified are important regulatory regions. Modified from Kaczmarek 2013.

coordination sequence found within some inwardly-rectifying K^+ channels[282], was identified in the RCK2 domain of $K_{Na}1.1$ channels, and further shown to convey Na^+-sensitivity[279]. K_{Na} channels display large unitary conductance, multiple subconductance states, and inward rectification at positive membrane potentials above +30mV[267,283]. K_{Na} channels also show weak voltage-sensitivity[284]. However, what conveys voltage-sensitivity is unclear as K_{Na} channels lack the pattern of positively charged residues within the S4 domain[284].

1.6.2 K_{Na} channel expression

$K_{Na}1.1$ and $K_{Na}1.2$ expression patterns have been observed throughout the CNS and in non-neuronal cell types in mammals. *$K_{Na}1.1$* and *$K_{Na}1.2$* transcript has been observed in the brain, kidney, testis, and heart of mice and rat[271,272]. Additionally, *$K_{Na}1.2$* transcript was found in mouse skeletal muscle, lung, and liver[272]. Upon RT-PCR inspection, *$K_{Na}1.2$* was shown to be more prominently expressed in the heart than *$K_{Na}1.1$*[285]. Within the brain, *$K_{Na}1.1$* and *$K_{Na}1.2$* are widely expressed. Initial *in situ* hybridization and immunohistochemistry experiments revealed expression in all brain regions tested[286,287]. Broadly, both are expressed in sensory circuits of rat CNS, such as olfactory bulb, auditory brainstem, and visual and somatosensory regions of the cerebral cortex[286–289]. Additionally, both were found in regions CA1, CA2,

CA3, and the Dentate Gyrus of the mouse hippocampus, cerebellum, hypothalamus, thalamus, brainstem, and amygdala[289]. Immunoreactivity of $K_{Na}1.1$ and $K_{Na}1.2$ confirmed expression of both in DRG neurons of mice and rat[278,290,291]. Subcellular examination revealed $K_{Na}1.1$ and $K_{Na}1.2$ channels are localized to the soma and central terminals of IB4+ small diameter nonpeptidergic nociceptors of the DRG[278,291], and in CGRP+ small and medium-sized DRG neurons, respectively[290]. Within DRG neurons, *$K_{Na}1.1$* transcript was found to be significantly higher than *$K_{Na}1.2$*[285]. These expression patterns of K_{Na} channels suggest a role in modulating external stimuli signaling.

Subcellular localization of K_{Na} channels seems to be specific to the cell type. For example, $K_{Na}1.2$ immunoreactivity was found in the somata of medial nucleus of the trapezoid body (MNTB), the globular bushy cell cross fibers, and dendritic region of hippocampal pyramidal cells[287]. Additionally, $K_{Na}1.1$ immunoreactivity was found in the somata of the mitral cell layer, the dendritic rich region of the plexiform layer, and axonal tracks of DRG neurons[286]. In addition to the immunoreactivity assays, a Na^+-dependent K^+ current was found to be localized to the axonal tracts of *Xenopus*[292]. As for dendritic localization, this is likely due to the putative PDZ binding motif found on the C-terminus that was further shown to bind to PSD-95[293]. Therefore, K_{Na} channels could function in different roles in different neurons depending on its subcellular localization.

1.6.3 K_{Na} channel activation

Studies have reported mixed levels of Na^+ needed to activate K_{Na} channels. Initial electrophysiological experiments showed that the Na^+-dependent K^+ current required levels of Na^+ to be significantly higher (20-180mM) than predicted physiological levels (4-15mM)[260,262,264,267,294]. Following cloning of the channel, similarly high levels of Na^+ (50mM) were required to activate $K_{Na}1.1$ channels in inside-out macropatches from *Xenopus* oocytes expressing rat $K_{Na}1.1$[272]. They did notice that increasing intracellular Cl^- levels well above the physiological range brought the Na^+-sensitivity of $K_{Na}1.1$ channels closer to physiological levels (20mM). With these combined results, researchers concluded that $K_{Na}1.1$ channels must only be active during extreme depolarization when intracellular Na^+ and Cl^- levels increase

substantially, such as hypoxic conditions. More recent evidence suggests K_{Na} channels can be activated by physiological levels of Na^+ when other factors are present. Following the Cl^- sensitivity data, the Jan lab has shown that a Ca^{2+}-activated Cl^- channel, TMEM16C, enhances $K_{Na}1.1$ Na^+-sensitivity when coexpressed in HEK293 cells[295]. Another group has shown that nicotinamide adenine dinucleotide (NAD+), when added to the intracellular side of DRG neurons, brought Na^+-sensitivity of $K_{Na}1.1$ channels to physiologically relevant levels[278]. The current state of the field suggests that K_{Na} channels likely act in both situations of extreme depolarization and in normal physiological functioning of excitable cells, although its role in either has not been clearly defined.

Other neuromodulators have also been shown to alter the activity of K_{Na} channels. It was initially shown in the Salkoff lab that $K_{Na}1.1$ and $K_{Na}1.2$ are alternatively regulated by protein kinase C (PKC) activity. They found that PKC inhibits $K_{Na}1.2$ channel currents while increasing $K_{Na}1.1$ channel currents expressed in *Xenopus* oocytes[281]. This was further expanded on by Nanou and Manira 2010[296], when they found that mGluR1 activity modulates AMPA-induced K_{Na} current in a Ca^{2+} and PKC dependent manner in lamprey spinal cord neurons. Additionally, protein kinase A (PKA) activity has been shown to inhibit $K_{Na}1.1$ channel activity in DRG neurons by internal trafficking of the channel from the plasma membrane[280]. Other regulatory elements that are altered during excessive neuronal activity have been shown to differentially regulate $K_{Na}1.1$ and $K_{Na}1.2$. For instance, there is a consensus ATP binding site found in the C-terminus of $K_{Na}1.2$ that is absent in $K_{Na}1.1$ and ATP was shown to inhibit $K_{Na}1.2$ activity[297]. Additionally, $K_{Na}1.2$ channels were shown to be activated and inhibited by cell volume increases and decreases, respectively[298]. This regulation was not seen in $K_{Na}1.1$ channels. The vast amount of options for regulating K_{Na} channel function suggest a variety of roles in different neuronal subtypes.

In addition to regulation of K_{Na} channels by many different neuromodulators, multiple sources of Na^+ have been shown to activate the channels. These sources include AMPA receptors, H-channels, and CNG channels[299–301]. Of particular interest for this dissertation, the Salkoff lab has provided evidence that a TTX-sensitive I_{NaP} activates $K_{Na}1.1$ channels[302,303]. They initially found that a TTX-sensitive and Na^+-

sensitive K^+ current exists in dissociated tufted/mitral cells, medium spiny neurons, and cortical pyramidal cells of the rat. This K_{Na} current was greatly diminished by the application of small interfering RNA (siRNA) directed against *$K_{Na}1.1$*. Furthermore, Riluzole, a blocker of the I_{NaP}, removed the Na^+-sensitive K^+ current (Fig. 1.4.A)[302]. This paper was the first to suggest that K_{Na} currents are activated by I_{NaP}. In a second paper, they greatly expanded upon their earlier findings. In this case, they found that a Na^+-sensitive K^+ current was not dependent on I_{NaT}. Using an outside-out patch clamp configuration, they found the K_{Na} channel opening depended upon extracellular Na^+ influx, and that this opening probability was blocked by either TTX or by substituting Na^+ with Li^+[303]. Additionally, they showed that application of Veratridine, which enhances the I_{NaP}, increased the open probability of K_{Na} channels (Fig. 1.4.B)[303]. A third and most recent paper suggests that $GABA_B$ receptor activation inhibits the I_{NaP} which leads to a decrease in the K_{Na} current[304]. Combined, these papers strongly suggest that K_{Na} channels are activated by I_{NaP} through voltage-gated Na^+ channels. My research in this dissertation expands on this finding and suggests that K_{Na} channels protect against increased I_{NaP} that causes seizure-like behavior in *Drosophila*.

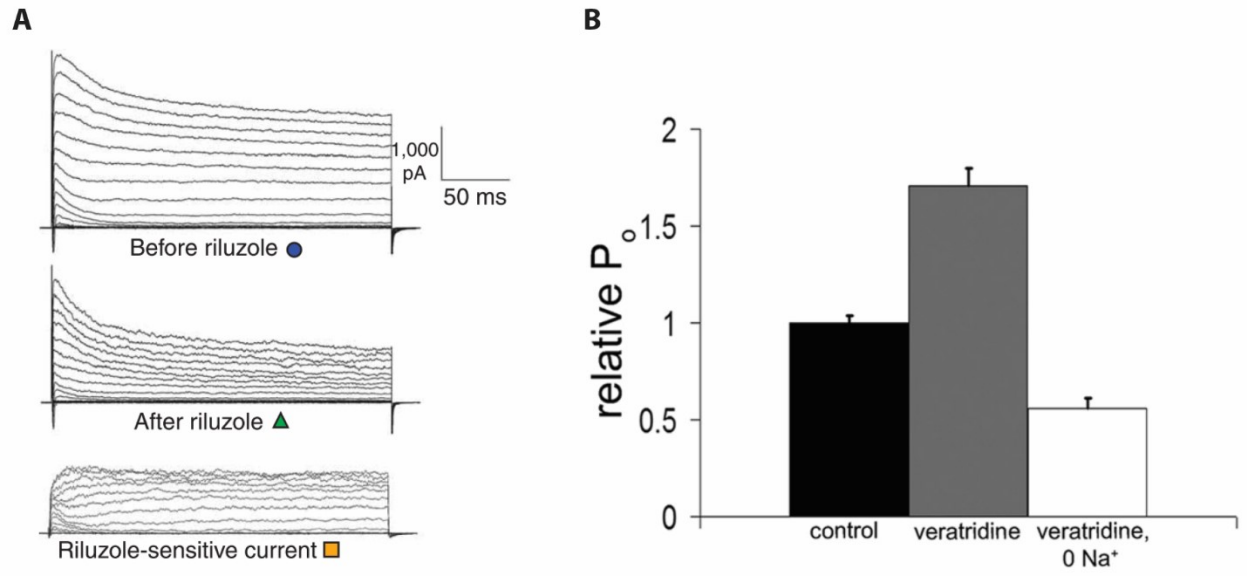

Figure 1.4: K_{Na} current activated by I_{NaP}. A) Riluzole was used to block I_{NaP} (middle). The measured Riluzole-sensitive K^+ current (bottom) shows a K^+ current that was present due to I_{NaP}. (Adapted from Budelli et al. 2008). B) Relative opening probability of K_{Na} channels was increased by Veratridine in the outside-out patch clamp configuration. (Adapted from Hage and Salkoff 2012).

1.6.4 Physiological roles of K_{Na} channels

It has been suggested that K_{Na} channels can regulate multiple aspects of cell excitability and action potential (AP) firing. Some of the earlier electrophysiological data suggest that K_{Na} channels contribute to the resting membrane potential of chick brain stem and quail trigeminal nerve ganglion cultures[262,268]. Additional electrophysiological data using peripheral myelinated axons of *Xenopus laevis* showed a K_{Na} current specific to the Nodes of Ranvier[292]. This location led the authors to hypothesize that these K_{Na} channels could be active under a single AP or upon a train of APs. Following this idea, multiple groups have found K_{Na} channels to modulate AP dynamics in a cell-specific manner. Evidence in mouse DRG neurons suggests that $K_{Na}1.1$ and $K_{Na}1.2$ channels play a role in increasing the rheobase, which is the minimum amount of injected current required to induce an AP. This suggests that both K_{Na} channels are acting to delay AP initiation[285,290]. Upon deletion of *$K_{Na}1.1$* and *$K_{Na}1.2$*, these DRG neurons exhibited an increased AP firing rate. In contrast, early electrophysiological data suggest a Na^+-dependent K^+ current might alter the repolarization phase of the AP[261,262,264]. Expanding on this, researchers found that upon application of fragile X mental retardation protein (FMRP), K_{Na} channels accelerated repolarization of bag cells neurons of *Aplysia*. This was confirmed by knocking down the channel using *$K_{Na}1.1$* siRNA[305]. In addition to affecting the initiation and repolarization phases, K_{Na} channels have also been implicated in affecting the AHP, thereby regulating firing frequency and bursting patterns of neurons. Using pharmacological and Na^+ substitution assays, a role of the Na^+-dependent K^+ current affecting the AHP has been observed in auditory neurons of the MNTB[306], neocortical intrinsically bursting neurons[307], and larval lamprey spinal cord neurons[308]. Important to note, most of these studies separated the Na^+-activated K^+ current using pharmacological methods, some of which, such as N-methyl-d-glucamine (NMDG) and choline substitution, have recently been called into question[309]. Nonetheless, the combined data suggest that K_{Na} channels have a diverse and cell specific role in regulating cell excitability.

Based on K_{Na} channel expression in the DRG neurons, it was postulated that they may regulate pain processing. Indeed, recent studies found that knock-out of both *$K_{Na}1.1$* and *$K_{Na}1.2$* is sufficient to increase AP firing rates in small diameter DRG neurons by decreasing rheobase, which was associated with

enhanced sensitivity to pruritic stimuli[285]. Another group, using spared nerve injury and paclitaxel induced hypersensitivity models of neuropathic pain, found that mice with *$K_{Na}1.1$* conditionally knocked out in $Na_V1.8$-sensory neurons displayed enhanced sensitivity to mechanical stimuli[291]. Furthermore, Evely et al. 2017[310] found that deletion of *$K_{Na}1.1$* increased presynaptic release from primary afferents which coincided with enhanced nociceptive responsiveness to thermal stimuli. A third group recently showed that knock-out of *$K_{Na}1.2$* is sufficient to cause increased heat sensitivity and exacerbated thermal hyperalgesia[290]. Combined, these studies suggest K_{Na} channels act at the level of the primary nociceptors to dampen painful stimuli signaling.

Following the expression patterns of K_{Na} channels in sensory regions of the brain, it has also been postulated that they are responsible for modulating other sensory input. More specifically, expression of both $K_{Na}1.1$ and $K_{Na}1.2$ in the olfactory bulb and medial nucleus of the trapezoid body suggests they modulate olfaction and auditory stimuli, respectively. The potential to alter olfactory input has been examined *in vitro* using electrophysiological methods to uncover the Na^+-activated K^+ current in mitral cells[267,300,302,303]. To our knowledge no studies have examined whether K_{Na} channels affect olfactory behavior. In the auditory system, neurons of the MNTB have similarly been examined *in vitro* to elucidate the role of K_{Na} channels in this system. In this case, it was found that K_{Na} currents affect the AHP of the AP; additionally, that increased activity of K_{Na} current enhanced the fidelity of timing at high frequency stimulations[306]. Expanding on these studies, a group recently identified both *$K_{Na}1.1$* and *$K_{Na}1.2$* expression in the primary auditory neurons (spiral ganglion neurons (SGNs)). Using a double knock-out (DKO) line of both *$K_{Na}1.1$* and *$K_{Na}1.2$*, they identified that the amplitude of auditory brainstem suprathreshold responses were reduced in the DKO line. This corresponded with reduced action potential thresholds and amplitudes in excised SGNs[311]. These data further suggest that K_{Na} channels alter incoming sensory information, in this case in the auditory system.

Based on expression data of both K_{Na} channels throughout the hippocampus, groups have suggested that K_{Na} channels may regulate learning and memory. Indeed, recent studies have suggested that humans

with mutated *KCNT1*, which usually cause a gain-of-function, show signs of intellectual disability (ID)[312–315]. However, these individuals also show comorbidity with different forms of early-onset epilepsy (see Section 1.6.5), making the actual cause of the ID unclear. A few groups have looked at learning and memory impairment in mouse knock-out models of $K_{Na}1.1$. The initial report found that $K_{Na}1.1$ knock-out mice showed normal working memory and motor functions, however, they differed in reversal learning abilities[316]. Reversal learning refers to the ability to forget a learned association to learn a new one. In this case, this was measured in the Morris water maze, in which the platform's location was moved following initial acquisition trials. After moving the platform, $K_{Na}1.1$ knock-out mice showed an increase in latency to reach the new platform. The authors postulate that this may be the result of an inability to depotentiate after learning a specific task. However, these behavioral results were mild. Additionally, this mouse model still left $K_{Na}1.2$ intact, which could compensate in the absence of $K_{Na}1.1$. More recently, Quraishi et al. 2020[317] further examined the role of $K_{Na}1.1$ in spatial and motor learning. These researchers found that $K_{Na}1.1$-deficient mice responded similarly to wild type mice in the spatial learning test, but they exhibited impaired motor learning in an accelerating rotarod test. However, $K_{Na}1.1$ knock-out mice also showed decreased locomotor activity and exploratory behavior in an open field test. Together, these results suggest that the absence of $K_{Na}1.1$ alone does not alter essential learning and memory function in mice.

1.6.5 Epileptogenic mutations in K_{Na} channels

Advances in whole genome sequencing have allowed for rapid identification of novel mutations associated with many different diseases. A few recent studies have identified mutations in *KCNT1* and *KCNT2* in individuals with different forms of epilepsy[312,313,318–321]. Pathologies linked to these mutations include malignant migrating partial seizures of infancy (MMPSI), autosomal dominant nocturnal frontal lobe epilepsy (ADNFLE), Ohtahara syndrome, sudden unexplained death in epilepsy (SUDEP), multifocal epilepsy, leukoencephalopathy and Brugada syndrome. Some of these mutations, found in individuals with MMPSI and ADNFLE, have been recapitulated in rat $K_{Na}1.1$ constructs and injected into *Xenopus* oocytes[322–324]. Electrophysiological recordings from these oocytes revealed a gain-of-function (GOF)

mutation in these channels due to increased Na^+-sensitivity[324]. The sites of these mutations are associated with regulatory regions that function as PKC phosphorylation sites as well as NAD+ binding sites[278,322]. Additional studies have identified increased positive cooperativity between mutant $K_{Na}1.1$ channels which leads to enhanced K^+ current[325]. These findings are surprising as an increase in K^+ current would be expected to decrease activity. A few recent studies have attempted to address this. One study found that induced pluripotent stem cell (iPSC)-derived neurons expressing the MMPSI-associated KCNT1 P924L mutation showed increased K_{Na} current. This current shortened the AP duration and increased the amplitude of the AHP. Surprisingly, the number of action potentials and maximal firing rates were increased in these neurons, suggesting an overall increase in activity[326]. Additionally, this group generated a mouse containing the R455H mutation in $K_{Na}1.1$, which was found in humans with epilepsy of infancy with migrating focal seizures (EIMFS). These mice showed spontaneous interictal epileptiform discharges measured by EEG and a decreased threshold for pentylenetetrazole (PTZ)-induced seizures[317]. Combined, these papers suggest a mechanism by which enhanced K_{Na} current could lead to increased excitability and epilepsy.

1.6.6 Role of K_{Na} channels in overexcitation

For a few reasons, K_{Na} channels have been suggested to play a neuroprotective role against overexcitation. First, initial experiments suggested that K_{Na} channels were likely to only function during situations of extreme depolarization due to higher than physiological levels of Na^+ required to activate the channel[260,262,264,267,272]. Additionally, Cl^- levels also increase the activity of K_{Na} channels[272,284,297], which are elevated in times of extreme depolarization, such as hypoxia. Second, expression of K_{Na} channels in auditory neurons has been suggested to be protective due to very high rates of energy utilization and AP firing[327,328]. Third, it has been shown that K_{Na} channels are coupled to AMPA receptor activation, and influence the AMPA-mediated current and amplitude of synaptic potential[329]. Combined, these data strongly suggest that K_{Na} channels could protect neurons against situations of extreme depolarization. However, we are only aware of three studies that attempt to address this role at the organismal level.

Two of these studies have examined the role of *slo-2*, the C. *elegans* orthologue of *K_{Na}1.1*, in hypoxia. Importantly, *slo-2* channels are activated by Ca^{2+} and not Na^{+}, as Ca^{2+} is the main ion that depolarizes neurons in C. *elegans*. In these experiments, nematodes were subjected to 0.1% O_2 levels for 16 hours, and subsequently survival rates were measured. Following treatment, the initial study found that *slo-2* knock-out mutants were susceptible to hypoxia-induced death[272]. However, another study similarly treated the same *slo-2* knock-out mutants and found they were resistant to hypoxia[330]. In addition to these studies, a recent study subjected *K_{Na}1.1*-deficient mice to electric shock and chemically induced seizure assays. These mice showed a slight decrease in threshold stimulus to induce hindlimb extension seizures and no significant increase in PTZ-induced seizures[317]. However, this study did not account for potential compensation by K_{Na}1.2, which is highly expressed in most brain regions in which K_{Na}1.1 is expressed[285,289]. What has yet to be addressed is whether or not K_{Na} channels can protect against overexcitation caused by increased Na^{+} influx. A major portion of my dissertation investigates the ability of K_{Na} channels to protect against seizure-like behavior in *Drosophila* epilepsy models.

1.7 Overview of this dissertation

This dissertation focuses on the ability of K_{Na} channels to protect against overexcitation. It expands upon previous hypotheses that these channels play a role under extreme depolarization, such as those found in pathological conditions. Additionally, it furthers research suggesting that K_{Na} channels are activated by I_{NaP}. My research suggests that K_{Na} channels protect against seizure-like behavior caused by increases in I_{NaP}. Results from these studies lay the groundwork that K_{Na} channels may be a therapeutic target in certain pathologies associated with hyperexcitability, and more specifically pathologies caused by increased I_{NaP}.

Chapter 3: In this chapter, I characterize expression of the *Drosophila* K_{Na} channel, dSlo2. To accomplish this, I generated multiple *Drosophila* lines that report expression of dSlo2. I found that dSlo2 is expressed in many different regions throughout the *Drosophila* CNS. This includes primary sensory organs in the fly. I additionally found that dSlo2 is expressed in cholinergic neurons and not in GABAergic neurons.

Furthermore, dSlo2 channels are localized to the axonal region of some neurons. Interestingly, dSlo2 expression was also found in a subset of glia important for regulation of the *Drosophila* blood-brain barrier.

Chapter 4: In this chapter, I test that hypothesis that dSlo2 protects against global overexcitation induced by a cholinergic agonist. I found that dSlo2 protects flies both through development and as adults to toxic levels of exposure to a specific cholinergic agonist, Imidacloprid. I also found that dSlo2 protects against hyperexcitable behavioral phenotypes induced by Imidacloprid exposure. Furthermore, dSlo2 could be preventing against overexcitation in neurons that are activated by Imidacloprid.

Chapter 5: In this chapter, I test the hypothesis that dSlo2 protects against overexcitation induced by increases in I_{NaP}. I found that in the absence of *dSlo2*, multiple *Drosophila* models of epilepsy show exacerbated seizure-like behavior. I further found that pharmacological increases of I_{NaP}, induced by Veratridine feeding, leads to exacerbated seizure-like behavior in *dSlo2*-deficient flies. Last, I found that flies which have an increased I_{NaP} display spontaneous seizure-like behavior only in the absence of *dSlo2*.

CHAPTER 2. MATERIALS AND METHODS

2.1 *Drosophila* strains

w1118 (Bloomington *Drosophila* Stock Center) were used as the wild-type (WT) flies. To test the role of dSlo2, *dSlo2-* (described below) flies were used. We used the following lines to examine seizure-like behavior in *Drosophila*: *GEFS+*[116], *DS*[117] (gift from Dr. Diane O'Dowd, University of California, Irvine), *bang-senseless* (*bss*[1]) originally denoted (*bas*^{MW1})[331], *slamdance* (*sda*$^{iso7.8}$)[203], *easily-shocked* (*eas*^{PC80})[194] (gifts from Dr. Mark Tanouye, University of California, Berkeley). The following were used to examine neurons in the PNS: *ppk-TdTom*, *ppk-Gal4* (gifts from Dr. Daniel Tracey, Indiana University). *ΔMdr65* (#14547, Bloomington Stock Center) was used to examine susceptibility to insecticide exposure. We used the following Gal4 lines to drive tissue-specific expression of genes under the control of the *Upstream Activating Sequence* (*UAS*): *elav-Gal4*, *ChAT-Gal4*, *201y-Gal4*, *30y-Gal4* (Bloomington *Drosophila* Stock Center), *nAchRα1*^{Mi00453}*-Gal4* (#66780, Bloomington *Drosophila* Stock Center). We used the following lines to drive expression of genes under the control of *LexA-op*: *dSlo2*^{Mi13397}*-LexA* (described below), *ChAT*^{Mi04508}*-LexA*, *GAD*^{Mi09277}*-LexA*, *VGlut*^{Mi04979}*-LexA* (gifts from Dr. Ben White[332], NIH), *R54C07-LexA* (Subperineural Glia) (#61562, Bloomington *Drosophila* Stock Center), *R85G01-LexA* (#54285, Bloomington *Drosophila* Stock Center). We used the following lines to label specific cells expressing either Gal4 or LexA: *LexAop-TdTom-nls* (gifts from Dr. Ben White, NIH), *UAS-CD8-GFP* (Bloomington *Drosophila* Stock Center). We used the following lines for the generation of the Trojan *dSlo2*^{Mi13397}*-Gal4* line (see below): *yw,UAS-2xEYFP;sp/CyO;Dr/TM3*, *yw;sp/CyO;pC(lox2-attB2-SA-T2A-Gal4-Hsp70)3*, *yw,{y+,hs-Cre},{vas-ΦC31};+;+* (gifts from Dr. Ben White, NIH), *yw;Mi13397;+* (#59336, Bloomington *Drosophila* Stock Center). We used the following lines for tissue-specific expression of wild-type, dominant-negative, or RNAi *dSlo2*: *UAS-dSlo2*, *UAS-dSlo2-DN* (both described below), *UAS-RNAi-dSlo2* (#10268, Vienna *Drosophila* Resource Center). We used a line in which

endogenous *dSlo2* was tagged with *myc* (*dSlo2-myc*, described below) to examine endogenous expression of dSlo2 protein.

2.2 Generation of *Drosophila* strains

2.2.1 *dSlo2* null mutant

CRISPR-cas9 techniques were employed to generate a null mutant of *dSlo2*[333,334]. We decided to target the sequence coding for the pore region of the channel instead of predicted start sites because the four predicted start sites span a range of ~73 kb. To target the pore region, the sequence spanning the S5-S6 transmembrane was inserted into the online tool: http://tools.flycrispr.molbio.wisc.edu/targetFinder. This tool identified multiple options for gRNA targets upstream and downstream of the *dSlo2* pore region. An upstream and downstream target were chosen based on the predicted specificity of the gRNA by the online tool. Primers were generated that code for the gRNA that would target the upstream (Fwd: 5'- CCT CGT GCT GGA TAC CAC AAA CGC -3', Rev: 5'- AAA CGC GTT TGT GGT ATC CAG CAC -3') and downstream (Fwd: 5'- CTT CGA TGA CCA TAT AAA GCT GCG -3', Rev: 5'-AAA CGC CAG CTT TAT ATG GTC ATC -3') targets flanking the *dSlo2* pore region. These were ordered from Integrated DNA Technologies. In addition to the gRNA sequences, these primers contained BbsI restriction ligation sites on the 5' and 3' ends, underlined above. Primers were separately annealed, phosphorylated, and ligated into previously digested pU6-BbsI-gRNA vectors. This generated two vectors that drive expression of gRNA specific for upstream and downstream sequences of the *dSlo2* pore region. In addition to the gRNA sequences, a donor plasmid was generated to allow for homology directed repair (HDR) following the double-stranded breaks (DSBs) generated by the cas9 protein in conjunction with the gRNA. To develop the donor plasmid, homologous regions flanking the gRNA target sequences were generated using PCR. The following primers were designed for generation of the Left Homologous Arm (LHA) (Fwd: 5'- TAC TCA CCT GCT ACT TCG CCA CTC AAC TGA CCC AAA TTC -3', Rev: 5'- TAC TCA CCT GCT ACT CTA CCG CTG GGG ATA AAT AAA AAA -3') and Right Homologous Arm (RHA) (Fwd: 5'- TAC TGC TCT TCA TAT AGC TTT ATA TGG TCA TCA TG -3', Rev: 5'- TAC TGC TCT TCA GAC

ATT ATT GGG CGG GTC CCA GA -3'). Genomic DNA was collected using standard phenol chloroform extraction followed by isopropanol precipitation. PCR using the LHA primers and RHA primers generated two separate products. Initially, the LHA product was digested with AarI (restriction site underlined above) and ligated into the AarI site in the pHD-DSRed-attp vector. Following successful ligation of LHA, the RHA was digested with SapI (restriction site underlined above) and ligated into the SapI site in the pHD-LHA-DSRed-attp, thereby generating the complete donor vector pHD-LHA-DSRed-RHA-attp. The gRNA plasmids, along with the donor vector, were sent to Rainbow Transgenic Flies Inc. for injection into a *Drosophila* line that expresses cas9 under the control of the *vas* promoter (#51323, Bloomington *Drosophila* Stock Center). Injected larvae were received, separated, and crossed to *w1118* lines containing balancer chromosomes to prevent recombination. Successful integration of the donor plasmid was screened for using a fluorescent stereoscope screening for DSRed expression in the eye. Fluorescent flies were backcrossed to offspring and homozygous mutant lines were isolated. *dSlo2* null lines were verified using RT-PCR and DNA sequencing.

2.2.2 Generation of *UAS-dSlo2* transgenic lines

Generating lines that allow for tissue specific expression of *dSlo2* would be advantageous to allow for rescue of phenotypes in the null background as well as overexpression. To accomplish this, *dSlo2* was placed under the control of the *UAS* to allow for Gal4 driven expression of *dSlo2*. First, *dSlo2* cDNA was generously donated by the Salkoff lab[274]. *dSlo2* cDNA was digested from the pOX-dSlo2 vector using KpnI and XhoI sites and ligated into the pENTR1A vector by Genewiz LLC. Additionally, mutagenesis was performed to insert a start codon at the 5' end of *dSlo2*. To then allow for P-element insertion of *dSlo2* under the control of *UAS*, the pENTR1A-dSlo2 vector was recombined with the pTW vector using the Gateway Cloning LR recombination technology. This placed *dSlo2* under the control of *UAS* flanked by P-feet, which allow for P-element mediated recombination into the *Drosophila* genome. Successful recombination of pENTR1A-dSlo2 with pTW was confirmed using restriction digestion in combination with DNA sequencing. Upon confirmation, pTW-dSlo2 was amplified using the Qiagen Maxiprep kit.

Subsequently, this plasmid was injected into *Drosophila* embryos by Rainbow Transgenic Flies, Inc. Injected larvae were received, and crossed individually to *w1118* flies containing balancer chromosomes to prevent recombination. Offspring were screened for w+ eyes, confirming insertion of the P-element. Positive lines were then crossed to *elav-Gal4* lines, and overexpression was confirmed using RT-PCR.

2.2.3 Generation of *UAS-dSlo2-DN* transgenic lines

To block dSlo2 conductance in specific tissues, I generated transgenic lines expressing a dominant-negative (DN) form of *dSlo2*. The pore forming amino acid sequence of K^+ channels is well conserved, containing either glycine-tryptophan-glycine (GWG) or glycine-tyrosine-glycine (GYG) residues. It has previously been shown that mutation of the hydrophobic tryptophan or tyrosine amino acid to a phenylalanine[335–337] or alanine[338] prevents K^+ conductance. Importantly, when this DN subunit was expressed in a wild-type background it completely blocked K^+ conductance[337,338]. This suggests that tetramerization of a DN subunit with a functional subunit will block K^+ conductance. To generate a *dSlo2-DN* construct, a *dSlo2* cDNA sequence was generated by Genewiz Inc. in which sequence encoding the pore was mutated from a glycine-tyrosine-glycine (5'-GGA TAC GGC-3') to alanine-alanine-alanine (5'-GCC GCC GCC-3') (GYG>AAA). This sequence was then digested using DpnIII and ScaI and ligated into the digested pENTR1A vector. Successful ligation was confirmed using DNA sequencing. Following ligation, pENTR1A-dSlo2-DN was recombined to the pTW vector using the Gateway Technology LR Recombination technology. Successful recombination was confirmed using restriction digest. pTW-dSlo2-DN was then sent to Rainbow Transgenic Flies, Inc. for injection into embryos. Injected larvae were received, crossed to *w1118* flies containing balancer chromosomes to prevent recombination, and offspring screened for w+ eyes. Successful insertion lines were isolated, and Gal4 driven expression of *dSlo2-DN* was confirmed using RT-PCR.

2.2.4 Generation of *dSlo2* reporter lines

dSlo2-T2A-Gal4 line

Initially, the minos-mediated integration cassette (MiMIC)[339,340] line *Mi13397* was identified as a potential target for Trojan-mediated expression of Gal4 (*T2A-Gal4*) under the control of the endogenous *dSlo2* promoter region. *Mi13397* is located in a 5' intronic region of all predicted splice forms of *dSlo2*. Integration of the *T2A-Gal4* cassette into the *Mi13397* location is predicted to terminate translation of *dSlo2* and instead translate *Gal4*[341]. As the phase of the MiMIC insertion was unknown, the *in vivo* method of *T2A-Gal4* insertion was used[332]. This method entails transient crosses of flies to genetically introduce to necessary components to replace the *Mi13397* insertion with the *T2A-Gal4* cassette. Initially, transgenic flies containing all 3 phases of the *T2A-Gal4*, flanked by attB sites as well as loxP sites, were crossed to the *Mi13397* line (Fig. 2.1, Cross 1). Progeny were crossed to a line expressing Cre as well as ΦC31-Integrase

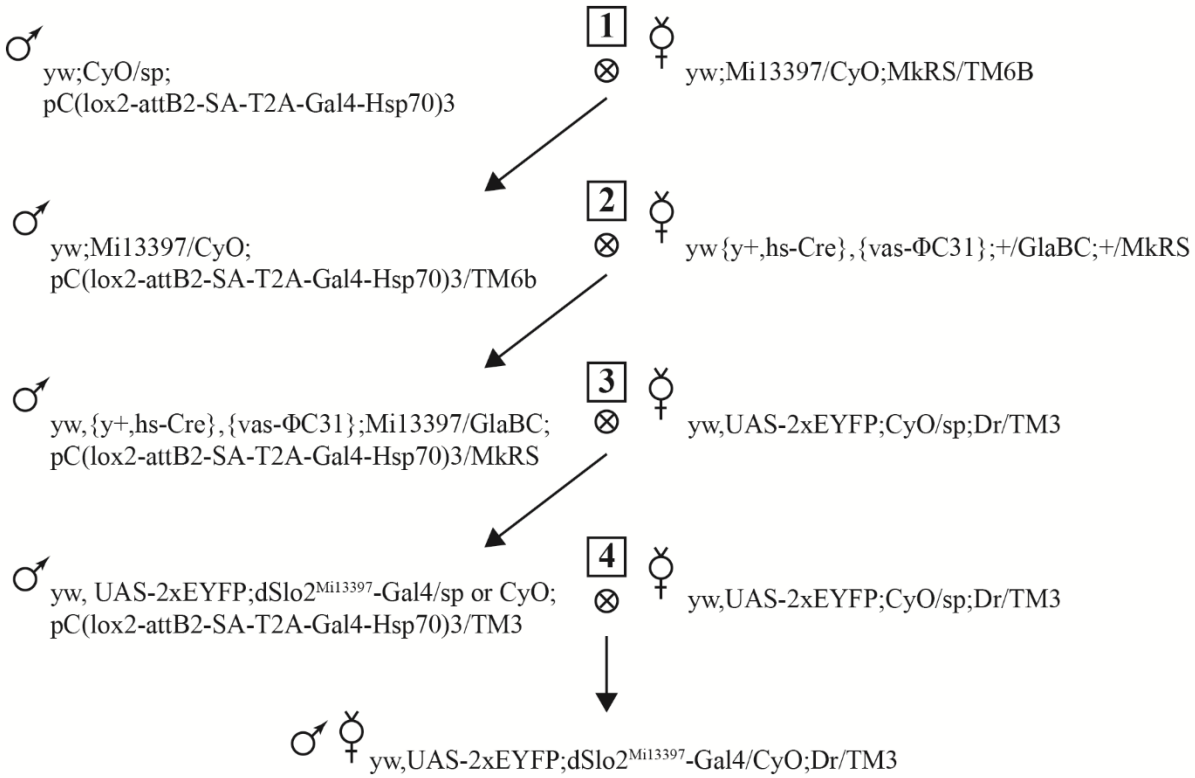

Figure 2.1: Crossing strategy to generate the *dSlo2^{Mi13397}-Gal4* line. Cross 1, took place in 5-7 bottles. CyO, non-sp, TM6B males were collected. Cross 2, took place in 5-7 bottles. GlaBC, MkRS males were collected. Cross 3, individual males from cross 2 were crossed with 3-5 females. A total of 162 crosses were set up. Yellow, sp or CyO males were collected. 59 total males were collected that were Yellow. Of these, 13 males were positive for EYFP. Cross 4, EYFP-positive individual males were crossed to 5 females. From these 13 crosses, 6 were viable, thereby generating 6 *yw,UAS-2xEYFP;dSlo2^{Mi13397}-Gal4/CyO;Dr/TM3* lines.

(Fig. 2.1, Cross 2). In these progeny, it is expected that Cre will excise the floxed *T2A-Gal4* signal. Additionally, the ΦC31-Integrase is expected to mediate recombination of *T2A-Gal4* into the MiMIC site using attB-guided recombination. In theory, offspring from these lines will contain *T2A-Gal4* insertions in one of three phases, only one of which will translate *Gal4* in-frame. Therefore, these progeny were crossed to transgenic *UAS-EYFP* lines (Fig. 2.1, Cross 3), and screened for EYFP using fluorescent microscopy. Successful insertions in the correct phase caused EYFP fluorescence. EYFP positive progeny were backcrossed to build and maintain a stable stock (Fig. 2.1, Cross 4), hereto referred to as *dSlo2*^{Mi13397}*-Gal4*. Successful insertions were further verified by DNA sequencing.

***dSlo2-T2A-LexA* line**

Due to the successful insertion of the *T2A-Gal4* insertion into the *Mi13397* site, we decided that the *Mi13397* site should similarly be used for insertion of the *T2A-LexA* cassette. Insertion of the *T2A-LexA* cassette into *Mi13397* is predicted to efficiently terminate translation of *dSlo2* and instead translate *LexA*[332,341]. To allow for proper translation of *LexA*, the correct phase of the Trojan insertion was predicted using the online tool from the Bellen lab (http://flypush.imgen.bcm.tmc.edu/pscreen/mimic.html) and found to be phase 2. Confirmation of the phase 2 insertion was further performed by sequencing of the successful *dSlo2*^{Mi13397}*-Gal4* insertion (see above). To replace the *Mi13397* insertion with *T2A-LexA*, the plasmid pBS-KS-attB2-SA(2)-T2A-LexA:QFAD-Hsp70 was kindly provided by Dr. Ben White[332]. This plasmid was transformed into DH5α E.coli strain, and amplified using Qiagen Maxiprep kit followed by isopropanol and sodium acetate precipitation. Microinjection of pBS-KS-attB2-SA(2)-T2A-LexA;QFAD-Hsp70 along with a ΦC31 integrase plasmid into *Mi13397* embryos was performed by Rainbow Transgenic Flies, Inc. Individual injected flies were crossed to *LexAop-TdTom-nls* flies and progeny were screened by TdTom fluorescence in the fly. Successful insertions were identified by TdTom fluorescence and backcrossed to fluorescent progeny from the same adult to build a stable stock, hereto referred to as *dSlo2*^{Mi13397}*-LexA*.

2.2.5 *dSlo2-myc* line

To determine the subcellular localization of dSlo2, I inserted a myc signal into the endogenous *dSlo2* locus. The CRISPR-cas9 system was used to accomplish this[333,334]. First, dSlo2 peptide sequence was aligned with $K_{Na}1.1$ sequence to identify known sites that affect channel trafficking and function[271,278,279,281,290,293,342]. These areas were specifically not chosen for incorporation of the myc tag to prevent altering channel expression patterns. Based on these alignments, a position in Exon 5 at the distal 3' end of *dSlo2* was chosen. Optimal guide RNA (gRNA) target sites within Exon 5 were identified using the online tool (http://tools.flycrispr.molbio.wisc.edu/targetFinger/). Based on these results, a sense primer 5'-CTT CGT TCT GCT CGA ACA TCA ACC -3' and antisense primer 5'- AAA CGG TTG ATG TTC GAG CAG AAC -3' encoding the gRNA with BbsI annealing sequences (underlined) were ordered from IDT. Primers were initially annealed, phosphorylated, and subsequently ligated into the BbsI sites of pU6-BbsI-chiRNA. Successful ligation was confirmed by PCR, and the plasmid was further amplified using a Qiagen Maxiprep kit. In addition to the gRNA, the homologous DNA sequence containing the in-frame myc sequence was generated as a single-stranded oligodeoxynucleotide (ssODN) by Integrated DNA Technologies, Inc. The single-stranded oligodeoxynucleotide (ssODN) repair template was designed such that *myc* was in-frame with *dSlo2* and flanked by homologous regions of 60 nt. Importantly, the *myc* sequence also disrupts the gRNA target sequence, preventing cas9 digestion of the repair template (Figure 2.2). Both the pU6-BbsI-gRNA-Exon5 plasmid and ssODN were injected into embryos expressing cas9 under control of the *vas* promoter (#51324) by Rainbow Transgenic Flies, Inc. Individually injected flies were crossed to a double-balanced line and progeny from these were backcrossed to each other. Once these flies began laying eggs, adults were pooled in groups of five and screened for successful insertion of the *myc* tag using PCR flanking the insertion followed by restriction digest with EarI, a site located within the *myc* sequence. Successful digestion suggested one of the adults contained the insertion. In this case, progeny from this vial were subsequently crossed individually to double-balancer lines. Again, once eggs were laid, the individual adult was screened for positive insertion. If digestion occurred, this line was then balanced and maintained. A total of five lines showed digestion and were kept as stocks. Following amplification of the line, successful insertion of in-frame *myc* sequence was confirmed using DNA sequencing.

TTGAAAATGCTCTTCTAAATTTGTTTTATTTTGTAAACTTTCCATTAAATACTTGGTGAGGCC

GTCGCCGTTCTCT[GCCCAAAAGACATTCGAGCGACACAACTCGCGCCGCAAGTCGAACATC

TCGTTCTGCTCGAACATCGAACAAAAACTCATCTCAGAAGAGGATCTGA/ACCTGGGTGCCA

CATGCGGCCCTCAAATGCCGCAAATGAACATGAACATGGCCAAC]ACCGCCGTCGGGGCTGG

ATCGCGTCGAGGATCCGGCATTGCCGGATTGAACCCCATGCAAATGCAGAGCGTTCAGACCT

TGGCCGGGTATGG

___ = myc Tag Insert In Frame

___ = CRISPR Target

___ = PAM

/ = cas9 Cut Site

__ = EarI site [ ] = ssODN sequence

Figure 2.2: *dSlo2-myc* generation strategy. *dSlo2* genomic sequence listed above with ssODN sequence in the brackets. The gRNA target sequence, highlighted in green, is separated by the *myc* sequence in frame with *dSlo2*.

2.3 Immunocytochemistry and confocal microscopy

2.3.1 L3 body wall staining

Wandering L3 larvae were collected from vials and washed in 1x Phosphate buffered saline (PBS). Following wash, larvae were fileted in cold PBS down the dorsal midline and slight cuts were made perpendicularly at each end. Each corner of the body wall was pinned down in sylgard. Tissue inside of the larvae was removed. The fileted prep was rinsed 3x in cold PBS. It was then fixed in 4% Paraformaldehyde (PFA) in PBS for 30 min. at room temperature. PFA was rinsed out 3 times with PBS. Larval body wall was then blocked in PBS with 0.5% Triton-X 100 (PBT) and 5% BSA for 2-3 hrs. Following block, larval body wall was incubated for 2 nights at 4˚C on rocker in PBT with 5% BSA and primary mouse anti-myc (Santa Cruz, 9E10) at 1:50. Body walls were subsequently washed 3 times for 30 min. each in PBT with

5% BSA. Following wash, body walls were incubated in secondary goat anti-mouse conjugated to Alexafluor 647 at 1:2000 overnight at 4˚C. Body walls were again washed 3 times for 30min. each in blocking solution. They were then rinsed 2 times in PBS followed by fixation in 4% PFA for 10 min. to secure antibodies to their targets. Body walls were then washed in PBS then H_2O and mounted in VectaShield. Images were acquired on an upright confocal microscope.

2.3.2 CNS staining

Adult and larval *Drosophila* CNS were dissected in cold PBS. Following dissection, CNS were fixed in 4% PFA in PBS at room temperature for 20 min. and subsequently washed 2 times in PBS then 2 times in PBT. Primary antibodies used were mouse anti-myc (1:50, Santa Cruz), chicken anti-GFP (1:2000, Aves Labs), rabbit anti-RFP (1:2000, Rockland Immunochemicals, Inc.), mouse anti-elav (1:10, Developmental Studies Hybridoma Bank). Primary antibodies were diluted in PBT with 5% BSA or NGS and incubated with CNS for 2-3 nights at 4˚C on rocker. Following primary staining, CNS were washed 3x times in PBT for 10 min. each. Alexa Fluorophores, anti-chicken 488, anti-rabbit 568, and anti-mouse 647 from Invitrogen were used at a 1:2000 dilution in PBT with 5% BSA or NGS and incubated on CNS for 1-2 nights at 4˚C on rocker. CNS were again washed 3 times for 10 min. each in PBT. They were then rinsed 2 times in PBS and fixed in 4% PFA for 10 min. to secure antibodies to their targets. Following fixation, CNS were rinsed in PBS then water and mounted using Vectashield or DABCO (90% glycerol in PBS and 2.5% DABCO). Larval brains were oriented with the dorsal side facing the coverslip, while the adult brains were oriented with the ventral side facing the coverslip.

2.3.3 Confocal microscopy

Images were acquired on either an upright Zeiss LSM 880 fluorescence confocal microscope or an inverted Zeiss LSM 800 fluorescence confocal microscope. On the LSM 880 microscope, light was collected using a 40x PlanApo 1.3 oil DIC objective. On the LSM 800 microscope, light was collected using either a 20x PlanApo 0.8 objective or a 63x PlanApo 1.4 oil DIC objective. Laser wavelengths of

488, 543, and 633 nm were used to excite fluorophores. Z-stacks and image tiling on the Zeiss ZEN software were used to acquire images of whole brains. Images were processed in ImageJ and maximum intensity Z-projections were generated when compiling Z-stack images.

2.4 Reverse transcription and PCR

Drosophila RNA was collected by mechanical squashing of 3 flies in 300 µL Trizol (ThermoFisher Scientific, Waltham, MA). 60 µL of chloroform was added to the sample, and vortexed for 30 sec. Samples were then centrifuged at 15,000 rpm at 4˚C for 15 min. 120 µL of supernatant was removed and placed in 150 µL isopropanol and 10 µL glycogen and mixed gently. Samples were then incubated at -20˚C for 30 min. to fully precipitate RNA. Samples were then centrifuged at 15,000 rpm at 4˚C for 10 min. to pellet the RNA. Supernatant was decanted, and RNA pellet was washed with 70% ethanol in diethyl pyrocarbonate (DEPC)-treated water. Samples were again centrifuged at 15,000 rpm at 4˚C for 10 min. and supernatant was decanted. Pellets were allowed to air dry for 5-15 min. and resuspended in 10 µL DEPC-treated nanopure water. RNA purity and concentration were verified using NanoDrop spectrophotometer and gel electrophoresis. Upon verification of RNA purity, 1µg of RNA was treated with 1 unit of DNaseI (ThermoFisher Scientific, Waltham, MA) by incubation at 37˚C for 15 min. DNaseI was then inactivated by adding 1 µL of 50 mM ethylenediaminetetraacetic acid (EDTA) and heat-treated at 65˚C for 10 min. Upon inactivation, 1µL 0.5µg/µL Oligo$(dT)_{12\text{-}18}$ primer and 1 µL 10 mM deoxynucleoside triphosphate (dNTP) (ThermoFisher Scientific, Waltham, MA) were added and incubated at 65˚C for 5min. to release any self-dimerizing oligos. Then, 4 µL of 5x First Strand Buffer, 1 µL of 0.1M dithiothreitol (DTT), and 1 µL 40U/µl RNAseOUT (ThermoFisher Scientific, Waltham, MA) were added to the samples and incubated briefly for 2 min. at 42˚C. Then 1 µL 200U/µL Superscript II RNase H (ThermoFisher Scientific, Waltham, MA) was added. Samples were incubated at 50˚C for 50 min. to allow for elongation and then at 70˚C for 15 min. to inactivate the enzyme. cDNA was then used for standard PCR reactions.

2.5 Thermonociception

Thermal nociception assays were performed as previously described[343–345]. Wandering 3rd instar larvae were collected and gently washed with water. Using a brush, larvae were gently placed into a 35mm petri dish containing a shallow layer of water. Larvae were allowed to adjust briefly to the new environment. A thermocouple probe (IT-23, Physitemp, Clifton, New Jersey) was welded to the end of a soldering iron, and the tip was filed down to a flat surface roughly 6mm wide. The probe was connected to at BAT-12 thermocouple (Physitemp, Clifton, New Jersey), allowing for real-time reading of the temperature of the tip of the probe within 0.1˚C. The temperature of the soldering iron was controlled using a variac transformer and regulating voltage supply. Once the described temperature was reached, the tip of the probe was gently placed on the side of a freely moving larvae and held against the body for 10 seconds. While stimulating the larvae, a video recording was taken using OMAX digital camera viewed through a stereoscope. Videos were analyzed offline and genotypes were blinded to the researcher. Latency to response was recorded as the time from which the stimulus probe was applied to the body wall of the larvae to the time in which the larvae completed a nocifensive escape locomotion (NEL). NEL was characterized by a complete 360˚ roll around the body axis of the larvae. Time to complete a NEL were binned into 1 second intervals and plotted per genotype at the different temperatures used.

2.6 Drug administration

2.6.1 Imidacloprid and Spinosad

Developmental exposure assays were performed as previously described[346–349]. Two insecticides which contained the active ingredients Imidacloprid (“Compare N Save Systemic Tree and Shrub Insect Drench”) or Spinosad (“Monterey Garden Insect Spray”) were diluted 1:100,000 in H2O. From these dilutions, the drugs were added to standard cornmeal and agar food at the listed concentrations and allowed to solidify overnight in the dark. Embryos were collected from adult flies of the listed genotypes on egg laying plates consisting of grape juice and agar. Embryos were aged for 24 hours to the L1 larval stage. 20 L1 larvae were gently collected from the egg laying plates using a brush and placed on the cornmeal and agar food containing different concentrations of the insecticides. Larvae were aged for 14-18 days in the

dark to prevent degradation of the drug by exposure to light. The larvae that made it to adulthood were counted and averaged over 3 separate feeding trials with 3 vials each. Survival was charted and compared across genotypes.

Acute exposure assays following eclosion were performed similar to previously described[350], however with partial adjustments. Food containing 5% sucrose and 1% agar was made to feed the flies. After boiling the food to bring the sucrose and agar into solution, the correct amount of the diluted Imidacloprid ("Compare N Save Systemic Tree and Shrub Insect Drench") was added to the food mixture and stirred thoroughly. 4mLs of the food mixture was then aliquoted into separate vials and allowed to solidify overnight in the dark. 0 day old males were collected and aged for 5 days in a 12 hr. light:dark cycle. On the 5th day, flies were starved in empty vials for 4 hours. Following starvation, flies were placed in the Imidacloprid food mixture vials and left in the dark. Every 24 hours, flies were analyzed for their ability to stand, walk, or groom. If flies were found to be stuck on their backs, unable to stand or walk, or were dead, they were counted as "affected". Totals of flies affected were counted each day for a total of 5 days.

To test whether exposure to Imidacloprid leads to an increased propensity for overexcitation, we exposed flies to a low percentage of Imidacloprid for 24 hours and then examined whether or not they exhibited seizure-like behavior following a mechanical stimulation. In these assays, Imidacloprid powder (Sigma-Aldrich CAS #138261-41-3) was dissolved in H_2O at 2.36mM and kept in the dark wrapped in foil. Dissolved Imidacloprid was added into the same food solution previously used (5% sucrose + 1% agar) at 0.0009%. Male flies were aged for 3 days in a 12 hr. light:dark cycle. On the morning of the 3rd day, flies were placed on the mock or Imidacloprid-laced food and left there for 24 hours in a 12 hr. light:dark cycle. Following treatment, flies were subjected to bang-sensitive assays blinded to the researcher. 5 flies were transferred to empty vials and allowed to acclimate for at least 5 minutes. Following acclimation, flies were subjected to 30 seconds of vortexing at a high speed. Immediately following vortex, flies were analyzed to

determine the fraction that were paralyzed. Scores were averaged across trials and compared across genotypes.

2.6.2 Veratridine and Anemone Toxin (ATX-II)

To test whether exposure to Veratridine leads to seizure-like behavior, flies were fed Veratridine, which has previously been shown to enhance I_{NaP}[303]. To perform these experiments, 0-1 day old male flies were collected, 5 per vial, and allowed to acclimate following CO_2 exposure for 1d in 12 hr. light:dark cycle. Following acclimation, flies were starved by placing them in an empty vial with H_2O-soaked filter paper. These vials were kept at 25˚C incubator at ~64% relative humidity for 24 hrs. Following starvation, the H_2O-soaked filter paper was replaced with filer paper soaked in 2% sucrose containing either 20μM Veratridine (V-110, Alomone Labs, Inc.) in dimethyl sulfoxide (DMSO) or the vehicle ("mock") .05% DMSO and left for 2 hrs. to feed. Immediately following feeding, flies were then tested for bang-sensitivity and spontaneous seizure activity. In the bang-sensitive assays, flies were considered to be exhibiting seizure-like behavior if they exhibited a period of uncontrollable motor movement immediately following the vortexing. In both assays, the researcher was blinded to the genotype and treatment during analysis.

ATX-II (STA-700, Alomone Labs, Inc.) was administered using two techniques. It was either embedded in a sucrose agar solution or administered in a sucrose solution on filter paper. For the sucrose agar feeding regimen, 0-1d old males were collected, 5 per vial, and aged for 1d in 12:12 light:dark cycle on normal cornmeal agar food. Flies were then placed on either vehicle (H_2O) or 100nM ATX-II in a 5% sucrose and 1% agar solution. Flies were left on food for 3 days. Vials were blinded by assigning a number to each. Flies were then recorded immediately following 30 sec. of vortexing. Seizure-like behavior was analyzed blinded to the genotype and treatment. In these assays, seizure-like behavior was scored if flies were exhibiting uncontrollable motor movement immediately following the vortex. For the sucrose-soaked filter paper regimen, 0d old males were collected, 5 per vial, and aged for 24 hrs. on normal cornmeal agar food at 12:12 light:dark cycle. Flies were then starved on H_2O-soaked filter paper for 24 hrs. Following starvation, flies were fed 1μM ATX-II in 5% sucrose on filter paper at 25°C with ~64% relative humidity

for 24 hrs. Immediately following feeding, filter paper was removed, and vials were blinded by assigning a number to each. Flies were then recorded following 30 sec. vortex. Videos were analyzed for seizure-like behavior with the researcher blinded to genotype. Seizure-like behavior was defined as uncontrollable motor movement immediately following vortexing.

2.6.3 Loxapine

Loxapine (L106, Sigma-Aldrich) was administered similar to the other Sucrose filter paper feeding methods. Loxapine was suspended in DMSO at a stock concentration of 10mM and kept at -20°C. 0d old male flies were collected, 5 per vial, and aged for 1 day at 12:12 light:dark cycle. Flies were then starved for 24 hrs. on H_2O-soaked filter paper. Immediately following starvation, flies were placed on either vehicle (0.1% DMSO), 10µM Loxapine, or 100µM Loxapine in 5% sucrose-soaked filter paper for 24 hrs. at 25°C in ~64% relative humidity. Immediately following feeding, filter paper was removed, and vials were blinded to genotype and treatment by assigning a number to each vial. Flies were vortexed for 10 sec. and video recordings were taken of the following response. Videos were analyzed for seizure-like behavior with the genotype and treatment blinded to the researcher.

2.6.4 Phenytoin and Avobenzone

Acute Phenytoin (PHR1139, Sigma-Aldrich) and Avobenzone (PHR1073, Sigma-Aldrich) assays were performed similar to the Sucrose-soaked filter paper experiments. 0d old males were collected, 5 per vial, and aged for 1 day on normal cornmeal agar food at 12:12 light:dark cycle. Flies were then starved for 24 hrs. on H_2O-soaked filter paper. Following starvation, flies were placed on either vehicle (1.6% DMSO), or .4mg/mL Phenytoin or Avobenzone in 5% sucrose-soaked filter paper at 25°C and ~64% relative humidity for 24 hrs. Immediately following feeding, vials were blinded to genotype and treatment by assigning a number to each vial. Flies were vortexed for 10 sec. and video recordings were taken of the subsequent response. Videos were analyzed for seizure-like behavior with the genotype and treatment blinded to the researcher.

2.7 Seizure induction

2.7.1 Bang-sensitive assays

Similar to the Imidacloprid overexcitation assays, bang-sensitive assays were performed. In these experiments, *Drosophila* lines (*bang-senseless* (*bss*^{1}), *easily-shocked* (*eas*^{PC80}), and *slamdance* (*sda*$^{iso7.8}$)) that display seizure-like behavior following a mechanical shock were used[194,196,201,202,204]. Males were aged for 2 days in 12 hr. light:dark cycle. Following aging, flies were gently transferred individually to empty vials using suction pipetting to avoid the use of CO_2. Flies were allowed to acclimate to the new vials for at least 5 minutes. Following acclimation, the vials were subjected to 10 seconds of vortexing on max speed. Immediately following vortexing, flies were videotaped and later analyzed for stereotypical seizure-like behavior. The time to each behavioral characteristic was noted by the researcher who was blinded to the genotype. These characteristics included the time to both the recovery seizure and to full recovery, characterized by the ability to stand or walk without exhibiting uncontrollable motor function. Additionally, flies were scored for a secondary paralysis period, characterized by a period of quiescence following the recovery seizure that lasted for at least 3 seconds. If flies exhibited a secondary paralysis, the time spent paralyzed was also counted. These characteristics were averaged across trials of roughly 20 flies and compared across genotypes.

2.7.2 Temperature-sensitive assays

Temperature-sensitive seizure assays were performed as previously described[116]. In these experiments, background temperature-sensitive *Drosophila* lines (*GEFS+*)[116] and (*DS*)[117] were used. Females were collected and aged for 2-3 days before running assays. To induce seizures, 5 flies were placed in empty vials and allowed to acclimate for at least 5 minutes. Following acclimation, flies were placed in a 40˚C or 42˚C water bath and behavior was videotaped. Analysis of recordings was done offline blinded to the genotype of the flies. Seizure-like behavior, defined as uncontrolled motor behavior or paralysis, was scored as a fraction of the total flies every 10 seconds per vial and averaged across trials.

2.7.3 Spontaneous seizure assays

0-1 day old male flies were collected on CO_2, and 10 were placed in vials containing normal cornmeal and yeast food. These flies were aged for 2 days in 12:12 light:dark cycle at room temperature. Before testing, flies were gently transferred to empty vials. These vials were placed sideways in a rack and flies were allowed to acclimate to the new environment for 30 minutes. Following acclimation, flies were videotaped for 15 minutes. Videos were then analyzed offline, with the researcher blinded to the genotype. Seizures were characterized as random bouts of uncontrollable motor movement in which the flies were unable to stand or walk. The number of overall seizures exhibited in a vial were totaled over the 15-minute period and averaged across genotypes.

CHAPTER 3. DSLO2 EXPRESSION IN THE NERVOUS SYSTEM

3.1 Overview

K_{Na} channels are widely expressed throughout the mammalian nervous system. K_{Na} channel expression has not yet been examined in *Drosophila*. To better understand the role of dSlo2, the *Drosophila* K_{Na} channel, I investigated expression of dSlo2 in the nervous system. To accomplish this, I generated two different *Drosophila* lines. The first is a reporter line in which translation of *dSlo2* is terminated, and instead Gal4 is translated. This line allows for Gal4 driven expression of fluorescent proteins in cells that would normally express dSlo2. The second is a line in which I tagged the C-terminus of the endogenous dSlo2 protein with a small epitope tag, myc.

Upon inspection of the reporter line, I found dSlo2 expression in primary sensory systems. These include the funiculus, Johnston's Organ, arista, and multidendritic neurons. These sensory regions are responsible for olfaction, mechanosensation, thermosensation, and noxious tactile sensation, respectively. Using the reporter line and dSlo2-myc line together, I also found that dSlo2 is expressed in anatomically distinct regions of the brain. These include the lamina, medulla, Kenyon cells, and antennal lobe. Expression in the lamina and medulla suggest a role in visual processing while expression in the antennal lobe suggests a role in olfactory processing. Additional expression in the Kenyon cells suggest a potential role in learning and memory. Expression in multiple primary sensory systems suggests a role in regulating sensory transduction both at the primary sensory level and in the downstream relay systems.

Further examination of dSlo2 expression in different cell types of the *Drosophila* CNS revealed expression in excitatory neurons but not inhibitory neurons. I found that most dSlo2-positive neurons in the *Drosophila* brain are cholinergic. Cholinergic neurons are considered the main excitatory neuron in the CNS, as opposed to mammalian systems where glutamatergic neurons are the main excitatory neurons in the brain. Furthermore, I found that dSlo2 is not expressed in GABAergic neurons in the CNS. This expression pattern suggests that dSlo2 is acting in excitatory neurons, with the potential role of dampening

excitability of cholinergic neurons. I test this hypothesis in Chapters 4 and 5. When I looked at expression of dSlo2 in glutamatergic neurons, I found that dSlo2 is not expressed in glutamatergic neurons in the brain; however, dSlo2 is expressed in the glutamatergic motor neurons in both larvae and adults. This suggests a potential role in modulating locomotive behaviors.

I also examined the subcellular localization of dSlo2 in the nervous system using the *dSlo2-myc* tagged line. I found that dSlo2 is localized to the axonal region of a specific subset of multidendritic neurons that are responsible for noxious stimuli sensation. I additionally found dSlo2-myc expression in the calyx and peduncle of the mushroom body and the neuropil region of the medulla. Expression of dSlo2-myc in the calyx of the mushroom body suggests it may regulate associative olfactory learning, as the calyx is a neuropil region containing dendrites from the Kenyon cells and axonal projections from the antennal lobe. Additionally, expression in the peduncle suggests a role in regulating axonal output of the Kenyon cells.

Interestingly, I also found expression of dSlo2 in glia responsible for establishing a diffusion barrier in the *Drosophila* blood-brain barrier (BBB). These glial cells function similarly to epithelial cells of the mammalian BBB. It has been previously found that K_{Na} channels function in non-neuronal cell types, such as cardiomyocytes and epithelial cells of the kidney[260,275]. Exploring the role of dSlo2 channels in these glia could help elucidate K_{Na} channel function in mammalian BBB cells.

3.2 dSlo2 expression in distinct regions of the *Drosophila* CNS

To first examine where dSlo2 is expressed in the *Drosophila* nervous system, I generated a line in which Gal4 is inserted into a coding intron immediately upstream of the S1 transmembrane domain coding exon. Gal4 will then be expressed under the control of native *dSlo2* regulatory regions. This line allows for Gal4 driven expression of fluorescent proteins under the control of the *Upstream Activating Sequence* (*UAS*), which subsequently label all dSlo2-positive cells. To do this, I utilized the relatively new "Trojan exon" recombination method developed in Dr. Ben White's lab[332]. In this system, a Trojan cassette containing a *T2A-Gal4* sequence is recombined into the location of a separate cassette that has already been

inserted in the genome, called a *Minos*-mediated integration cassette (MiMIC)[339,340]. MiMIC cassettes are transposons that incorporate randomly into the *Drosophila* genome. These cassettes were designed with ΦC31 integrase target *attP* sites flanking the cassette. These sites allow for cassette replacement via recombinase-mediated cassette exchange[340]. Previously, large scale transgenic insertion projects were performed that generated many different lines containing a MiMIC insertion[340]. Using this library of MiMIC insertion lines, I targeted a MiMIC insertion, *Mi13397*, which is located in a coding intronic region between exon *33* and exon *32* of the *dSlo2* gene. These exons are downstream of all predicted start sites and are immediately upstream of the coding exon for the S1 transmembrane domain (Fig. 3.1A). Within the Trojan cassette, the T2A signal is a viral peptide motif that disrupts translation by the ribosome, forcing it to skip an amino acid and begin translation of the next encoded peptide sequence[351,352]. To generate this line, multiple genetic crosses were performed that incorporate the necessary components to induce recombination and replace the *Mi13397* insertion with the *T2A-Gal4* cassette (See Section 2.2.4). The first cross generates a fly with chromosomes containing both the *Mi13397* cassette and the replacement cassette containing the *T2A-Gal4* signal. Importantly, this insertion (*pC(lox2-attB2-SA-T2A-Gal4-Hsp70)*) contains the *T2A-Gal4* sequence in all three phases. This guarantees that the correct phase needed for in-frame translation of Gal4 will incorporate into the *Mi13397* location. Each one of these phases is flanked by a *lox* site, allowing for Cre-mediated excision of *T2A-Gal4* in each phase. Progeny from this cross were then crossed to a transgenic line that expresses both Cre and ΦC31 integrase. Cre is expected to excise each phase of the *T2A-Gal4* sequence and ΦC31 integrase will recombine the *T2A-Gal4* cassette into the *Mi13397* location. As each recombination event is a single event, individual flies were collected from this cross to isolate potential recombination events. These flies were then crossed to a transgenic line containing a *UAS-EYFP* insertion. If incorporation of the *T2A-Gal4* signal in the correct phase occurred, then progeny of this cross would express EYFP under the control of Gal4 (Fig. 3.1B). These progeny were screened for EYFP (3.1C), and EYFP-positive lines were maintained. DNA sequencing was performed to confirm

incorporation of the *T2A-Gal4* cassette. For a visual depiction of these crosses, see Fig. 2.1. These flies, now referred to as *dSlo2*^{Mi13397}*-Gal4*, were subsequently balanced and kept as a stock.

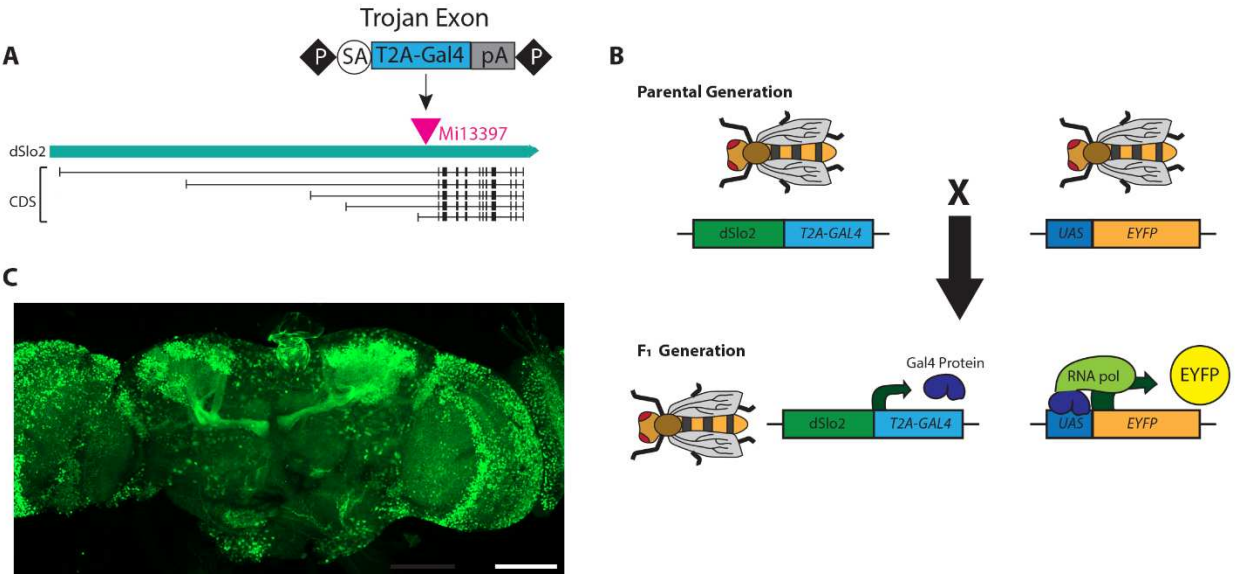

Figure 3.1: Generation of *dSlo2*^{Mi13397}*-Gal4* line. A) Replacement of the *Mi13397* MiMIC insertion, located within an intronic region of *dSlo2* predicted to be in all splice forms, with the Trojan exon containing the *T2A-Gal4* cassette. B) Crossing the *dSlo2*^{Mi13397}*-Gal4* line with a transgenic line containing *UAS-EYFP* allows for Gal4 driven expression of EYFP. C) Confirmation of endogenously driven EYFP in adult *dSlo2*^{Mi13397}*-Gal4 Drosophila* brain. Scale Bar: 100µm.

I then examined expression of dSlo2 throughout the CNS of both larvae and adult *Drosophila*. The *Drosophila* CNS has distinct neuronal populations and brain structures that have been anatomically described in great detail[353]. I found dSlo2 reporter expression in the Kenyon cells of both larvae and adult *Drosophila* (Fig. 3.2A and 3.2B). Kenyon cells extend their processes into the calyx region as well as into α, β, and γ lobes of the mushroom body[354]. The mushroom body has been identified to play a key role in associative visual and olfactory learning and memory[355–358]. dSlo2 reporter expression was also observed in the Ventral Nerve Cord (VNC) of both larvae and adults (Fig. 3.2A and 3.2B). Within the VNC, dSlo2 reporter expression was observed in the motor neurons, which are situated in a very distinct pattern in both larvae and adults[359,360]. Reporter expression of dSlo2 in the motor neurons suggests it may play a role in regulating locomotor functions of both larvae and adults. dSlo2 reporter expression was also observed in other cells within the VNC, whose identity was not further explored in my dissertation.

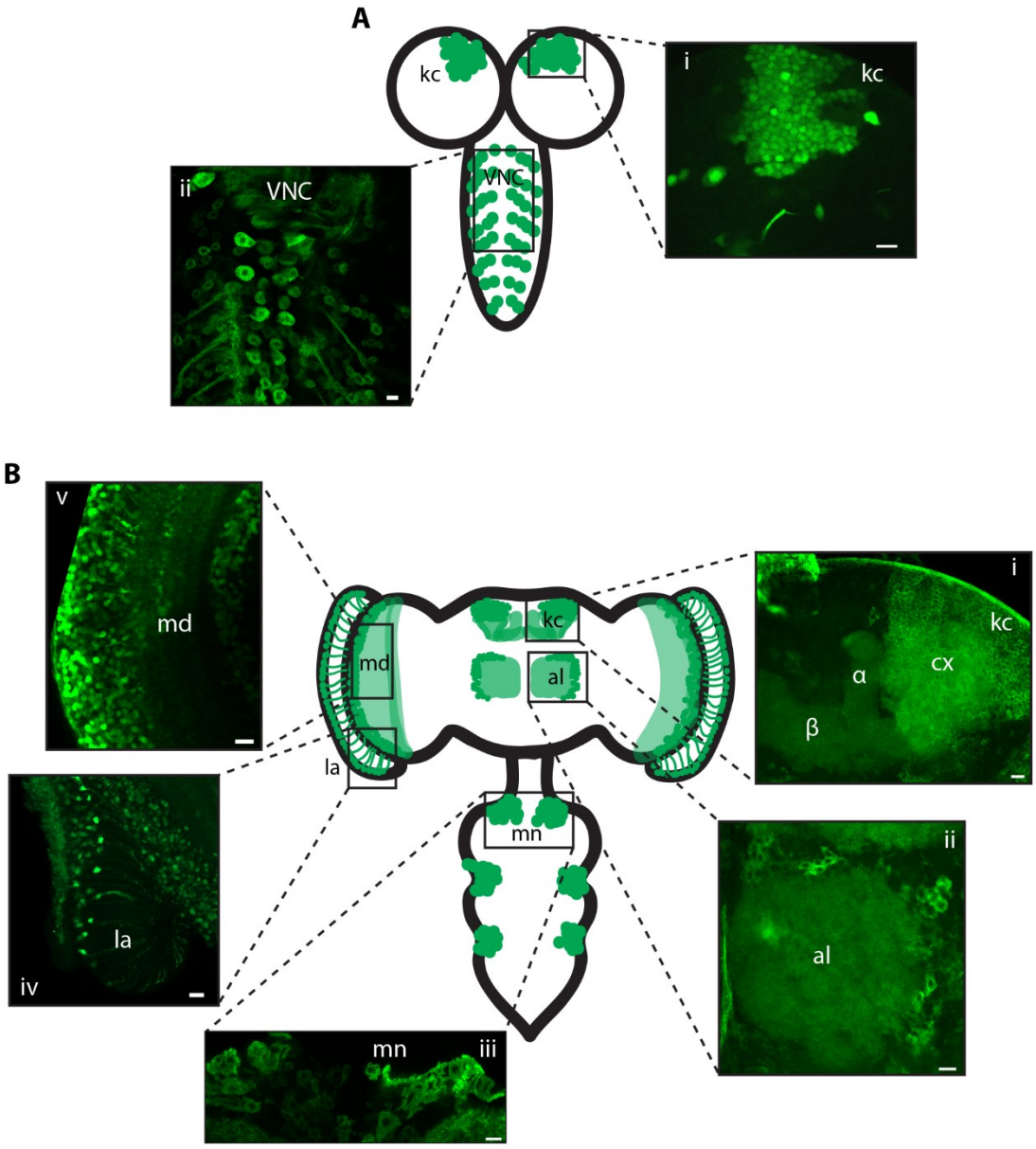

Figure 3.2: dSlo2 reporter expression in the nervous system. A) dSlo2 reporter expression in L3 larval CNS, depicted in the drawing. dSlo2 reporter expression was seen in the kenyon cells (kc, i) as well as the Ventral Nerve Cord (VNC, ii). B) dSlo2 reporter expression in different regions of the adult CNS, depicted in the drawing. dSlo2 reporter expression was found in the kenyon cells (kc, i), antennal lobe (al, ii), medulla (md, v), and lamina (la, iv) in the brain and motor neurons (mn, iii) in the VNC. All images were taken of either *dSlo2^{Mi13397}-Gal4>>UAS-EYFP* or *dSlo2^{Mi13397}-Gal4>>UAS-CD8-GFP*. Scale Bars: 10µm.

In addition to those regions observed in both the larvae and adult CNS, dSlo2 reporter expression was also found in other anatomically distinct regions in the adult CNS known to regulate sensory

processing. These include the medulla and lamina, as well as the antennal lobe (Fig. 3.2B). The medulla and lamina are second order processing cells that receive input from the photoreceptors and are located in the optic lobe of the adult brain. Neurons in the lamina and medulla play a key role in regulating visual processing, such as motion and color[361–363]. The dSlo2-positive cells located in the medulla cortex project both internally within the medulla as well as into the lobula and lobula plate[363,364]. The antennal lobe is responsible for processing of olfactory information from the olfactory neurons and further relaying this information to higher order regions of the brain such as the mushroom body and lateral horn[365].

3.3 dSlo2 expressed in primary sensory organs

I further examined whether dSlo2 may be expressed in the primary sensory organs of *Drosophila*. I found that the dSlo2 reporter line showed expression in cells located in primary sensory organs. These include the funiculus, Johnston's Organ, arista, and multidendritic (md) neurons (Fig. 3.3). Neurons within the third segment of the antenna, the funiculus, express olfactory receptor proteins, and are the main cells responsible for olfaction in the adult fly[366]. These olfactory sensory neurons project to the antennal lobe[366] where further odorant processing takes place[365,367]. The Johnston's Organ, which is located in the second segment of the antenna, is a mechanosensory organ. It plays a major role in many behaviors, such as geotaxis, flight regulation, wind sensation, and courtship[368–372]. Additionally, the arista is a long bristle which extends out of the antenna. Deflections in the arista excite mechanosensory neurons in the Johnston's Organ, which is thought to enhance sound and wind sensation[373,374]. It is also responsible for sensing temperature changes, and subsequent avoidance behaviors[375,376]. The multidendritic neurons are located in the larval body wall[377]. These neurons are responsible for gentle and noxious tactile sensation, thermosensation, and proprioception[343,344,378–380]. dSlo2 reporter expression in multiple primary sensory organs is consistent with the hypothesis that dSlo2 channels may regulate sensory transduction.

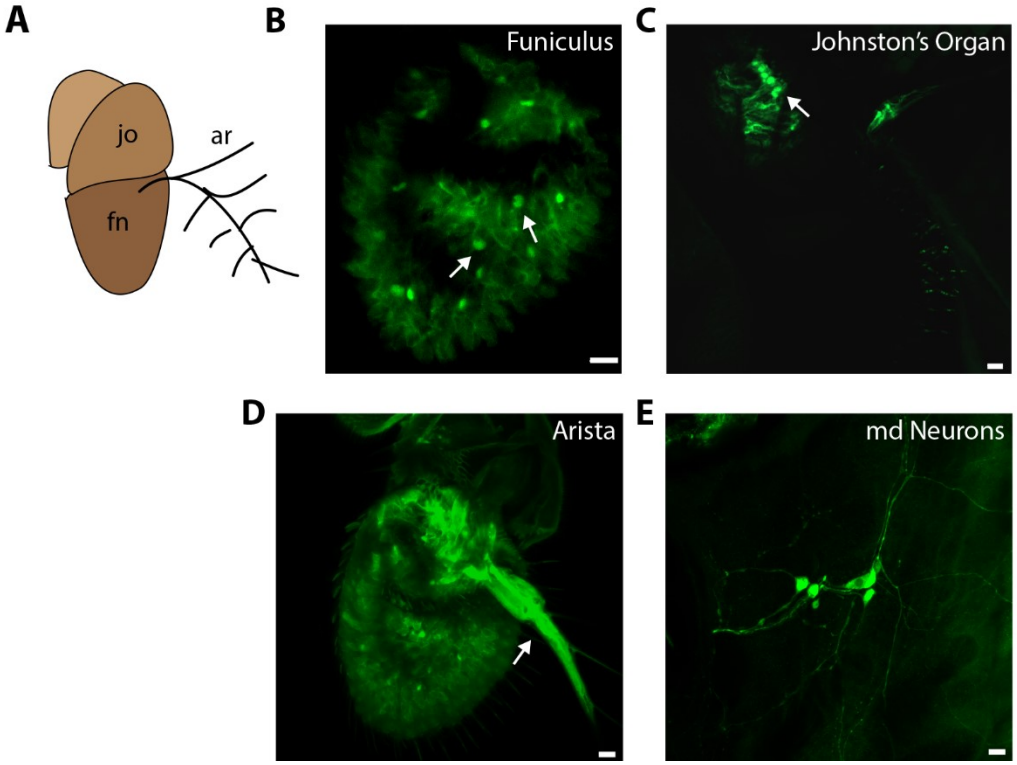

Figure 3.3: dSlo2 reporter expressed in primary sensory systems. A) Depiction of the fly antenna. The second segment of the antenna is the Johnston's Organ (jo), the third segment is the funiculus (fn), and the arista (ar) protrudes out of the antenna. B) dSlo2 reporter expressed in cells located in the funiculus (Arrow). C) dSlo2 reporter expressed in cells of the Johnston Organ (Arrow). D) dSlo2 reporter expressed in the Arista (Arrow). E) dSlo2 reporter expressed in multidendritic (md) neurons in the larval body wall. All images were taken from *dSlo2*^{Mi13397}*-Gal4>>UAS-EYFP*. Scale Bars: 10μm.

3.4 Subcellular localization of dSlo2

Subcellular localization of ion channels greatly influences the role they have in regulating neuronal excitability. For example, a K^+ channel located in the dendrites could differentially affect neuronal excitability compared to the same channel located in the axon. Therefore, I examined the subcellular localization of dSlo2 in neurons to better understand how it may be regulating excitation. To accomplish this, I generated a line in which endogenous dSlo2 is tagged on the C-terminus with the small epitope tag, myc. Using CRISPR-cas9, I designed a guide RNA (gRNA) sequence that targets exon *5*, which encodes a portion of the C-terminus of dSlo2. This gRNA would guide cas9 to this genomic location, where cas9

would induce a double-stranded break (DSB). Homology-directed repair (HDR) mechanisms will fix the DSB using a repair template. I designed a repair template in which the *myc* sequence is in frame with the coding of exon *5* (Fig. 3.4A), such that the myc epitope would be fused to the C-terminus (Fig. 3.4B). Flies were initially screened for the insertion using PCR from genomic DNA followed by restriction digest. The *myc* sequence contains an EarI restriction site, which is not found in the surrounding DNA sequences. The PCR primers were designed such that the EarI site would be located in the middle of the PCR. Therefore, if the *myc* sequence was inserted, the PCR product would be digested, and bands would appear at roughly half the size of the overall product (See Section 2.2.5). Upon successful digestion of the PCR product, these

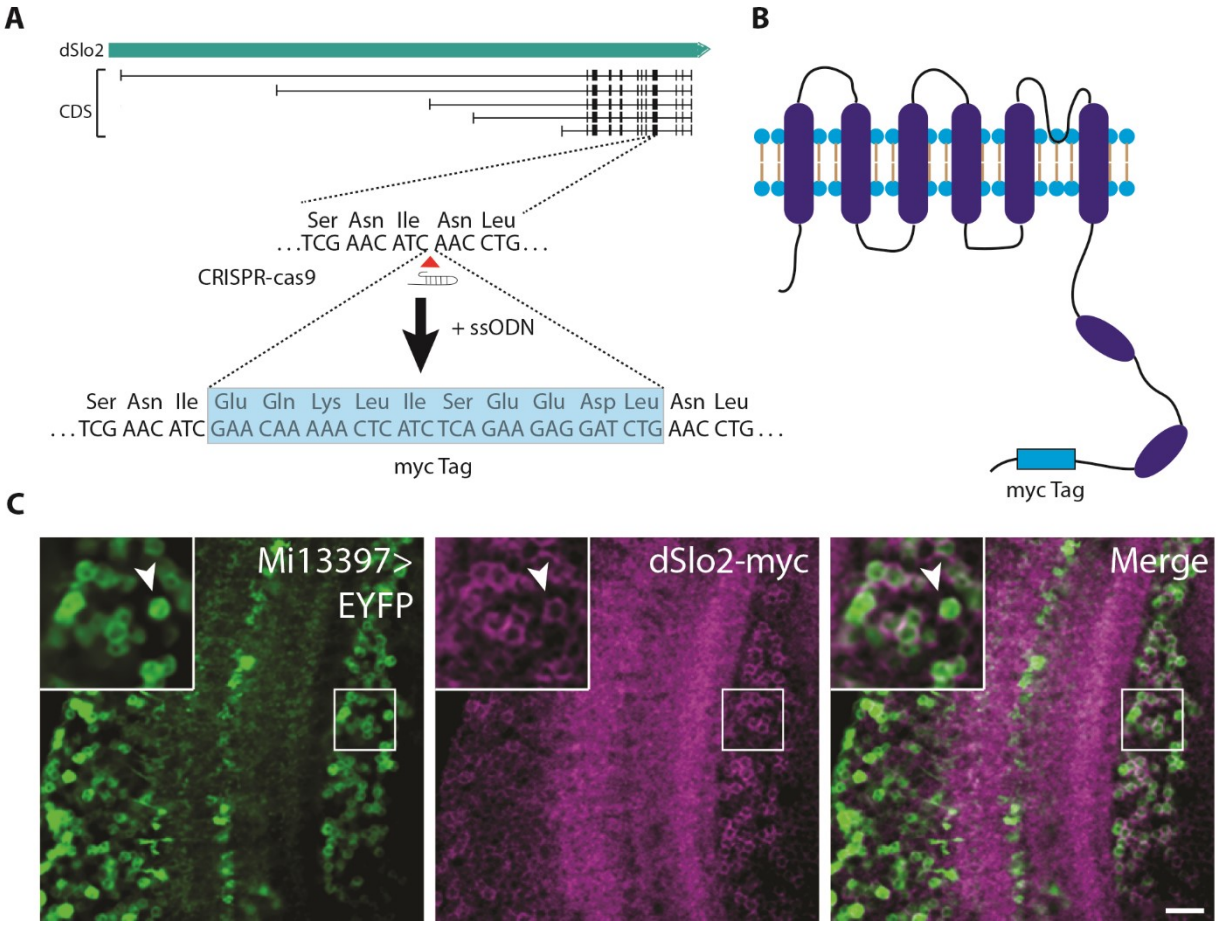

Figure 3.4: Generation of the *dSlo2-myc* line. A) CRISPR-cas9 in conjunction with gRNA were used to generate a double-stranded break within an exon in the C-terminus of *dSlo2*. A single-stranded oligodeoxynucleotide (ssODN) sequence was provided as a repair template containing the in-frame *myc* tag. B) dSlo2 protein depiction containing the in-frame myc tag in the intracellular C-terminus. C) *dSlo2*^{Mi13397}*-Gal4* was used to drive EYFP (left) and crossed with the *dSlo2-myc* line (middle). Co-expression was found in the same cells in the adult CNS (right). Scale Bar: 10µm.

flies were balanced and sequenced to confirm successful integration of the *myc* sequence. To confirm expression of dSlo2-myc in dSlo2-positive cells, the *dSlo2-myc* line was crossed to the *dSlo2^{Mi13397}-Gal4>>UAS-EYFP* line and co-expression was examined. Co-expression was seen throughout the brain. Highlighted in Figure 3.4C, overlap of dSlo2-myc and EYFP was seen in neurons of the medulla. Confirmation of the insertion by DNA sequencing, as well as co-expression with the previously generated reporter line, suggested that the myc epitope was indeed fused to the endogenously expressed dSlo2 channel.

To identify the subcellular compartments dSlo2-myc is localized to, I decided to examine the multidendritic (md) neurons located in the larval body wall. Md neurons are primary sensory neurons that display stereotypical neuronal architecture. They have a vast array of dendritic arborizations that tile the larval body wall and a single axon which relays sensory information to the VNC (Fig. 3.5A)[377,381]. This architecture allows for clear distinction between axonal and dendritic neuronal compartments. I first needed to focus on a specific subset of md neurons to allow for clear distinction of dSlo2-myc expression[343,378]. I decided to examine if the dSlo2 reporter line was expressed in Class IV md neurons. It was previously shown that these neurons express a Deg/NaC channel, pickpocket (*ppk*)[378,382]. Based on this, the Jan lab generated a line that expresses CD4-TdTom under the control of the *ppk* promoter region[383]. Therefore, I crossed *dSlo2^{Mi13397}-Gal4>>UAS-EYFP* to the *ppk>>CD4-TdTom* line and examined if EYFP and TdTom were co-expressed in body wall neurons. I found that *ppk*-positive neurons were also positive for *dSlo2^{Mi13397}-Gal4* driven *UAS-EYFP* (Fig. 3.5B). I then examined subcellular localization of dSlo2-myc in the *ppk*-positive Class IV neurons. After staining the *Drosophila* body wall for myc, I found that dSlo2-myc was mainly localized to the axonal regions of the Class IV md neurons and minimally in the dendrites (Fig. 3.5C). Axons were identified in the stack of images, as they extend in the z-axis and join nerve bundles that travel to the VNC. This subcellular localization of the channel could greatly affect the role it plays in regulating excitability and action potential firing of these neurons. Worth noting, other K^+ channels, Elk and Shal, have also been found to localize to this region in other md neurons[381].

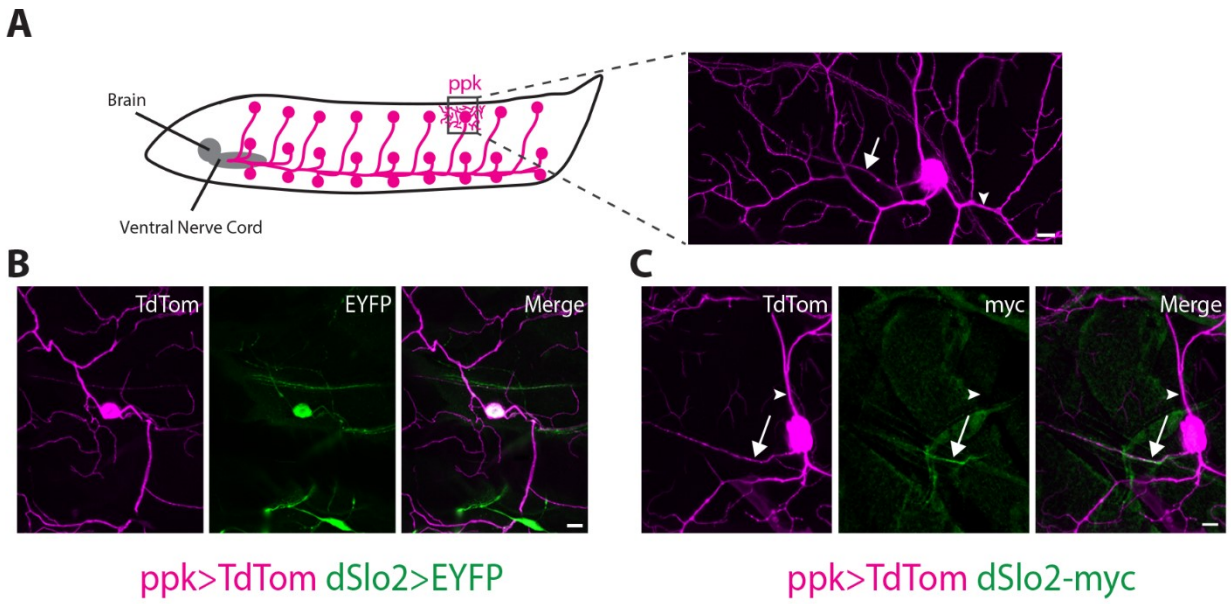

Figure 3.5: dSlo2 localizes to the axonal region of ppk neurons. A) Depiction of ppk neurons lining the bodywall of Drosophila larvae. The image is of a ppk neuron, with a single axon (arrow) and multiple dendritic arborizations (arrowhead). B) *dSlo2^{Mi13397}-Gal4>>UAS-EYFP* co-localizes with *ppk>>CD4-TdTom*. C) Staining for dSlo2-myc shows localization to the proximal region of the axon (arrow) and lack of expression in the dendrites (arrowhead). Scale Bars: 10µm.

I further examined the subcellular localization of dSlo2-myc in regions of the adult brain. I found dSlo2-myc localized to the processes of the medulla (Fig. 3.6A). Subcellular localization of dSlo2 to the processes of the medulla suggests that it is likely regulating processing of visual stimulation. The medulla region of the optic lobe contains processes from many different neuronal types, including cholinergic, GABAergic, and glutamatergic[384], which work together to regulate directional selectivity. However, this region is difficult to distinguish between axonal and dendritic compartments. I therefore examined the Kenyon cells, which have more distinct neuronal compartments (3.6B). I found that dSlo2-myc was localized to the calyx region and peduncle of the Kenyon cells, but not in the mushroom body lobes (Fig. 3.6C, 3.6D, and 3.6E). The calyx region of the mushroom body is a neuropil region containing mainly dendritic arborizations from the Kenyon cells along with axonal projections from the antennal lobe[385] (Fig. 3.6B). As the reporter line suggested that dSlo2 is expressed in both Kenyon cells and antennal lobe neurons (Fig. 3.2B), it is hard to distinguish whether dSlo2-myc localization in the calyx is from dendritic expression in the Kenyon cells or presynaptic connections from the antennal lobe. The peduncle is thought to be the

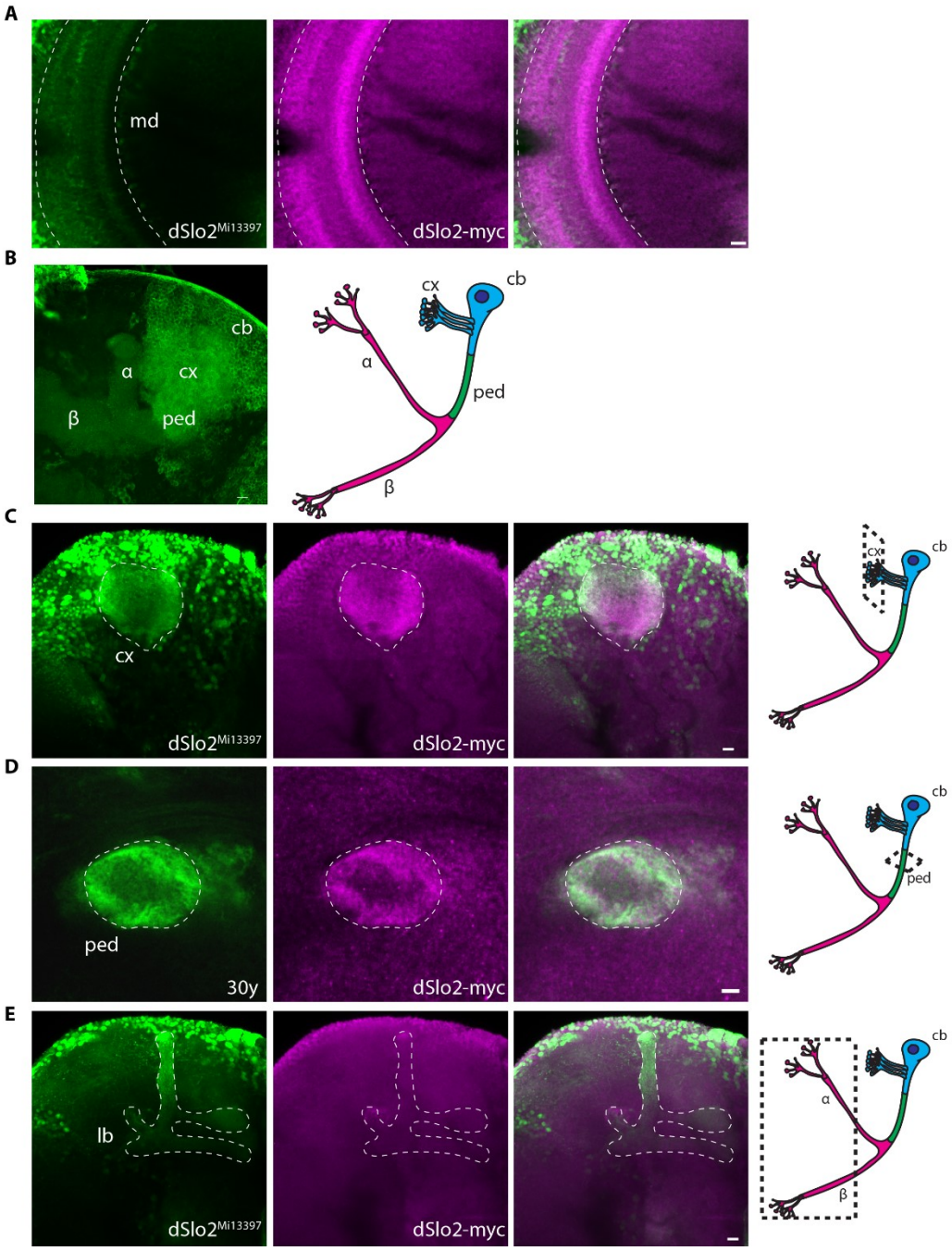

Figure 3.6: Subcellular localization of dSlo2-myc in adult CNS. A) Image from Figure 3.3 showing different segments of the mushroom body (left). A cartoon drawing of a Kenyon cell, with the cell body (cb), dendritic branching into the calyx (cx), the peduncle (ped), and the α and β lobes (right). B) dSlo2-myc staining was strong in the cx of the mushroom bodies. C) dSlo2-myc staining was strong in the ped of the mushroom body, shown by 30y>>CD8-RFP. D) dSlo2-myc staining was very low in the lobes of the mushroom bodies (lb, outlined). E) dSlo2-myc localized to the medulla region of the optic lobe (md, outlined). All images taken from *dSlo2*^{Mi13397}*-Gal4>>UAS-EYFP*, *dSlo2-myc* unless otherwise stated. Scale Bars: 10 µm.

distal axonal region, where processes begin to send signals to the α and β lobes[386] (Fig. 3.6B). Furthermore,

the voltage-gated Na^+ channel, para, was found to be localized to this region[386]. The finding that dSlo2-myc channels are localized to the peduncle (Fig. 3.6D) suggests they might be activated by para channels.

3.5 dSlo2 expressed in excitatory neurons but not inhibitory neurons

Most of the regions in which dSlo2 reporter expression was found, such as the Kenyon cells, consist mainly of cholinergic neurons. This suggests that dSlo2 is likely expressed in excitatory neurons. To test what types of neurons dSlo2 is expressed in, I employed the use of the LexA/LexAop binary expression system. In this case, I utilized transgenic lines that express LexA in cholinergic, GABAergic, or glutamatergic neurons. These classes of neurons provide insight into whether or not dSlo2 may be affecting excitatory, inhibitory, or motor function, respectively. I decided to image the medulla cortex which contains cholinergic, GABAergic, and glutamatergic neurons[384]. It is important to note that different from mammalian systems, cholinergic neurons are the main excitatory neurons in the *Drosophila* brain.

Expression comparisons were made between excitatory and inhibitory neurons in the brain. I examined if dSlo2 reporter was expressed in cholinergic neurons. To do this, I crossed the *dSlo2^{Mi13397}-Gal4* line with a choline acetyltransferase (ChAT) reporter line[332], *ChAT^{Mi04508}-LexA*. I also examined whether dSlo2 was expressed in GABAergic neurons. To do this, I crossed the *dSlo2^{Mi13397}-Gal4* line with a glutamate decarboxylase (GAD) reporter line[332], *Gad1^{Mi09277}-LexA*. In both cases, the transgenic progeny also contained the insertions *UAS-EYFP* and *LexAop-TdTom-nls*. This allowed for Gal4-mediated expression of EYFP in the dSlo2-positive cells and LexA-mediated expression of TdTom-nls (nuclear localization sequence) in cholinergic or GABAergic neurons. Upon examination of the medulla cortex, I found that most dSlo2-positive neurons were cholinergic (Fig. 3.7A). Not shown here, this pattern existed in other regions of the brain such as the Kenyon cells. Additionally, based on levels of EYFP, it seems as though the dSlo2 reporter is more highly expressed in certain cholinergic neurons compared to others. Although, this was never quantified as EYFP expression is driven by Gal4 and does not report exact levels of dSlo2. Contrastingly, I found that dSlo2 is not expressed in GABAergic neurons (Fig. 3.7B). Not shown here, lack of dSlo2 in GABAergic neurons was observed in other regions of the brain. Expression of dSlo2

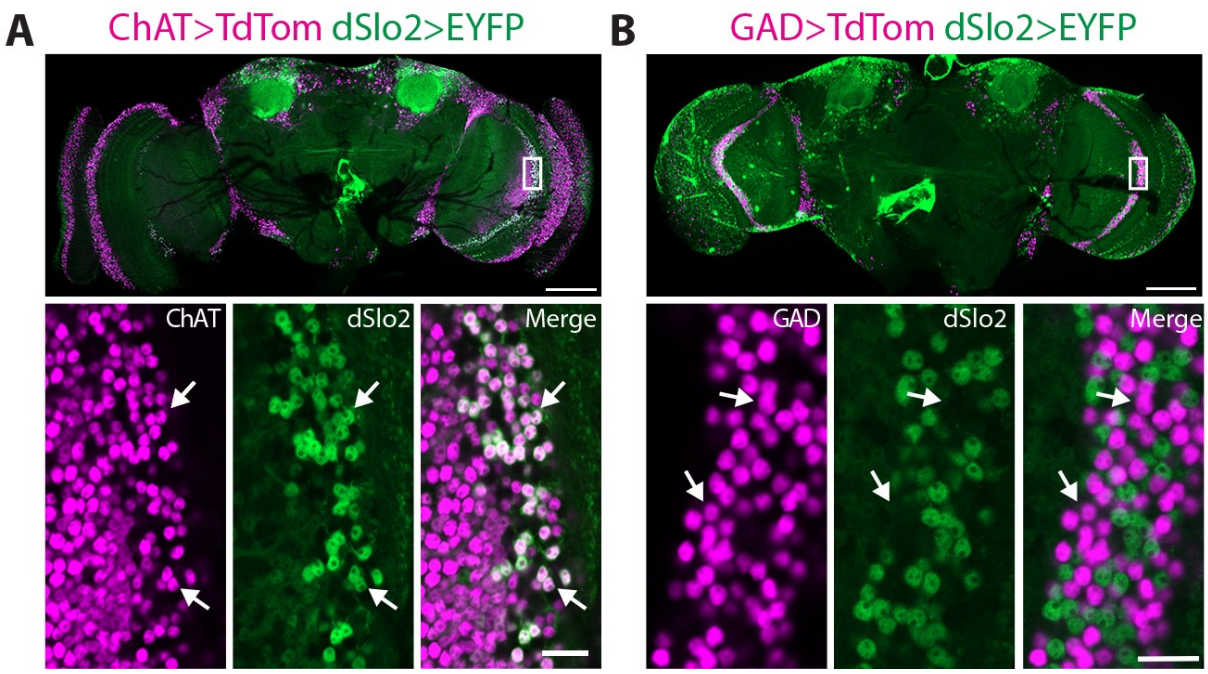

Figure 3.7: dSlo2 expression is specific to cholinergic neurons in *Drosophila* brain. A) Co-localization of EYFP from *dSlo2*^{Mi13397}*-Gal4>>UAS-EYFP* and cholinergic neurons labeled with *Cha*^{Mi04508}*-LexA>>LexAop-TdTom-nls*. B) No co-localization is seen between *dSlo2*^{Mi13397}*-Gal4>>UAS-EYFP* and GABAergic neurons labeled with *Gad1*^{Mi09277}*-LexA>>LexAop-TdTom-nls*. Scale Bars: 100µm in top panels, 10µm in lower panels.

in excitatory, cholinergic neurons, while being seemingly absent in inhibitory, GABAergic neurons, suggests that dSlo2 may dampen signaling in excitatory neurons. This hypothesis is the basis for experiments conducted in the following chapters.

I also examined whether dSlo2 is expressed in glutamatergic neurons. To accomplish this, I crossed *dSlo2*^{Mi13397}*-Gal4* with a vesicular glutamate transporter (VGlut) reporter line[332], *VGlut*^{Mi14979}*-LexA*. I found dSlo2 expression in glutamatergic neurons to be region specific. While glutamatergic neurons mainly function as motor neurons in the *Drosophila* VNC, there is also a subset located in the brain of the fly. I found that dSlo2 is not expressed in most glutamatergic neurons throughout the brain of the fly (Fig. 3.8). However, when examining the VNC, I found clear expression of dSlo2 in the motor neurons which are morphologically distinct from other neurons in the VNC (Fig. 3.8). This pattern suggests that dSlo2

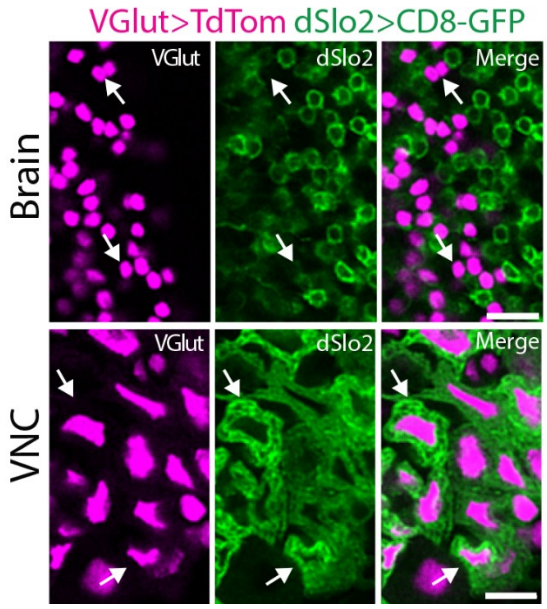

Figure 3.8: dSlo2 reporter is expressed in glutamatergic neurons in the ventral nerve cord but not in the brain. *VGlut^{Mi14979}-LexA>>TdTom-nls* (left) combined with *dSlo2^{Mi13397}-Gal4>>CD8-GFP* (middle) did not overlay in the brain (top right). However, co-expression was found within the morphologically distinct motor neurons in the ventral nerve cord (bottom right). Scale Bars: 10µm.

channels could play a role in altering motor neuron output and thereby affect locomotion and other coordinated motor movement.

3.6 Expression of dSlo2 in glia of the blood brain barrier

When examining the *dSlo2^{Mi13397}-Gal4>>UAS-EYFP* line, I also noticed expression in extremely large, non-neuronal cells located throughout the periphery of the brain. After a literature search, I found that these were likely to be cells of the *Drosophila* BBB. They matched the anatomical and morphological descriptions. The BBB in *Drosophila* consists of 3 cellular layers, the neural lamella, the perineural glia (PG), and the subperineural glia (SPG) (Fig. 3.9A). These layers ensheath the entirety of the *Drosophila* CNS, acting as a barrier between the hemolymph and the nervous tissue (Reviewed by Hindle and Bainton 2014[387]). Expression of the dSlo2 reporter resembled the morphological description of either the PG or SPG cells. To determine which they were, I crossed the *dSlo2^{Mi13397}-Gal4* line to lines specifically expressing LexA in either the PG (*R85G01-LexA*) or SPG (*R54C07-LexA*) cells[353,388]. Upon examination, I found that dSlo2 is not expressed in the PG cells (Fig. 3.9B) but is expressed in the SPG cells (Fig 3.9C).

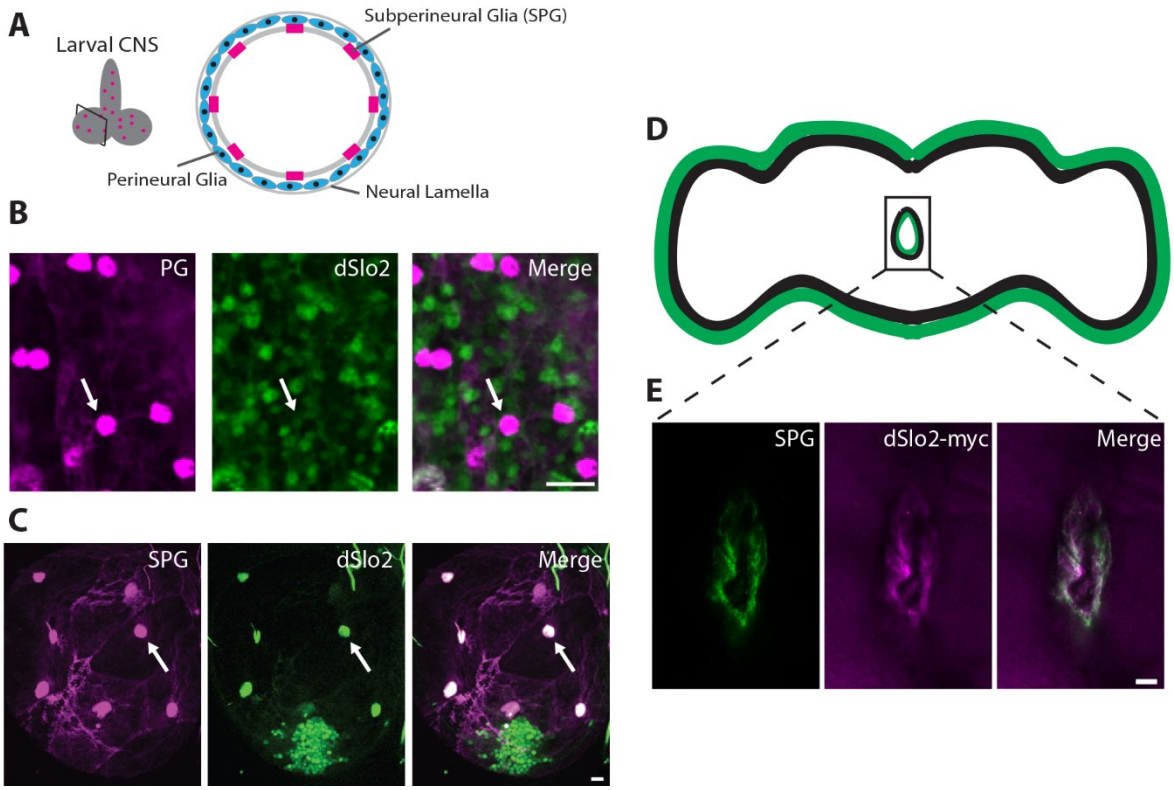

Figure 3.9: dSlo2 expression in subperineural Glia of the BBB. A) Depiction of the *Drosophila* BBB in larval brain. B) *R85G01-LexA>>TdTom-nls* in PG (left). *dSlo2*^{Mi13397}*-Gal4>>UAS-EYFP* (middle). No overlap was found between the two (right) in the adult brain. C) *R54C07-LexA>>TdTom-nls* in SPG (left). *dSlo2*^{Mi13397}*-Gal4>>UAS-EYFP* (middle). Co-expression was found between the two (right panel, arrow) in larval brain. Scale Bars: 10µm. D) Depiction of the adult *Drosophila* brain (black) with the SPG layer ensheathing the outside of the brain and the inner layer of the esophageal hole (green). E) *R54C07-Gal4>>CD8-GFP* (left) in conjunction with dSlo2-myc staining (middle) revealed clear overlap in the esophageal hole region (right). Scale bar: 10µm.

As this expression pattern was unexpected, I wanted to further verify expression of dSlo2 in these cells. To accomplish this, I examined whether dSlo2-myc staining was positive in the SPG cell layer. Normal methods of imaging were complicated by the shape and anatomical position of the SPG. These cells are extremely thin, roughly 2-3 µm[388], and their thin processes expand in an uncharacteristic manner encasing the CNS. Since dSlo2 was broadly expressed throughout neurons in the brain, I had to image an area where background staining of dSlo2-myc was low and yet the SPG layer was still visible. A region known as the esophageal hole, which traverses through the center of the brain and is lined with BBB cells, was used to examine expression (Fig. 3.9D). Images taken through this region of multiple fly brains showed positive staining of dSlo2-myc that overlaid with expression of CD8-GFP driven in SPG cells (Fig. 3.9E).

The combination of both the reporter *dSlo2*^{Mi13397}*-Gal4* line as well as dSlo2-myc staining strongly suggests that dSlo2 is expressed in SPG glia.

3.7 Conclusion

Examining the expression of dSlo2 in the *Drosophila* nervous system revealed expression in multiple regions during both larval and adult stages. Additionally, expression of dSlo2 was observed in primary sensory organs. Widespread expression of dSlo2 in primary and higher order sensory processing centers in the brain suggests it may play a role in vision, olfaction, mechanosensation, thermosensation, and auditory sensation. It additionally may regulate integration of sensory stimuli in the mushroom body. Indeed, the mushroom body receives direct input from the antennal lobe which relays much of the sensory stimuli coming from the antenna. Not only was dSlo2 expression found in both the Kenyon cells of the mushroom body and the antennal lobe, but subcellular localization of the channel was found in the calyx of the mushroom body. The calyx is a neuropil region where antennal lobe neurons synapse onto dendritic processes from the Kenyon cells. Whether expression of dSlo2 in this region is coming from antennal lobe or Kenyon cell projections, it indicates dSlo2 may contribute to the transmission of these signals. In addition to expression in sensory systems, dSlo2 is expressed in the glutamatergic motor neurons that regulate locomotion of both larvae and adult flies. Combined, these expression results suggest that dSlo2 may contribute to signaling at every stage of the circuit; from the initial sensation of the external stimuli, to processing and integration of these signals, to locomotive responses to these signals.

The biophysical properties of the K_{Na} channel, being that it is activated by internal Na^+, suggests that it may act as a brake to excitation. However, this type of negative feedback would act differently depending on whether the channels are acting in excitatory or inhibitory neurons. My results suggest that in *Drosophila*, dSlo2 is specifically expressed in excitatory neurons and not inhibitory neurons. Currently, only indirect evidence suggests expression of mammalian K_{Na} channels in GABAergic neurons. This includes expression in the frontal lobe, which is rich in GABAergic neurons[286,389,390], as well as recordings from putative inhibitory lamina II interneurons[310]. Expression of dSlo2 in excitatory neurons of *Drosophila*

provide a unique model to better understand the role of K_{Na} channels in dampening neuronal signaling by acting in excitatory neurons. I explore the hypothesis that dSlo2 protects against neuronal overexcitation induced by exposure to a cholinergic agonist in the following chapter.

An interesting and unexpected result of this chapter is that dSlo2 is expressed in glial cells that function in the *Drosophila* BBB. It is possible that K_{Na} channels may also be expressed in human BBB cells. In a large transcriptomics screen, *K_{Na}1.2* (*KCNT2*) transcript was identified in cultured human cerebrovascular endothelial cells[391]. While the mammalian BBB is more complex than the *Drosophila* BBB, its function is relatively similar. This has led to recent explorations in the use of the *Drosophila* BBB as a model to test the role and function of different cellular components in development and maintenance of the barrier[392–394]. Indeed, very similar cellular functions have been observed, such as acting as a chemical barrier through efflux of xenobiotic compounds[393]. An interesting study recently found that efflux of xenobiotic compounds in *Drosophila* is altered by the circadian clock, with potential implications for drug efficacy depending on the time of day[395]. Other K^+ channels have been found in BBB endothelial cells and are thought to maintain proper ionic gradients across the membranes (Reviewed by Hladky and Barrand 2016[396]). This gradient is extremely important for the proper transport of water across the barrier as water transport is regulated by the Na^+-K^+-Cl^- cotransporter (NKCC)[397–399]. Proper functioning of the BBB has also been implicated in different forms of epilepsy (Reviewed by van Vliet et al. 2015[400]). While my studies did not continue to examine the role of dSlo2 in SPG cells, I believe this area of study is very intriguing for future investigation.

CHAPTER 4. DSLO2 PROTECTS AGAINST BEHAVIORAL ABNORMALITIES CAUSED BY CHOLINERGIC OVEREXCITATION

4.1 Overview

K_{Na} channels have long been hypothesized to protect against overexcitation[260,262]. Due to the levels of Na^+ required to activate the channels (reviewed by Dryer 1994[401]), it has been suggested that only during times of extreme depolarization would K_{Na} channels play a protective role. However, this hypothesis has not been directly tested. Therefore, in this chapter I test this hypothesis by feeding *Drosophila* cholinergic agonists and examining whether the loss of *dSlo2* increases susceptibility to both toxic effects as well as seizure-like activity.

I used two compounds, Imidacloprid and Spinosad, which were shown to have agonistic properties on different invertebrate nicotinic acetylcholine receptors (nAChRs). Both are also commonly used in insecticides[402], suggesting that overactivation of nAChRs results in neurotoxic effects. To examine whether the loss of dSlo2 channels might exacerbate these neurotoxic effects, I generated a *dSlo2* null line (*dSlo2*-) using the CRISPR-cas9 system. I then fed *dSlo2*- and wild-type larvae Spinosad or Imidacloprid and examined the percentage that eclosed. I found that in the absence of *dSlo2*, larvae were significantly less likely to eclose when exposed to Imidacloprid but not Spinosad. This suggests that endogenous dSlo2 channels are somehow protective against exposure to Imidacloprid during development.

I next examined if adult flies acutely fed Imidacloprid exhibit detectable behavioral alterations. I found, similar to the larval exposure assays, that the loss of *dSlo2* exacerbated behavioral abnormalities caused by Imidacloprid feeding. In these assays, *dSlo2*- flies were more likely to exhibit uncontrolled motor behavior and an inability to stand or walk compared to wild-type flies. Furthermore, this behavioral phenotype was rescued by expressing *dSlo2* in a *dSlo2* null background.

As these assays did not necessarily link behavioral abnormalities to overexcitation induced by Imidacloprid exposure, I tested whether Imidacloprid exposure enhanced susceptibility to seizure-like behavior. I found that following exposure to a low level of Imidacloprid, *dSlo2*- flies were significantly more likely to exhibit paralysis following mechanical stimulation compared to wild-type flies. These results suggest that endogenous *dSlo2* indeed protects against overexcitation caused by Imidacloprid.

It has previously been shown that Imidacloprid binds to and activates Dα1 nicotinic acetylcholine receptors (nAChRs)[403–405]. Additionally, the loss of Dα1 protects flies against toxic exposure to Imidacloprid[346]. I therefore examined whether dSlo2 may act in neurons expressing Dα1 nAChR subunits. To test this, I generated a Trojan exon line in which LexA is expressed in the place of dSlo2. I then examined whether dSlo2 and Dα1 are co-expressed in the nervous system. I found that most Dα1-positive cells were also positive for dSlo2. Therefore, it is possible that dSlo2 channels hyperpolarize Dα1-positive neurons when exposed to Imidacloprid.

4.2 *dSlo2*- larvae exhibit decreased survival following Imidacloprid exposure

To test the hypothesis that dSlo2 channels prevent overexcitation, I first generated a *dSlo2* null line. To accomplish this, I employed the CRISPR-cas9 system. I designed gRNA sequences to target sequences flanking the pore region of the channel. This region was chosen instead of the start site as there are four predicted start sites spanning roughly 73kb (Fig. 4.1.A). This 73kb region encodes for multiple other genes, making deletion of the pore region a more precise strategy that would not affect other genes. These gRNA sequences would guide cas9 to sites spanning the pore region, thereby inducing double-stranded breaks at both sites. I additionally designed a repair template that contained a selection marker, 3xP3-DsRed, which when incorporated causes expression of DsRed in the *Drosophila* eye. This selection marker was flanked by a left homologous arm (LHA) and a right homologous arm (RHA), which allow for homology-directed repair (HDR). Flies were screened based on fluorescence of DsRed in the eye. After isolating DsRed-positive flies, I verified the incorporation of the repair template using PCR and DNA sequencing. I

additionally confirmed the absence of *dSlo2* transcript by RT-PCR (Fig. 4.1.C). Once confirmed, these flies were then used in behavioral assays.

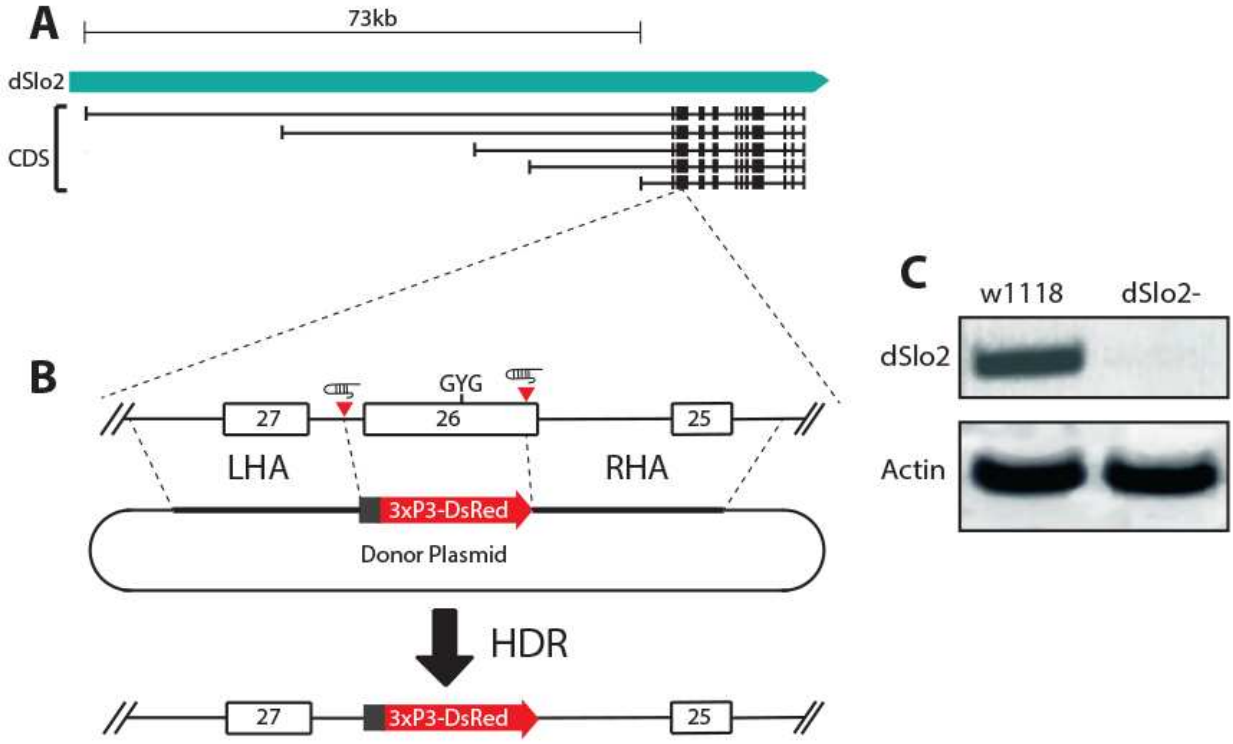

Figure 4.1: Generation of the *dSlo2* null line, *dSlo2-*. A) Depiction of the *dSlo2* gene with all predicted coding sequences (CDS) displayed below. B) gRNA sequences target regions flanking the pore-coding region (GYG) located in *Exon 26*. A donor plasmid was provided that allows for homology-directed repair (HDR), and insert the selection marker, 3xP3-DsRed. C) *dSlo2* RNA expression was examined in wild-type (*w1118*) and *dSlo2-* lines using RT-PCR. *Actin* was used as a positive control.

To examine whether *dSlo2* protects against overexcitation, I exposed wild-type and *dSlo2-* larvae to toxic levels of two cholinergic agonists during development and tested how many eclosed. The two cholinergic agonists, Imidacloprid and Spinosad, have different mechanisms of action. Imidacloprid is a compound classified under the group neonicotinoids and is the second most commonly used insecticide affecting nAChRs[402]. It has been shown to have partial agonist properties, such that it induces a smaller current than acetylcholine (ACh) in invertebrate neuronal cell cultures and in *Xenopus* oocytes expressing invertebrate nAChRs[403–405]. Additionally, a tonic inward current was observed in cholinergic neurons of acutely dissected honeybee brains following application of Imidacloprid[406]. *Drosophila* have a total of 10

pore forming nAChR subunits, Dα1-7 and Dβ1-3. *Drosophila* mutants for Dα1 or β2 nAChRs show strong resistance to neonicotinoid toxicity, including Imidacloprid. Meanwhile, mutants for Dα2, Dα5, Dα6, Dα7, Dβ1, and Dβ3 did not protect against Imidacloprid exposure[346]. This suggests specificity of Imidacloprid for Dα1 and Dβ2 nAChRs in *Drosophila*. Spinosad consists of multiple compounds called Spinosyns and is the fourth most commonly used insecticide affecting nAChRs[402]. Spinosyn A, the main ingredient in Spinosad, has been shown to increase nerve firing in *Drosophila* larvae[407]. Additionally, exposure to Spinosyn A in oocytes expressing Dα5 and Dα6 caused a significant inward current, greater than that of Ach[407]. Furthermore, multiple groups have found that mutations within Dα6 confer resistance to Spinosad in *Drosophila*[348,349,408]. This suggests that Spinosad is specific for Dα6 nAChRs.

It has previously been shown that increasing or decreasing neuronal excitability during development can drastically affect growth of the organism and neuronal function[151,156–161]. I therefore sought to test the hypothesis that dSlo2 channels defend against chronic overexcitation during development. Experimental setup of these assays was performed similar to those previously conducted in other studies[347–349]. 20 L1 larvae from wild-type and *dSlo2*- lines were grown on standard food containing either the vehicle, water ("mock"), or increasing concentrations of Imidacloprid or Spinosad. As previously described, exposure to either compound at certain concentrations will kill a percentage of larvae during development[346,408], although it is unclear exactly what causes death of the larvae. The finding that *Dα1*-null and *Dα6*-null lines were resistant to Imidacloprid and Spinosad exposure, respectively, suggests that activation of these receptors contributes to death of the larvae[346,348,349,408]. The number of larvae that eclosed were counted after 14-16 days and averaged over multiple trials. To verify larval susceptibility to either compound, I also included larvae from the line *ΔMdr65*, which has previously been shown to be extremely susceptible to insecticide exposure[350,409]. *ΔMdr65* contains a mutation in an ABC transporter, which disrupts efflux of xenobiotic compounds. This causes an increase in retention of the insecticide within the larvae, which likely causes the increased susceptibility to insecticide-induced death[350]. *dSlo2^{Mi13397}-Gal4* was used as another *dSlo2* null line, as it is expected to end translation of dSlo2 shortly after the start codon, thereby

producing a truncated protein and acting like a null line (See Section 3.2). Importantly, when larvae were mock treated (0ppm) there was no difference in survival rates between wild-type, *dSlo2*-, or *dSlo2*^{Mi13397}-*Gal4* (Fig. 4.2.A). There was a decrease in *ΔMdr65* survival when fed on the vehicle-laced food, suggesting that this mutation alone decreases survival of the larvae. At 0.6ppm Imidacloprid, there was a significant reduction in *ΔMdr65* survival, suggesting that the treatment regimen was successful. However, there was no difference between wild-type, *dSlo2*-, or *dSlo2*^{Mi13397}-*Gal4* (Fig. 4.2.A). Upon doubling this concentration to 1.2ppm, I found that both *dSlo2*- and *dSlo2*^{Mi13397}-*Gal4* both showed greater susceptibility to Imidacloprid exposure compared to wild-type, with only 18% of either *dSlo2* null flies eclosing compared to 50% of wild-type (Fig. 4.2.A). At the highest concentration of Imidacloprid tested, 1.8ppm, both *dSlo2* null lines showed increased death compared to wild-type, with roughly 35% of wild-type surviving compared to roughly 6% of either *dSlo2* null line (Fig. 4.2.A).

At the lowest concentration of Spinosad exposure, 0.8ppm, I found a significant decrease in *ΔMdr65* survival. Unexpectedly, I found a significant decrease in *dSlo2*^{Mi13397}-*Gal4* survival but not in

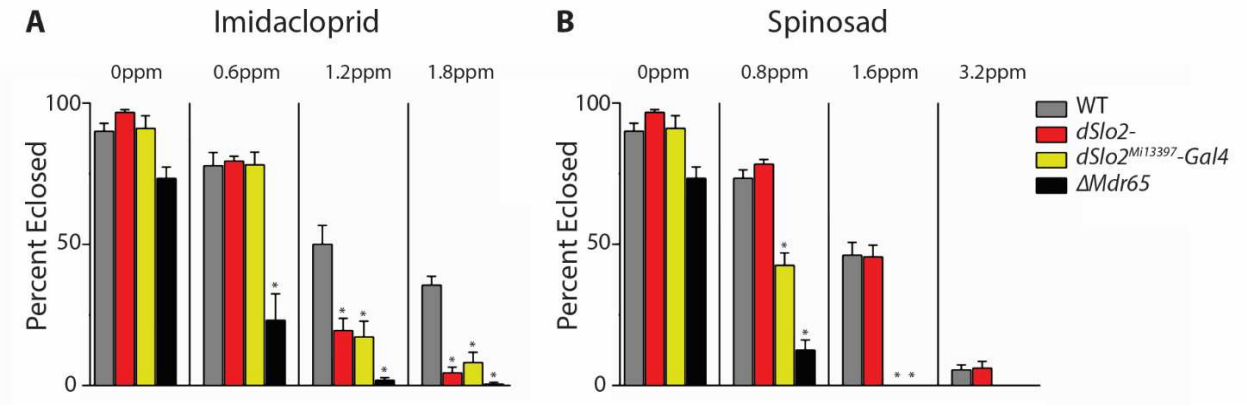

Figure 4.2: *dSlo2*- flies show enhanced susceptibility to developmental Imidacloprid exposure. A) Percentage of flies eclosing from 20 L1 larvae was measured in *w1118* (WT), *dSlo2*, *dSlo2*^{Mi13397}-*gal4,* and *ΔMdr65* lines when grown on standard cornmeal food containing 0ppm, 0.6ppm, 1.2ppm and 1.8ppm Imidacloprid. n = 6 trials for 0ppm and 8-9 trials for all other concentrations, 20 larvae per genotype per trial. $p < .01$ compared to WT (Student's t-test). B) Percentage of flies eclosing from 20 L1 larvae was measured in *w1118* (WT), *dSlo2*, *dSlo2*^{Mi13397}-*gal4,* and *ΔMdr65* lines when grown on standard cornmeal food containing 0ppm, 0.8ppm, 1.6ppm and 3.2ppm Spinosad. n = 6 trials for 0ppm and 0.8ppm and 3 trials for *dSlo2*^{Mi13397}-*gal4* and *ΔMdr65* and 9 trials for *w1118* (WT) and *dSlo2*- at 1.6ppm and 3.2ppm. $p < .01$ compared to WT (Student's t-test).

dSlo2- (Fig. 4.2.B). This difference between *dSlo2*- and *dSlo2*^{Mi13397}*-Gal4* continued at 1.6ppm Spinosad. However, no difference in survival was observed between wild-type and *dSlo2*- at either concentration (Fig. 4.2.B). These results suggest that the absence of *dSlo2* does not enhance susceptibility to Spinosad, as there was no difference in survival between wild-type and *dSlo2*-. However, it does seem as though Gal4 alone enhances toxicity, as the *dSlo2*^{Mi13397}*-Gal4* line showed a significant decrease in survival at 0.8ppm Spinosad compared to *dSlo2*-.

Together, these results suggest that endogenous *dSlo2* protects against developmental exposure to Imidacloprid but not Spinosad. This is shown by the decrease in survival rates of both *dSlo2*- and *dSlo2*^{Mi13397}*-Gal4* larvae at 1.2ppm and 1.8ppm Imidacloprid. As *Dα1*-null larvae are resistant to Imidacloprid toxicity through development[346], this suggests that dSlo2 channels might hyperpolarize neurons while they experience increased cholinergic activity during development. Since many physiological changes occur during development, I wanted to expand on these findings and tested whether *dSlo2*- adults were susceptible to behavioral abnormalities induced by Imidacloprid.

4.3 The loss of *dSlo2* exacerbates Imidacloprid induced behavioral abnormalities

To next test whether dSlo2 channels protect against cholinergic overexcitation after development, I fed adult flies Imidacloprid over a shorter period of time and tested whether the loss of *dSlo2* exacerbated behavioral abnormalities compared to wild-type flies. To do this, I placed young adult males on food containing a lower and higher concentration of Imidacloprid and examined their behavior every day for up to 5 days. I initially observed that common behavioral abnormalities caused by ingestion of Imidacloprid included uncoordinated motor movement, spasms, paralysis, and death. Flies were therefore scored as "affected" by Imidacloprid if they were unable to stand or walk. Similar behavioral defects were previously reported in response to Spinosad feeding[408]. At the lower concentration of Imidacloprid, 0.0018%, I found that roughly two times as many *dSlo2*- flies were scored as "affected" compared to wild-type flies at days 4 and 5 on Imidacloprid food (Fig. 4.3). Additionally, I found at the higher concentration of Imidacloprid, 0.0055%, that roughly 1.5 times more *dSlo2*- flies were scored as "affected" compared to wild-type flies at

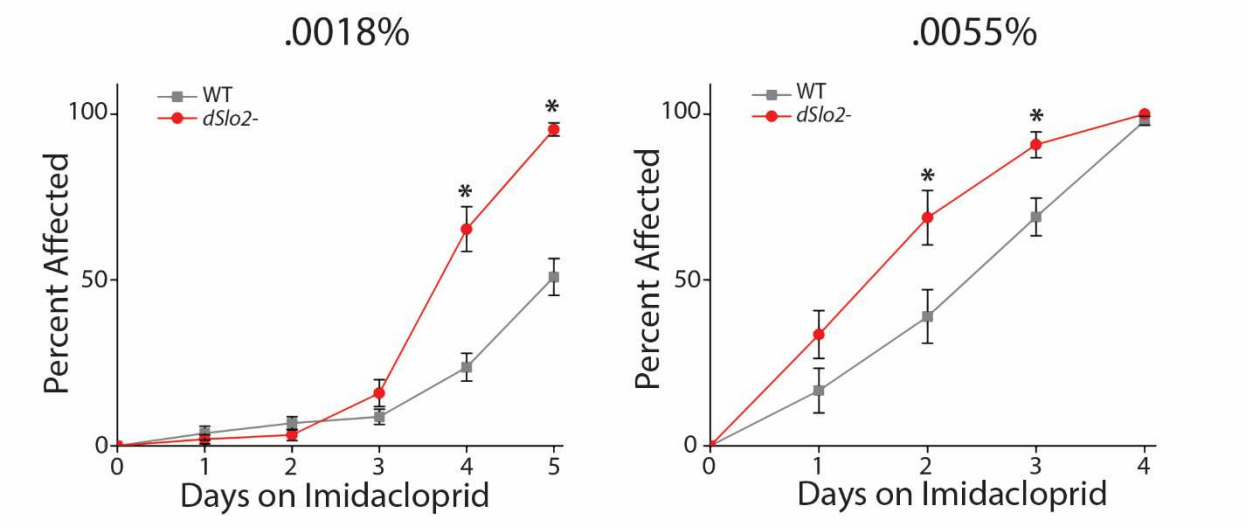

Figure 4.3: Increased behavioral abnormalities in *dSlo2-* line due to acute Imidacloprid exposure. Percentage of flies unable to stand or walk were scored as "affected" every day while feeding Imidacloprid at 0.0018% (Left). Percentage of flies unable to stand or walk were scored as "affected" every day while feeding Imidacloprid at 0.0055% (Right). n = 10 trials with 10 flies per genotype per trial. $p < .01$ (Student's t-test).

days 2 and 3 (Fig. 4.3). These results suggest that endogenous *dSlo2* attenuates locomotive dysfunction caused by Imidacloprid feeding.

To determine if *dSlo2* was indeed responsible for this protection against Imidacloprid exposure, I tested whether expression of *dSlo2* in a *dSlo2* null background would rescue the percent of flies displaying behavioral dysfunctions. To accomplish this, I generated transgenic lines containing *dSlo2* coding sequence downstream of the Upstream Activating Sequence (*UAS*). Lines were screened for positive incorporation of *UAS-dSlo2* and crossed to a pan-neuronal Gal4 line, *elav-Gal4*. I then confirmed enhanced expression of *dSlo2* transcript compared to WT using RT-PCR (Fig. 4.4). I additionally used a positive control line, $dSlo2^{f00048}$ that I previously found, when crossed to the *elav-Gal4* line, caused overexpression of *dSlo2*. Expression levels between lines might differ due to the position effect of the *UAS-dSlo2* cassette in the genome. Lines exhibiting greater expression of *dSlo2* compared to background levels were kept. I then used the $dSlo2^{Mi13397}$*-Gal4* line as the null background. As stated previously, the *T2A-Gal4* sequence is expected to terminate translation of *dSlo2* shortly after the start codon, thereby generating a null line that expresses Gal4 in all dSlo2-positive cells.

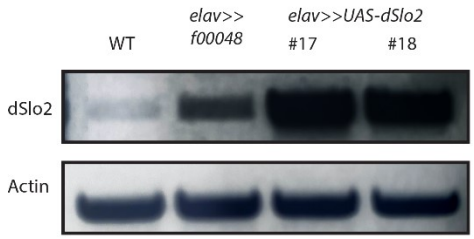

Figure 4.4: *UAS-dSlo2* allows for *dSlo2* overexpression. *dSlo2* transcript levels were measured in *elav-Gal4>>UAS-dSlo2* lines compared to *w1118*. *elav>>f00048* was used as a positive control. Shown here are just two lines, #17 and #18. Note Actin levels are similar in all samples. Primers span intronic region, and separation by size confirms this is indeed *dSlo2* RNA.

Similar to *dSlo2-* flies, the *dSlo2*^{Mi13397}*-Gal4* line showed a significant increase in the percent of affected flies at both concentrations of Imidacloprid compared to wild-type (Fig. 4.5). However, the *dSlo2*^{Mi13397}*-Gal4* line displayed a significant increase in percentage affected compared to the *dSlo2-* flies. I found that this was likely due to Gal4, as other Gal4 expressing backgrounds exhibited an increased number of affected flies compared to wild-type flies. High levels of Gal4 has previously been shown to induce apoptosis[410], which may explain these results. One of the transgenic *UAS-dSlo2* lines was crossed with *dSlo2*^{Mi13397}*-Gal4* to generate a rescue line. Compared to the *dSlo2*^{Mi13397}*-Gal4* background, the rescue

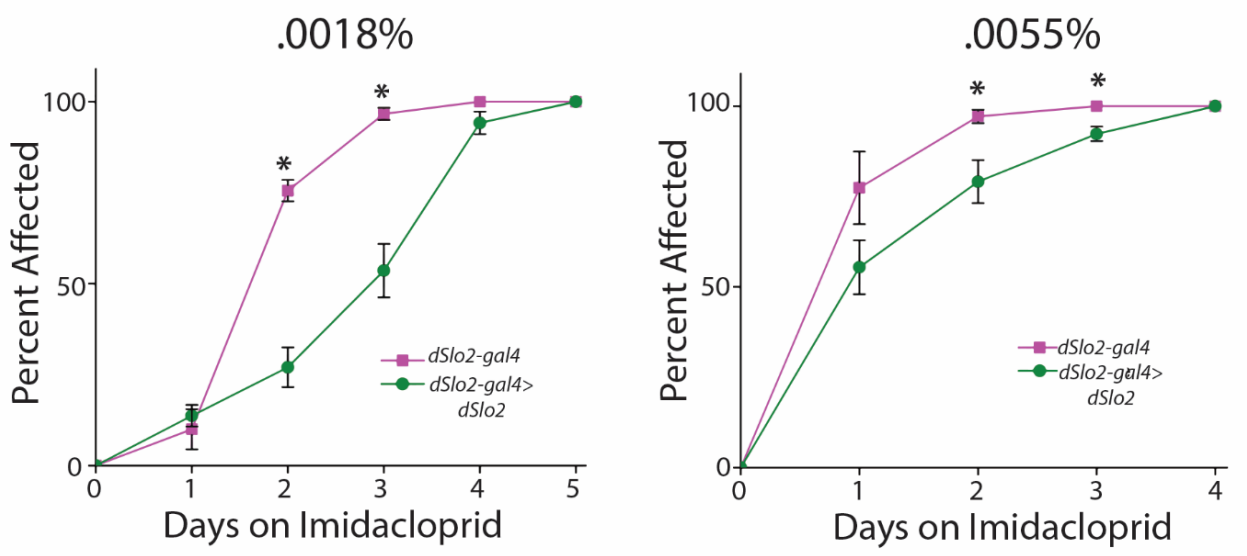

Figure 4.5: Increased behavioral abnormalitiese in *dSlo2* null background rescued by *dSlo2* expression. Percentage of flies unable to stand or walk were scored as "affected" every day while feeding 0.0018% (Left) and 0.0055% (Right) Imidacloprid to *dSlo2*^{Mi13397}*-Gal4* and *dSlo2*^{Mi13397}*-Gal4>>UAS-dSlo2* flies. n = 8-10 trials with 10 flies per genotype per trial. $p < .05$ (Student's t-test).

line *dSlo2*^{Mi13397}*-Gal4>>UAS-dSlo2* showed enhanced resistance to Imidacloprid exposure at both the lower and higher concentration on days 2 and 3 (Fig. 4.5). Rescue of the behavioral abnormalities further suggests that it is indeed the loss of *dSlo2* that results in enhanced susceptibility to Imidacloprid exposure.

Since a majority of dSlo2-positive cells are cholinergic, I tested whether *dSlo2* protection against Imidacloprid exposure was specific to cholinergic neurons. I attempted to rescue behavior by expressing *dSlo2* in all cholinergic neurons in the *dSlo2* null background. Similar to the *dSlo2*^{Mi13397}*-Gal4* experiment, Gal4 seems to exacerbate the phenotype. Note that the *dSlo2-;Chat-Gal4* line was significantly worse after 2 days of exposure to 0.0018% Imidacloprid (Fig. 4.6) compared to the *dSlo2-* background (Fig. 4.3). However, when combined with two separate *UAS-dSlo2* lines, #18 and #55, roughly half were scored as "affected" compared to the *dSlo2-;Chat-Gal4* background line after 2 days of exposure. Although the Gal4 phenotype complicates the interpretation of these results, the decrease in flies scored as affected upon expression of *dSlo2* in cholinergic neurons suggests that dSlo2 channels indeed attenuate Imidacloprid induced behavioral abnormalities in cholinergic neurons.

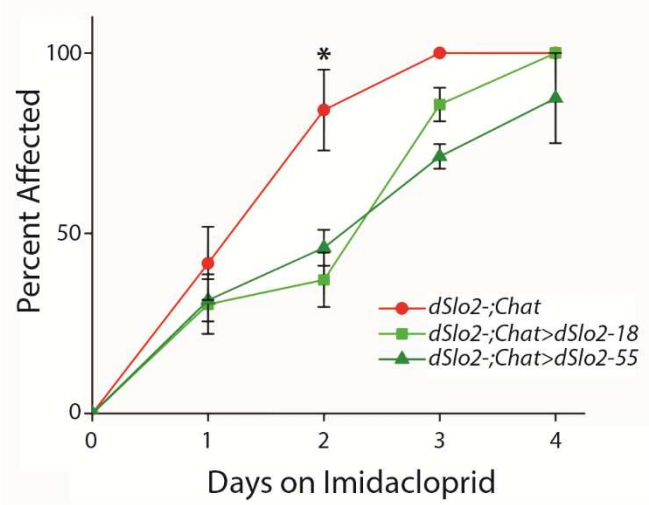

Figure 4.6: *dSlo2* protects against behavioral abnormalities in cholinergic neurons. Percentage of flies unable to stand or walk were scored as "affected" every day while fed 0.0018% Imidacloprid in *dSlo2-;Chat-Gal4* and *dSlo2-;Chat-Gal4>>UAS-dSlo2* flies. n = 3-8 trials with 9-10 flies per genotype per trial. $p < .01$ (Student's t-test).

4.4 The loss of *dSlo2* increases the fraction of flies exhibiting Imidacloprid induced seizure-like behavior

To test if the loss of *dSlo2* exacerbates hyperactivity caused by Imidacloprid, I assayed the flies for mechanically induced seizure-like behavior following Imidacloprid feeding. Mechanical stimulation has been well documented to stress flies, and in some mutants, such as the bang-sensitive mutants, leads to a stereotypic seizure-like behavior (See Section 1.4.2). One of these stereotypic behaviors is paralysis, which immediately follows the mechanical stimulation (reviewed by Parker et al. 2011[195]) and was examined in these assays. Flies were fed Imidacloprid for 24 hours at a concentration of 0.0009%, half of the lowest concentration used in the previous experiments. I found that after 24 hours of exposure to Imidacloprid, wild-type flies did not exhibit a significant increase in paralysis (Fig. 4.7). However, following Imidacloprid feeding roughly 80% of the *dSlo2*- flies exhibited mechanically induced paralysis (Fig. 4.7). This is compared to only 3% exhibiting paralysis when mock fed (Fig. 4.7). These results suggest that dSlo2 channels prevent mechanically induced hyperactivity that is caused by Imidacloprid feeding.

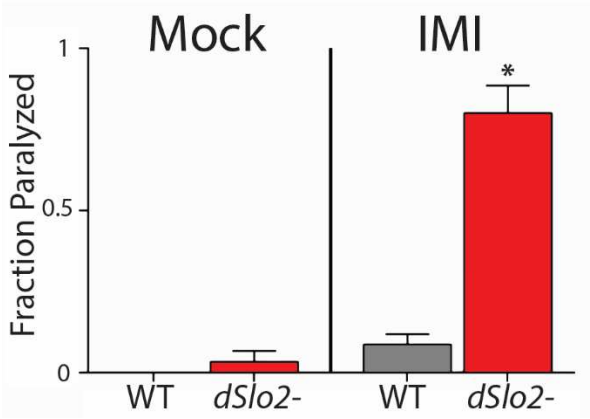

Figure 4.7: Imidacloprid induces hyperexcitable phenotype in *dSlo2*- flies. Fraction of adult flies paralyzed following mechanical stimulation when fed either vehicle ("Mock") or 0.0009% Imidacloprid (IMI) was measured. n = 12-16 trials with 5 flies per genotype per trial. $p < .01$ (Student's t-test).

To test whether dSlo2 is protecting against overexcitation in cholinergic neurons, I tested whether cholinergic expression of *dSlo2* in the *dSlo2*-null background would rescue the mechanically induced paralysis. I similarly fed adult flies 0.0009% Imidacloprid for 24 hours. Following feeding, flies were tested for paralysis caused by mechanical stimulation. *Chat-Gal4* alone exhibited a significant increase in paralysis following Imidacloprid exposure and mechanical stimulation, roughly 70% of flies (Fig. 4.8),

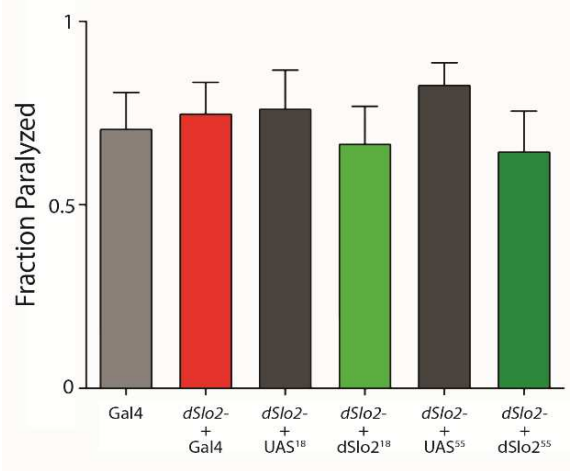

Figure 4.8: Cholinergic expression of *dSlo2* does not prevent paralysis. Fraction of adult flies show paralyzed following mechanical stimulation when fed 0.0009% Imidacloprid (IMI) was measured. Comparisons were made between the background lines (*Gal4, dSlo2- + Gal4*, *dSlo2- + UAS*^{18}, and *dSlo2-+ UAS*^{55}) and the rescue lines (*dSlo2- + dSlo2*^{18} or *dSlo2- + dSlo2*^{55}).

compared to roughly 8% in wild-type flies (Fig. 4.7). This suggests that similar to results from the previous section, Gal4 expression alone increases toxicity of Imidacloprid. Additionally, cholinergic expression of *dSlo2* in the *dSlo2-* line did not prevent paralysis in two separate *UAS-dSlo2* transgenic lines (Fig. 4.8). Interpretation of these results is difficult due to the *Chat-Gal4* line showing such a strong susceptibility to this phenotype compared to the wild-type background.

Results from the previous sections suggest that dSlo2 channels protect against larval death and behavioral dysfunctions in adults caused by Imidacloprid exposure. However, neither of these experiments directly link Imidacloprid exposure to subsequent overexcitation. The findings in this section suggest that dSlo2 channels diminish hyperexcitable behavior caused by Imidacloprid feeding.

4.5 dSlo2 and Dα1 reporters are co-expressed throughout the CNS

After testing whether *dSlo2* protects against Imidacloprid induced hyperactivity, I examined if dSlo2 channels are co-expressed in Dα1-positive neurons. This is important because previous results suggest that Dα1 nAChRs are a specific target of Imidacloprid[346,403–405]. Therefore, if dSlo2 channels are co-expressed with Dα1 nAChRs, it is possible that they prevent overexcitation in neurons activated by Imidacloprid. To test this, I generated a reporter line similar to the *T2A-Gal4* line that expresses LexA in

dSlo2-positive cells. To generate the *dSlo2-LexA* reporter line, I again utilized the "Trojan exon" approach[332] (Section 3.2). I had already verified that the MiMIC insertion, *Mi13397*, when replaced, successfully reported dSlo2 expression. Therefore, I targeted *Mi13397* with a *T2A-LexA* cassette. Additionally, based on the successful incorporation of the *T2A-Gal4* cassette into *dSlo2^{Mi13397}-Gal4*, I knew that the *T2A-LexA* sequence needed to be in phase 2 for proper in-frame translation of *LexA*. Using this information, I obtained a plasmid (gift from Dr. Ben White) that contained the *T2A-LexA* cassette situated in the correct frame such that the *T2A* sequence would terminate translation of *dSlo2* and begin translation of *LexA*. This plasmid was injected into *Drosophila* embryos for recombinase-mediated integration into the *Mi13397* site. Injected flies were crossed to a transgenic line containing the insertion *LexAop-TdTom-nls* and screened for positive insertion of the *T2A-LexA* cassette using fluorescent microscopy. Lines positive for TdTom were then kept as stable stocks, referred to as *dSlo2^{Mi13397}-LexA*.

dSlo2^{Mi13397}-LexA>>LexAop-TdTom-nls was then crossed to the Dα1 reporter line, *Dα1^{Mi00453}-Gal4>>UAS-CD8-GFP* to examine TdTom and CD8-GFP, which would indicate dSlo2 and Dα1 expression, respectively. I found that most Dα1-positive cells also express dSlo2 (Fig. 4.8). In this figure, I have highlighted two regions of the CNS where co-expression was clear. The first was in the motor neurons located in the VNC (Fig. 4.9, left). The second is the Kenyon cells (Fig. 4.9, right). These regions are particularly pertinent for the Imidacloprid induced behavioral abnormalities discussed in this chapter. Both motor neurons and Kenyon cells regulate locomotive behavior in adult flies[411,412]. In both the adult Imidacloprid exposure assay (Section 4.3) as well as the mechanically induced paralysis assay (Section 4.4), flies displayed abnormal locomotor function. Speculatively, expression data suggests that Imidacloprid could activate either or both motor neurons and central neurons, causing disruptions in motor control and leading to the inability to stand or walk, paralysis, and eventually death. Since dSlo2 is expressed in most cells that express Dα1 nAChRs, one possibility is that dSlo2 channels protect neurons that are directly activated by Imidacloprid.

4.6 Conclusion

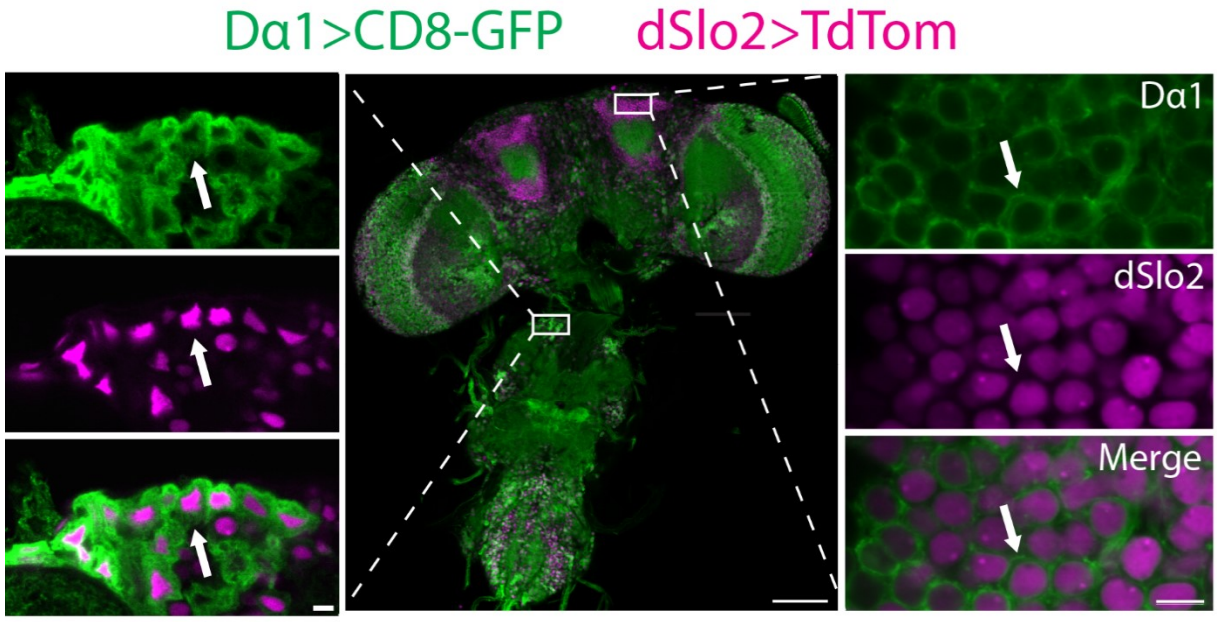

Figure 4.9: Dα1 and dSlo2 are co-expressed throughout the CNS. *dSlo2^{Mi13397}-LexA>>TdTom-nls*;*Da1^{Mi00453}-Gal4>>CD8-GFP* show dSlo2 and Dα1 are co-expressed in cells throughout the CNS, including motor neurons (left) and Kenyon cells (right). Scale Bars: 100µm middle, 10µm left and right.

It has long been hypothesized that the main function of K_{Na} channels is to protect against situations of extreme depolarization[260,262]. Based on early calculations of Na^+ concentrations needed to activate K_{Na} channels, it was hypothesized that these channels might act as a reserve mechanism to repolarize cells following prolonged depolarization[401]. Experiments performed in this chapter set out to test this hypothesis. I exposed flies to cholinergic agonists, with the goal of inducing global hyperexcitability. In the initial experiments, I exposed flies to two different types of cholinergic agonists that have well characterized mechanisms of action (reviewed by Crossthwaite et al. 2017[402]). I found that the loss of *dSlo2* increases susceptibility to Imidacloprid exposure during development, but not to Spinosad. As mentioned previously, this may be due to the binding of these compounds to different nAChRs or due to their differing agonistic properties on the nAChRs. Worth noting, Imidacloprid has been found to have partial agonistic properties, inducing a small amount of inward current through nAChRs, roughly 10% of that induced by Ach in cholinergic *Drosophila* neurons[404]. Spinosad was found to induce a rather large inward current through Dα6 receptors, roughly 5 times as much as Ach when Dα6 was expressed in oocytes[407]. While I did not explore

this further, the ability of dSlo2 channels to hyperpolarize the neurons upon a lower level of depolarizing current but not a significantly larger depolarizing current is an interesting idea. One potential explanation for this is a relatively low level of dSlo2 current. If this were the case, it would then make sense why they may be able to protect against lower levels of depolarization, but unable to hyperpolarize the neuron upon a much greater depolarization. Consistent with this idea, Dr. Hahm in our lab found that the TTX-sensitive K^+ current, encoded by *dSlo2*, is 7% of the total sustained K^+ current in cholinergic neurons. I also did not explore co-expression of dSlo2 and Dα6 receptors in the nervous system. However, indirect evidence from other labs suggests that they are likely co-expressed in multiple regions of the brain. This includes the Kenyon cells, the medulla cortex, and the antennal lobe[413]. Lacking direct evidence of co-expression of dSlo2 channels and Dα6 nAChRs makes it difficult to postulate whether it is indeed the difference in agonistic properties between Imidacloprid and Spinosad that dSlo2 channels protect against.

The second set of experiments showed that the loss of *dSlo2* increased adult fly's susceptibility to behavioral abnormalities caused by Imidacloprid. Combined with the previous results, this suggests that dSlo2 channels are able to protect against overexcitation of the developing nervous system as well as in the adult nervous system. It is worth noting that the *dSlo2^{Mi13397}-Gal4* line exhibited significantly worse behavioral defects following Imidacloprid exposure compared to the *dSlo2-* line. Additionally, when *dSlo2-* was combined with *Chat-Gal4*, flies were much more affected than the *dSlo2-* line. These results indicate that similar to the Spinosad developmental assays, Gal4 may somehow be enhancing the toxicity of insecticide exposure. One potential reason for this is that Gal4 aggregation has previously been associated with apoptosis[410]. Efforts were made to rescue behavior by cholinergic expression of *dSlo2* in the *dSlo2-* line. However, susceptibility of the background Gal4 lines made these results difficult to interpret. Nonetheless, adult exposure results combined with the developmental results suggest a role of dSlo2 channels in attenuating detrimental behavioral effects due to Imidacloprid exposure.

I next tested whether the loss of *dSlo2* would exacerbate behavioral hyperexcitability by examining seizure-like behavior following Imidacloprid feeding. While previous research has strongly suggested that

the toxic effects of Imidacloprid are due to its actions through Dα1 nAChRs[346], it may also have secondary effects that eventually lead to the consequential behavioral deficits and death. It was therefore more informative to test whether Imidacloprid indeed caused a hyperexcitable phenotype, and additionally whether the loss of *dSlo2* exacerbated this behavior. To my knowledge, my results are the first that link Imidacloprid exposure to a hyperexcitable behavioral phenotype. The finding that *dSlo2*- flies were susceptible to Imidacloprid induced seizure-like behavior suggests that the protection that dSlo2 provides against exposure to Imidacloprid is at least partially due to its ability to attenuate hyperexcitability caused by the neonicotinoid. Furthermore, based on co-expression of dSlo2 in most Dα1-positive neurons in the CNS, it is possible dSlo2 channels attenuate excitability directly in neurons stimulated by Imidacloprid.

Upon finding that dSlo2 channels protect against global overexcitation induced by a cholinergic agonist, I wanted to further examine its ability to attenuate other forms of hyperactivity associated with seizure-like behavior. In the following chapter, I test the hypothesis that the loss of dSlo2 channels exacerbates overexcitation in *Drosophila* seizure models with an increased persistent Na^+ current.

CHAPTER 5. DSLO2 PROTECTS AGAINST SPONTANEOUS AND INDUCED SEIZURE-LIKE BEHAVIOR ASSOCIATED WITH AN INCREASED PERSISTENT NA^+ CURRENT

5.1 Overview

In this chapter, I test the hypothesis that dSlo2 channels protect against overexcitation caused by an increase in I_{NaP}. This hypothesis stems from findings in the Salkoff lab that suggest that at least one mode of K_{Na} channel activation is through the I_{NaP}[302,303]. I use *Drosophila* seizure models to test this hypothesis. There are both temperature-sensitive and bang-sensitive mutant lines that exhibit seizure-like behavior associated with an increase in I_{NaP}. The temperature-sensitive line, *GEFS+*, contains a mutation in the voltage gated Na^+ channel, *para*, that is homologous to a mutation in humans that causes Generalized Epilepsy with Febrile Seizures Plus (GEFS+)[116,125]. I found that the *GEFS+;dSlo2-* double mutants were significantly more sensitive to heat induced seizure-like behavior compared to the *GEFS+* background flies. I also examined bang-sensitive mutants which have an increased I_{NaP} associated with the seizure-like behavior. Bang-sensitive flies are sensitive to mechanical stimulation, such that a "bang" on the benchtop, or vortexing, elicits seizure-like behavior[193]. The loss of *dSlo2* prolonged seizure-like behavior following mechanical stimulation in all bang-sensitive lines. Combined, these results suggest that *dSlo2* protects against stress induced seizure-like behavior caused by an increase in I_{NaP}.

I next tested whether dSlo2 channels play a protective role in excitatory neurons of the CNS. I tested this because dSlo2 channels were found to be expressed in cholinergic neurons of the brain (Fig. 3.8). I found that expression of a dominant negative *dSlo2* subunit (*dSlo2-DN*) in cholinergic neurons exacerbates seizure-like behavior in all of the bang-sensitive mutants. I furthermore found that cholinergic expression of *RNAi* specific for *dSlo2* exacerbates seizure-like behavior in one of the bang-sensitive mutants. These findings suggest that dSlo2 channels act protectively in cholinergic neurons.

To further test whether *dSlo2* protects against an increase in I_{NaP}, I examined whether pharmacologically-induced increases in I_{NaP} cause seizure-like behavior, and whether this is exacerbated in the *dSlo2*- mutants. I found that feeding flies Veratridine, a compound that enhances I_{NaP}[303], causes seizure-like behavior in *dSlo2*- flies following mechanical stimulation. Furthermore, this phenotype is not observed in flies lacking either the Ca^{2+}-activated K^+ channel, SK, or the A-type voltage-gated K^+ channel, Shaker. These findings are consistent with the hypothesis that dSlo2 channels protect against increased I_{NaP}, in this case induced by exposure to Veratridine.

While bang-sensitive mutants are well known to require mechanical stimulation to induce seizure-like behavior, I noticed that when combined with the *dSlo2*- mutation, a number of flies exhibited spontaneous seizure-like behavior. I therefore sought to quantify this behavior to determine if my observations were significant. In these assays, I analyzed flies during normal behavior and recorded the number of times they exhibited spontaneous seizure activity. I found that all backgrounds containing an increased I_{NaP}, either caused by bang-sensitive mutations or Veratridine feeding, do not exhibit increased spontaneous seizures. It is only when combined with the *dSlo2* mutation that these flies began to exhibit spontaneous seizures. *dSlo2*- mutants themselves displayed minimal spontaneous seizure activity, suggesting that spontaneous seizure-like activity was induced by the enhancement of I_{NaP}, although only revealed in the absence of dSlo2 channels.

Altogether, these findings strongly suggest that K_{Na} channels protect against hyperactivity caused by an increase in I_{NaP}. These results may have strong implications for human disorders associated with an increase in I_{NaP}. Not only does this include multiple forms of epilepsy[213], but other pathologies such as amyotrophic lateral sclerosis (ALS)[80,250], Fragile X Syndrome (FXS)[248], ischemia[44], and neuropathic pain[249]. As a potential therapeutic target for many different pathologies, the protective nature of K_{Na} channels in other neuropathological models deserves further examination.

5.2 The loss of *dSlo2* exacerbates temperature induced seizure-like behavior caused by increased I_{NaP}

To test the hypothesis that *dSlo2* protects against increased I_{NaP} *in vivo*, I investigated whether the absence of *dSlo2* would exacerbate seizure-like behavior in temperature-sensitive mutants. To first test if dSlo2 channels may affect temperature induced seizure-like behavior, I examined if the loss of *dSlo2* alone would cause a heat induced seizure-like phenotype. I compared wild-type and *dSlo2-* flies placed in a 42˚C water bath. I found that about 50% of the *dSlo2-* flies exhibited seizure-like behavior after 270 seconds, whereas 50% of wild-type flies did not begin to exhibit seizure-like behavior until 360 seconds (Figure 5.1).

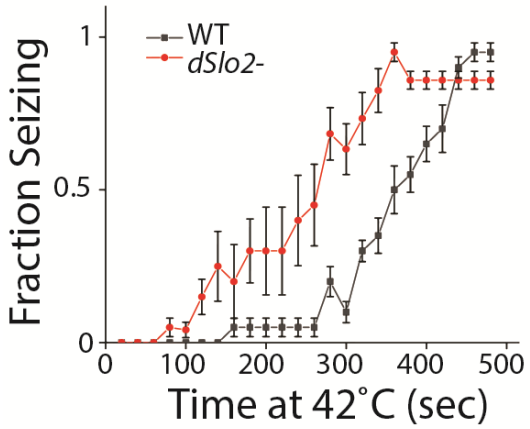

Figure 5.1: Loss of *dSlo2* exacerbates 42˚C seizure-like behavior. Fraction of flies seizing out of 5 was measured at 42˚C. Fraction was counted every 20 seconds. Averages are compared between wild-type (WT) and *dSlo2-*. n = 4 vials with 5 flies each.

This suggests that at elevated temperatures that induce seizure-like behavior in wild-type flies, dSlo2 channels protect against overexcitation. In the temperature-sensitive mutant assays, I examined flies containing mutations homologous to those causing Generalized Epilepsy with Febrile Seizures Plus (GEFS+) and Dravet Syndrome (DS) in humans[116,117]. The temperature-sensitive flies have been shown to display seizure-like behavior at a lower temperature of 40˚C which is the temperature I used in the following experiments[116,117]. Importantly, neither wild-type nor *dSlo2-* flies exhibited seizure-like behavior after 5 minutes of exposure to 40°C (Fig. 5.3B). These temperature-sensitive mutations, recapitulated from the human *SCN1A* gene into the *Drosophila* voltage-gated Na^+ channel, *para*, cause different physiological alterations in the channel function. The GEFS+ mutation (K1270T) leads to an increase in the I_{NaP}, while the DS mutation (S1231R) leads to a decrease in the I_{NaT}[117] (See Chapter 1.4.1). Testing whether the loss of dSlo2 channels exacerbates seizure-like behavior in one or both of these mutant lines will help elucidate

the physiological conditions that the channels protect against. I combined these flies with the *dSlo2* null line and tested whether a greater fraction of the double mutants exhibit heat induced seizure-like behavior at an earlier time point compared to the background line. I found that in the *DS* line, the absence of *dSlo2*, did not exacerbate the seizure-like behavior (Fig. 5.2). Surprisingly, I found that the loss of *dSlo2* slightly protected against seizure-like behavior, as it only took 10 seconds for 50% of the *DS* flies to exhibit seizure-

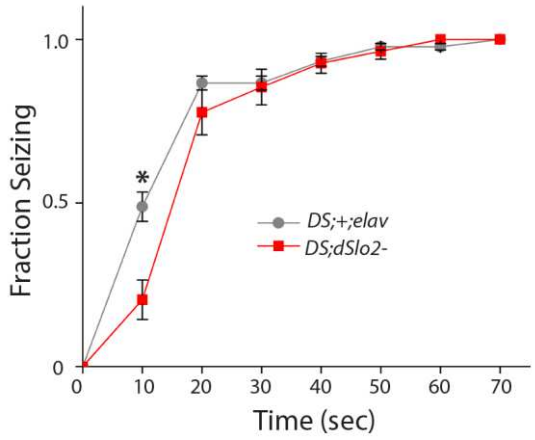

Figure 5.2: Loss of dSlo2 slightly protects against *DS* seizure-like behavior. Fraction of flies seizing out of 5 was measured every 10 seconds at 40˚C. n = 9-11 trials per genotype, 5 flies per trial. $p < .05$ (Student's t-test).

like behavior compared to roughly 15 seconds for 50% of the double mutant line (Fig. 5.2). However, the DS phenotype occurs so quickly after exposure to an elevated temperature that it is difficult to definitively conclude whether the absence of dSlo2 channels provide any protection against the seizure-like behavior caused by a decreased I_{NaT}. In contrast, when I combined the *dSlo2* null line with the *GEFS+* mutation, I found that the loss of dSlo2 channels worsened seizure-like behavior in both the heterozygous and homozygous *GEFS+* flies (Fig. 5.3A and 5.3B) The heterozygous line has previously been shown to be about 50% as likely to exhibit seizure-like behavior compared to the homozygous line after 2 minutes at 40˚C[116], suggesting it is a semidominant mutation. When examining the heterozygous *GEFS+* flies, I found that 50% of the background flies exhibited seizure-like behavior after about 10 minutes. The loss of *dSlo2* caused this to decrease to roughly 5 minutes (Fig. 5.3A). Similarly, 50% of the homozygous double mutant lines exhibited seizure-like behavior at 60 seconds compared to the background *GEFS+* line at 100 seconds (Fig. 5.3B). It would additionally be worth examining whether the combination of the *GEFS+* mutation

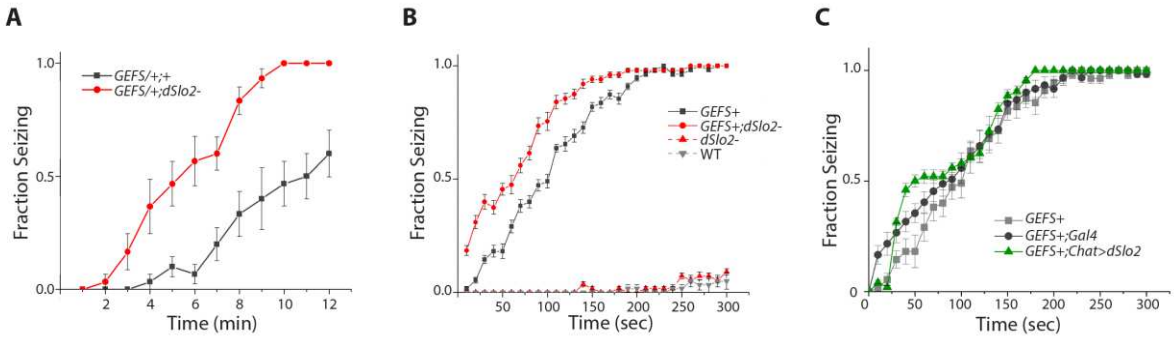

Figure 5.3: Absence of *dSlo2* exacerbates *GEFS+* seizure-like behavior. A) Fraction of flies seizing out of 5 was measured every minute while exposed to 40˚C. n = 6 vials with 5 flies each. $p < .05$ at 4 minutes and $p < .01$ at 5-12 minutes. (Student's t-test) B) Fraction of flies seizing out of 5 was measured every 10 seconds while exposed to 40˚C. n = 10 vials for *GEFS+;Slo2-*, 11 vials for *GEFS+* and *Slo2-*, 12 vials for WT. 5 flies per vial. $p < .05$ at times (10-50, 80-150 sec.) (Student's t-test). C) Fraction of flies seizing out of 5 was measured every 10 seconds while exposed to 40˚C. n = 9-11 vials per genotype, 5 flies per vial.

with the *dSlo2*^{Mi13397}*-Gal4* line causes a decrease in the time for 50% of the flies to exhibit seizure-like behavior. If so, it could be tested whether expression of *UAS-dSlo2* in this background would rescue the increased sensitivity to heat induced seizures. This has not yet been completed. To further test whether *dSlo2* may protect against the *GEFS+* mutation, I attempted to overexpress *dSlo2* to see if this might increase the time it takes to exhibit seizure-like behavior. I overexpressed *dSlo2* in cholinergic neurons, as the majority of *dSlo2*-positive neurons in the brain were previously found to be cholinergic (Fig. 3.8). I found that cholinergic overexpression of *dSlo2* did not alter the time at which 50% of the flies exhibited seizure-like behavior (Fig. 5.3C). One possibility is that overexpression of exogenous *dSlo2* in cholinergic neurons does not increase K_{Na} current. This would need to be tested before these results can be further interpreted.

5.3 The loss of *dSlo2* exacerbates bang-sensitive seizure-like behavior caused by increased I_{NaP}

In addition to testing seizure models induced by heat, I also examined whether *dSlo2* may protect against bang-sensitive seizures caused by an increase in I_{NaP}. These include bang-sensitive flies *bang-senseless* (*bss*), *easily-shocked* (*eas*), and *slamdance* (*sda*)[201,202] (See Chapter 1.4.2). The mechanism underlying the enhanced I_{NaP} in each mutant is different. *sda* and *eas* have been shown to affect alternative

splicing of the single voltage-dependent Na^+ channel gene, *para*, such that there is increased inclusion of exon L^{205}. The increase in I_{NaP} in the *bss* line, however, is caused by a point mutation in the *para* gene itself[201]. These bang-sensitive flies exhibit stereotypic behavioral responses to mechanical stimulation, such as a bang on the benchtop or vortexing[193,199] (Fig. 5.4A). Immediately following the "bang", or during

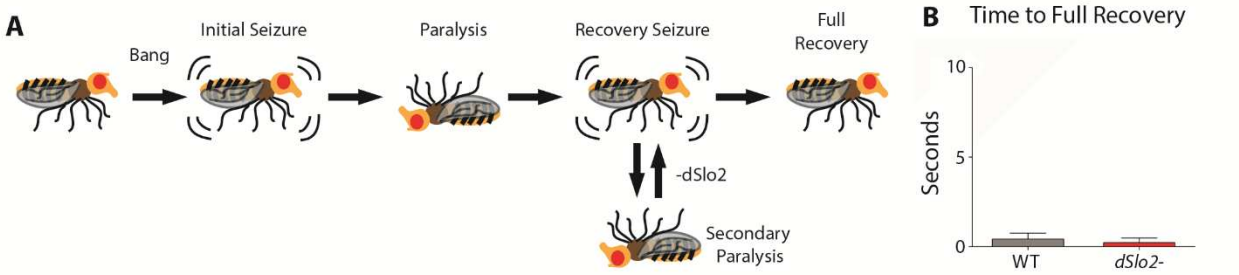

Figure 5.4: *dSlo2*- flies are not bang-sensitive. A) Schematic of typical bang-sensitive behavior. Following a "bang" or vortex for 10 seconds, flies elicit an Initial Seizure followed by a period of Paralysis. Following Paralysis, flies exhibit a Recovery Seizure from which leads to Full Recovery defined as walking or standing without further seizures. When *dSlo2* is knocked out, bang-sensitive flies regularly re-enter a Secondary Paralysis phase following the recovery seizure. B) Time to full recovery following mechanical stimulation was measured in wild-type (WT) and *dSlo2*- flies. n = 18-19 flies per genotype.

stimulation in the case of vortexing, flies exhibit an "Initial Seizure". This is followed by a period of paralysis, in which the fly is not exhibiting any motor function and is usually on its back. Towards the end of the paralytic phase, flies exhibit a "Recovery Seizure", in which they again display uncontrollable motor movement and are unable to stand or walk. In *sda* and *eas*, this recovery seizure is almost always followed by "Full Recovery", in which the fly is able to stand and walk. In the more severe line, *bss*, this recovery seizure usually lasts for roughly 280 seconds, in which it is described to have a prolonged "tonic-clonic-like" behavior, exhibiting multiple bouts of muscle spasms and paralysis[195,201]. Eventually, *bss* flies also fully recover. To first determine whether dSlo2 channels may play a role in mechanically induced seizure-like behavior, I compared the *dSlo2*- flies to wild-type, to determine if they were any more susceptible to mechanically induced seizure-like behavior. I found that both wild-type and *dSlo2*- flies recover almost immediately following the mechanical shock, within 2-3 seconds (Fig. 5.4B). They also do not exhibit any of the stereotypical seizure-like behavior that is seen in the bang-sensitive mutants. This suggests that the absence of *dSlo2* alone does not increase the likelihood of mechanically induced seizure-like behavior.

Following this, I combined the *dSlo2-* line with each of the bang-sensitive lines listed above (*dSlo2-;sda, eas;dSlo2-,* and *bss;dSlo2-*) to test whether the absence of *dSlo2* exacerbates seizure-like behavior in these flies. Flies were placed individually into empty vials and video recordings were taken for the entirety of the behavioral assays. Videos were then analyzed offline, with the genotype blinded to the researcher. I measured time to recovery seizure, which is the amount of time following the 10 second vortex to the time when the recovery seizure began. Also, the fraction of flies exhibiting a secondary paralysis was recorded, which was defined as a period of immobility following the recovery seizure that lasted at least 3 seconds. If flies exhibited a secondary paralysis period, the time spent in the secondary paralysis phase was also measured. Finally, the time to full recovery, which is the total time from the end of the vortex to the fly resuming normal standing or walking behavior, was quantified. I found that in the *sda* line, both the time to recovery seizure and time to full recovery was increased by 41% and 169%, respectively, in the absence of *dSlo2* (Fig. 5.5A). Additionally, I found that all of the *sda* flies went directly from the recovery seizure to full recovery. However, when *dSlo2* was absent, 72% of these double mutant flies exhibited a secondary paralysis phase. This was likely the reason why the time to full recovery increased by 169% in the *dSlo2-;sda* flies. Similarly, the absence of *dSlo2* increased both the time to recovery seizure and time to full recovery in the *eas* line by 19% and 103%, respectively (Fig. 5.5B). Only 16% of *eas* flies exhibited a secondary paralysis. However, roughly 95% of the double mutant *eas;dSlo2-* flies exhibited a secondary paralysis phase. Within the flies that did exhibit a secondary paralysis, the *dSlo2* null flies took roughly 13 seconds longer to recover from this paralytic phase.

When examining whether *dSlo2* plays a role in the *bss* line, which exhibits the most severe phenotype of these three bang-sensitive mutants, I tested both heterozygous and homozygous lines. *bss* mutants have previously been shown to have dominant seizure-like behavior, that is less severe in heterozygotes than the homozygous lines. For example, the *bss/+* line fully recovered much sooner than the homozygous *bss* line, 69.2 seconds and 311.5 seconds, respectively (Fig. 5.5C and 5.5D); suggesting that flies containing the homozygous *bss* mutation in *para* are much more susceptible to mechanical

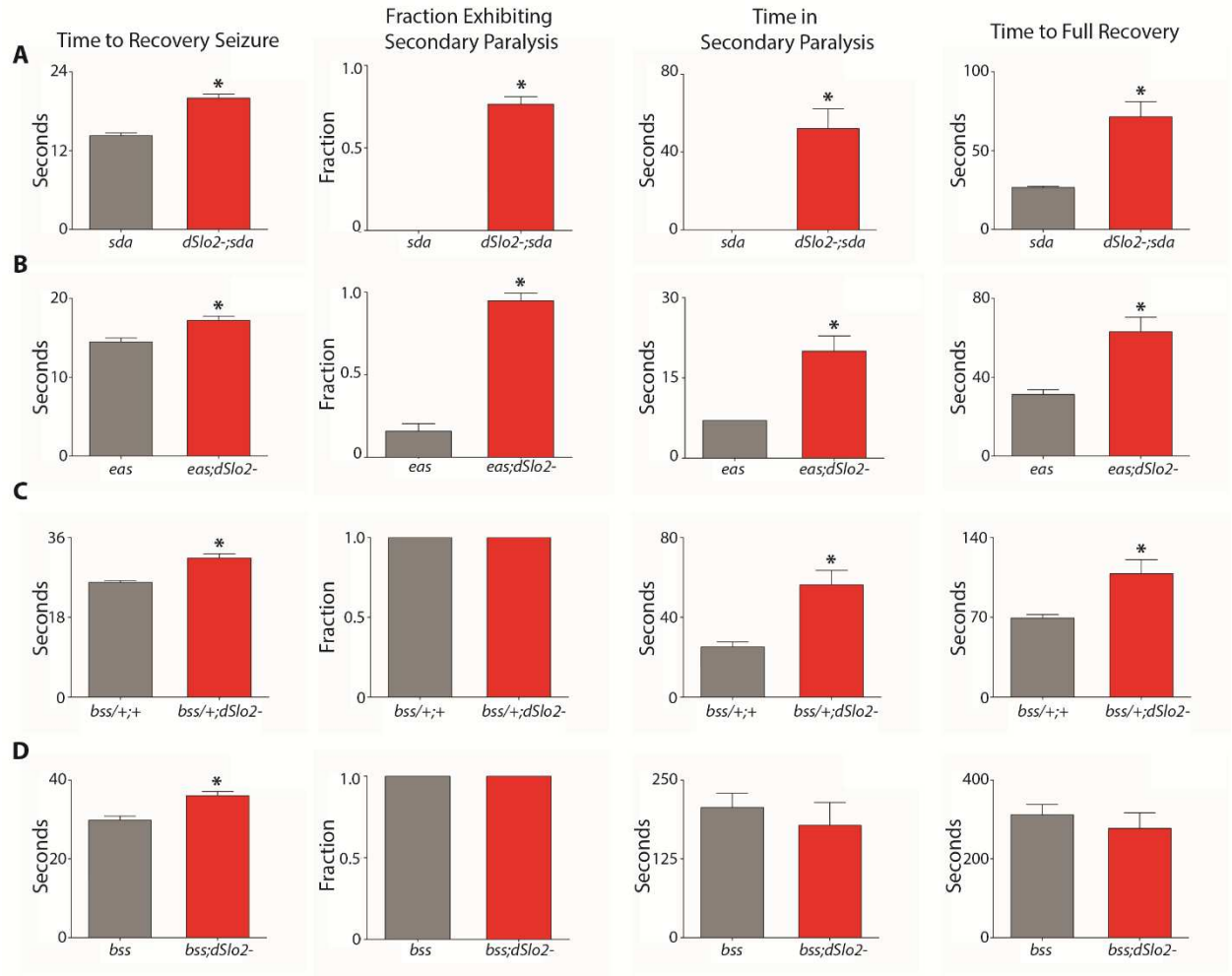

Figure 5.5: Absence of *dSlo2* exacerbates bang-sensitive behaviors. Time to recovery seizure, fraction of flies exhibiting secondary paralysis, time spent paralyzed following the recovery seizure, and time to full recovery were measured in single flies following mechanical stimulation. A) *sda* and *dSlo2-;sda* compared. n = 17-18 flies per genotype. $p < .01$ (Student's t-test). B) *eas* and *eas;dSlo2-* compared. n = 17-18 flies per genotype. $p < .01$ (Student's t-test). C) *bss/+* and *bss/+;dSlo2-* compared. n = 18-19 flies per genotype. $p < .01$ (Student's t-test). D) *bss* and *bss;dSlo2-* compared. n = 18 flies per genotype. $p < .01$ (Student's t-test).

stimulation than the heterozygous line. Unlike the *bss* mutation, both *sda* and *eas* are recessive and must be homozygous to exhibit mechanically induced seizure-like behavior in adult flies. In the heterozygous *bss/+* line, I found that the absence of *dSlo2* increased both the time to recovery seizure and time to full recovery by 22% and 56%, respectively (Fig. 5.5C). Similar to previous descriptions of a prolonged "tonic-clonic" behavior in *bss* flies following mechanical stimulation[195,201], I found that all of the *bss/+* flies exhibited a secondary paralysis phase. Therefore, the loss of *dSlo2* did not increase this phenotype. However, I did find that the loss of *dSlo2* increased the time spent paralyzed during the secondary paralysis

phase by 124%. These results differed from the homozygous *bss* mutants. In these lines, I found that the absence of *dSlo2* only increased the time to recovery seizure, but no other behavioral characteristics (Fig. 5.5D). Combined, these results suggest that endogenous *dSlo2* protects against bang-sensitive seizure behavior. Interestingly, the ability of dSlo2 channels to protect against this behavior is relative to the severity of the behavior, as the less severe *sda, eas,* and *bss/+* showed exacerbated behavior upon the loss of *dSlo2*, but *bss* homozygous flies did not.

To further test whether *dSlo2* is responsible for protection against seizure-like behavior, I tested whether exogenous expression of *dSlo2* in a *dSlo2* null background would rescue or decrease the time to full recovery. To test this, I used the Trojan exon line, *dSlo2^{Mi13397}-Gal4* (previously generated in Chapter 3.2) in combination with the *UAS-dSlo2* transgenic lines generated in Chapter 4.3. As a reminder, the *T2A-Gal4* sequence in *dSlo2^{Mi13397}-Gal4* is expected to terminate translation of *dSlo2* upstream of the S1 transmembrane domain[332,341], thereby acting as a *dSlo2* null line. If combined with *UAS-dSlo2*, it is expected that exogenous *dSlo2* would then be expressed in all cells that normally express *dSlo2*. I examined whether the time to full recovery in the *eas* line might be decreased in this rescue experiment. In preparation for the experiments, I found that *eas;dSlo2^{Mi13397}-Gal4* flies would only survive as heterozygous flies for the *dSlo2^{Mi13397}-Gal4* insertion. Therefore, I performed transient crosses between *eas;dSlo2-* and *eas;dSlo2^{Mi13397}-Gal4* lines, to produce progeny that were null for *dSlo2* but still express Gal4 in *dSlo2*-positive cells. The time to full recovery was compared between the background lines, and two other transgenic lines containing insertions of *UAS-dSlo2*, lines #18 and #55. Importantly, the *eas;dSlo2^{Mi13397}-Gal4/dSlo2-* line increased the time to recovery similar to that of *eas;dSlo2-* (Fig. 5.6), suggesting that it indeed acts as a *dSlo2* null line. Expression of exogenous *UAS-dSlo2* in the *eas;dSlo2^{Mi13397}-Gal4/dSlo2-* background did not decrease the time to full recovery (Fig. 5.6). Since the *eas;dSlo2^{Mi13397}-Gal4* line only lives as a heterozygote for the *dSlo2^{Mi13397}-Gal4* insertion, while *eas;dSlo2-* flies live as homozygotes, Gal4 may be detrimental to these flies and perhaps this prevents them living as homozygotes; Gal4 aggregation has been found to be toxic in some cases[410]. With only one copy of the *dSlo2^{Mi13397}-Gal4* and *UAS-dSlo2*

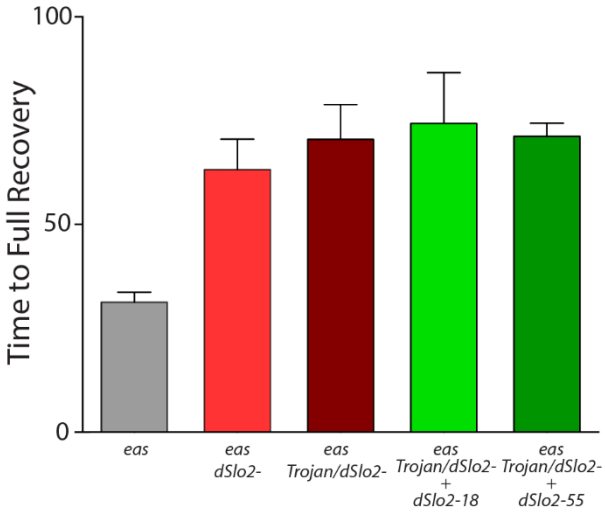

Figure 5.6: *dSlo2*^{Mi13397}*-Gal4* driving *dSlo2* expression did not rescue *dSlo2* null phenotype. Time to full recovery of individual flies was measured. *eas* and *eas;dSlo2-* data from Fig. 5.5, added for comparison. n = 7-11 flies per genotype.

transgenes, the inability to decrease the time to recovery could be due to insufficient exogenous *dSlo2* expression.

Overall, these findings suggest that endogenous dSlo2 channels protect against mechanically induced seizure-like behavior that is caused by increases in I_{NaP}.

5.4 dSlo2 channels protect flies from mechanically triggered seizure-like behavior actuated by pharmacological enhancement of I_{NaP}

To further explore the hypothesis that dSlo2 protects against seizure-like behavior caused by an increase in I_{NaP}, I examined whether *dSlo2-* flies would be more susceptible to mechanically induced seizure-like behavior following feeding of pharmacological drugs shown to increase I_{NaP}. To do this, I used two separate compounds that have been shown to enhance I_{NaP}, Anemone toxin (ATX-II) and Veratridine[303,414]. To my knowledge, only one study has examined the consequences of feeding *Drosophila* Veratridine, which examined the poisonous effects in adults[415]. Additionally, I'm aware of only one study that fed *Drosophila* larvae ATX-II to examine consequences of an increased I_{NaP}[202]. Therefore, I first had

to troubleshoot feeding methods and drug concentrations to determine if flies exhibited any seizure-like behavior following feeding.

For the ATX-II experiments, I tested two different concentrations as well as feeding methods. The first method used a lower concentration of ATX-II, 100nM, and flies were fed over three days. This concentration was sufficient to prolong recovery time in wild-type larvae similar to that of *sda* larvae following electrical shock[202]. In these assays, the drug was embedded in a sucrose-agar solution for feeding. Following feeding, flies were vortexed and examined for seizure-like behavior immediately following mechanical stimulation. In these assays, similar to the observation in Section 5.3, neither the wild-type or *dSlo2-* flies exhibited the stereotypic behavior seen in the bang-sensitive flies. Flies were instead scored for uncontrollable motor movements or an inability to stand or walk immediately following stimulation. I found that ATX-II treatment did not increase the fraction of flies seizing in either wild-type or *dSlo2-* flies (Fig. 5.7A). There is a large variability in these results due to the limited number of trials, which were abandoned

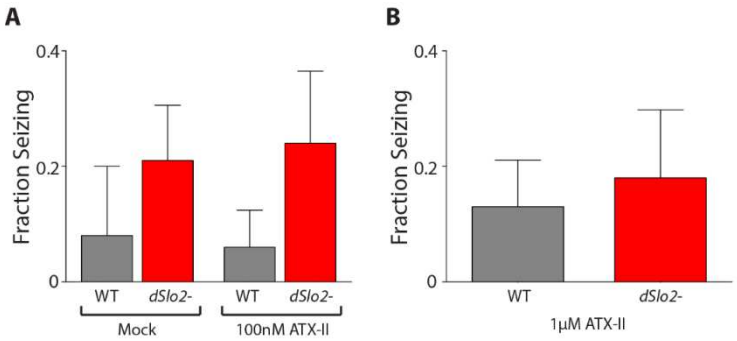

Figure 5.7: ATX-II does not cause mechanically induced seizure-like behavior. A) Fraction of flies exhibiting mechanically induced seizure-like behavior was examined in both vehicle ("mock") and 100nM ATX-II fed flies. n = 5 vials in Mock and 10 vials in 100nM ATX-II, 5 flies per vial. B) Fraction of flies exhibiting mechanically induced seizure-like behavior was examined in flies fed 1μM ATX-II. n = 5 vials per genotype, 5 flies per vial.

as there was no indication this treatment regimen was increasing seizure-like behavior. I therefore attempted to increase the concentration and alter the feeding method. In this assay, I fed flies ATX-II at 1μM for 24 hrs. on filter paper soaked in a sucrose solution. Similar to the previous assay, I found that ATX-II treatment did not increase the fraction of wild-type flies seizing above the fraction of *dSlo2-* flies (Fig. 5.7B).

Therefore, I ended the trials with ATX-II and moved forward with experiments utilizing Veratridine instead.

For Veratridine feeding, I decided to use the sucrose-soaked filter paper feeding method. In this case, flies were first starved on H_2O soaked filter paper for 24 hrs. This was done to try and increase the likelihood that flies would consume sufficient amounts of the Veratridine-sucrose solution. Following starvation, flies were fed with the Veratridine-sucrose soaked filter paper for an additional 2 hrs. Immediately following feeding, flies were tested for bang-sensitive seizure-like behavior. I found that *dSlo2-* flies were significantly more likely to exhibit seizure-like behavior compared to wild-type in the mock fed control trials (Fig. 5.8, left). Worth noting, the mock treatment in this assay differs from the mock treatment shown in Figure 5.7A in that these assays used sucrose-soaked filter paper for drug feeding for 2 hours whereas the previous experiment used a sucrose-agar solution, and flies were fed over 3 days. This

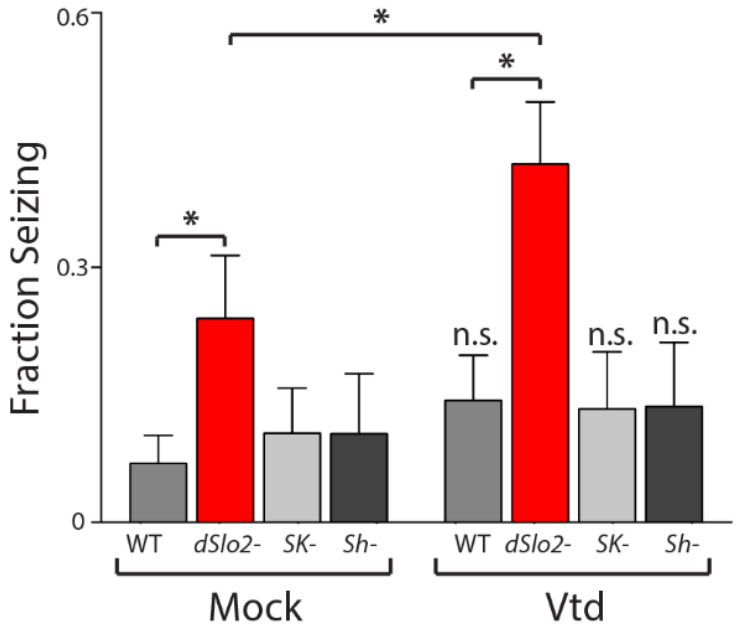

Figure 5.8: *dSlo2-* flies susceptible to mechanically induced seizure-like behavior actuated by Veratridine. Fraction of flies seizing out of 5 following mechanical stimulation was examined in flies either vehicle ("Mock") or Veratridine ("Vtd") fed. n = 21-23 vials for WT and *dSlo2-* and 10-12 vials for *SK-* and Sh^{ks133} per treatment, 5 flies per vial. $p < .05$ (Student's t-test) (*). Also, $p < .05$ for *dSlo2-* Vtd compared to all genotypes, but not highlighted. Vtd treated WT, *SK-*, and Sh^{ks133} were not significant (n.s.) compared to the same genotype mock treated.

difference may be the cause for the change in significance. Additionally, I found a significant increase in mechanically induced seizure-like behavior in the *dSlo2*- flies fed Veratridine compared to the mock treatment (Fig. 5.8). This increase was not observed in wild-type flies. To test whether protection against Veratridine is specific to dSlo2 channel function, and not just a general K^+ channel phenotype, I also tested whether mutants for other K^+ channels exhibit seizure-like behavior following treatment with Veratridine. I tested mutants for the small conductance Ca^{2+}-activated K^+ channel (*SK*-)[338] and the A-type voltage-gated K^+ channel Shaker (Sh^{ks133})[194]. I found that the fraction of *SK*- and Sh^{ks133} flies seizing did not increase following Veratridine treatment and were not greater than the fraction of wild-type flies seizing following Veratridine treatment (Fig. 5.8). Furthermore, *dSlo2*- flies were significantly more likely to exhibit seizure-like behavior than both *SK*- and Sh^{ks133} mutants after treatment with Veratridine.

Results in the Veratridine treatment assays are consistent with the hypothesis that dSlo2 protects against increases in I_{NaP}. The loss of *dSlo2* exacerbated seizure-like behavior when I_{NaP} was increased either genetically, as in the bang-sensitive and temperature-sensitive flies, or pharmacologically with Veratridine. Furthermore, the *SK*- and Sh^{ks133} mutant flies do not exhibit worsened seizure-like behavior actuated by increased I_{NaP}. This suggests that the protective nature of dSlo2 channels may be due to their activation by internal Na^+. These results suggest that K_{Na} channels may play a critical role in protecting against epilepsy caused by an increased I_{NaP}.

5.5 Bang-sensitive seizure-like behavior is exacerbated by blocking dSlo2 conductance in cholinergic neurons

To test if *dSlo2* protects against seizure-like behavior specifically in cholinergic neurons, I drove expression of *UAS-dSlo2-RNAi* in cholinergic neurons using a Choline Acetyltransferase (ChAT) Gal4 line (*ChAT-Gal4*). The *UAS-dSlo2-RNAi* transgene is located on the third chromosome, the same chromosome containing the mutation for *sda*. Since the *sda* mutation must be homozygous to cause bang-sensitivity, I was only able to test *eas* and *bss* flies in this experiment. Additionally, as the *bss* flies only showed

exacerbated seizure-like behavior as a heterozygote with *dSlo2*-, I only tested the heterozygous *bss/+* line in this assay. I found that knockdown of *dSlo2* in cholinergic neurons increased the time to full recovery in the *eas* line (Fig. 5.9A). However, I did not find a similar exacerbated phenotype in the heterozygous *bss/+*

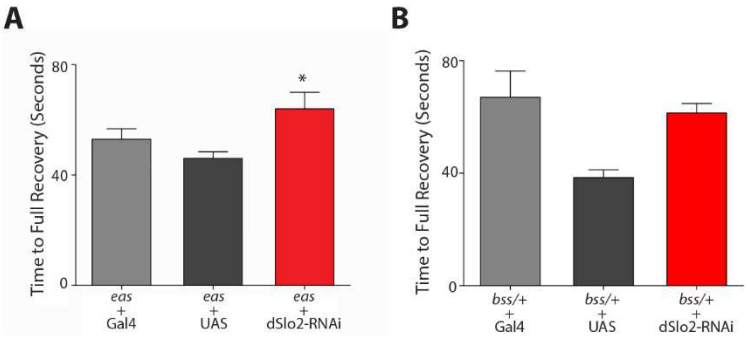

Figure 5.9: Expression of *dSlo2-RNAi* in cholinergic neurons prolongs time to full recovery in *eas* flies. Time to full recovery was measured in individual flies following mechanical stimulation. A) Cholinergic expression of *dSlo2-RNAi* in *eas* background. n = 17-19 flies per genotype. $p < .05$ (Student's t-test). B) Cholinergic expression of *dSlo2-RNAi* in *bss/+* background. n = 14-19 flies per genotype.

line (Fig. 5.9B). This *RNAi* line was made in a large transgenic generation project, and to my knowledge has not been tested for efficacy. Therefore, it is possible that it only acts as a partial knockdown. It would be useful to test the level of knockdown caused by the *RNAi* by examining dSlo2 protein levels by Western blot. This would help determine whether or not dSlo2 protein levels are actually decreased as a result of *dSlo2-RNAi* expression. Due to the minimal increase in time to recovery when driving cholinergic expression of *dSlo2-RNAi* in *eas* and *bss/+* backgrounds, I sought to use a different technique to test the hypothesis that endogenous dSlo2 channels protect cholinergic neurons against hyperxcitability. In these assays, I generated a transgenic line that expresses a dominant negative coding sequence for dSlo2 (*dSlo2-DN*). To do this, the *UAS-dSlo2* sequence was mutated to alter the coding sequence for the pore region. The pore sequence was mutated such that the consensus K^+ channel pore forming glycine-tyrosine-glycine amino acids would instead code for alanine-alanine-alanine (GYG>AAA). Importantly, mutation of the hydrophobic tyrosine amino acid to an alanine prevents K^+ conductance[336–338], thereby generating a dominant negative subunit (Fig. 5.10). The *UAS-dSlo2-DN* transgene was inserted in the *Drosophila*

genome, and lines positive for the insertion were confirmed using RT-PCR and tested for overexpression using *elav-Gal4* similar to the *UAS-dSlo2* confirmation in Chapter 4.3.

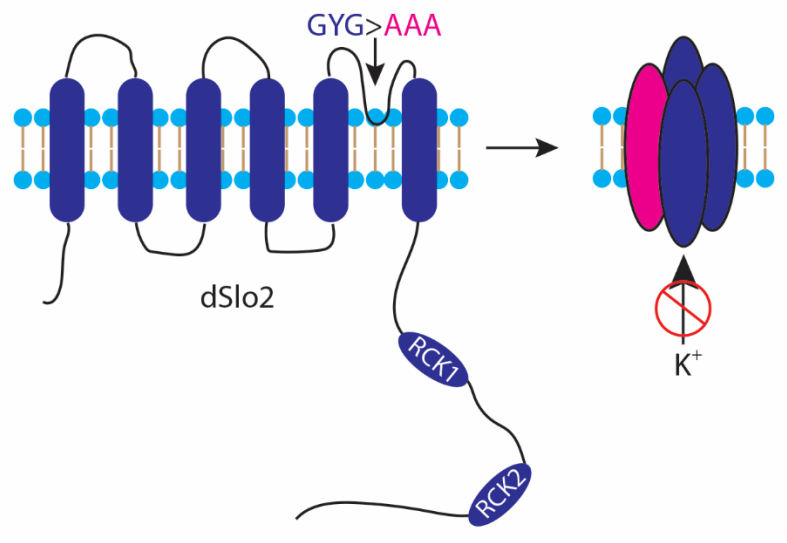

Figure 5.10: Dominant-negative dSlo2 subunit. Schematic of dSlo2 protein with the mutation of the consensus pore amino acid sequence GYG to AAA. When this dSlo2-DN subunit tetramerizes with wild-type subunits, it will prevent K^+ conductance (Barry et al. 1998, Ping et al. 2011, About Tayoun et al. 2011).

Based on the results from Chapter 5.2 that the loss of *dSlo2* exacerbates bang sensitive seizure-like behavior, I tested whether cholinergic expression of *dSlo2-DN* would similarly worsen seizure-like behavior in *sda*, *eas*, and heterozygous *bss/+* lines. In all of these experiments, I used both the *ChAT-Gal4* and *UAS-dSlo2-DN* lines as genetic backgrounds. When combined with *sda*, I found that both the time to recovery seizure as well as full recovery was increased by roughly 20% and 73%, respectively, when *dSlo2-DN* was expressed in cholinergic neurons (Fig. 5.11A). Also, similar to the *dSlo2-;sda* double mutant, only when *dSlo2-DN* was expressed in cholinergic neurons did the *sda* flies exhibit a secondary paralysis period following the recovery seizure (Fig. 5.11A). I found that cholinergic expression of *dSlo2-DN* in *eas* and *bss/+* led to an increase in the full time to recovery but did not alter the other behavioral phenotypes (Fig. 5.11B and 5.11C). It is worth noting that the time to full recovery was increased roughly 23% in *eas;Chat>>dSlo2-DN* compared to background lines and 8% in *bss/+;Chat>>dSlo2-DN* compared to background lines (Fig. 5.11B and 5.11C); In contrast, the loss of *dSlo2* caused an increase of 103% in

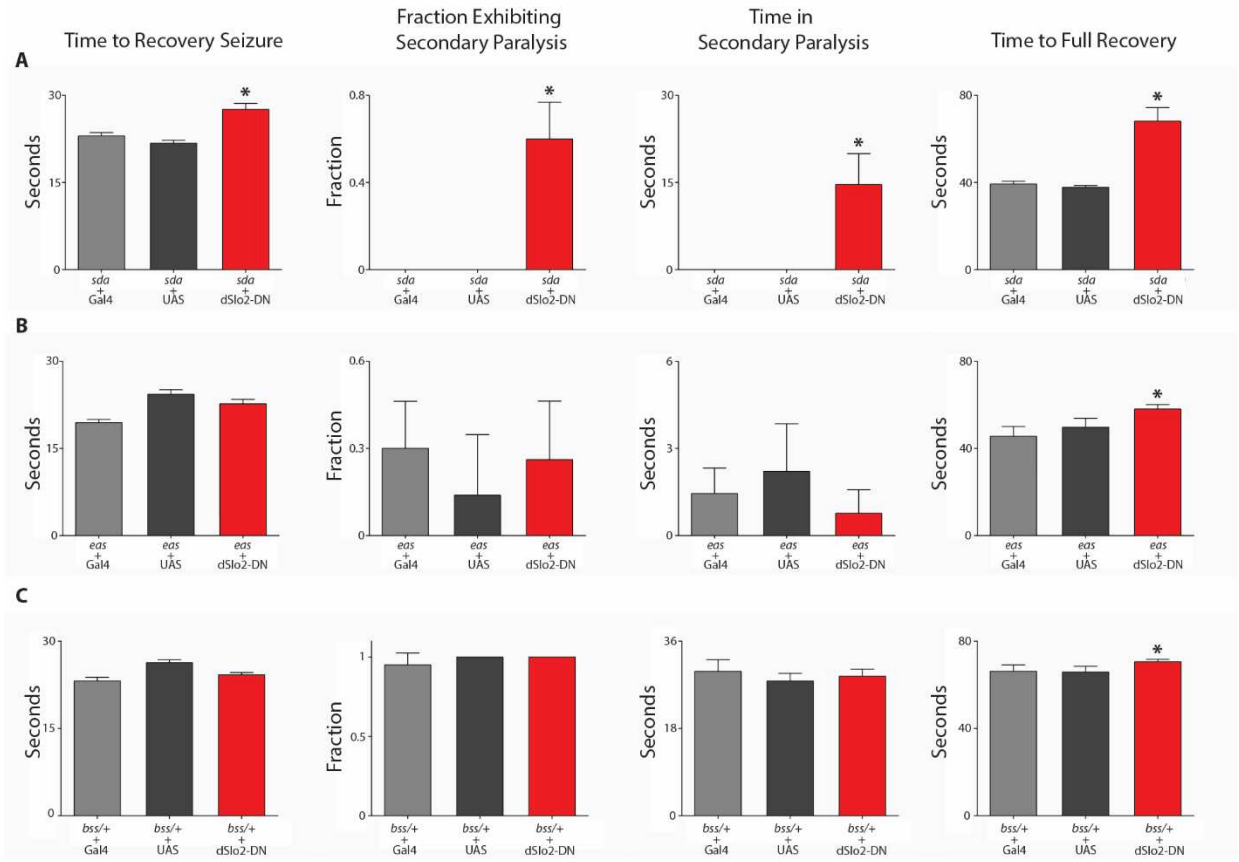

Figure 5.11: Expression of *dSlo2-DN* in cholinergic neurons prolongs seizure-like behavior. Time to recovery seizure, fraction of flies exhibiting secondary paralysis, time spent paralyzed following the recovery seizure, and time to full recovery were measured in single flies following mechanical stimulation. A) *ChAT-Gal4>>UAS-dSlo2-DN* examined in the *sda* background. n = 19-22 flies per genotype. $p < .01$ (Student's t-test). B) *ChAT>>UAS-dSlo2-DN* examined in *eas* background. n = 18-20 flies per genotype. $p < .05$ (Student's t-test). C) *ChAT-Gal4>>UAS-dSlo2-DN* examined in *bss/+* background. n = 18-19 flies per genotype. $p < .05$ (Student's t-test).

eas;dSlo2- and 56% in *bss/+;dSlo2-* compared to their background lines (Fig. 5.5B and 5.5C). The less severe increase in the time to full recovery could be the result of the dominant negative subunit not completely blocking K_{Na} current in cholinergic neurons. An alternative reasoning could be that *dSlo2* is not only protecting against overexcitation in cholinergic neurons but may also be playing an important role in other neurons such as the glutamatergic motor neurons. Also worth noting is that similar to the assays testing the *dSlo2-* line (Fig. 5.5), the greatest increase in seizure-like behavior is in the least severe bang-sensitive mutant *sda*. This suggests that dSlo2 channels are able to protect most against the least severe

seizure-like behavior; implying that there may be some limit of overexcitation that dSlo2 channels are able to counteract, but beyond this limit they no longer can protect against the seizure-like behavior.

Based on expression data from Chapter 3, I further examined whether *dSlo2* may protect against seizure-like behavior in a subset of cholinergic neurons, the Kenyon cells. Kenyon cells are most known for their role in associative learning[355–358]. However, they have also been implicated in motor control[411] as well as the initiation of the bang-sensitive seizure-like behavior[207]. Therefore, dSlo2 channels may be ameliorating seizure-like behavior by dampening excitability in this subset of neurons. To test this hypothesis, I drove either *dSlo2-DN* or *dSlo2-RNAi* specifically in the Kenyon cells using the *201y-Gal4* driver line, which has previously been shown to express Gal4 in the Kenyon cells[416]. I found that in the *sda* background, driving expression of two separate *dSlo2-DN* transgenes did not increase the time to full recovery compared to their backgrounds (Fig. 5.12A). I additionally did not see an increase in the time to full recovery in *eas* when I expressed either *dSlo2-DN* or two separate *UAS-dSlo2-RNAi* transgenes (Fig. 5.12B). Lastly, the *bss/+* heterozygous background also did not exhibit an increased time to full recovery when *dSlo2-RNAi* was expressed in the Kenyon cells (Fig. 5.12C). These findings suggest that endogenous *dSlo2* does not protect against seizure-like behavior in just the Kenyon cells. It is possible that dSlo2

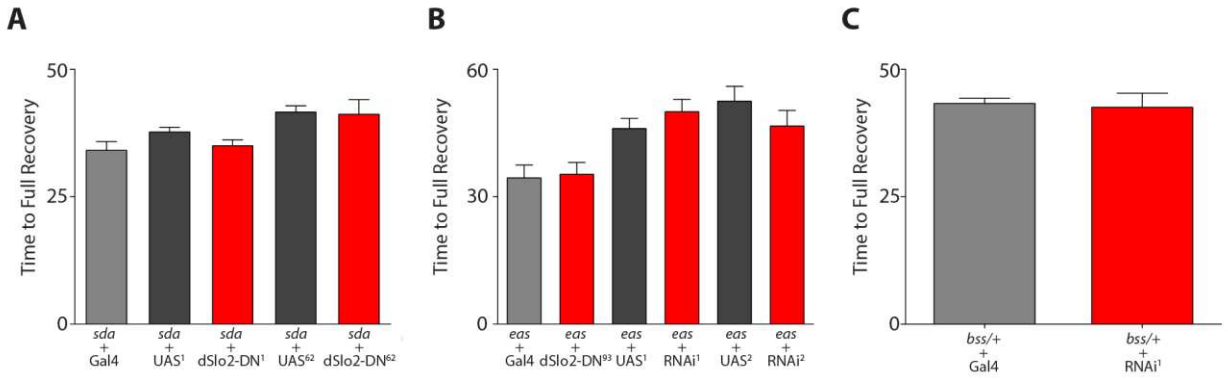

Figure 5.12: Blocking dSlo2 function in the Kenyon cells does not exacerbate time to full recovery in bang-sensitive flies. Time to full recovery following mechanical stimulation was examined in individual flies. A) *201y-Gal4>>UAS-dSlo2-DN* wass examined in the *sda* background. n = 6-19 flies per genotype. B) *201y-Gal4>>UAS-dSlo2-DN* or *UAS-dSlo2-RNAi* was examined in the *eas* background. n = 17-19 flies per genotype. C) *201y-Gal4>>UAS-dSlo2-RNAi* was examined in the *bss/+* background. n = 16-18 flies per genotype.

channels protect against seizure-like behavior in another subset of cholinergic neurons. It is also possible that dSlo2 channels are only able to protect against overexcitation in a large group of cholinergic neurons and are not acting within just a subset of neurons to attenuate seizure-like behavior.

5.6 Attempts to increase dSlo2 activity or pharmacologically decrease I_{NaP} did not attenuate seizure-like behavior in bang-sensitive seizure models

Since endogenous *dSlo2* expression seems to protect against seizure-like behavior, I tested the hypothesis that enhancing dSlo2 channel current pharmacologically would decrease the time to full recovery in the bang-sensitive mutants. To accomplish this, I fed *eas* flies Loxapine which was found to be a potent activator of K_{Na} channels[417]. In these experiments, I fed *eas* flies Loxapine at two different concentrations and then tested whether this would decrease the time to full recovery following mechanical stimulation. I found that feeding *eas* flies either 10μM or 100μM Loxapine for 24 hours did not reduce the time to full recovery (Fig. 5.13A and 5.13B). I additionally tested if Loxapine decreased the time to full recovery in *eas;dSlo2-* flies to examine the specificity of Loxapine for dSlo2 channels. However, as no prevention was seen in the *eas* line, this portion of the experiment did not confirm this. These findings are difficult to interpret as there was no significant decrease in seizure-like behavior in either experiment. This may result from an inability of Loxapine to reach dSlo2 channels, not enough Loxapine being fed to the flies, or minimal to no effect of Loxapine on dSlo2 channels.

In addition to pharmacological activation of dSlo2 channels, I hypothesized that increased expression of *dSlo2* might decrease the severity of seizure-like behavior. To test this hypothesis, I examined if *dSlo2* overexpression in cholinergic neurons may decrease the time to full recovery in the bang-sensitive flies. To do this, I used the transgenic *UAS-dSlo2* lines described in Chapter 3.3, in combination with a *ChAT-Gal4* line. This allowed for targeted overexpression of *dSlo2* in all cholinergic neurons. I used multiple transgenic lines containing the *UAS-dSlo2* insertion, as the insertion site of the transgene typically affects expression levels of exogenous *dSlo2*. I tested both the *eas* and *bss* lines. In these experiments, I

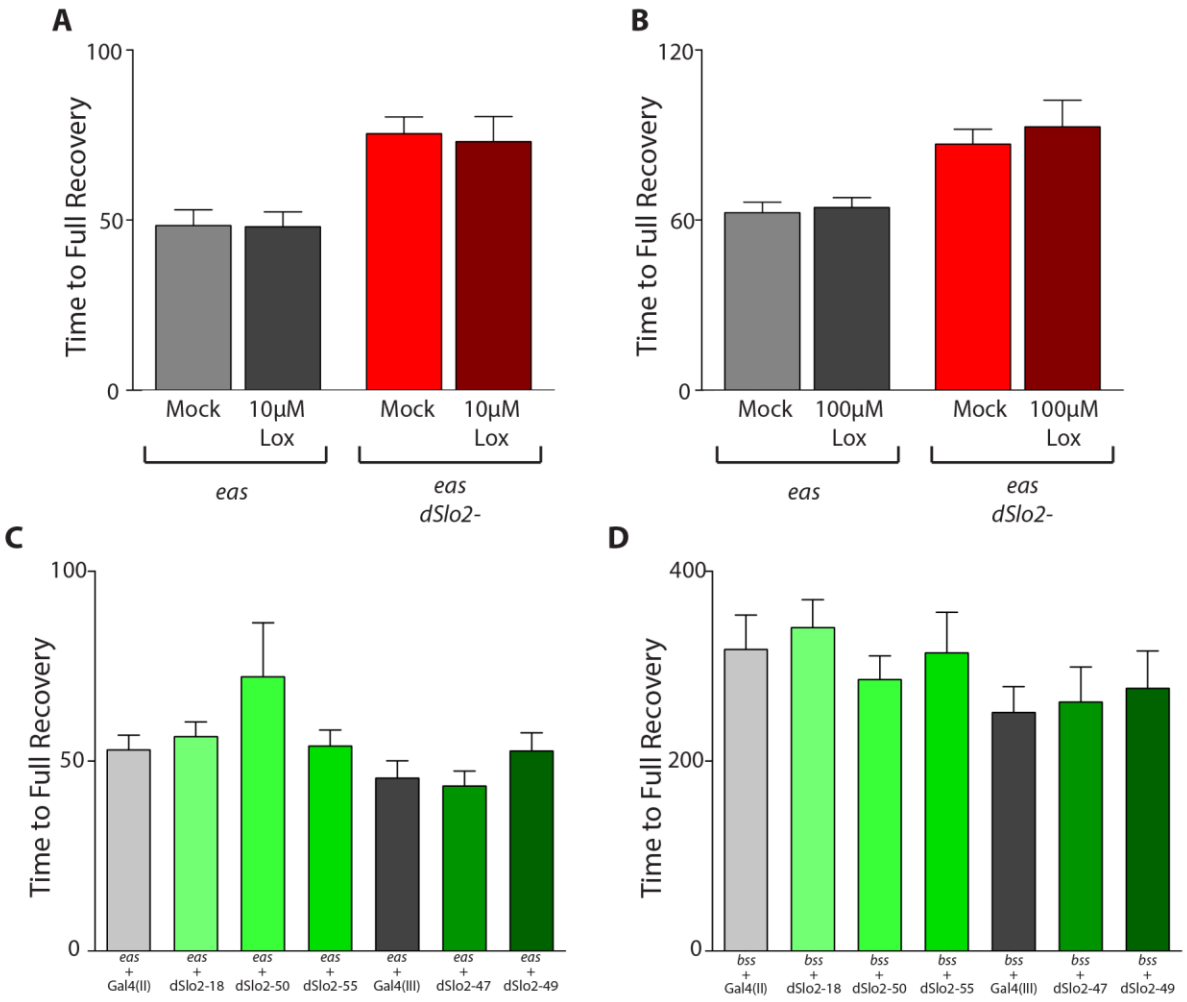

Figure 5.13: Pharmacological activation or cholinergic overexpression of dSlo2 do not attenuate time to full recovery. A) *eas* and *eas;dSlo2-* were fed either vehicle ("mock") or 10μM Loxapine and the time to full recovery following mechanical stimulation was tested. B) *eas* and *eas;dSlo2-* were fed either vehicle ("mock") or 100μM Loxapine and the time to full recovery following mechanical stimulation was tested. C) Time to full recovery was examined in *eas* flies overexpressing *dSlo2* in cholinergic neurons. D) Time to full recovery was examined in *bss* flies overexpressing *dSlo2* in cholinergic neurons.

found that in both *eas* and *bss*, cholinergic overexpression of *dSlo2* did not lead to a decrease in the time to full recovery (Fig. 5.13C and 5.13D). For these experiments I used two transgenic *ChAT-Gal4* lines, which were inserted on either the second or third chromosome. These were combined with five different *UAS-dSlo2* lines, #18, #50, and #55 with *ChAT-Gal4* on the second chromosome, and #47 and #49 with *ChAT-Gal4* on the third chromosome. The inability to decrease the time to full recovery in all lines suggests that overexpression of *dSlo2* is not able to protect against this behavior. However, multiple controls have not

been performed to confirm that this is the case. For instance, it has not been shown that overexpression of *dSlo2* leads to an increased K_{Na} current. Without knowing this, it is difficult to discern whether increasing the K_{Na} current in cholinergic neurons indeed does not protect against bang-sensitive seizure behavior.

I also hypothesized that decreasing I_{NaP} in bang-sensitive mutants might protect them against seizure-like behavior. Furthermore, if dSlo2 channels attenuate hyperexcitability caused by the increased I_{NaP}, then the absence of *dSlo2* should no longer exacerbate the phenotype upon a decrease in I_{NaP}. Therefore, the double mutant lines would be expected to behave similarly to the background. To test this hypothesis, I fed flies either Phenytoin or Avobenzone. These drugs have previously been shown to decrease I_{NaP} in bang-sensitive flies, and decrease the time to full recovery[202,256]. Phenytoin was found to decrease alternative splicing of exon *L* into *para*, thereby decreasing the I_{NaP} of *sda* mutants to levels of that observed in wild-type flies[202]. Avobenzone feeding was found to increase expression of *pumilio*, a translation represser, whose increased expression correlated with a decreased I_{NaP} in *bss* mutants[256]. Based on these findings, I fed *sda* and *eas* flies Phenytoin or Avobenzone to determine if this would decrease the time to full recovery. However, I found there was not a significant reduction in the time to full recovery following treatment as previously reported (Fig. 5.14A and 5.14B). Additionally, double mutant bang-sensitive flies lacking *dSlo2* did not exhibit a decreased time to full recovery (Fig. 5.14A and 5.14B). These findings are difficult to interpret, as there was no protection observed in the *sda* and *eas* lines treated with Phenytoin or Avobenzone. Differing from previous studies that fed Phenytoin and Avobenzone to *sda* and *eas* larvae[202,256], I fed them to adult flies. Therefore, mechanisms of the drug in the adult, as well as the ability of the drug to reach its target, may differ from the larvae. I attempted increasing the concentration two-fold to see if that reduced the time to full recovery, but this concentration caused adverse effects in the flies. Therefore, it was unclear how best to proceed with these drugs in the adult bang-sensitive assays.

While the results of the studies in this section were inconclusive, the underlying hypotheses could be pursued further. For instance, other drugs besides Loxapine have been suggested to activate K_{Na} channels, such as bithionol and niclosamide[417]. These could be fed to bang-sensitive flies at varying

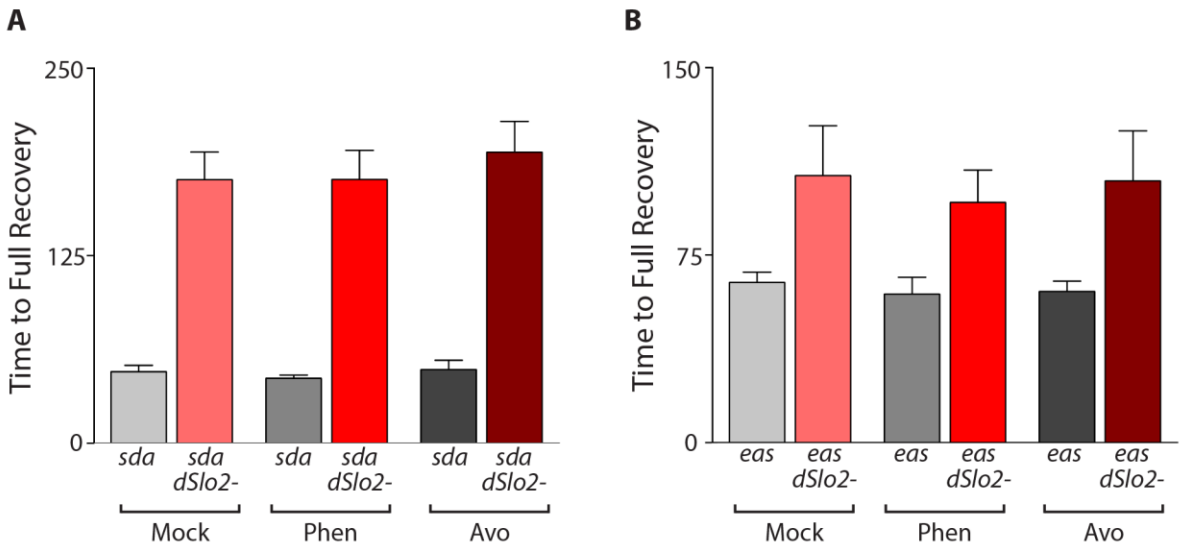

Figure 5.14: Pharmacologically decreasing I_{NaP} does not decrease the time to full recovery. A) Time to full recovery following mechanical stimulation was tested following treatment of *sda* or *dSlo2-;sda* with either 4mg/mL Phenytoin or 4mg/mL Avobenzone. B) Time to full recovery following mechanical stimulation was tested following treatment of *eas* or *eas;dSlo2-* with either 4mg/mL Phenytoin or 4mg/mL Avobenzone.

concentrations to see if they reduce the time to full recovery. To further test if decreased I_{NaP} reduces the time to full recovery in both the bang-sensitive mutants with and without *dSlo2*, there have been reports of genetic manipulation of an RNA binding protein, *pasilla*, that alters the splicing in of exon *L* in *sda* flies, thereby decreasing I_{NaP} and the time to recovery[205]. Future experiments could combine the *dSlo2-* and *pasilla* mutant lines, and test whether this brings the time to full recovery down to levels similar to that of the background bang sensitive flies.

5.7 The loss of dSlo2 reveals a spontaneous seizure phenotype in I_{NaP}-affected seizure models

To further examine whether dSlo2 channels may protect against seizure-like behavior that is not mechanically induced, I tested whether an increase in I_{NaP} may cause spontaneous seizure-like behavior in the absence of *dSlo2*. I was unaware of any previous studies examining spontaneous seizure-like behavior in flies, and therefore needed to establish a definition of a spontaneous seizure. Upon examining flies, I found that rarely they would exhibit a bout of uncontrollable motor movement that resembled the recovery seizures observed in the bang-sensitive flies. However, this behavior was not induced by external factors

and seen in flies otherwise behaving normally. I therefore labeled these bouts as spontaneous seizures as they occurred seemingly randomly without clear induction as in the bang-sensitive and temperature-sensitive assays.

I then tested whether *dSlo2*- flies may be more susceptible to spontaneous seizures in backgrounds that have increased I_{NaP}. To test this, I placed 10 flies in an empty vial and let them acclimate for 30 minutes to the new environment. I then videotaped the flies for 15 minutes, with the genotypes blinded to the researcher. Videos were later analyzed offline, and the number of total seizures observed in the 15-minute period per vial was recorded. I observed that there was no difference in the number of spontaneous seizures between wild-type and *dSlo2*- flies (Fig. 15A). There similarly was not an increased number of spontaneous seizures in either *sda* or heterozygous *bss/+* flies compared to wild-type flies (Fig. 15A). However, the absence of *dSlo2* in *sda* flies increased the average number of spontaneous seizures observed in a group of 10 from 0.6 to 7.75 in a 15-minute period (Fig. 15A). Similarly, the loss of *dSlo2* in the *bss/+* line increased the average spontaneous seizures from 0.2 to 6.3 (Fig. 15A). I also tested the hypothesis that dSlo2 channels might protect against spontaneous seizures in cholinergic neurons. I found that expression of *dSlo2-DN* in cholinergic neurons in the *sda* background increased the average number of spontaneous seizures seen in a group of 10 flies to 4.6 compared to the averages of each genetic background line, which were between 0-1.1 (Fig. 15B). However, this was not the case in the heterozygous *bss/+* mutants (Fig. 15C). It is unclear why cholinergic expression of *dSlo2-DN* worsened the spontaneous seizure phenotype in *sda* but not *bss/+*. To further test whether the increase in spontaneous seizures in the absence of *dSlo2* was due to an increase in I_{NaP}, wild-type flies were tested for spontaneous seizures following feeding of Veratridine. Similar to the experiments in Section 5.6, flies were fed Veratridine for 2 hours before testing for spontaneous seizures. I found that feeding Veratridine to wild-type flies did not increase the average number of spontaneous seizures seen in a group of 10 flies (Fig. 15D). Contrastingly, feeding *dSlo2*- flies Veratridine significantly increased the average number of spontaneous seizures to 4.9 compared to the mock fed flies which averaged only 0.7 (Fig. 15D). To further test whether the increase in spontaneous seizures is specific to dSlo2 channel

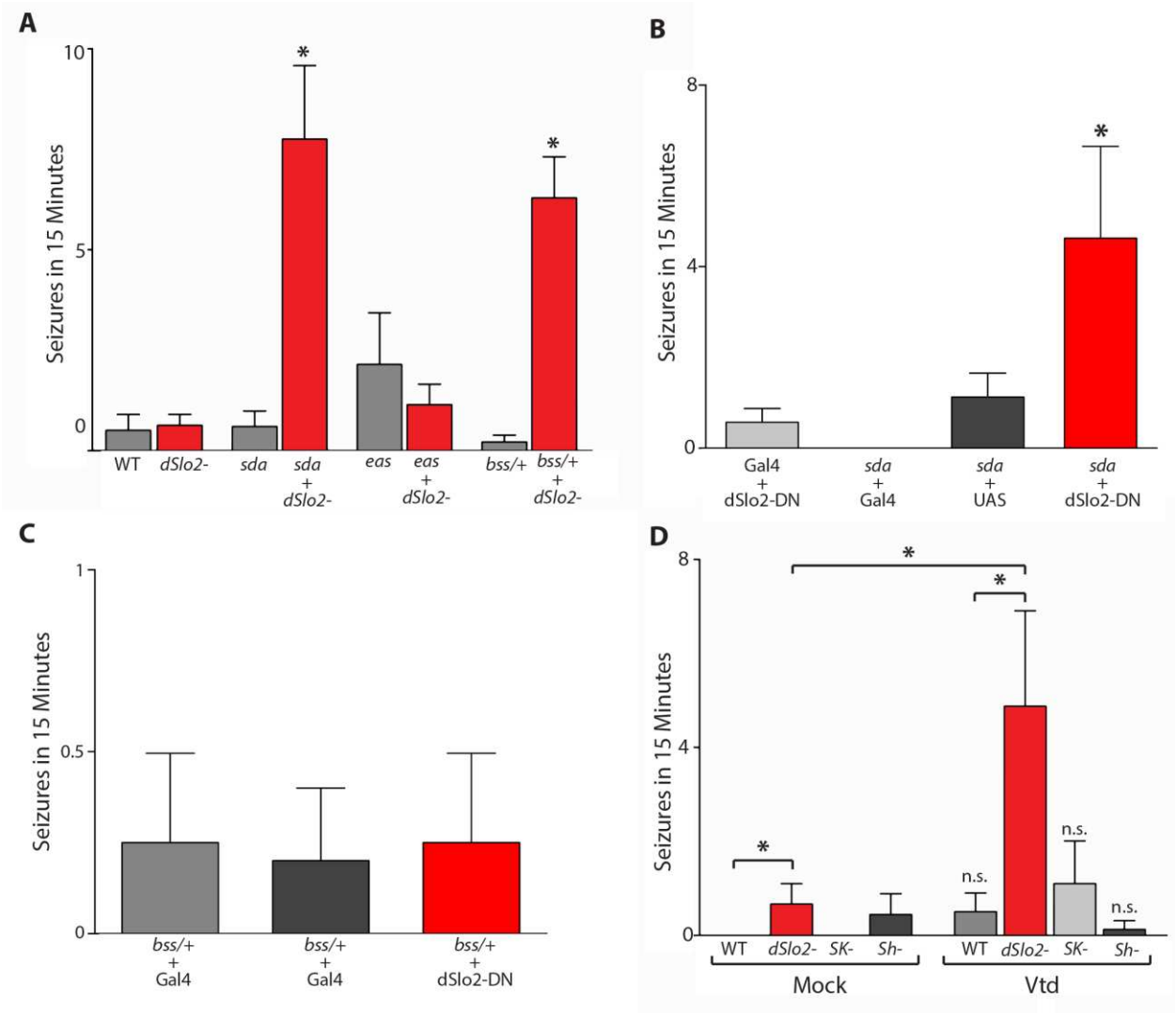

Figure 5.15: Loss of *dSlo2* reveals a spontaneous seizure phenotype in I_{NaP}-affected seizure models. Number of spontaneous seizures observed out of 10 flies in a 15 minute period was measured and averaged across trials. A) *dSlo2-* compared in the bang-sensitive backgrounds. n = 7-8 vials for WT and *dSlo2-* genotypes and 14-16 vials for *sda*, *dSlo2-;sda*, *bss/+*, and *bss/+;dSlo2-* genotypes, 10 flies per vial. $p < .01$ (Student's t-test). B) *ChAT-Gal4>>UAS-dSlo2-DN* and its combination with *sda* flies was compared. n = 7-8 vials per genotype, 10 flies per vial. $p < .05$ (Student's t-test). C) *ChAT-Gal4>>UAS-dSlo2-DN* and its combination with *bss/+* background was compared. D) Number of spontaneous seizures observed out of 10 flies in a 15 minute period was measured when flies were treated with either vehicle ("mock") or 20μM Veratridine (Vtd) for 2 hrs. n = 8-10 vials per genotype, 9-10 flies per vial. $p < .05$ for Vtd-treated *dSlo2-* flies compared to every other treatment.

function, I tested whether the *SK-* or Sh^{ks133} flies exhibited a greater number of spontaneous seizures following Veratridine treatment. I found that feeding *SK-* and Sh^{ks133} flies Veratridine did not significantly increase the average number of spontaneous seizures (Fig. 15D). Furthermore, following Veratridine

treatment, *dSlo2-* flies exhibited significantly more spontaneous seizures on average compared to treated *SK-* and Sh^{ks133} flies (Fig. 15D).

To further examine the spontaneous seizure phenotype, I analyzed the time spent in spontaneous seizures for each genotype. I found that while there were only a total of 7 seizures in the *sda* line out of 150 flies observed, each seizure lasted for a very brief period, with 92% lasting less than 2 seconds (Fig. 16A). In contrast, 40% of the spontaneous seizures in the double mutant *dSlo2-;sda* lasted for longer than 2 seconds (Fig. 16A). Interestingly, this was slightly different in the *bss/+* flies. In the absence of *dSlo2*, only 7% of the spontaneous seizures lasted longer than 2 seconds while the majority of the seizures in both lines lasted less than 2 seconds (Fig. 16B). It is currently unclear why the loss of *dSlo2* prolongs the spontaneous seizure duration in the *sda* flies but not in the *bss/+* flies. I also analyzed the duration of each spontaneous seizure when *dSlo2-DN* was expressed in cholinergic neurons. I found minimal differences in the length of spontaneous seizure between the background *ChAT>>dSlo2-DN* flies compared to the combination of *ChAT>>dSlo2-DN;sda* (Fig. 16C). I also compared the spontaneous seizure duration in the Veratridine treated flies and found that the length of spontaneous seizures in wild-type flies treated with Veratridine all lasted less than 10 seconds (Fig. 16D). In the *dSlo2-* flies fed Veratridine, a significant portion of these spontaneous seizures, 37%, lasted longer than 10 seconds (Fig. 16D).

In this section, I show a novel protective role of dSlo2 against increases in I_{NaP}. Neither increases in I_{NaP} nor the deletion of dSlo2, alone, increased the probability of exhibiting spontaneous seizures. It was only when these two components were combined that flies began to exhibit spontaneous seizures. These results strongly suggest that dSlo2 channels are playing an important role in protecting against increases in I_{NaP}, even when flies are behaving normally. This further suggests that dSlo2 channels are activated by I_{NaP} *in vivo*, expanding upon the *in vitro* experiments conducted in Dr. Salkoff's lab[302,303]. Altogether, these results support the model that dSlo2 channels protect against seizure-like behavior caused by increases in I_{NaP}.

5.7 Conclusion

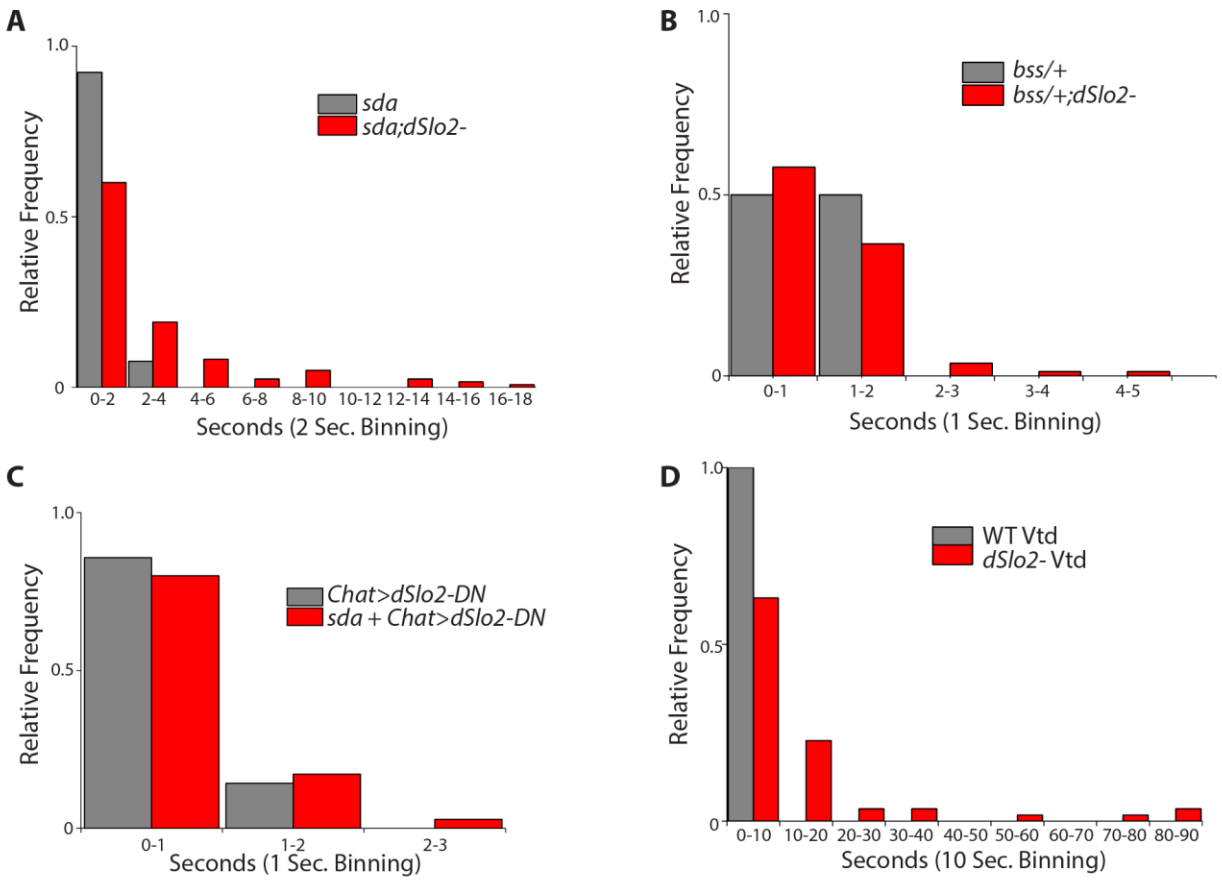

Figure 5.16: Time spent in spontaneous seizures is exacerbated by the loss of *dSlo2*. A) Time spent seizing during each spontaneous seizure observed from 5.15A. n = *sda*: 13, *dSlo2-;sda*: 120. B) Time spent seizing during each spontaneous seizure observed from 5.15A. n = *bss/+*: 2, *bss/+;dSlo2-*: 86. C) Time spent seizing during each spontaneous seizure observed from 5.15B. n = *ChAT-Gal4>>UAS-dSlo2-DN*: 7, *ChAT-Gal4>>UAS-dSlo2-DN;sda*: 35. D) Time spent seizing during each spontaneous seizure observed from B. n = WT Vtd: 6, *dSlo2-* Vtd: 57.

The results of this chapter strongly suggest that K_{Na} channels protect against overexcitation induced by increases in I_{NaP}. Our findings indicate that endogenous *dSlo2* protects against bang sensitive seizure-like behavior, and also seizure-like behavior in the *GEFS+* line. Humans with the homologous mutation exhibit seizures as children that are usually associated with an increase in body temperature, such as a fever, vaccination, or a hot water bath[119,120]. K_{Na} channels may therefore be a potential therapeutic target to prevent seizure onset or severity in GEFS+ patients. This hypothesis would need to be further examined in mammalian models of GEFS+. Indirectly, these findings also suggest that K_{Na} channels may protect against other forms of epilepsy associated with increases in I_{NaP}, such as severe myoclonic epilepsy of infancy

(SMEI) and intractable childhood epilepsy with generalized tonic-clonic seizures (ICEGTC)[213]. These syndromes were associated with different mutations in *SCN1A* that increase I_{NaP}[252,255,259,418–420].

The results that dSlo2 channels protect against these different mutations that cause bang-sensitivity and are associated with an increase in I_{NaP} is significant. This is most evident in the *bss* mutant, which contains a point mutation in the voltage-gated Na^+ channel that causes the increased I_{NaP}[201]. This is more direct than the mutations in aminopeptidase N (*sda*)[203] and ethanolamine kinase (*eas*)[204], whose mechanism of increased I_{NaP} is less direct, causing alternative splicing of exon *L* into *para*[205,206]. These mutations could also affect other cellular physiological processes, which could lead to alterations in neuronal activity. The use of all three mutants also provided intriguing evidence that *dSlo2* protection correlates with the severity of the behavior. This is evident in the fact that in the absence of *dSlo2*, *sda* and *eas* flies took roughly 2 times as long to reach full recovery. As the severity of the phenotype increased in *bss* mutants, the time to full recovery was increased by 1.5 times in the heterozygous *bss* flies. Additionally, the loss of *dSlo2* in homozygous *bss* flies did not exacerbate the time to full recovery. Since the severity of the phenotype increases from *sda* to *eas* to *bss*, these results suggest that there is some limit of hyperexcitability that dSlo2 channels can prevent, but beyond that it is no longer able to protect against overexcitation. While my results do not directly test this, they provide evidence that this may be the case.

In *Drosophila*, it seems that K_{Na} channels function to dampen excitatory signaling by specifically acting in cholinergic neurons. The finding that specifically blocking dSlo2 channel function in cholinergic neurons alone exacerbated bang-sensitive seizure-like behavior supports this hypothesis. This provides a unique model to study the role of K_{Na} channels specifically in cholinergic neurons. While there is indirect evidence of K_{Na} channel expression in inhibitory neurons in mammals[286,310,389,390], this has not been directly tested. These results, combined with dSlo2 expression seemingly absent in GABAergic neurons of *Drosophila*, suggests K_{Na} channel expression in mammalian neuronal subtypes should be further examined. Expression of K_{Na} channels in different neuronal subtypes would greatly alter their role in regulating excitability of the circuit and organism as a whole. For example, if expressed in excitatory neurons, it is

possible that they dampen signaling and therefore decrease overall excitability. However, if K_{Na} channels are expressed in inhibitory neurons they could cause disinhibition, and lead to an overall increase in excitability. While these models are overly simplistic, this information would help better understand the role of K_{Na} channels in the mammalian brain.

The finding that dSlo2 channels protect against seizure-like behavior induced by Veratridine feeding further supports the model that this channel protects against overexcitation induced by increased I_{NaP}. Additionally, the lack of seizure-like behavior in other K^+ channel mutants suggests that K_{Na} channels may be critically important for preventing hyperexcitability caused by an increase in I_{NaP}. While I did not test mutants for every K^+ channel, these two at least suggest that two types of K^+ channels, voltage-gated and Ca^{2+}-activated, do not protect against increased I_{NaP}. Additionally, the other Ca^{2+}-activated K^+ channel, BK (dSlo1), might protect against bang sensitive seizure-like behavior. However, I was unable to test this due to the lack of *dSlo1* null flies that would live as homozygotes. These lines could instead be tested as heterozygotes or hypomorphs to test if this prolongs seizure-like behavior in bang-sensitive models. This would help elucidate whether protection against increased I_{NaP}-actuated seizure-like behavior is particular to Na^+-activated K^+ channels and not Ca^{2+}-activated K^+ channels. If so, these results would further support the hypothesis that K_{Na} channels specifically protect against I_{NaP} induced hyperexcitability.

Perhaps the most intriguing and unexpected result of this chapter was the finding that in the absence of *dSlo2*, flies with increased I_{NaP} began to exhibit spontaneous seizures. To my knowledge, this type of behavioral phenotype has not been reported in *Drosophila*. Unlike the induced seizure-like behavior in bang-sensitive and temperature-sensitive flies, these spontaneous seizures have no stressor that causes the seizure-like behavior. Instead, these seizures likely occur solely due to a basally increased level of I_{NaP}, which manifests only when *dSlo2* is absent. Furthermore, *dSlo2*- flies did not exhibit spontaneous seizures, suggesting this channel is working in conjunction with the I_{NaP} *in vivo*. These findings suggest that K_{Na} channels may function under times of greater excitation induced by an external stressor, as well as basally

to preclude the effects of an increased I_{NaP}. These results help elucidate the role of K_{Na} channels and suggest that they are indeed activated *in vivo* by the persistent Na^+ current.

Altogether, the results in this chapter are consistent with the model that K_{Na} channels protect against overexcitation induced by increases in I_{NaP}. Further, they suggest that K_{Na} channels may be a potential therapeutic target in specific forms of epilepsy, which may help to prevent or decrease the severity of seizures. Indirectly, this evidence also suggests that K_{Na} channels may protect against other neuropathologies associated with increased I_{NaP}. These pathologies include ALS[80,250], FXS[248], ischemia[44], and neuropathic pain[249]. Overall, this chapter provides strong evidence for the continued exploration of K_{Na} channel protection against I_{NaP} induced hyperexcitability.

CHAPTER 6: DISCUSSION

6.1 Possible roles of dSlo2 channels based on expression

6.1.1 dSlo2 tempers activity of excitatory neurons

In Chapter 3, I showed that dSlo2-positive neurons in the brain mainly consist of cholinergic neurons. In contrast, dSlo2 is specifically not expressed in GABAergic or glutamatergic neurons in the brain. Based on these findings, in Chapter 5 I tested whether dSlo2 channels protect against seizure-like behavior in bang-sensitive flies specifically in cholinergic neurons. I addressed this hypothesis in two ways. The first was to express a dominant-negative transgene for *dSlo2* in cholinergic neurons that is predicted to block channel conductance. The second utilized expression of RNAi specific for *dSlo2* to knockdown channel expression in cholinergic neurons. RNAi directed against *dSlo2* exacerbated the time to full recovery in the *eas* line, but not the *bss/+* line. Alternatively, I found that cholinergic expression of the *dSlo2-DN* transgene mimicked the *dSlo2* null phenotypes in all bang-sensitive flies, albeit to a lesser extent than the loss of *dSlo2*. These results are consistent with the idea that the *dSlo2-DN* transgene may not completely block channel function in cholinergic neurons. Alternatively, these results could suggest that dSlo2 channels may also function in other non-cholinergic neurons to attenuate seizure-like behavior. To this point, dSlo2 expression was also found in glutamatergic motor neurons in both the larvae and adults. Previous reports suggest that in bang-sensitive mutants, these motor neurons exhibit an increased I_{NaP}[202]. This possibility is worth further exploration, as an effect in these neurons would vastly increase the experimental assays available to elucidate the role of dSlo2. These experiments would similarly express the *dSlo2-DN* transgene in motor neurons and examine whether this exacerbates the time to full recovery in the bang-sensitive flies. If so, further exploration of the role of *dSlo2* in tempering excitability of these neurons in an *in vitro* prep could be performed as similarly described[202]. In these assays, it is possible to directly examine neuronal properties in the intact larval ventral nerve cord. Examining how the loss of dSlo2 affects

action potential firing dynamics in the bang-sensitive backgrounds would increase our understanding of how these channels affect neuronal excitability when there is an increased I_{NaP}.

6.1.2 Subcellular localization of dSlo2 channels

During my research, I also examined subcellular localization by generating a line in which endogenous dSlo2 channels are tagged with the small peptide, myc. Using this line, I found that dSlo2 localization seems to be widespread in cholinergic neurons. I examined the multidendritic neurons which line the larval body wall, as they display clear separation of neuronal dendrites and a single axon[377,381]. In these neurons, it was clear that dSlo2 was localized to the axonal region while being mostly absent in the dendritic compartments. When looking the in brain, subcellular localization of dSlo2 channels was less clear. For instance, when examining the Kenyon cells whose arms constitute the mushroom body, I found that dSlo2 channels were mainly localized to the calyx and peduncle regions. The calyx region is a combination of dendritic processes from the Kenyon cells as well as axonal terminals from multiple regions of the brain, including the projection neurons (PNs) that originate in the antennal lobe. Because the *dSlo2^{Mi13397}-Gal4* reporter line showed expression in both Kenyon cells and antennal lobe neurons, I was unable to distinguish whether dSlo2 localization in the calyx was from the Kenyon cell's dendritic processes or PN axonal terminals. In addition to expression seen in the calyx, I also noticed that dSlo2-myc staining continued into the peduncle of the mushroom body, which is considered the distal axonal processes from the Kenyon cells[421]. Localization of dSlo2 channels to this axonal region matches localization found in the *ppk*-positive multidendritic neurons. More pertinent to my findings in this dissertation, the distal axonal region is where para channels are localized[386]. If both channels are localized to the same subcellular compartment, this would be consistent with the model that dSlo2 channels are specifically being activated by the I_{NaP} generated through para channels. If dSlo2 localization to the calyx of the mushroom body was indeed from the dendritic processes of the Kenyon cells, then subcellular localization would seem to be specific to the neuronal subtype as dendritic localization was not found in the *ppk* neurons. This is similar to findings of mammalian K_{Na} channels, which have been found localized to dendrites, somata, and axons

depending on the neurons examined[292,327]. Additionally, a putative PDZ binding motif was found localized to the C-terminus of $K_{Na}1.1$ channels and further shown to bind PSD-95[293]. Differential localization would be expected to alter the role dSlo2 channels play in those neurons. For instance, dendritic localization of dSlo2 might be expected to dampen incoming signaling from presynaptic neurons by reacting to Na^+ influx through ligand-gated post-synaptic channels. This may be different for dSlo2 channels localized to the axonal process, which could affect action potential properties in multiple ways. If localized near voltage-gated Na^+ channels in axons, K_{Na} channels could possibly prevent action potential firing by repolarizing the neuron during the initial phase of the action potential, thereby preventing the neuron from reaching threshold for action potential firing. Alternatively, K_{Na} channels may act during the repolarization phase of the action potential, thereby decreasing the refractory period and allowing for more rapid action potential firing rates. Indeed, both of these roles have been suggested of K_{Na} channels[285,290,326,417]. Findings that K_{Na} channels can differentially affect action potential firing rates further complicates hypothesized roles of K_{Na} channels and emphasizes their complexity. Therefore, different neuronal populations within *Drosophila* could be examined to better understand the role of K_{Na} channels based on their subcellular localization.

6.1.3 Hypothetical role of dSlo2 channels in sensory adaptation

When examining expression of dSlo2 throughout the *Drosophila* nervous system, I found that it is expressed in both primary sensory organs as well as secondary sensory relay regions. These sensory regions are responsible for regulating somatosensory, visual, auditory, and olfactory input. Expression of K_{Na} channels in mammals also suggests that they may regulate sensory processing in somatosensory and auditory systems[278,285,290,306,311]. Within these systems, some experiments have been conducted to examine what K_{Na} channels may be doing. For instance, in the somatosensory system, $K_{Na}1.1$ and $K_{Na}1.2$ expression has been observed in the DRG neurons[278,290]. Based on these findings, researchers have examined whether K_{Na} channel knock-out alters nociceptive behavior. Results from these experiments, overall, suggest that the loss of K_{Na} channels increases activity of DRG neurons, which corresponded with enhanced pain and itch sensation[285,290]. In the auditory systems, expression of K_{Na} channels have been observed in the spiral

ganglion neurons, which are the primary auditory neurons[311]. These researchers found that double-knockout of $K_{Na}1.1$ and $K_{Na}1.2$ resulted in reduced action potential thresholds that were associated with an increased amplitude of the auditory brainstem response[311]. Results from these researchers suggest that K_{Na} channels do regulate primary sensory neurons in mammals.

dSlo2 channel expression in *Drosophila* provides a unique opportunity to test the role of K_{Na} channels in primary sensory systems. For instance, the Johnston's Organ in *Drosophila* has been shown to regulate many different behaviors, including auditory sensation important for courtship[368–372]. Using the tools generated through my research, it would be feasible to examine whether the loss of dSlo2 channels in these primary sensory neurons alters stereotypical courtship behavior. Additionally, extracellular potentials can be recorded from the antennal nerve that occur in response to courtship sounds[422]. If behavioral alterations are observed, these could potentially be linked to physiological alterations in Johnston's Organ signaling. Similarly, olfactory sensation has been studied extensively in *Drosophila*, with mapping of specific odorant receptors to different regions of the antenna[367]. Similar to the proposed auditory experiments, dSlo2 channel function could be assayed in specific olfactory receptor neurons known to be stimulated by different odorants. Both physiological and behavioral analyses[423] could be done to see if dSlo2 channels indeed regulate olfactory sensation and corresponding behavior. For the somatosensory system, I did perform experiments to determine if the loss of *dSlo2* would alter nociceptive behavior. Interestingly, *dSlo2*- larvae exhibited behavior that was opposite of that seen in K_{Na} knockout mice[285,290] (See Appendix A.1). Further research into the causes of this behavioral phenotype in *Drosophila* could help understand differing roles of K_{Na} channels in regulating neuronal excitability. For instance, if the loss of dSlo2 channels was found to decrease action potential firing rates of Class IV *ppk* neurons, this would provide a model that could provide insight into the role of K_{Na} channels in increasing neuronal output, which has recently been suggested[326]. Nonetheless, *Drosophila* are a valuable model to further examine the role of K_{Na} channels in regulating sensory systems.

6.1.4 What business does a K_{Na} channel have in the blood brain barrier?

Expression data also suggests that dSlo2 channels are expressed in a specific glial cell type, the subperineural glia (SPG), that constitute the *Drosophila* blood brain barrier (BBB). Mammalian BBB epithelial cells have been found to express *$K_{Na}1.2$* transcript[391], suggesting this phenomena is not invertebrate-specific. The SPG are responsible for acting as a chemical barrier. This includes the prevention of paracellular diffusion by the formation of tight junctions, active efflux of lipophilic molecules, and solute transport[387,392–394,424,425]. To achieve active transport, the SPG cells contain ATP-binding cassette (ABC) transporters that cause the efflux of xenobiotic compounds out of the brain and solute carrier (SLC) transporters for maintenance of proper solute concentrations within the CNS[393,395,399]. Both ABC and SLC transporters can be regulated by ionic concentration gradients across the plasma membrane[395,426]. K_{Na} channels could regulate these ionic gradients and thereby effect efflux of xenobiotic compounds and retention of solutes. Also, it has previously been shown that a member of the SLC family, the Na^+-K^+-Cl^- cotransporter, NKCC1, is critical for solute transport across the BBB[424]. Lieserson et al. found that the *Drosophila* analog of this transporter, Ncc69, is expressed in the SPG. Additionally, they showed that loss of Ncc69 resulted in extracellular fluid accumulation in the larval nerves[399]. Using the tools generated in this dissertation, combined with assays to examine xenobiotic efflux[395], solute transport[424], and fluid retention[399], it is feasible to test whether the loss of *dSlo2* affects any of these critical processes performed by the SPG.

SPG cells have additionally been found to release insulin-like peptide (ILP) into the larval CNS[427]. These authors found that release of ILP from these cells induced neural stem cell reactivation and growth in the larval brain. Furthermore, proper release of ILP was dependent upon electrical synchronicity of the SPG cells as shown by Ca^{2+} reporters. As such, it is possible that K_{Na} channels could regulate electrical signaling within the SPG, thereby affecting ILP release. It would be possible to examine Ca^{2+} oscillations, neural stem cell reactivation, and ILP release in *dSlo2* null larvae to test whether any of these processes are altered compared to wild-type. Interestingly, epithelial cells have also been shown to exhibit Ca^{2+} oscillations[428], however the function and underlying mechanism are unknown.

While these ideas are purely hypothetical, there are clear ways of testing whether dSlo2 channels may be functioning in any of these pathways. The transgenic and knockout flies generated throughout my dissertation would allow for specific analysis of dSlo2 function in SPG, which could have implications for mammalian physiology.

6.2 Is the protective nature of dSlo2 due to Na^+ activation?

6.2.1 Does decreasing Na^+ sensitivity of dSlo2 mimic the *dSlo2*- behavioral phenotypes?

The majority of my results, especially regarding the I_{NaP}-actuated seizure-like behavior, suggest that dSlo2 channels are responding to increases in intracellular Na^+. This is consistent with previous electrophysiological experiments that show that K_{Na} channels are activated by intracellular Na^+[260,272]. However, I never directly tested whether Na^+ sensitivity of the channel is indeed responsible for protecting against the exacerbated seizure-like behavior caused by increased I_{NaP}. To this point, Na^+ coordination sites have been examined in mammalian K_{Na} channels. A consensus Na^+ binding motif, DX(R/K)XXH, originally identified in K_{ir} channels[282] was searched for in rat $K_{Na}1.1$ and $K_{Na}1.2$ channels[279,429]. This revealed six potential Na^+ binding sites located in the C-terminus of $K_{Na}1.1$[279]. These researchers found that mutation of the aspartic acid residue, D818, to an asparagine (N) or arginine (R), significantly reduced Na^+ sensitivity of rat $K_{Na}1.1$ expressed in *Xenopus* oocytes[279]. Mutation of this homologous site in $K_{Na}1.2$ similarly decreased Na^+ sensitivity of the channel[429]. I aligned dSlo2 and $K_{Na}1.1$ amino acid sequences to determine if Na^+ coordination sites in $K_{Na}1.1$ are homologous to dSlo2 sequences[279]. I additionally searched through the dSlo2 sequence and identified two other potential Na^+-binding sites matching the consensus sequence DX(R/K)XXH identified in K_{ir} channels[282]. These results show that five of the potential six Na^+-binding sites in $K_{Na}1.1$ are homologous in dSlo2 (Fig. 6.1). Importantly, the Na^+ coordination sequence identified in $K_{Na}1.1$ that heavily regulates Na^+ sensitivity (D818) is similar at two of the three essential amino acids in dSlo2. Alignment of this site with dSlo2 shows that the initial aspartic acid (D) is a glutamic acid (E) in dSlo2 (Fig. 6.1). Previous experiments found that the mutation D818E barely decreased Na^+ sensitivity of $K_{Na}1.1$[279], suggesting that the similarly charge glutamic acid (E) could act as a Na^+ sensor.

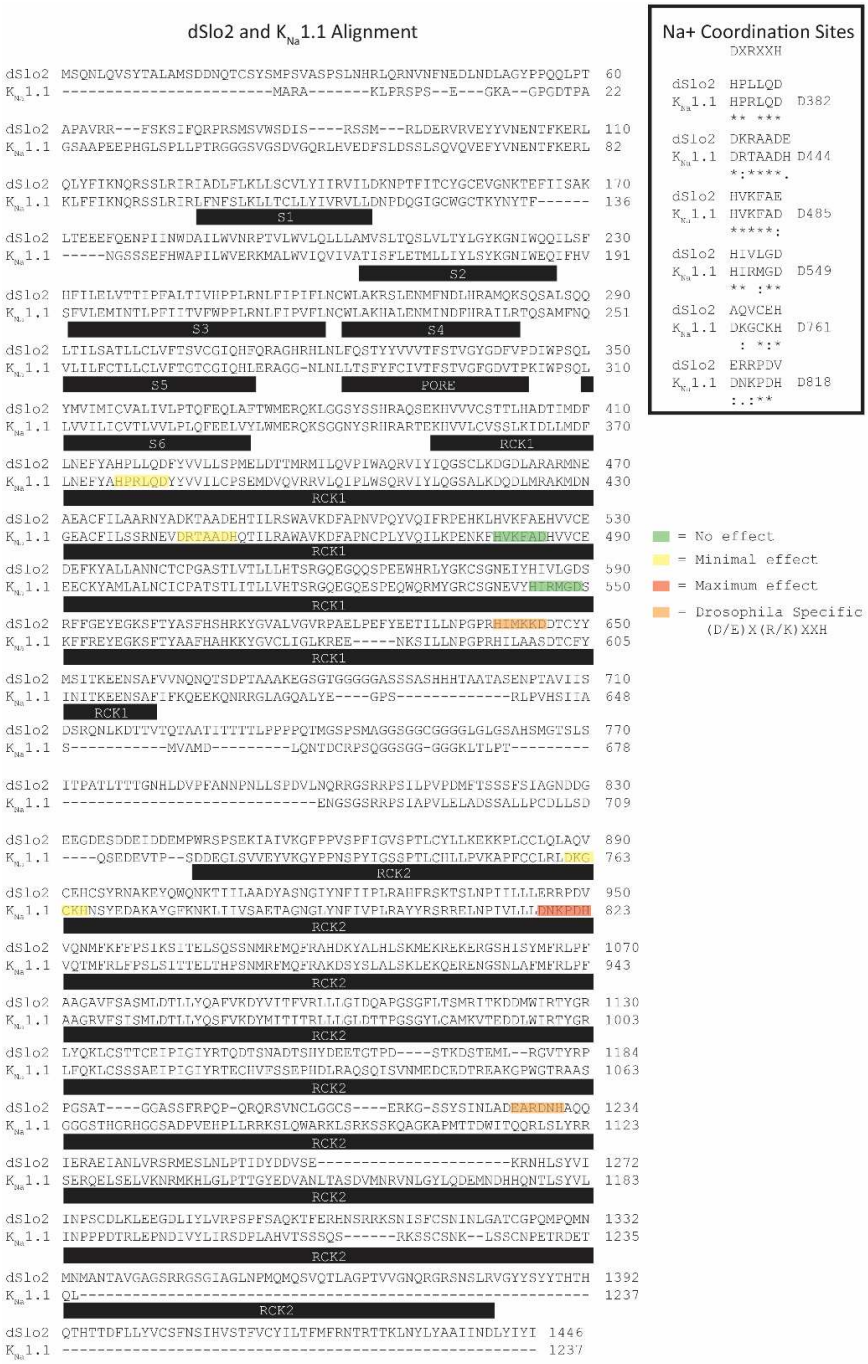

Figure 6.1: Similarity between dSlo2 and K_{Na}1.1 Na^+ sensitivity sites. dSlo2 amino acid sequence is aligned with rat K_{Na}1.1 sequence. Functional regions of the channel are identified below the sequence, such as transmembrane domains, pore forming region, and Regulators of Conductance of K^+ (RCK) domains. Constitutive Na^+ binding domains previously found (Zhang et al. 2010) are highlighted. Additionally, colors were used to exemplify how much of an effect mutating the site had on overall Na^+ sensitivity of the channel (Zhang et al. 2010). Two sites matching consensus Na^+ binding sequences were found that might be specific to dSlo2.

The sequences do differ, however, at the last amino acid in the motif. In the previous study, the authors

found that mutation of the histidine (H) at the end of the motif to an alanine (A), an amino acid very similar to valine (V) found at the end of the dSlo2 motif, significantly decreased Na^+ sensitivity[279]. This suggests that if this site is indeed the Na^+ coordination site in dSlo2, that it may have a significantly reduced Na^+ sensitivity when compared to $K_{Na}1.1$. Nonetheless, the aspartic or glutamic acid residue could be mutated to either asparagine or arginine in each of the consensus Na^+ coordination sites in dSlo2. These mutants could be examined in the bang-sensitive assays. If Na^+ sensitivity is indeed essential for channel function, then it is expected that the decreased Na^+ sensitive mutants would increase the time to full recovery similar to the *dSlo2* null flies. Another possibility is that it is the combination of multiple sites that causes Na^+ sensitivity of dSlo2 *in vivo*. To test this, multiple mutations would need to be made within the same channel. Another possibility is that Na^+ sensitivity of the channel is not the only property responsible for protecting against overactivity and seizure-like behavior. Other channel properties, such as Cl^- binding, NAD+ binding, kinase regulation, or others could be responsible for channel protection.

6.2.2 Does increasing Na^+ sensitivity of dSlo2 attenuate seizure-like behavior?

In addition to mutations that decrease Na^+ sensitivity of K_{Na} channels, other mutations have been found that increase the Na^+ sensitivity[312,313,318–321]. Interestingly, many of these mutations are associated with different forms of epilepsy in humans (See Section 1.6.5). Similar to the previous section, alignment of these sites with dSlo2 reveals sequence homology between sites shown to increase Na^+ sensitivity in $K_{Na}1.1$ channels. These mutations and homologous sites have been listed in Table 6.1. This poses the hypothesis that increasing Na^+ sensitivity of dSlo2 channels may attenuate seizure-like behavior in I_{NaP}-affected seizure models. To increase Na^+ sensitivity of the channel, it would be ideal to generate these mutations in a transgenic line and then express the channels in a *dSlo2* null background. This is important because it is unclear whether mutant channels will increase Na^+ sensitivity when tetramerized with endogenous wild-type channel. Using this strategy, dSlo2 channels with increased Na^+ sensitivity could be expressed either in all dSlo2-positive cells using the *dSlo2^{Mi13397}-Gal4* line, in all cholinergic cells using *ChAT-Gal4*, or any other subset of neurons thought to be responsible for bang-sensitive behavior. The

Table 6.1: Mutations that increase Na^+ sensitivity of K_{Na} channels. Epileptogenic mutations found in KCNT1 channels are homologous to sites found in dSlo2.

Mutation	KCNT1 Site	dSlo2 Site	Disease	Increased Na -Sensitivity
H257D	H257	H277	MMFSI	Unknown
G288S	G288	G308	ADNFLE 6x	Yes
R428Q	R428	R449	MMFSI 4x	Yes
I760M	I760	I866	MMFSI	No
Y796H	Y796	Y902	ADNFLE	Yes
R928C	R928	R1034	ADNFLE 3x	Yes
F932I	F932	F1038	Leuko	Yes
A934T	A934	A1040	MMFSI 4x	No
A966T	A966	A1072	Ohtahara	No

expected results of these experiments would be that an increase in Na^+ sensitivity would result in a decreased time to full recovery compared to the bang-sensitive flies lacking mutations in *dSlo2*. However, this prediction is solely based on the assumption that the channel functions to decrease excitability. Contrastingly, increasing channel function may lead to an increase in action potential firing by decreasing the repolarization phase. Overall, this would increase neuronal excitability. Indeed, this has been previously found as a result of increased Na^+ sensitivity[326]. If this were the case, then seizure-like behavior may be exacerbated when expressing dSlo2 channels with an increased Na^+ sensitivity. It is therefore difficult to predict the outcome of these experiments. Regardless, they may reveal pertinent information regarding channel function in overexcitable models.

6.3 Na^+ activation pathways for K_{Na} channels

6.3.1 Does I_{NaP} directly activate dSlo2 channels?

The results of Chapter 5 strongly suggest that dSlo2 channels are protecting against hyperexcitability induced by an increase in I_{NaP}. This is shown by the finding that the loss of *dSlo2* significantly exacerbates seizure-like behavior in all three bang sensitive lines, *sda*, *eas*, and *bss*. Importantly, all three lines have mutations in different genes but similarly exhibit an increase in I_{NaP}. This bolsters the idea that dSlo2 channels are specifically protecting against I_{NaP}. Consistent with this finding are the results that the absence of *dSlo2* reveals a spontaneous seizure-like phenotype that is only present in backgrounds with an increased I_{NaP}. This suggests that even in the absence of an external stimuli, dSlo2

channels protect against the increased I_{NaP}. Combined, these results support the model proposed by the Salkoff lab, which suggest that K_{Na} channels are activated by I_{NaP} in neurons[302,303]. This hypothesis could be further examined electrophysiologically in *Drosophila* neurons. To accomplish this, one could examine whether an increase in I_{NaP} induced either pharmacologically with veratridine or genetically with the bang-sensitive mutations, causes an increase in the K_{Na} current. If so, it would be expected that this increased K_{Na} current would be absent in neurons from the *dSlo2-* line.

Other data suggests that the I_{NaP} can affect intracellular Na^+ concentrations, especially in microdomains located throughout the neuron. Previously, it has been observed that fluctuations in bulk intracellular Na^+ levels can occur within the range of 5mM[430]. Furthermore, much larger fluctuations of Na^+ levels in subcellular compartments, such as axons and dendritic spines, can rise up to 45mM and 100mM, respectively[431,432]. Additional evidence suggests that there could be microdomains of Na^+ inside the cell, and that it does not freely diffuse throughout the cell. Results from ventricular myocytes show that there are discreet pockets of increased Na^+ levels, localized roughly 20nm from the plasma membrane[433]. These pockets saw increases of Na^+ levels to roughly 40mM, while the bulk Na^+ levels were effectively unchanged. Also, using Na^+-sensitive dyes, researchers have identified I_{NaP} as a sufficient source of Na^+ influx localized to the dendrites, soma, and axon of cortical neurons[434,435]. Altogether, these results suggest that I_{NaP} could result in discreet microdomains of increased intracellular Na^+ concentrations. When paired with data suggesting that the I_{NaP} activates K_{Na} channels[302,303], one possibility is that the voltage-gated Na^+ channels are in close proximity to the K_{Na} channels. This idea could be tested in a few different ways. The first of which could be to test whether dSlo2 and para channels co-immunoprecipitate together. If so, this would suggest that endogenous channels are actually interacting with each other and therefore are in very close proximity. Other techniques could employ microscopy analysis to examine relative closeness of the channels. This includes both electron microscopy and fluorescence resonance energy transfer (FRET) microscopy. In the case of electron microscopy, relative distances could be reliably measured between channels. For FRET microscopy, if fluorescence was observed when co-expressed in the same cells, this

would suggest that dSlo2 and para channels are at least within about 10 nanometers[436]. This distance would be close enough for dSlo2 channels to be activated by smaller pockets of increased Na^+ previously found to occur within 20nm of the plasma membrane[433]. Therefore, if any of these experiments were positive, it would strongly support the hypothesis that K_{Na} channels are activated by the Na^+ current coming from voltage-gated Na^+ channels.

6.3.2 Does the level of I_{NaP} affect the protective capacity of dSlo2?

In my studies, I found that the loss of *dSlo2* exacerbated multiple facets of seizure-like behavior associated with an increase in I_{NaP}. Interestingly, the severity of the increase in time to full recovery caused by the loss of *dSlo2* seemed to correlate strongly with the severity of the seizure-like behavior. The severity of the seizure-like behavior increased from *sda*<*eas*<*bss/+*<*bss*. While increasing in severity, the percentage increase in time to full recovery upon the loss of *dSlo2* increased by 95%, 102%, 56%, and -11%, respectively. Additionally, when expressing *dSlo2-DN* in the cholinergic neurons, the increase in time to full recovery increased by 73%, 17%, and 6% as the severity increased from *sda*<*eas*<*bss/+*, respectively. These results could be due to a few things. First, as mentioned previously, each mutation is in a separate gene. This could differentially affect how dSlo2 interacts with and protects against the increased I_{NaP}. The more interesting possibility is that each mutant's severity of seizure-like behavior corresponds with the increase in I_{NaP}. This would suggest that dSlo2 channels are able to better protect against lower levels of increased I_{NaP}, but as this worsens, they are unable to prevent overactivity. To my knowledge, no groups have examined or correlated the increase in I_{NaP} to the severity of the seizure-like behavior. Therefore, we would first need to examine whether the increase in I_{NaP} correlates with the severity of the behavior. This could be accomplished by culturing neurons from each line and examining I_{NaP} amplitudes in cholinergic neurons. This would provide information on whether indeed the I_{NaP} is most increased in neurons containing the *bss* mutation and progressively gets less in neurons from the *eas* and *sda* lines. If this was found to be the case, the corresponding K_{Na} currents could be examined in each. If these currents reached a maximal level, and no longer increased with the increase in I_{NaP}, this would support the hypothesis

that dSlo2 channels indeed can only protect against a certain level of increased I_{NaP}. Additionally, excitability and action potential firing dynamics could be examined in the bang-sensitive mutant neurons with and without *dSlo2*. If excitability, such as increased action potential firing, was most affected in the *sda;dSlo2-* neurons, and less so in the *bss;dSlo2-*, this would be consistent with this hypothesis.

Additionally, electrophysiological experiments in the intact brain could help better understand if this hypothesis is true at the network level. Previous experiments have shown that there is increased synaptic drive from central neurons onto motor neurons in *sda* larvae[202]. These researchers showed that spontaneous currents in motor neurons, elicited from activity coming from central neurons, exhibited a greater amplitude and duration, which was associated with greater excitation of the motor neurons[202]. Similar experiments could examine whether synaptic excitation of the bang-sensitive flies increases with behavioral severity. If so, synaptic drive could be examined in each bang-sensitive fly with and without *dSlo2*. If the increase in synaptic drive was most in the *sda;dSlo2-* line compared to *sda*, and least in *bss/+;dSlo2-* compared to *bss/+*, this would be consistent with the hypothesis that the protective capacity of dSlo2 channels is limited by the amount of overexcitation. While this hypothesis is solely based on behavioral data, it would be interesting and informative to follow up with these types of experiments to test this hypothesis. This information would help understand how much overactivity K_{Na} channels are able to protect against, and when other mechanisms may need to act to prevent overexcitation.

6.3.3 Other potential Na^+ entry pathways stimulating K_{Na} channels

Previous research suggests that K_{Na} channels are activated by multiple sources of Na^+ influx. These include AMPA receptors, H-channels, and CNG channels[299–301]. While my research mainly focuses on the ability of dSlo2 channels to protect against increases in I_{NaP} coming from the voltage-gated Na^+ channel, data from Chapter 4 suggests that it also may be protecting against Na^+ influx through nAChRs. More specifically, it may be that Na^+ influx through the Dα1 nAChR, and not the Dα6 nAChR, activate dSlo2 channels. This was shown by the *dSlo2* null line being more susceptible to behavioral alterations and seizure-like behavior induced by Imidacloprid exposure, which is specific for Dα1 nAChRs[346,403–405].

Additionally, it was found that most Dα1-positive neurons also express dSlo2. Expanding on these findings, it would be advantageous to know whether dSlo2 and Dα1 channels are localized to similar subcellular compartments. This could be accomplished utilizing the *dSlo2-myc* line generated in my research in combination with another line containing an endogenously tagged Dα1 channel. Indeed, I attempted to examine subcellular localization of two lines predicted to tag Dα1 nAChRs with either GFP or myc (#60150 and #84662, Bloomington *Drosophila* Stock Center). However, I was unable to obtain positive staining in dissected adult brains from either line. Therefore, these experiments would entail generating a line that tags Dα1 nAChRs with a small peptide using genetic approaches similar to that used to tag dSlo2. Additionally, examining whether Dα1 activation in cultured neurons activates a K_{Na} current could be explored. This could be accomplished by blocking voltage-gated Na^+ channels and applying Imidacloprid to the cultures. If a K_{Na} current is observed, then it is expected that it would be absent in *dSlo2* null neurons. If true, these results would support the hypothesis that dSlo2 channels are also activated by Na^+ influx through nAChRs. These results would extend the possible sources of Na^+ that activates K_{Na} channels, and could inform future experiments looking at the role of K_{Na} channels in mammalian neurons expressing nAChRs.

6.4 What is the physiological mechanism for dSlo2 protection in the fly?

6.4.1 Does motor output mimic *dSlo2* null seizure-like behavior in bang-sensitive flies?

As mentioned in Section 1.4.2, motor output from the Giant Fiber (GF) pathway has been shown to correlate with seizure-like behavior in bang-sensitive flies[199]. Since this is a physiological readout of what is occurring following stimulation, it would be an advantageous assay to examine how dSlo2 channels are altering motor responses in seizure models. In these assays, an electrical shock is administered to the brain of the fly, thereby stimulating axons of the GF neurons in the brain. These neurons then synapse onto downstream neurons in the ventral nerve cord. These motor neurons then transmit the signal to muscles responsible for the startle response and flight in the adult flies[198]. Recording from these muscles, researchers have previously shown that muscle activity strongly correlates with the seizure-like behavior caused by mechanical stimulation. It would be interesting to determine if the secondary paralysis phase observed in

the *dSlo2-;sda* flies is also apparent in these recordings, as shown by a secondary synaptic failure period. Additionally, this experimental setup allows for examination of seizure threshold, which cannot be measured in the behavioral assays. In this case, increasing levels of stimulation are applied to the brain to determine what threshold is necessary to elicit a seizure-like response in the muscles. For example, it was found that wild-type flies require 46 volts to elicit a seizure-like response, whereas in *bss* flies 3 volts is sufficient to elicit a similar response[200]. The same assays could be conducted on the bang-sensitive flies to determine if the absence of *dSlo2* increases or decreases the seizure threshold. In addition to recording from the giant fiber pathways, recordings from the motor neurons themselves would further our understanding of the role of dSlo2 channels. For example, it has previously been shown that spontaneous rhythmic currents recorded from motor neurons of *sda* larvae exhibit an increase in amplitude and duration[202]. Correspondingly, the spontaneous excitability of these neurons was increased due to increased synaptic drive. These results indicate that central cholinergic neurons, which synapse onto the motor neurons, exhibit increased activity in the *sda* flies. This is particularly pertinent to my results, which suggest that dSlo2 channels act in cholinergic neurons to attenuate seizure-like behavior. Similar recordings from *sda* motor neurons could be compared both with and without *dSlo2*, and when *dSlo2-DN* is expressed in cholinergic neurons. The spontaneous activity of the motor neurons would be expected to increase with the loss of *dSlo2*. This would suggest that indeed dSlo2 channels are attenuating hyperexcitability of upstream cholinergic neurons. Results from these proposed assays would help elucidate the physiological mechanism of dSlo2 channels acting to prevent hyperexcitability caused by an increase in I_{NaP}.

6.4.2 Does the loss of *dSlo2* affect synchronicity observed in I_{NaP}-affected mutants?

Previous reports have shown that synchronous firing patterns between larval motor neurons is increased in flies exhibiting an increased I_{NaP}. In these experiments, they expressed GCaMP in motor neurons in the larval ventral nerve cord. They found that under normal conditions, Ca^{2+} driven activity between segments of these motor neurons usually had a gap time over 200ms, which reflects forward and reverse locomotion patterns. However, in *bss* and *GEFS+* mutant flies, the time between activities of

neuronal segments decreased, thereby exhibiting an increase in synchrony[214]. Additionally, exposure to antiepileptic drugs known to reduce I_{NaP}, such as phenytoin, decreased synchrony close to that seen in wild-type flies. This data strongly suggests that it is the increased I_{NaP} that is responsible for the increased synchrony. It would be informative to use a similar technique to examine whether dSlo2 channels are preventing this increase in synchrony. In these experiments, alterations in synchronicity due to the loss of dSlo2 channels would be tested in *sda*, *eas*, *bss*, and *GEFS+* larvae. Based on the loss of *dSlo2* leading to an exacerbated mechanically induced seizure-like behavior, as well as a spontaneous seizure phenotype, I hypothesize that there would indeed be an increase in synchronicity. This is predicted because an increase in synchronicity between these motor neurons would suggest motor defects in these flies, such as those observed in the behavioral results reported in Chapters 4 and 5. If true, these results would help elucidate the underlying mechanisms of the increased seizure-like behavior due to the loss of *dSlo2*. More importantly, this would have larger implications for human epilepsy associated with an increased I_{NaP}. This is because multiple recent studies have suggested that synchronicity of neuronal firing patterns, observed as gamma oscillations in EEG recordings, is increased in response to an enhanced I_{NaP}[245,246]. Impaired gamma oscillations are associated with multiple pathologies, including FXS, AD, and epilepsy[242–244]. If endogenous dSlo2 channels prevent increased synchronicity between motor neurons, this would suggest that mammalian K_{Na} channels might decrease synchronicity observed in these pathologies. This would warrant further examination of whether mammalian models of these diseases are exacerbated by the knockout of $K_{Na}1.1$ and $K_{Na}1.2$. Additionally, studies could examine if K_{Na} channel activators, such as loxapine, might protect against increased neuronal synchronicity and subsequent symptoms.

6.5 Do K_{Na} channels protect against non-epileptic hyperexcitable disorders?

As mentioned in Section 1.5.3, multiple human disorders have been associated with an increase in I_{NaP}. These include ischemia, FXS, neuropathic pain, ALS, and epilepsy[44,80,213,248–250,437]. While my research implicates K_{Na} channels as a potential therapeutic target for this category of epilepsies, it also suggests they may prevent or alleviate symptoms associated with the increase in I_{NaP}. For example, mutant *SOD1* mouse

models of ALS exhibit an increased I_{NaP} in cultured motor neurons and cortical neurons[80,250]. The same *SOD1* mutation from these mouse models, G93A, has also been found to cause oxidative stress induced degeneration in cholinergic neurons using a C. *elegans* model[438]. Additionally, knock-in ALS models using *SOD1* mutations have been generated in *Drosophila*, and shown to exhibit neurodegeneration and locomotive dysfunction[439]. Therefore, it is feasible to examine whether the loss of dSlo2 may exacerbate these *SOD1* mutant *Drosophila* phenotypes. Additionally, if the loss of K_{Na} channels exacerbates neuronal excitability in the *SOD1* mutant mice, it would suggest that endogenous channels are indeed protecting against the increased I_{NaP}. Also, pharmacological activation of K_{Na} channels could be tested to determine if this attenuates dysfunctional neuromotor behaviors observed in *SOD1* mutant mice, such as forelimb pacing[81].

Neuropathic pain has also been associated with alterations in I_{NaP}. First, persistent Na^+ currents have been observed in both human and rat DRG neurons[249,440]. Furthermore, studies showed that in a compressed DRG rat model of neuropathic pain, that the I_{NaP} was significantly increased[249]. As K_{Na} channels are expressed in DRG and alter neuronal activity, it may be that K_{Na} channels and I_{NaP} work together to affect DRG signaling in both normal physiological states as well as during neuropathic pain. It would therefore be useful to test whether pharmacological activation of K_{Na} channels decreases behavioral sensitivity in these mouse models of neuropathic pain. As mentioned, I did examine the role of dSlo2 channels in affecting acute thermal nociceptive responses in larvae. However, I did not test whether the absence of *dSlo2* modulates neuropathic pain responses. In *Drosophila*, neuropathic pain models use methods to increase sensitivity of the larvae to mechanical or thermal stimulation, such as exposure to UV light or vinca alkaloids[441,442]. Similar treatments could be used to determine whether *dSlo2*- larvae exhibit hyperalgesic behavior.

Researchers have also identified an increase in I_{NaP} in a mouse model of FXS[248]. Using the established *Fmr1* knockout mouse model for FXS, these studies found an increase in I_{NaP} that was associated with increased action potential firing in entorhinal cortex neurons. Similar to above, it would be of interest

to determine whether K_{Na} channels functionally alter the hyperexcitability in this model of FXS. If so, it would offer a potential novel therapeutic target to attenuate some of the cognitive and behavioral impairments associated with the disease. Additionally, *Drosophila* have also been used to study FXS by generating homologous mutations to the *dFMR1* gene. These flies exhibit a number of altered cellular and behavioral characteristics, some of which are similar to human FXS symptoms (reviewed by Drozd et al. 2018[443]). Therefore, combining the genetic dSlo2 mutants generated in this dissertation with the *dFMR1* mutants may help elucidate whether K_{Na} channels function in FXS.

Lastly, an increase in I_{NaP} has been found in both cardiac myocytes and cortical neurons in response to hypoxic conditions[44,444]. Therefore, it is possible that K_{Na} channels may be activated during ischemic episodes, and possibly protect against prolonged depolarization. Indeed, two studies have examined whether the loss of *slo-2* in C. *elegans* exacerbates hypoxic-induced death[272,330]. However, one study found that knock-out of *slo-2* was protective[330] while the other found that it caused the worms to be more susceptible to hypoxia[272]. I similarly conducted experiments on *dSlo2*- flies to test whether they may be more susceptible to hypoxia-induced death. In these assays, flies were exposed to roughly 2% O_2 for 5 hours and replaced to normoxic conditions immediately afterwards. The percentage of flies alive 24 hours following hypoxic treatment was scored and compared between wild-type and *dSlo2*- flies. However, similar to previous studies, results between trials were inconclusive and subsequently abandoned. The experimental setup and technical aspects of these assays were not ideal and could be improved upon in future studies. For example, the hypoxic chamber was large and took over an hour to reach the proper O_2 levels. This led to a large variation between trials. Therefore, a smaller arena could be generated to improve consistency across tests. Previously used hypoxic assays, such as chronic and intermittent hypoxia[445], were not explored and could be examined in future studies. Additionally, hypoxic treatment for 90 minutes has previously been reported to cause susceptibility to mechanically induced seizure-like behavior in wild-type flies[446]. It would be interesting to test whether *dSlo2*- flies may be more susceptible to seizure-like behavior following hypoxic treatment.

6.6 Piece of the Puzzle

When considering the progression of science and our understanding of nature, it is useful to envision a puzzle. Within the puzzle are multiple pieces, which alone do not construct a clear picture. It is only when the pieces are combined that the observer is able to ascertain the overall picture. Almost all scientific hypotheses, discoveries, and theories rely upon the foundation established by numerous studies, or pieces, to combine and form a larger picture. This combination is the result of many scientists working diligently over many years to test and re-test hypotheses. Indeed, the original hypotheses my research is based on were first formulated over 30 years ago. Since then, multiple studies have built upon those initial discoveries, the beginnings of a puzzle. The research completed during my graduate degree attempts to expand upon these findings. Just as scientific discoveries must build upon each other to create a clear picture, my findings are just another piece of this puzzle. However, just as it addresses some questions posed previously, it also creates even more questions and possibilities. Hopefully, these findings help guide future experiments and further our understanding of neuroscience.

BIBLIOGRAPHY

1. Breitenfeld, T., Jurasic, M. J. & Breitenfeld, D. Hippocrates: The forefather of neurology. *Neurol. Sci.* **35**, 1349–1352 (2014).

2. Hodgkin, A. L. & Huxley, A. F. Action Potentials Recorded from Inside a Nerve Fibre. *Nature* **144**, 710–711 (1939).

3. Goldman, D. Potential, Impedance, and Rectification in Membranes. *J. Gen. Physiol.* 37–60 (1943).

4. Hodgkin, A. L. & Katz, B. The effect of Sodium Ions on the Electrical Activity of the Giant Axon of the Squid. *Dev. Brain Res.* **108**, 37–77 (1949).

5. Hodgkin, A. L. & Huxley, A. F. Currents carried by sodium and potassium ions through the membrane of the giant axon of Loligo. *J. Physiol.* **116**, 449–472 (1952).

6. Hodgkin, A. L. & Keynes, R. D. The potassium permeability of a giant nerve fibre. *J. Physiol.* **128**, 61–88 (1955).

7. Agnew, W. S., Levinson, S. R., Brabson, J. S. & Raftery, M. A. Purification of the tetrodotoxin-binding component associated with the voltage-sensitive sodium channel from Electrophorus electricus electroplax membranes. *Proc. Natl. Acad. Sci. U. S. A.* **75**, 2606–2610 (1978).

8. Tamkun, M. M., Talvenheimo, J. A. & Catterall, W. A. The sodium channel from rat brain. *J. Biol. Chem.* **259**, 1676–1688 (1984).

9. Hartshorne, R. P. & Catterall, W. A. The sodium channel from rat brain. Purification and subunit composition. *J. Biol. Chem.* **259**, 1667–1675 (1984).

10. Hartshorne, R., Keller, B. U., Talvenheimo, J. A., Catterall, W. A. & Montal, M. Functional Reconstitution of Purified Sodium Channels from Brain in Planar Lipid Bilayers. *Proc. Natl. Acad. Sci.* **82**, 240–244 (1985).

11. Tempel, B. L., Papazian, D. M., Schwarz, T. L., Jan, Y. N. & Jan, L. Y. Sequence of a Probable Potassium Channel Component Encoded at Shaker Locus of Drosophila. *Science.* **237**, 770–775 (1987).

12. Papazian, D. M., Schwarz, T. L., Tempel, B. L., Jan, Y. N. & Jan, L. Y. Cloning of genomic and complementary DNA from Shaker, a putative potassium channel gene from Drosophila. *Science.* **237**, 749–753 (1987).

13. Butler, A. *et al.* A Family of Putative Potassium Channel Genes in Drosophila. *Science.* **243**, 943–947 (1989).

14. Wei, A. *et al.* K+ Current Diversity Is Produced by an Extended Gene Family Conserved in Drosophila and Mouse. *Science.* **248**, 599–603 (1990).

15. Tsunoda, S. & Salkoff, L. The Major Delayed Rectifier in Both Drosophila Neurons and Muscle is Encoded by Shab. *J. Neurosci.* **15**, 5209–5221 (1995).

16. Tsunoda, S. & Salkoff, L. Genetic analysis of Drosophila neurons: Shal, Shaw, and Shab encode most embryonic potassium currents. *J. Neurosci.* **15**, 1741–1754 (1995).

17. Doyle, D. A. *et al.* The structure of the potassium channel: Molecular basis of K+ conduction and

selectivity. *Science.* **280**, 69–77 (1998).

18. Jiang, Y. *et al.* X-ray structure of a voltage-dependent K+ channel. *Nature* **423**, 33–41 (2003).

19. Long, S. B., Campbell, E. B. & MacKinnon, R. Crystal structure of a mammalian voltage-dependent Shaker family K + channel. *Science.* **309**, 897–903 (2005).

20. Geschwind, D. H. Advances in autism. *Annu. Rev. Med.* **60**, 367–380 (2009).

21. Zhang, Y. *et al.* Dendritic channelopathies contribute to neocortical and sensory hyperexcitability in Fmr1-/y mice. *Nat. Neurosci.* **17**, 1701–1709 (2014).

22. Gallagher, A. & Hallahan, B. Fragile X-associated disorders: A clinical overview. *J. Neurol.* **259**, 401–413 (2012).

23. Penagarikano, O., Mulle, J. G. & Warren, S. T. The pathophysiology of fragile X syndrome. *Annu. Rev. Genomics Hum. Genet.* **8**, 109–129 (2007).

24. Chen, L. & Toth, M. Fragile X mice develop sensory hyperreactivity to auditory stimuli. *Neuroscience* **103**, 1043–1050 (2001).

25. Gibson, J. R., Bartley, A. F., Hays, S. A. & Huber, K. M. Imbalance of neocortical excitation and inhibition and altered UP states reflect network hyperexcitability in the mouse model of fragile X syndrome. *J. Neurophysiol.* **100**, 2615–2626 (2008).

26. Contractor, A., Klyachko, V. A. & Portera-Cailliau, C. Altered Neuronal and Circuit Excitability in Fragile X Syndrome. *Neuron* **87**, 699–715 (2015).

27. Booker, S. A. *et al.* Altered dendritic spine function and integration in a mouse model of fragile X syndrome. *Nat. Commun.* **10**, (2019).

28. Bülow, P., Murphy, T. J., Bassell, G. J. & Wenner, P. Homeostatic Intrinsic Plasticity Is Functionally Altered in Fmr1 KO Cortical Neurons. *Cell Rep.* **26**, 1378–1388 (2019).

29. Zhang, L., He, J., Jugloff, D. G. M. & Eubanks, J. H. The MeCP2-null mouse hippocampus displays altered basal inhibitory rhythms and is prone to hyperexcitability. *Hippocampus* **18**, 294–309 (2008).

30. Rivell, A. & Mattson, M. P. Intergenerational Metabolic Syndrome and Neuronal Network Hyperexcitability in Autism. *Trends Neurosci.* **42**, 709–726 (2019).

31. Antoine, M. W., Langberg, T., Schnepel, P. & Feldman, D. E. Increased Excitation-Inhibition Ratio Stabilizes Synapse and Circuit Excitability in Four Autism Mouse Models. *Neuron* **101**, 648-661.e4 (2019).

32. Van Hecke, O., Austin, S. K., Khan, R. A., Smith, B. H. & Torrance, N. Neuropathic pain in the general population: A systematic review of epidemiological studies. *Pain* **155**, 654–662 (2014).

33. Calvo, M. *et al.* The Genetics of Neuropathic Pain from Model Organisms to Clinical Application. *Neuron* **104**, 637–653 (2019).

34. Veluchamy, A., Hébert, H. L., Meng, W., Palmer, C. N. A. & Smith, B. H. Systematic review and meta-analysis of genetic risk factors for neuropathic pain. *Pain* **159**, 825–848 (2018).

35. Fertleman, C. R. *et al.* SCN9A Mutations in Paroxysmal Extreme Pain Disorder: Allelic Variants Underlie Distinct Channel Defects and Phenotypes. *Neuron* **52**, 767–774 (2006).

36. Yang, Y. *et al.* Mutations in SCN9A, encoding a sodium channel alpha subunit, in patients with

primary erythermalgia. *J. Med. Genet.* **41**, 171–174 (2004).

37. Blesneac, I. *et al.* Rare NaV1.7 variants associated with painful diabetic peripheral neuropathy. *Pain* **159**, 469–480 (2018).

38. Dib-Hajj, S. D. & Waxman, S. G. Sodium Channels in Human Pain Disorders: Genetics and Pharmacogenomics. *Annu. Rev. Neurosci.* **42**, 87–106 (2019).

39. Finnerup, N. B. *et al.* Pharmacotherapy for neuropathic pain in adults: A systematic review and meta-analysis. *Lancet Neurol.* **14**, 162–173 (2015).

40. Jones, M. R. *et al.* A Brief History of the Opioid Epidemic and Strategies for Pain Medicine. *Pain Ther.* **7**, 13–21 (2018).

41. Meyer, F. B. Calcium, neuronal hyperexcitability and ischemic injury. *Brain Res. Rev.* **14**, 227–243 (1989).

42. Lee, J. M., Zipfel, G. J. & Choi, D. W. The changing landscape of ischaemic brain injury mechanisms. *Nature* **399**, 7–14 (1999).

43. Nicholls, D. & Attwell, D. The release and uptake of excitatory amino acids. *Trends Pharmacol. Sci.* **11**, 462–468 (1990).

44. Hammarström, A. K. M. & Gage, P. W. Inhibition of oxidative metabolism increases persistent sodium current in rat CA1 hippocampal neurons. *J. Physiol.* **510**, 735–741 (1998).

45. Hammarström, A. K. M. & Gage, P. W. Hypoxia and persistent sodium current. *Eur. Biophys. J.* **31**, 323–330 (2002).

46. Wang, W., Ma, J., Zhang, P. & Luo, A. Redox reaction modulates transient and persistent sodium current during hypoxia in guinea pig ventricular myocytes. *Pflugers Arch. Eur. J. Physiol.* **454**, 461–475 (2007).

47. Xuan Chi, X. & Xu, Z. C. Potassium currents in CA1 neurons of rat hippocampus increase shortly after transient cerebral ischemia. *Neurosci. Lett.* **281**, 5–8 (2000).

48. Huang, H., Gao, T. M., Gong, L. W., Zhuang, Z. Y. & Li, X. Potassium channel blocker TEA prevents CA1 hippocampal injury following transient forebrain ischemia in adult rats. *Neurosci. Lett.* **305**, 83–86 (2001).

49. Wei, L. *et al.* Potassium channel blockers attenuate hypoxia- and ischemia-induced neuronal death in vitro and in vivo. *Stroke* **34**, 1281–1286 (2003).

50. Pal, S., Hartnett, K. a, Nerbonne, J. M., Levitan, E. S. & Aizenman, E. Mediation of neuronal apoptosis by Kv2.1-encoded potassium channels. *J. Neurosci.* **23**, 4798–4802 (2003).

51. Shah, N. H. & Aizenman, E. Voltage-Gated Potassium Channels at the Crossroads of Neuronal Function, Ischemic Tolerance, and Neurodegeneration. *Transl. Stroke Res.* **5**, 38–58 (2014).

52. Misonou, H., Mohapatra, D. P., Menegola, M. & Trimmer, J. S. Calcium- and metabolic state-dependent modulation of the voltage-dependent Kv2.1 channel regulates neuronal excitability in response to ischemia. *J. Neurosci.* **25**, 11184–11193 (2005).

53. Fox, P. D. *et al.* Induction of stable ER-plasma-membrane junctions by Kv2.1 potassium channels. *J. Cell Sci.* **128**, 2096–2105 (2015).

54. Johnson, B., Leek, A. N. & Tamkun, M. M. Kv2 channels create endoplasmic reticulum / plasma

membrane junctions: a brief history of Kv2 channel subcellular localization. *Channels* **13**, 88–101 (2019).

55. Schulien, A. J. *et al.* Targeted disruption of Kv2.1-VAPA association provides neuroprotection against ischemic stroke in mice by declustering Kv2.1 channels. *Sci. Adv.* **6**, 1–14 (2020).

56. Carron, S. F., Alwis, D. S. & Rajan, R. Traumatic brain injury and neuronal functionality changes in sensory cortex. *Front. Syst. Neurosci.* **10**, 1–17 (2016).

57. Lowenstein, D. H. Epilepsy after head injury: An overview. *Epilepsia* **50**, 4–9 (2009).

58. Cantu, D. *et al.* Traumatic Brain Injury Increases Cortical Glutamate Network Activity by Compromising GABAergic Control. *Cereb. Cortex* **25**, 2306–2320 (2015).

59. Khan, M. *et al.* S-Nitrosoglutathione reduces oxidative injury and promotes mechanisms of neurorepair following traumatic brain injury in rats. *J. Neuroinflammation* **8**, (2011).

60. Readnower, R. D. *et al.* Post-injury administration of the mitochondrial permeability transition pore inhibitor, NIM811, is neuroprotective and improves cognition after traumatic brain injury in rats. *J. Neurotrauma* **28**, 1845–1853 (2011).

61. Fox, G. B., Fan, L., Levasseur, R. A. & Faden, A. I. Sustained sensory/motor and cognitive deficits with neuronal apoptosis following controlled cortical impact brain injury in the mouse. *J. Neurotrauma* **15**, 599–614 (1998).

62. Zhou, H., Chen, L., Gao, X., Luo, B. & Chen, J. Moderate Traumatic Brain Injury Triggers Rapid Necrotic Death of Immature Neurons in the Hippocampus. *J. Neuropahtol Exp Neurol* **71**, 348–359 (2012).

63. Huttunen, J. K. *et al.* Detection of Hyperexcitability by Functional Magnetic Resonance Imaging after Experimental Traumatic Brain Injury. *J. Neurotrauma* **35**, 2708–2717 (2018).

64. Ding, M. C., Wang, Q., Lo, E. H. & Stanley, G. B. Cortical excitation and inhibition following focal traumatic brain injury. *J. Neurosci.* **31**, 14085–14094 (2011).

65. Ping, X. & Jin, X. Transition from Initial Hypoactivity to Hyperactivity in Cortical Layer v Pyramidal Neurons after Traumatic Brain Injury in Vivo. *J. Neurotrauma* **33**, 354–361 (2016).

66. Busche, M. A. *et al.* Clusters of Hyperactive Neurons Near Amyloid Plaques in a Mouse Model of Alzheimer's Disease. *Science.* **321**, 1686–1690 (2008).

67. Bishop, M. W. *et al.* Hyperexcitable substantia nigra dopamine neurons in PINK1- and HtrA2/omi-deficient mice. *J. Neurophysiol.* **104**, 3009–3020 (2010).

68. Kim, J. *et al.* Changes in the excitability of neocortical neurons in a mouse model of amyotrophic lateral sclerosis are not specific to corticospinal neurons and are modulated by advancing disease. *J. Neurosci.* **37**, 9037–9053 (2017).

69. Zhang, C. *et al.* Presenilins are Essential for Regulating Neurotransmitter Release. *Nature* **460**, 632–636 (2009).

70. Liss, B. *et al.* K-ATP channels promote the differential degeneration of dopaminergic midbrain neurons. *Nat. Neurosci.* **8**, 1742–1751 (2005).

71. Hahm, E. *et al.* Cholinergic Homeostatic Synaptic Plasticity Drives the Progression of A b -Induced Changes in Neural Article Cholinergic Homeostatic Synaptic Plasticity Drives the Progression of A b -Induced Changes in Neural Activity. *Cell Rep.* **24**, 342–354 (2018).

72. Vucic, S. & Kiernan, M. C. Novel threshold tracking techniques suggest that cortical hyperexcitability is an early feature of motor neuron disease. *Brain* **129**, 2436–2446 (2006).

73. Vucic, S., Nicholson, G. A. & Kiernan, M. C. Cortical hyperexcitability may precede the onset of familial amyotrophic lateral sclerosis. *Brain* **131**, 1540–1550 (2008).

74. Geevasinga, N. *et al.* Cortical Function in Asymptomatic Carriers and Patients With C9orf72 Amyotrophic Lateral Sclerosis Nimeshan. *JAMA Neurol.* **72**, 1268–1274 (2015).

75. Vucic, S. & Kiernan, M. C. Transcranial Magnetic Stimulation for the Assessment of Neurodegenerative Disease. *Neurotherapeutics* **14**, 91–106 (2017).

76. Shibuya, K. *et al.* Motor cortical function determines prognosis in sporadic ALS. *Neurology* **87**, 513–520 (2016).

77. Eisen, A. *et al.* Cortical influences drive amyotrophic lateral sclerosis. *J. Neurol. Neurosurg. Psychiatry* **88**, 917–924 (2017).

78. LoRusso, E., Hickman, J. J. & Guo, X. Ion channel dysfunction and altered motoneuron excitability in ALS. *Neurol. Disord. epilepsy J.* **3**, 1–13 (2019).

79. Kuo, J. J. *et al.* Hyperexcitability of Cultured Spinal Motoneurons from Presymptomatic ALS Mice. *J. Neurophysiol.* **91**, 571–575 (2004).

80. Kuo, J. J., Siddique, T., Fu, R. & Heckman, C. J. Increased persistent Na+ current and its effect on excitability in motoneurones cultured from mutant SOD1 mice. *J. Physiol.* **563**, 843–854 (2005).

81. Van Zundert, B. *et al.* Neonatal neuronal circuitry shows hyperexcitable disturbance in a mouse model of the adult-onset neurodegenerative disease amyotrophic lateral sclerosis. *J. Neurosci.* **28**, 10864–10874 (2008).

82. Shibuya, K. *et al.* Markedly reduced axonal potassium channel expression in human sporadic amyotrophic lateral sclerosis: An immunohistochemical study. *Exp. Neurol.* **232**, 149–153 (2011).

83. Bellingham, M. C. A Review of the Neural Mechanisms of Action and Clinical Efficiency of Riluzole in Treating Amyotrophic Lateral Sclerosis: What have we Learned in the Last Decade? *CNS Neurosci. Ther.* **17**, 4–31 (2011).

84. Tubert, C. & Murer, M. G. What's wrong with the striatal cholinergic interneurons in Parkinson's disease? Focus on intrinsic excitability. *Eur. J. Neurosci.* 1–17 (2020). doi:10.1111/ejn.14742

85. Tubert, C. *et al.* Decrease of a Current Mediated by Kv1.3 Channels Causes Striatal Cholinergic Interneuron Hyperexcitability in Experimental Parkinsonism. *Cell Rep.* **16**, 2749–2762 (2016).

86. Katzenschlager, R., Sampaio, C., Costa, J. & Lees, A. Anticholinergics for symptomatic management of Parkinson´s disease. *Cochrane Database Syst. Rev.* (2002). doi:10.1002/14651858.cd003735

87. Bennett, B. D. & Wilson, C. J. Spontaneous activity of neostriatal cholinergic interneurons in vitro. *J. Neurosci.* **19**, 5586–5596 (1999).

88. Grace, A. A. & Onn, S. P. Morphology and electrophysiological properties of immunocytochemistry identified rat dopamine neurons recorded in vitro. *J. Neurosci.* **9**, 3463–3481 (1989).

89. Association, A. Alzheimer ' s disease facts and figures. **12**, 459–509 (2013).

90. Masters, C. L. *et al.* Neuronal origin of a cerebral amyloid: neurofibrillary tangles of Alzheimer's disease contain the same protein as the amyloid of plaque cores and blood vessels. *EMBO J.* **4**, 2757–2763 (1985).

91. Hardy, J. A. & Higgins, G. A. Alzheimer's disease: The amyloid cascade hypothesis. *Science.* **256**, 184–185 (1992).

92. Lambert, M. P. *et al.* Diffusible, nonfibrillar ligands derived from Aβ1-42 are potent central nervous system neurotoxins. *Proc. Natl. Acad. Sci. U. S. A.* **95**, 6448–6453 (1998).

93. Ferreira, S. T., Lourenco, M. V., Oliveira, M. M. & De Felice, F. G. Soluble amyloid-β oligomers as synaptotoxins leading to cognitive impairment in Alzheimer's disease. *Front. Cell. Neurosci.* **9**, 1–17 (2015).

94. Ping, Y. *et al.* Linking Aβ42-Induced Hyperexcitability to Neurodegeneration, Learning and Motor Deficits, and a Shorter Lifespan in an Alzheimer's Model. *PLOS Genet.* **11**, e1005025 (2015).

95. Ren, S. Q. *et al.* Amyloid β causes excitation/inhibition imbalance through dopamine receptor 1-dependent disruption of fast-spiking GABAergic input in anterior cingulate cortex. *Sci. Rep.* **8**, 1–10 (2018).

96. Brown, J. T., Chin, J., Leiser, S. C., Pangalos, M. N. & Randall, A. D. Altered intrinsic neuronal excitability and reduced Na+ currents in a mouse model of Alzheimer's disease. *Neurobiol. Aging* **32**, 2109.e1-2109.e14 (2011).

97. Busche, M. A. *et al.* Critical role of soluble amyloid-β for early hippocampal hyperactivity in a mouse model of Alzheimer's disease. *Proc. Natl. Acad. Sci. U. S. A.* **109**, 8740–8745 (2012).

98. Coelho, D. S. & Moreno, E. Neuronal Selection Based on Relative Fitness Comparison Detects and Eliminates Amyloid-β-Induced Hyperactive Neurons in Drosophila. *iScience* **23**, 101468 (2020).

99. Davis, K. E., Fox, S. & Gigg, J. Increased hippocampal excitability in the 3xTgAD mouse model for Alzheimer's disease in vivo. *PLoS One* **9**, (2014).

100. Ghatak, S. *et al.* Mechanisms of hyperexcitability in alzheimer's disease hiPSC-derived neurons and cerebral organoids vs. Isogenic control. *Elife* **8**, 1–22 (2019).

101. Kuchibhotla, K. V. *et al.* Aβ Plaques Lead to Aberrant Regulation of Calcium Homeostasis In Vivo Resulting in Structural and Functional Disruption of Neuronal Networks. *Neuron* **59**, 214–225 (2008).

102. Minkeviciene, R. *et al.* Amyloid β-induced neuronal hyperexcitability triggers progressive epilepsy. *J. Neurosci.* **29**, 3453–3462 (2009).

103. Palop, J. J. *et al.* Aberrant Excitatory Neuronal Activity and Compensatory Remodeling of Inhibitory Hippocampal Circuits in Mouse Models of Alzheimer's Disease. *Neuron* **55**, 697–711 (2007).

104. Small, D. H. Network dysfunction in Alzheimer's disease: does synaptic scaling drive disease progression? *Trends Mol. Med.* **14**, 103–108 (2008).

105. Moshé, S. L., Perucca, E., Ryvlin, P. & Tomson, T. Epilepsy: New advances. *Lancet* **385**, 884–898 (2015).

106. Fisher, R. S. *et al.* Response: Definitions proposed by the International League Against Epilepsy

(ILAE) and the International Bureau for Epilepsy (IBE) [4]. *Epilepsia* **46**, 1701–1702 (2005).

107. Falco-Walter, J. J., Scheffer, I. E. & Fisher, R. S. The new definition and classification of seizures and epilepsy. *Epilepsy Res.* **139**, 73–79 (2018).

108. Lindy, A. S. *et al.* Diagnostic outcomes for genetic testing of 70 genes in 8565 patients with epilepsy and neurodevelopmental disorders. *Epilepsia* **59**, 1062–1071 (2018).

109. Deng, H., Xiu, X. & Song, Z. The molecular biology of genetic-based epilepsies. *Mol. Neurobiol.* **49**, 352–367 (2014).

110. Catterall, W. A., Kalume, F. & Oakley, J. C. NaV1.1 channels and epilepsy. *J. Physiol.* **588**, 1849–1859 (2010).

111. Niday, Z. & Tzingounis, A. V. Potassium Channel Gain of Function in Epilepsy: An Unresolved Paradox. *Neuroscientist* (2018). doi:10.1177/1073858418763752

112. Heyne, H. O. *et al.* Targeted gene sequencing in 6994 individuals with neurodevelopmental disorder with epilepsy. *Genet. Med.* **21**, 2496–2503 (2019).

113. Menezes, L. F. S., Sabiá Júnior, E. F., Tibery, D. V., Carneiro, L. dos A. & Schwartz, E. F. Epilepsy-Related Voltage-Gated Sodium Channelopathies: A Review. *Front. Pharmacol.* **11**, (2020).

114. Ogiwara, I. *et al.* Nav1.1 haploinsufficiency in excitatory neurons ameliorates seizure-associated sudden death in a mouse model of dravet syndrome. *Hum. Mol. Genet.* **22**, 4784–4804 (2013).

115. Martin, M. S. *et al.* Altered function of the SCN1A voltage-gated sodium channel leads to γ-aminobutyric acid-ergic (GABAergic) interneuron abnormalities. *J. Biol. Chem.* **285**, 9823–9834 (2010).

116. Sun, L. *et al.* A knock-in model of human epilepsy in Drosophila reveals a novel cellular mechanism associated with heat-induced seizure. *J. Neurosci.* **32**, 14145–55 (2012).

117. Schutte, R. J. *et al.* Knock-in model of Dravet syndrome reveals a constitutive and conditional reduction in sodium current. *J. Neurophysiol.* **112**, 903–912 (2014).

118. Schutte, S. S., Schutte, R. J., Barragan, E. V. & O'Dowd, D. K. Model systems for studying cellular mechanisms of SCN1A-related epilepsy. *J. Neurophysiol.* **115**, 1755–1766 (2016).

119. Scheffer, I. E. & Berkovic, S. F. Generalized epilepsy with febrile seizures plus. A genetic disorder with heterogeneous clinical phenotypes. *Brain* **120**, 479–490 (1997).

120. Dravet, C. The core Dravet syndrome phenotype. *Epilepsia* **52**, 3–9 (2011).

121. Kalume, F., Yu, F. H., Westenbroek, R. E., Scheuer, T. & Catterall, W. A. Reduced sodium current in Purkinje neurons from Nav1.1 mutant mice: Implications for ataxia in severe myoclonic epilepsy in infancy. *J. Neurosci.* **27**, 11065–11074 (2007).

122. Yu, F. H. *et al.* Reduced sodium current in GABAergic interneurons in a mouse model of severe myoclonic epilepsy in infancy. *Nat. Neurosci.* **9**, 1142–1149 (2006).

123. Fujiwara, T. *et al.* Mutations of sodium channel α subunit type 1 (SCN1A) in intractable childhood epilepsies with frequent generalized tonic-clonic seizures. *Brain* **126**, 531–546 (2003).

124. Tang, B. *et al.* A BAC transgenic mouse model reveals neuron subtype-specific effects of a Generalized Epilepsy with Febrile Seizures Plus (GEFS +) mutation. *Naurobiol Dis.* **35**, 91–102

(2009).

125. Abou-Khalil, B. *et al.* Partial and generalized epilepsy with febrile seizures plus and a novel SCN1A mutation. *Neurology* **57**, 2265–2272 (2001).

126. Lukmanji, S. *et al.* The co-occurrence of epilepsy and autism: A systematic review. *Epilepsy Behav.* **98**, 238–248 (2019).

127. Hoon Lee, B., Smith, T. & Paciorkowski, A. R. Autism Spectrum Disorder and Epilepsy: disorders with a shared biology. *Epilepsy Behav.* 191–201 (2015). doi:10.1016/j.yebeh.2015.03.017.Autism

128. Menon, B. & Shorvon, S. D. Ischaemic stroke in adults and epilepsy. *Epilepsy Res.* **87**, 1–11 (2009).

129. Jungehulsing, G. J., Heuschmann, P. U., Holtkamp, M., Schwab, S. & Kolominsky-Rabas, P. L. Incidence and predictors of post-stroke epilepsy. *Acta Neurol. Scand.* **127**, 427–430 (2013).

130. Zhang, C. *et al.* Risk factors for post-stroke seizures: A systematic review and meta-analysis. *Epilepsy Res.* **108**, 1806–1816 (2014).

131. Pitkänen, A., Roivainen, R. & Lukasiuk, K. Development of epilepsy after ischaemic stroke. *Lancet Neurol.* **15**, 185–197 (2016).

132. Lowenstein, D. H. Epilepsy after head injury: An overview. *Epilepsia* **50**, 4–9 (2009).

133. Agrawal, A., Timothy, J., Pandit, L. & Manju, M. Post-traumatic epilepsy: An overview. *Clin. Neurol. Neurosurg.* **108**, 433–439 (2006).

134. Ferguson, P. L. *et al.* A population-based study of risk of epilepsy after hospitalization for traumatic brain injury. *Epilepsia* **51**, 891–898 (2010).

135. Salazar, A. M. & Grafman, J. Post-traumatic epilepsy. clinical clues to pathogenesis and paths to prevention. *Handb. Clin. Neurol.* **128**, 525–538 (2015).

136. Sharma, R. *et al.* Neuroinflammation in post-traumatic epilepsy: Pathophysiology and tractable therapeutic targets. *Brain Sci.* **9**, (2019).

137. Amatniek, J. C. *et al.* Incidence and Predictors of Seizures in Patients with Alzheimer's Disease. *Epilepsia* **47**, 867–872 (2006).

138. Hebb, D. O. The Organization of Behavior: A Neuropsychological Theory. (1949). doi:10.2307/1418888

139. Bliss, T. V. . & Lomo, T. Long-Lasting Potentiation of Synaptic Transmission in the Dentate Area of the Anasthetized Rabbit following Stimulation of the Perforant Path. *J. Physiol.* 331–356 (1973).

140. Kandel, E. R. The Molecular Biology of Memory Storage: A Dialogue Between Genes and Synapses. **294**, 1030–1039 (2001).

141. Herron, C. E., Lester, R. A. J., Coan, E. J. & Collingridge, G. L. Frequency-dependent involvement of NMDA receptors in the hippocampus: A novel synaptic mechanism. *Nature* **322**, 265–268 (1986).

142. Morris, R. G. M., Anderson, E., Lynch, G. S. & Baudry, M. Selective Impairment of Learning and Blockade of Long-Term Potentiation by an N-methyl-D-aspartate receptor antagonist, AP5.

Nature **319**, 75–77 (1986).

143. Bliss, T.V.P. & Collingridge, G. L. A synaptic model of memory: LTP in the hippocampus. *Nature* **361**, 31–39 (1993).

144. Tang, Y. P. *et al.* Genetic enhancement of learning and memory in mice. *Nature* **401**, 63–69 (1999).

145. Dudek, S. M. & Bear, M. F. Homosynaptic long-term depression in area CA1 of hippocampus and effects of N-methyl-D-aspartate receptor blockade. *Proc. Natl. Acad. Sci. U. S. A.* **89**, 4363–4367 (1992).

146. Kemp, N. & Bashir, Z. I. Long-term depression: A cascade of induction and expression mechanisms. *Prog. Neurobiol.* **65**, 339–365 (2001).

147. Massey, P. V. & Bashir, Z. I. Long-term depression: multiple forms and implications for brain function. *Trends Neurosci.* **30**, 176–184 (2007).

148. Fox, K. & Stryker, M. Integrating Hebbian and homeostatic plasticity: Introduction. *Philos. Trans. R. Soc. B Biol. Sci.* **372**, (2017).

149. Turrigiano, G. G. The dialectic of hebb and homeostasis. *Philos. Trans. R. Soc. B Biol. Sci.* **372**, 4–6 (2017).

150. Turrigiano, G. G., Leslie, K. R., Desai, N. S., Rutherford, L. C. & Nelson, S. B. Activity-dependent scaling of quantal amplitude in neocortical neurons. *Nature* **391**, 892–896 (1998).

151. Desai, N. S., Cudmore, R. H., Nelson, S. B. & Turrigiano, G. G. Critical periods for experience-dependent synaptic scaling in visual cortex. *Nat. Neurosci.* **5**, 783–789 (2002).

152. Goel, A. *et al.* Cross-modal regulation of synaptic AMPA receptors in primary sensory cortices by visual experience. *Nat. Neurosci.* **9**, 1001–1003 (2006).

153. Goel, A. & Lee, H. K. Persistence of experience-induced homeostatic synaptic plasticity through adulthood in superficial layers of mouse visual cortex. *J. Neurosci.* **27**, 6692–6700 (2007).

154. Kim, J. & Tsien, R. W. Synapse-Specific Adaptations to Inactivity in Hippocampal Circuits Achieve Homeostatic Gain Control while Dampening Network Reverberation. *Neuron* **58**, 925–937 (2008).

155. Goold, C. P. & Nicoll, R. A. Single-Cell Optogenetic Excitation Drives Homeostatic Synaptic Depression. *Neuron* **68**, 512–528 (2010).

156. Benevento, L. A., Bakkum, B. W. & Cohen, R. S. Gamma-aminobutyric acid and somatostatin immunoreactivity in the visual cortex of normal and dark-reared rats. *Brain Res.* **689**, 172–182 (1995).

157. Hendry, S. H. C. *et al.* GABA(A) receptor subunit immunoreactivity in primate visual cortex: Distribution in macaques and humans and regulation by visual input in adulthood. *J. Neurosci.* **14**, 2383–2401 (1994).

158. Hendry, S. H. C. & Jones, E. G. Reduction in number of immunostained BAGAergic neurones in deprived-eye dominance columns of monkey area 17. *Nature* **320**, 750–753 (1986).

159. Hendry, S. H. C. & Jones, E. G. Activity-dependent regulation of GABA expression in the visual cortex of adult monkeys. *Neuron* **1**, 701–712 (1988).

160. Marty, S., Da, M. & Berninger, B. Neurotrophins and activity-dependent plasticity of cortical interneurons. *Trends Neurosci.* **20**, 198–202 (1997).

161. Rutherford, L. C., DeWan, A., Lauer, H. M. & Turrigiano, G. G. Brain-derived neurotrophic factor mediates the activity-dependent regulation of inhibition in neocortical cultures. *J. Neurosci.* **17**, 4527–4535 (1997).

162. Hartman, K. N., Pal, S. K., Burrone, J. & Murthy, V. N. Activity-dependent regulation of inhibitory synaptic transmission in hippocampal neurons. *Nat. Neurosci.* **9**, 642–649 (2006).

163. Kilman, V., Van Rossum, M. C. W. & Turrigiano, G. G. Activity deprivation reduces miniature IPSC amplitude by decreasing the number of postsynaptic GABAA receptors clustered at neocortical synapses. *J. Neurosci.* **22**, 1328–1337 (2002).

164. Albuquerque, E. X., Pereira, E. F. R., Alkondon, M. & Rogers, S. W. Mammalian nicotinic acetylcholine receptors: From structure to function. *Physiol. Rev.* **89**, 73–120 (2009).

165. Steinlein, O. K. & Bertrand, D. Neuronal nicotinic acetylcholine receptors: From the genetic analysis to neurological diseases. *Biochem. Pharmacol.* **76**, 1175–1183 (2008).

166. Ping, Y. & Tsunoda, S. Inactivity-induced increase in nAChRs upregulates Shal K + channels to stabilize synaptic potentials. *Nat. Neurosci.* **15**, 90–97 (2012).

167. Turrigiano, G., Abbott, L. F. & Marder, E. Activity-Dependent Changes in the Intrinsic Properties of Cultured Neurons. *Science.* **264**, 974–977 (1994).

168. LeMasson, G., Marder, E. & Abbott, L. F. Activity-dependent regulation of conductances in model neurons. *Science.* **259**, 1915–1917 (1993).

169. Golowasch, J., Abbott, L. F. & Marder, E. Activity-dependent regulation of potassium currents in an identified neuron of the stomatogastric ganglion of the crab Cancer borealis. *J. Neurosci.* **19**, 1–5 (1999).

170. Marder, E. & Prinz, A. A. Modeling stability in neuron and network function: The role of activity in homeostasis. *BioEssays* **24**, 1145–1154 (2002).

171. Desai, N. S., Rutherford, L. C. & Turrigiano, G. G. Plasticity in the intrinsic excitability of cortical pyramidal neurons. *Nat. Neurosci.* **2**, 515–520 (1999).

172. Fan, Y. *et al.* Activity-dependent decrease of excitability in rat hippocampal neurons through increases in Ih. *Nat. Neurosci.* **8**, 1542–1551 (2005).

173. Frick, A., Magee, J. & Johnston, D. LTP is accompanied by an enhanced local excitability of pyramidal neuron dendrites. *Nat. Neurosci.* **7**, 126–135 (2004).

174. Cudmore, R. H., Fronzaroli-Molinieres, L., Giraud, P. & Debanne, D. Spike-time precision and network synchrony are controlled by the homeostatic regulation of the D-type potassium current. *J. Neurosci.* **30**, 12885–12895 (2010).

175. Nataraj, K., Le Roux, N., Nahmani, M., Lefort, S. & Turrigiano, G. Visual deprivation suppresses L5 Pyramidal Neuron Excitability by Preventing the Induction of Intrinsic Plasticity. *Neuron* **68**, 750–762 (2010).

176. Breton, J. D. & Stuart, G. J. Loss of sensory input increases the intrinsic excitability of layer 5 pyramidal neurons in rat barrel cortex. *J. Physiol.* **587**, 5107–5119 (2009).

177. Kim, E. Z., Vienne, J., Rosbash, M. & Griffith, L. C. Nonreciprocal homeostatic compensation in

drosophila potassium channel mutants. *J. Neurophysiol.* **117**, 2125–2136 (2017).

178. Apostolopoulou, A. A. & Lin, A. C. Mechanisms underlying homeostatic plasticity in the Drosophila mushroom body in vivo. *Proc. Natl. Acad. Sci. U. S. A.* **117**, 16606–16615 (2020).

179. Eadaim, A., Hahm, E. T., Justice, E. D. & Tsunoda, S. Cholinergic Synaptic Homeostasis Is Tuned by an NFAT-Mediated α7 nAChR-Kv4/Shal Coupled Regulatory System. *Cell Rep.* **32**, 108119 (2020).

180. Grubb, M. S. & Burrone, J. Activity-dependent relocation of the axon initial segment fine-tunes neuronal excitability. *Nature* **465**, 1070–1074 (2010).

181. Kuba, H., Oichi, Y. & Ohmori, H. Presynaptic activity regulates Na+ channel distribution at the axon initial segment. *Nature* **465**, 1075–1078 (2010).

182. Catsch, A. Eine Erbliche Storung des Bewegungsmechanismus bei Drosophila Melanogaster. 64–66 (1944).

183. Fahmy, O. G. & Fahmy, M. J. Differential Gene Response to Mutagens in Drosophila Melanogaster. *Genetics* **44**, 1149–71 (1959).

184. Kaplan, W. D. & Trout, W. E. The behavior of four neurological mutants of Drosophila. *Genetics* **61**, 399–409 (1969).

185. Lee, J. & Wu, C. F. Genetic modifications of seizure susceptibility and expression by altered excitability in Drosophila Na+ and K+ channel mutants. *J. Neurophysiol.* **96**, 2465–2478 (2006).

186. Suzuki, D. T., Grigliatti, T. & Williamson, R. Temperature-Sensitive Mutations in Drosophila melanogaster, VII, A Mutation (parats) Causing Reversible Adult Paralysis. *P.N.a.S* **68**, 890–893 (1971).

187. Wu, C. F., Ganetzky, B., Jan, L. Y., Jan, Y. N. & Benzer, S. A Drosophila mutant with a temperature-sensitive block in nerve conduction. *Proc. Natl. Acad. Sci. U. S. A.* **75**, 4047–4051 (1978).

188. Grigliatti, T. A., Hall, L., Rosenbluth, R. & Suzuki, D. T. Temperature-Sensitive Mutations in Drosophila melanogaster XIV. A Selection of Immobile Adults. *Mol. Genet.* **120**, 107–114 (1972).

189. Jackson, F. R., Gitschier, J., Strichartz, G. R. & Hall, L. M. Genetic modifications of voltage-sensitive sodium channels in Drosophila: Gene dosage studies of the seizure locus. *J. Neurosci.* **5**, 1144–1151 (1985).

190. Loughney, K., Kreber, R. & Ganetzky, B. Molecular analysis of the para locus, a sodium channel gene in Drosophila. *Cell* **58**, 1143–1154 (1989).

191. Siddiqi, O. & Benzer, S. Neurophysiological defects in temperature sensitive paralytic mutants of Drosophila melanogaster. *Proc. Natl. Acad. Sci. U. S. A.* **73**, 3253–3257 (1976).

192. Brunklaus, A., Ellis, R., Reavey, E., Semsarian, C. & Zuberi, S. M. Genotype phenotype associations across the voltage-gated sodium channel family. *J. Med. Genet.* **51**, 650–658 (2014).

193. Benzer, S. From the Gene to Behavior. *JAMA* **218**, 1015–1022 (1971).

194. Ganetzky, B. & Wu, C.-F. Indirect Suppression Involving Behavioral Mutants. *Genetics* 597–614 (1982).

195. Parker, L., Howlett, I. C., Rusan, Z. M. & Tanouye, M. a. Seizure and epilepsy: Studies of seizure

disorders in drosophila. *Int. Rev. Neurobiol.* **99**, 1–21 (2011).

196. Pavlidis, P. & Tanouye, M. a. Seizures and failures in the giant fiber pathway of Drosophila bang-sensitive paralytic mutants. *J. Neurosci.* **15**, 5810–5819 (1995).

197. Lee, J. & Wu, C. F. Electroconvulsive seizure behavior in Drosophila: Analysis of the physiological repertoire underlying a stereotyped action pattern in bang-sensitive mutants. *J. Neurosci.* **22**, 11065–11079 (2002).

198. Tanouye, M. A. & Wyman, R. J. Motor outputs of giant nerve fiber in Drosophila. *J. Neurophysiol.* **44**, 405–421 (1980).

199. Song, J. & Tanouye, M. A. From bench to drug: Human seizure modeling using Drosophila. *Prog. Neurobiol.* **84**, 182–191 (2008).

200. Kuebler, D. & Tanouye, M. A. Modifications of seizure susceptibility in Drosophila. *J. Neurophysiol.* **83**, 998–1009 (2000).

201. Parker, L., Padilla, M., Du, Y., Dong, K. & Tanouye, M. a. Drosophila as a model for epilepsy: bss is a gain-of-function mutation in the para sodium channel gene that leads to seizures. *Genetics* **187**, 523–534 (2011).

202. Marley, R. & Baines, R. a. Increased persistent Na+ current contributes to seizure in the slamdance bang-sensitive Drosophila mutant. *J. Neurophysiol.* **106**, 18–29 (2011).

203. Zhang, H. *et al.* The Drosophila slamdance gene: A mutation in an aminopeptidase can cause seizure, paralysis and neuronal failure. *Genetics* **162**, 1283–1299 (2002).

204. Pavlidis, P., Ramaswami, M. & Tanouye, M. A. The Drosophila easily shocked gene: A mutation in a phospholipid synthetic pathway causes seizure, neuronal failure, and paralysis. *Cell* **79**, 23–33 (1994).

205. Lin, W.-H., Gunay, C., Marley, R., Prinz, a. a. & Baines, R. a. Activity-Dependent Alternative Splicing Increases Persistent Sodium Current and Promotes Seizure. *J. Neurosci.* **32**, 7267–7277 (2012).

206. Lin, W.-H., He, M. & Baines, R. a. Seizure suppression through manipulating splicing of a voltage-gated sodium channel. *Brain* 1–11 (2015). doi:10.1093/brain/awv012

207. Saras, A., Wu, V. V., Brawer, H. J. & Tanouye, M. A. Investigation of seizure-susceptibility in a drosophila melanogaster model of human epilepsy with optogenetic stimulation. *Genetics* **206**, 1739–1746 (2017).

208. Hekmat-Scafe, D. S. *et al.* Seizure sensitivity is ameliorated by targeted expression of K +-Cl-cotransporter function in the mushroom body of the Drosophila brain. *Genetics* **184**, 171–183 (2010).

209. Kuebler, D. & Tanouye, M. Anticonvulsant valproate reduces seizure-susceptibility in mutant Drosophila. *Brain Res.* **958**, 36–42 (2002).

210. Reynolds, E. R. *et al.* Treatment with the Antiepileptic Drugs Phenytoin and Gabapentin Ameliorates Seizure and Paralysis of Drosophila Bang-Sensitive Mutants. *J. Neurobiol.* **58**, 503–513 (2004).

211. Tan, J. S., Lin, F. & Tanouye, M. A. Potassium bromide, an anticonvulsant, is effective at alleviating seizures in the Drosophila bang-sensitive mutant bang senseless. *Brain Res.* **1020**, 45–52 (2004).

212. Kuebler, D., Zhang, H., Ren, X. & Tanouye, M. A. Genetic suppression of seizure susceptibility in Drosophila. *J. Neurophysiol.* **86**, 1211–1225 (2001).

213. Stafstrom, C. E. Persistent Sodium Current and Its Role in Epilepsy. *Epilepsy Curr.* **7**, 15–22 (2007).

214. Streit, A. K., Fan, Y. N., Masullo, L. & Baines, R. A. Calcium imaging of neuronal activity in Drosophila can identify anticonvulsive compounds. *PLoS One* **11**, 1–15 (2016).

215. Uhlhaas, P. J. & Singer, W. Neural Synchrony in Brain Disorders: Relevance for Cognitive Dysfunctions and Pathophysiology. *Neuron* **52**, 155–168 (2006).

216. Crill, W. E. Persistent sodium current in mammalian central neurons. *Annu. Rev. Physiol.* **58**, 349–362 (1996).

217. Hotson, J. R., Prince, D. A. & Schwartzkroin, P. A. Anomalous inward rectification in hippocampal neurons. *J. Neurophysiol.* **42**, 889–895 (1979).

218. Lin, W. H., Wright, D. E., Muraro, N. I. & Baines, R. A. Alternative splicing in the voltage-gated sodium channel DmNav regulates activation, inactivation, and persistent current. *J. Neurophysiol.* **102**, 1994–2006 (2009).

219. Gao, R. *et al.* Sequence variations at I260 and A1731 contribute to persistent currents in Drosophila sodium channels. *Neuroscience* **268**, 297–308 (2014).

220. Lu, B. *et al.* The Neuronal Channel NALCN Contributes Resting Sodium Permeability and Is Required for Normal Respiratory Rhythm. *Cell* **129**, 371–383 (2007).

221. Lear, B. C. *et al.* The ion channel narrow abdomen is critical for neural output of the Drosophila circadian pacemaker. *Neuron* **48**, 965–976 (2005).

222. Moose, D. L., Haase, S. J., Aldrich, B. T. & Lear, B. C. The narrow abdomen ion channel complex is highly stable and persists from development into adult stages to promote behavioral rhythmicity. *Front. Cell. Neurosci.* **11**, 1–14 (2017).

223. Alzheimer, C., Schwindt, P. C. & Crill, W. E. Modal gating of Na+ channels as a mechanism of persistent Na+ current in pyramidal neurons from rat and cat sensorimotor cortex. *J. Neurosci.* **13**, 660–673 (1993).

224. Marder E. & Bucher D. Central pattern generators and the control of rhythmic movements. *Curr. Biol.* **11**, R986–R996 (2001).

225. Kiehn, O. Locomotor circuits in the mammalian spinal cord. *Annu. Rev. Neurosci.* **29**, 279–306 (2006).

226. Ramirez, J. M., Koch, H., Garcia, A. J., Doi, A. & Zanella, S. The role of spiking and bursting pacemakers in the neuronal control of breathing. *J. Biol. Phys.* **37**, 241–261 (2011).

227. Tazerart, S., Viemari, J. C., Darbon, P., Vinay, L. & Brocard, F. Contribution of persistent sodium current to locomotor pattern generation in neonatal rats. *J. Neurophysiol.* **98**, 613–628 (2007).

228. Tazerart, S., Vinay, L. & Brocard, F. The persistent sodium current generates pacemaker activities in the central pattern generator for locomotion and regulates the locomotor rhythm. *J. Neurosci.* **28**, 8577–8589 (2008).

229. Yamanishi, T., Koizumi, H., Navarro, M. A., Milescu, L. S. & Smith, J. C. Kinetic properties of persistent Na+ current orchestrate oscillatory bursting in respiratory neurons. *J. Gen. Physiol.* **150**,

1523–1540 (2018).

230. Grillner, S. *et al.* The intrinsic function of a motor system - From ion channels to networks and behavior. *Brain Res.* **886**, 224–236 (2000).

231. Wu, N. *et al.* Persistent sodium currents in mesencephalic V neurons participate in burst generation and control of membrane excitability. *J. Neurophysiol.* **93**, 2710–2722 (2005).

232. Reboreda, A., Sánchez, E., Romero, M. & Lamas, J. A. Intrinsic spontaneous activity and subthreshold oscillations in neurones of the rat dorsal column nuclei in culture. *J. Physiol.* **551**, 191–205 (2003).

233. Jinno, S., Ishizuka, S. & Kosaka, T. Ionic currents underlying rhythmic bursting of ventral mossy cells in the developing mouse dentate gyrus. *Eur. J. Neurosci.* **17**, 1338–1354 (2003).

234. Van Drongelen, W. *et al.* Role of persistent sodium current in bursting activity of mouse neocortical networks in vitro. *J. Neurophysiol.* **96**, 2564–2577 (2006).

235. Darbon, P., Yvon, C., Legrand, J. C. & Streit, J. INaP underlies intrinsic spiking and rhythm generation in networks of cultured rat spinal neurons. *Eur. J. Neurosci.* **20**, 976–988 (2004).

236. Zhong, G., Masino, M. A. & Harris-Warrick, R. M. Persistent sodium currents participate in fictive locomotion generation in neonatal mouse spinal cord. *J. Neurosci.* **27**, 4507–4518 (2007).

237. Haider, B. & McCormick, D. A. Rapid Neocortical Dynamics: Cellular and Network Mechanisms. *Neuron* **62**, 171–189 (2009).

238. Buzsaki, G. & Wang, X.-J. Mechanisms of Gamma Oscillations. *Annu Rev Neurosci* **35**, 203–225 (2012).

239. Wang, X. J. Neurophysiological and computational principles of cortical rhythms in cognition. *Physiol. Rev.* **90**, 1195–1268 (2010).

240. Colgin, L. L. *et al.* Frequency of gamma oscillations routes flow of information in the hippocampus. *Nature* **462**, 353–357 (2009).

241. Colgin, L. L. & Moser, E. I. Gamma oscillations in the hippocampus. *Physiology* **25**, 319–329 (2010).

242. Mably, A. J. & Colgin, L. L. Gamma oscillations in cognitive disorders. *Curr. Opin. Neurobiol.* **52**, 182–187 (2018).

243. Nakazono, T., Jun, H., Blurton-Jones, M., Green, K. N. & Igarashi, K. M. Gamma oscillations in the entorhinal-hippocampal circuit underlying memory and dementia. *Neurosci. Res.* **129**, 40–46 (2018).

244. Dugladze, T. *et al.* Impaired hippocampal rhythmogenesis in a mouse model of mesial temporal lobe epilepsy. *Proc. Natl. Acad. Sci. U. S. A.* **104**, 17530–17535 (2007).

245. Kang, Y.-J. *et al.* Cell type-specific intrinsic perithreshold oscillations in hippocampal GABAergic interneurons. *Neuroscience* **376**, 80–93 (2018).

246. Kang, Y. J. *et al.* The critical role of persistent sodium current in hippocampal gamma oscillations. *Neuropharmacology* **162**, (2020).

247. Hammarström, A. K. M. & Gage, P. W. Inhibition of oxidative metabolism increases persistent sodium current in rat CA1 hippocampal neurons. *J. Physiol.* **510**, 735–741 (1998).

248. Deng, P. Y. & Klyachko, V. A. Increased Persistent Sodium Current Causes Neuronal Hyperexcitability in the Entorhinal Cortex of Fmr1 Knockout Mice. *Cell Rep.* **16**, 3157–3166 (2016).

249. Xie, R. G. *et al.* Blockade of persistent sodium currents contributes to the riluzole-induced inhibition of spontaneous activity and oscillations in injured DRG neurons. *PLoS One* **6**, 1–10 (2011).

250. Pieri, M., Carunchio, I., Curcio, L., Mercuri, N. B. & Zona, C. Increased persistent sodium current determines cortical hyperexcitability in a genetic model of amyotrophic lateral sclerosis. *Exp. Neurol.* **215**, 368–379 (2009).

251. Lossin, C., Wang, D. W., Rhodes, T. H., Vanoye, C. G. & George Jr., A. L. Molecular basis of an inherited epilepsy. *Arch. Neurol.* **61**, 473–478 (2004).

252. Vanoye, C. G., Lossin, C., Rhodes, T. H. & George, A. L. Single-channel properties of human NaV1.1 and mechanism of channel dysfunction in SCN1A-associated epilepsy. *J. Gen. Physiol.* **127**, 1–14 (2006).

253. Chen, S. *et al.* An increase in persistent sodium current contributes to intrinsic neuronal bursting after status epilepticus. *J. Neurophysiol.* **105**, 117–129 (2011).

254. Isaeva, E., Hernan, A., Isaev, D. & Holmes, G. L. Thrombin Facilitates Seizures through Activation of Persistent Sodium Current. *Ann Neurol* **72**, 192–198 (2012).

255. Kearney, J. A. *et al.* A gain-of-function mutation in the sodium channel gene Scn2a results in seizures and behavioral abnormalities. *Neuroscience* **102**, 307–317 (2001).

256. Lin, W. H., Giachello, C. N. G. & Baines, R. A. Seizure control through genetic and pharmacological manipulation of Pumilio in Drosophila: A key component of neuronal homeostasis. *DMM Dis. Model. Mech.* **10**, 141–150 (2017).

257. Anderson, L. L. *et al.* Antiepileptic Activity of Preferential Inhibitors of Persistent Sodium Current. *Epilepsia* **55**, 1274–1283 (2014).

258. Wolff, M. *et al.* Genetic and phenotypic heterogeneity suggest therapeutic implications in SCN2A-related disorders. *Brain* **140**, 1316–1336 (2017).

259. Vreugdenhil, M., Hoogland, G., Van Veelen, C. W. M. & Wadman, W. J. Persistent sodium current in subicular neurons isolated from patients with temporal lobe epilepsy. *Eur. J. Neurosci.* **19**, 2769–2778 (2004).

260. Kameyama, M. *et al.* Intracellular Na+ activates a K+ channel in mammalian cardiac cells. *Nature* **309**, 354–356 (1984).

261. Bader, C. R., Bernheim, L. & Bertrand, D. Sodium-activated potassium current in cultured avian neurones. *Nature* **317**, 540–542 (1985).

262. Dryer, S. E., Fujiit, J. T. & Martin, A. R. A Na+-Activated K+ Current in Cultured Brain Stem Neurones from Chicks. *J. Physiol.* **410**, 283–296 (1989).

263. Schwindt, P. C. Long-Lasting Reduction of Excitability by a Sodium- Dependent Potassium Current in Cat Neocortical Neurons. *J. Neurophy* **61**, 233–244 (1989).

264. Haimann, C., Bernheim, L., Bertrand, D. & Bader, C. R. Potassium current activated by intracellular sodium in quail trigeminal ganglion neurons. *J. Gen. Physiol.* **95**, 961–979 (1990).

265. Dryer, S. E. Na+-Activated K+ Channels and Voltage-Evoked Ionic Currents in Brain Stem and Parasympathetic Neurones of the Chick. *J. Physiol.* **435**, 513–532 (1991).

266. Saito, M. & Wu, C. F. Expression of ion channels and mutational effects in giant Drosophila neurons differentiated from cell division-arrested embryonic neuroblasts. *J. Neurosci.* **11**, 2135–2150 (1991).

267. Egan, T. M., Dagan, D., Kupper, J. & Levitan, I. B. Properties and rundown of sodium-activated potassium channels in rat olfactory bulb neurons. *J. Neurosci.* **12**, 1964–1976 (1992).

268. Haimann, C., Magistretti, J. & Pozzi, B. Sodium-activated potassium current in sensory neurons: a comparison of cell-attached and cell-free single-channel activities. *Pflügers Arch. Eur. J. Physiol.* **422**, 287–294 (1992).

269. Dale, N. A large, sustained Na+- and voltage-dependent K+ current in spinal neurons of the frog embryo. *J. Physiol.* **462**, 349–372 (1993).

270. Bischoff, U., Vogel, W., Safronov, B. V, Institut, P. & Giessen, J. Na+-activated K+ channels in small dorsal root ganglion neurones of rat. *J. Physiol.* **510**, 743–754 (1998).

271. Joiner, W. J. *et al.* Formation of intermediate-conductance calcium-activated potassium channels by interaction of Slack and Slo subunits. *Nat. Neurosci.* **1**, 462–469 (1998).

272. Yuan, A. *et al.* The sodium-activated potassium channel is encoded by a member of the Slo gene family. *Neuron* **37**, 765–773 (2003).

273. Wallén, P. *et al.* Sodium-dependent potassium channels of a Slack-like subtype contribute to the slow afterhyperpolarization in lamprey spinal neurons. *J. Physiol.* **585**, 75–90 (2007).

274. Budelli, G. *et al.* SLO2 Channels Are Inhibited By All Divalent Cations That Activate SLO1 K+ Channels. *J. Biol. Chem.* **291**, jbc.M115.709436 (2016).

275. Paulais, M., Lachheb, S. & Teulon, J. A Na+- and Cl--activated K+ channel in the thick ascending limb of mouse kidney. *J. Gen. Physiol.* **127**, 205–215 (2006).

276. Kaczmarek, L. K. *et al.* International union of basic and clinical pharmacology. C. Nomenclature and properties of calcium-activated and sodium-activated potassium channels. *Pharmacol. Rev.* **69**, 1–11 (2017).

277. Hite, R. K. *et al.* Cryo-electron microscopy structure of the Slo2.2 Na+-activated K+ channel. *Nature* **647**, 641–647 (2015).

278. Tamsett, T. J., Picchione, K. E. & Bhattacharjee, A. NAD+ Activates KNa Channels in Dorsal Root Ganglion Neurons. *J. Neurosci.* **29**, 5127–5134 (2009).

279. Zhang, Z., Rosenhouse-Dantsker, A., Tang, Q.-Y., Noskov, S. & Logothetis, D. E. The RCK2 domain uses a coordination site present in Kir channels to confer sodium sensitivity to Slo2.2 channels. *J. Neurosci.* **30**, 7554–62 (2010).

280. Nuwer, M. O., Picchione, K. E. & Bhattacharjee, A. PKA-induced internalization of slack KNa channels produces dorsal root ganglion neuron hyperexcitability. *J. Neurosci.* **30**, 14165–72 (2010).

281. Santi, C. M. *et al.* Opposite regulation of Slick and Slack K+ channels by neuromodulators. *J. Neurosci.* **26**, 5059–5068 (2006).

282. Zhang, H., He, C., Yan, X., Mirshahi, T. & Logothetis, D. E. Activation of inwardly rectifying K+

channels by distinct PtdIns(4,5)P2 interactions. *Nat. Cell Biol.* **1**, 183–188 (1999).

283. Wang, B. Y. Z., Kimitsuki, T. & Noma, A. Conductance Properties of the Na-Activated K Channel in Guinea-pig Ventricular Cells. *J. Physiol.* **433**, 241–257 (1991).

284. Yuan, A. *et al.* SLO-2, a K+ channel with an unusual Cl- dependence. *Nat. Neurosci.* **3**, 771–779 (2000).

285. Martinez-Espinosa, P. L. *et al.* Knockout of Slo2.2 enhances itch, abolishes K_{Na} current, and increases action potential firing frequency in DRG neurons. *Elife* **4**, 1–27 (2015).

286. Bhattacharjee, A., Gan, L. & Kaczmarek, L. K. Localization of the Slack potassium channel in the rat central nervous system. *J. Comp. Neurol.* **454**, 241–254 (2002).

287. Bhattacharjee, A., Von Hehn, C. A. A., Mei, X. & Kaczmarek, L. K. Localization of the Na+-activated K+ channel slick in the rat central nervous system. *J. Comp. Neurol.* **484**, 80–92 (2005).

288. Brown, M. R. *et al.* Amino-termini isoforms of the Slack K+ channel, regulated by alternative promoters, differentially modulate rhythmic firing and adaptation. *J. Physiol.* **586**, 5161–5179 (2008).

289. Rizzi, S., Knaus, H. G. & Schwarzer, C. Differential distribution of the sodium-activated potassium channels slick and slack in mouse brain. *J. Comp. Neurol.* **524**, 2093–2116 (2016).

290. Tomasello, D. L., Hurley, E., Wrabetz, L. & Bhattacharjee, A. Slick (Kcnt2) sodium-activated potassium channels limit peptidergic nociceptor excitability and hyperalgesia. *J. Exp. Neurosci.* **11**, (2017).

291. Lu, R. *et al.* Slack Channels Expressed in Sensory Neurons Control Neuropathic Pain in Mice. *J. Neurosci.* **35**, 1125–1135 (2015).

292. Koh, D. S., Jonas, P. & Vogel, W. Na(+)-activated K+ channels localized in the nodal region of myelinated axons of Xenopus. *J. Physiol.* **479**, 183–197 (1994).

293. Uchino, S. *et al.* Slo2 sodium-activated K+ channels bind to the PDZ domain of PSD-95. *Biochem. Biophys. Res. Commun.* **310**, 1140–1147 (2003).

294. Rose, C. R. Na+signals at central synapses. *Neuroscientist* **8**, 532–539 (2002).

295. Huang, F. *et al.* TMEM16C facilitates Na(+)-activated K(+) currents in rat sensory neurons and regulates pain processing. *Nat. Neurosci.* **16**, 1284–1290 (2013).

296. Nanou, E. & Manira, A. El. Mechanisms of Modulation of AMPA-Induced Na+-Activated K+ Current by mGluR1. *J. Neurophysiol.* **103**, 441–445 (2010).

297. Bhattacharjee, A. *et al.* Slick (Slo2.1), a rapidly-gating sodium-activated potassium channel inhibited by ATP. *J. Neurosci.* **23**, 11681–11691 (2003).

298. Tejada, M. A. *et al.* Cell volume changes regulate slick (Slo2.1), but not slack (Slo2.2) K+ channels. *PLoS One* **9**, (2014).

299. Nanou, E. & Manira, A. El. A postsynaptic negative feedback mediated by coupling between AMPA receptors and Na+-activated K+ channels in spinal cord neurones. *Eur. J. Neurosci.* **25**, 445–450 (2007).

300. Lu, S., Das, P., Fadool, D. A. & Kaczmarek, L. K. The Slack Sodium-Activated Potassium Channel Provides a Major Outward Current in Olfactory Neurons of Kv1.3 -/- Super-Smeller

Mice. *J. Neurophysiol.* **103**, 3311–3319 (2010).

301. Aoki, I. *et al.* SLO potassium channels antagonize premature decision making in C. elegans. *Commun. Biol.* **1**, 1–15 (2018).

302. Budelli, G. *et al.* Na+-activated K+ channels express a large delayed outward current in neurons during normal physiology. *Nat. Neurosci.* **12**, 745–750 (2009).

303. Hage, T. a. & Salkoff, L. Sodium-Activated Potassium Channels Are Functionally Coupled to Persistent Sodium Currents. *J. Neurosci.* **32**, 2714–2721 (2012).

304. Li, P. *et al.* GABA-B Controls Persistent Na+ Current and Coupled Na+ -Activated K+ Current. *eNeuro* **4**, 1–8 (2017).

305. Zhang, Y. *et al.* Regulation of neuronal excitability by interaction of fragile X mental retardation protein with slack potassium channels. *J. Neurosci.* **32**, 15318–27 (2012).

306. Yang, B., Desai, R. & Kaczmarek, L. K. Slack and Slick K(Na) channels regulate the accuracy of timing of auditory neurons. *J. Neurosci.* **27**, 2617–2627 (2007).

307. Franceschetti, S. *et al.* Na+-Activated K+ Current Contributes to Postexcitatory Hyperpolarization in Neocortical Intrinsically Bursting Neurons. *J. Neurophysiol.* **89**, 2101–2111 (2003).

308. Hess, D., Nanou, E. & El Manira, A. Characterization of Na+-activated K+ currents in larval lamprey spinal cord neurons. *J. Neurophysiol.* **97**, 3484–3493 (2007).

309. Thuma, J. B. & Hooper, S. L. Choline and NMDG directly reduce outward currents: reduced outward current when these substances replace Na^+ is alone not evidence of Na^+ -activated K^+ currents. *J. Neurophysiol.* **120**, 3217–3233 (2018).

310. Evely, K. M. *et al.* Slack K_{Na} channels influence dorsal horn synapses and nociceptive behavior. *Mol. Pain* **13**, 174480691771434 (2017).

311. Reijntjes, D. O. J. *et al.* Sodium-activated potassium channels shape peripheral auditory function and activity of the primary auditory neurons in mice. *Sci. Rep.* **9**, 1–18 (2019).

312. Møller, R. S. *et al.* Mutations in KCNT1 cause a spectrum of focal epilepsies. *Epilepsia* **56**, e114–e120 (2015).

313. Heron, S. E. *et al.* Missense mutations in the sodium-gated potassium channel gene KCNT1 cause severe autosomal dominant nocturnal frontal lobe epilepsy. *Nat. Genet.* **44**, 1188–90 (2012).

314. Kim, G. E. & Kaczmarek, L. K. Emerging role of the KCNT1 Slack channel in intellectual disability. *Front. Cell. Neurosci.* **8**, 209 (2014).

315. Lim, C. X., Ricos, M. G., Dibbens, L. M. & Heron, S. E. KCNT1 mutations in seizure disorders: the phenotypic spectrum and functional effects. *J. Med. Genet.* **53**, 217–25 (2016).

316. Bausch, A. E. *et al.* The sodium-activated potassium channel Slack is required for optimal cognitive flexibility in mice. *Learn. Mem.* **22**, 323–335 (2015).

317. Quraishi, I. H. *et al.* Impaired motor skill learning and altered seizure susceptibility in mice with loss or gain of function of the Kcnt1 gene encoding Slack (KNa1.1) Na+-activated K+ channels. *Sci. Rep.* **10**, (2020).

318. Ishii, A. *et al.* A recurrent KCNT1 mutation in two sporadic cases with malignant migrating partial seizures in infancy. *Gene* **531**, 467–471 (2013).

319. Gururaj, S. *et al.* A De Novo Mutation in the Sodium-Activated Potassium Channel KCNT2 Alters Ion Selectivity and Causes Epileptic Encephalopathy. *Cell Rep.* **21**, 926–933 (2017).

320. Ambrosino, P. *et al.* De novo gain-of-function variants in KCNT2 as a novel cause of developmental and epileptic encephalopathy. *Ann. Neurol.* **83**, 1198–1204 (2018).

321. Mao, X. *et al.* The Epilepsy of Infancy With Migrating Focal Seizures: Identification of de novo Mutations of the KCNT2 Gene That Exert Inhibitory Effects on the Corresponding Heteromeric KNa1.1/KNa1.2 Potassium Channel. *Front. Cell. Neurosci.* **14**, 1–12 (2020).

322. Barcia, G. *et al.* De novo gain-of-function KCNT1 channel mutations cause malignant migrating partial seizures of infancy. *Nat. Genet.* **44**, 1255–9 (2012).

323. Milligan, C. J. *et al.* KCNT1 gain of function in 2 epilepsy phenotypes is reversed by quinidine. *Ann. Neurol.* **75**, 581–590 (2014).

324. Tang, Q. Y. *et al.* Epilepsy-Related Slack Channel Mutants Lead to Channel Over-Activity by Two Different Mechanisms. *Cell Rep.* **14**, 129–139 (2016).

325. Kim, G. E. *et al.* Human Slack Potassium Channel Mutations Increase Positive Cooperativity between Individual Channels. *Cell Rep.* **9**, 1661–1673 (2014).

326. Quraishi, I. H. *et al.* An Epilepsy-Associated KCNT1 Mutation Enhances Excitability of Human iPSC-Derived Neurons by Increasing Slack KNa Currents. *J. Neurosci.* **39**, 7438–7449 (2019).

327. Bhattacharjee, A. & Kaczmarek, L. K. For K+ channels, Na+ is the new Ca2+. *Trends Neurosci.* **28**, 422–428 (2005).

328. Markham, M. R., Kaczmarek, L. K. & Zakon, H. H. A sodium-activated potassium channel supports high-frequency firing and reduces energetic costs during rapid modulations of action potential amplitude. *J. Neurophysiol.* **109**, 1713–1723 (2013).

329. Nanou, E. *et al.* Na+-mediated coupling between AMPA receptors and KNa channels shapes synaptic transmission. *Proc. Natl. Acad. Sci.* **105**, 20941–20946 (2008).

330. Zhang, Z. *et al.* SLO-2 isoforms with unique Ca2+- and voltage-dependence characteristics confer sensitivity to hypoxia in C. elegans. *Channels* **7**, 194–205 (2013).

331. Jan, Y. N. & Jan, L. Y. Genetic dissection of short-term and long-term facilitation at the Drosophila neuromuscular junction. *Proc. Natl. Acad. Sci. U. S. A.* **75**, 515–519 (1978).

332. Diao, F. *et al.* Plug-and-play genetic access to drosophila cell types using exchangeable exon cassettes. *Cell Rep.* **10**, 1410–1421 (2015).

333. Gratz, S. J. *et al.* Genome engineering of Drosophila with the CRISPR RNA-guided Cas9 nuclease. *Genetics* **194**, 1029–1035 (2013).

334. Gratz, S. J., Rubinstein, C. D., Harrison, M. M., Wildonger, J. & O'Connor-Giles, K. M. CRISPR-Cas9 Genome Editing in *Drosophila*. *Curr. Protoc. Mol. Biol.* 31.2.1-31.2.20 (2015). doi:10.1002/0471142727.mb3102s111

335. Perozo, E., Mackinnon, R., Bezanilla, F. & Stefanis, E. Gating Currents from a Nonconducting Reveal Open-Closed Conformations in Shaker K+ Channels. *Neuron* **11**, 353–358 (1993).

336. Barry, D. M., Xu, H., Schuessler, R. B. & Nerbonne, J. M. Functional Knockout of the Transient Outward Current, Long-QT Syndrome, and Cardiac Remodeling in Mice Expressing a Dominant-Negative Kv4 a Subunit. *Circ. Res.* **83**, 560–567 (1998).

337. Ping, Y. *et al.* Shal/Kv4 channels are required for maintaining excitability during repetitive firing and normal locomotion in Drosophila. *PLoS One* **6**, 15–20 (2011).

338. Abou Tayoun, a. N. *et al.* The Drosophila SK Channel (dSK) Contributes to Photoreceptor Performance by Mediating Sensitivity Control at the First Visual Network. *J. Neurosci.* **31**, 13897–13910 (2011).

339. Metaxakis, A., Oehler, S., Klinakis, A. & Savakis, C. Minos as a genetic and genomic tool in Drosophila melanogaster. *Genetics* **171**, 571–581 (2005).

340. Venken, K. J. T. *et al.* MiMIC : a highly versatile transposon insertion resource for engineering Drosophila melanogaster genes. *Nat. Methods* **8**, 737–743 (2011).

341. Diao, F. & White, B. H. A novel approach for directing transgene expression in Drosophila: T2A-Gal4 in-frame fusion. *Genetics* **190**, 1139–1144 (2012).

342. Quirk, J. C. & Reinhart, P. H. Identification of a novel tetramerization domain in large conductance K(ca) channels. *Neuron* **32**, 13–23 (2001).

343. Tracey, W. D., Wilson, R. I., Laurent, G. & Benzer, S. painless, a Drosophila gene essential for nociception. *Cell* **113**, 261–273 (2003).

344. Hwang, R. Y. *et al.* Nociceptive Neurons Protect Drosophila Larvae from Parasitoid Wasps. *Curr. Biol.* **17**, 2105–2116 (2007).

345. Honjo, K., Robertson, J. & Jr, W. D. T. Nociception. in *Behavioral Genetics of the Fly* 66–76 (2014).

346. Perry, T., Heckel, D. G., McKenzie, J. A. & Batterham, P. Mutations in Dα1 or Dβ2 nicotinic acetylcholine receptor subunits can confer resistance to neonicotinoids in Drosophila melanogaster. *Insect Biochem. Mol. Biol.* **38**, 520–528 (2008).

347. Perry, T. *et al.* Effects of mutations in Drosophila nicotinic acetylcholine receptor subunits on sensitivity to insecticides targeting nicotinic acetylcholine receptors. *Pestic. Biochem. Physiol.* **102**, 56–60 (2012).

348. Somers, J., Nguyen, J., Lumb, C., Batterham, P. & Perry, T. In vivo functional analysis of the Drosophila melanogaster nicotinic acetylcholine receptor Dα6 using the insecticide spinosad. *Insect Biochem. Mol. Biol.* **64**, 116–127 (2015).

349. Perry, T., Somers, J., Yang, Y. T. & Batterham, P. Expression of insect α6-like nicotinic acetylcholine receptors in Drosophila melanogaster highlights a high level of conservation of the receptor: Spinosyn interaction. *Insect Biochem. Mol. Biol.* **64**, 106–115 (2015).

350. Denecke, S., Fusetto, R. & Batterham, P. Describing the role of Drosophila melanogaster ABC transporters in insecticide biology using CRISPR-Cas9 knockouts. *Insect Biochem. Mol. Biol.* **91**, 1–9 (2017).

351. Donnelly, M. L. L. *et al.* Analysis of the aphthovirus 2A/2B polyprotein 'cleavage' mechanism indicates not a proteolytic reaction, but a novel translational effect: A putative ribosomal 'skip'. *J. Gen. Virol.* **82**, 1013–1025 (2001).

352. Donnelly, M. L. L. *et al.* The 'cleavage' activities of foot-and-mouth disease virus 2A site-directed mutants and naturally occurring '2A-like' sequences. *J. Gen. Virol.* **82**, 1027–1041 (2001).

353. Jenett, A. *et al.* A GAL4-Driver Line Resource for Drosophila Neurobiology. *Cell Rep.* **2**, 991–1001 (2012).

354. Tanaka, N. K., Tanimoto, H. & Ito, K. Neuronal assemblies of the Drosophila mushroom body. *J. Comp. Neurol.* **508**, 711–755 (2008).

355. Heisenberg, M., Borst, A., Wagner, S. & Byers, D. Drosophila mushroom body mutants are deficient in olfactory learning: Research papers. *J. Neurogenet.* **2**, 1–30 (1985).

356. McGuire, S. E., Le, P. T. & Davis, R. L. The role of Drosophila mushroom body signaling in olfactory memory. *Science.* **293**, 1330–1333 (2001).

357. van Swinderen, B. Fly Memory: A Mushroom Body Story in Parts. *Curr. Biol.* **19**, R855–R857 (2009).

358. Vogt, K. *et al.* Shared mushroom body circuits underlie visual and olfactory memories in Drosophila. *Elife* **3**, e02395 (2014).

359. Kim, M. D., Wen, Y. & Jan, Y. N. Patterning and organization of motor neuron dendrites in the Drosophila larva. *Dev. Biol.* **336**, 213–221 (2009).

360. Baek, M. & Mann, R. S. Lineage and birth date specify motor neuron targeting and dendritic architecture in adult Drosophila. *J. Neurosci.* **29**, 6904–6916 (2009).

361. Meinertzhagen, I. A. & Sorra, K. E. Synaptic organization in the fly's optic lamina: Few cells, many synapses and divergent microcircuits. *Prog. Brain Res.* **131**, 53–69 (2001).

362. Morante, J. & Desplan, C. The Color-Vision Circuit in the Medulla of Drosophila. *Curr. Biol.* **18**, 553–565 (2008).

363. Neriec, N. & Desplan, C. From the Eye to the Brain: Development of the Drosophila Visual System. *Curr. Top. Dev. Biol.* **116**, 247–271 (2016).

364. Fischbach, K. F. & Dittrich, A. P. M. The optic lobe of Drosophila melanogaster. I. A Golgi analysis of wild-type structure. *Cell Tissue Res.* **258**, 441–475 (1989).

365. Grabe, V. *et al.* Elucidating the Neuronal Architecture of Olfactory Glomeruli in the Drosophila Antennal Lobe. *Cell Rep.* **16**, 3401–3413 (2016).

366. Stocker, R. F. The organization of the chemosensory system in Drosophila melanogaster: a rewiew. *Cell Tissue Res.* **275**, 3–26 (1994).

367. Vosshall, L. B. & Stocker, R. F. Molecular Architecture of Smell and Taste in *Drosophila*. *Annu. Rev. Neurosci.* **30**, 505–533 (2007).

368. Sun, Y. *et al.* TRPA channels distinguish gravity sensing from hearing in Johnston's organ. *Proc. Natl. Acad. Sci. U. S. A.* **106**, 13606–11 (2009).

369. Kamikouchi, A. *et al.* The neural basis of Drosophila gravity-sensing and hearing. *Nature* **458**, 165–171 (2009).

370. Yorozu, S. *et al.* Distinct sensory representations of wind and near-field sound in the Drosophila brain. *Nature* **458**, 201–205 (2009).

371. Mamiya, A. & Dickinson, M. H. Antennal mechanosensory neurons mediate wing motor reflexes in flying Drosophila. *J. Neurosci.* **35**, 7977–7991 (2015).

372. Coen, P. & Murthy, M. Singing on the fly: Sensorimotor integration and acoustic communication in Drosophila. *Curr. Opin. Neurobiol.* **38**, 38–45 (2016).

373. Matsuo, E. *et al.* Identification of novel vibration- and deflection-sensitive neuronal subgroups in

Johnston's organ of the fruit fly. *Front. Physiol.* **5**, 1–13 (2014).

374. Ishikawa, Y., Fujiwara, M., Wong, J., Ura, A. & Kamikouchi, A. Stereotyped Combination of Hearing and Wind/Gravity-Sensing Neurons in the Johnston's Organ of Drosophila. *Front. Physiol.* **10**, 1–8 (2020).

375. Budelli, G. *et al.* Ionotropic Receptors Specify the Morphogenesis of Phasic Sensors Controlling Rapid Thermal Preference in Drosophila. *Neuron* **101**, 738-747.e3 (2019).

376. Moilanen, L. J. & Voets, T. A Fly's Cool Way to Escape the Heat. *Neuron* **101**, 550–552 (2019).

377. Bodmer, R. & Jan, Y. N. Morphological differentiation of the embryonic peripheral neurons in Drosophila. *Roux's Arch. Dev. Biol.* **196**, 69–77 (1987).

378. Zhong, L., Hwang, R. Y. & Tracey, W. D. Pickpocket Is a DEG/ENaC Protein Required for Mechanical Nociception in Drosophila Larvae. *Curr. Biol.* **20**, 429–434 (2010).

379. Zhong, L. *et al.* Thermosensory and Nonthermosensory Isoforms of Drosophila melanogaster TRPA1 Reveal Heat-Sensor Domains of a ThermoTRP Channel. *Cell Rep.* **1**, 43–55 (2012).

380. Caldwell, J. C., Miller, M. M., Wing, S., Soll, D. R. & Eberl, D. F. Dynamic analysis of larval locomotion in Drosophila chordotonal organ mutants. *Proc. Natl. Acad. Sci.* **100**, 16053–16058 (2003).

381. Jegla, T. *et al.* Bilaterian Giant Ankyrins Have a Common Evolutionary Origin and Play a Conserved Role in Patterning the Axon Initial Segment. *PLoS Genet.* **12**, e1006457 (2016).

382. Adams, C. M. *et al.* Ripped Pocket and Pickpocket, Novel Drosophila DEG/ENaC Subunits Expressed in Early Development and in Mechanosensory Neurons. *J. Cell Biol.* **140**, 143–152 (1998).

383. Han, C., Jan, L. Y. & Jan, Y.-N. Enhancer-driven membrane markers for analysis of nonautonomous mechanisms reveal neuron-glia interactions in Drosophila. *Proc. Natl. Acad. Sci.* **108**, 9673–9678 (2011).

384. Strother, J. A. *et al.* The Emergence of Directional Selectivity in the Visual Motion Pathway of Drosophila. *Neuron* **94**, 168-182.e10 (2017).

385. Aso, Y. *et al.* The neuronal architecture of the mushroom body provides a logic for associative learning. *Elife* **3**, e04577 (2014).

386. Ravenscroft, T. A. *et al.* Drosophila voltage-gated sodium channels are only expressed in active neurons and are localized to distal axonal initial segment-like domains. *J. Neurosci.* **40**, 7999–8024 (2020).

387. Hindle, S. J. & Bainton, R. J. Barrier mechanisms in the Drosophila blood-brain barrier. *Front. Neurosci.* **8**, 1–12 (2014).

388. Kremer, M. C., Jung, C., Batelli, S., Rubin, G. M. & Gaul, U. The glia of the adult Drosophila nervous system. *Glia* **65**, 606–638 (2017).

389. Joshi, D., Fung, S. J., Rothwell, A. & Weickert, C. S. Higher gamma-aminobutyric acid neuron density in the white matter of orbital frontal cortex in schizophrenia. *Biol. Psychiatry* **72**, 725–733 (2012).

390. Soumier, A. & Sibille, E. Opposing effects of acute versus chronic blockade of frontal cortex somatostatin-positive inhibitory neurons on behavioral emotionality in mice.

Neuropsychopharmacology **39**, 2252–2262 (2014).

391. Kalari, K. R. *et al.* BBBomics-Human Blood Brain Barrier Transcriptomics Hub. *Front. Neurosci.* **10**, 1–7 (2016).

392. Bainton, R. J. *et al.* moody encodes two GPCRs that regulate cocaine behaviors and blood-brain barrier permeability in Drosophila. *Cell* **123**, 145–156 (2005).

393. Mayer, F. *et al.* Evolutionary Conservation of Vertebrate Blood-Brain Barrier Chemoprotective Mechanisms in Drosophila. *J. Neurosci.* **29**, 3538–3550 (2009).

394. Schwabe, T., Bainton, R. J., Fetter, R. D., Heberlein, U. & Gaul, U. GPCR signaling is required for blood-brain barrier formation in Drosophila. *Cell* **123**, 133–144 (2005).

395. Zhang, S. L., Yue, Z., Arnold, D. M., Artiushin, G. & Sehgal, A. A Circadian Clock in the Blood-Brain Barrier Regulates Xenobiotic Efflux. *Cell* **173**, 130-139.e10 (2018).

396. Hladky, S. B. & Barrand, M. A. Fluid and ion transfer across the blood-brain and blood-cerebrospinal fluid barriers; a comparative account of mechanisms and roles. *Fluids Barriers CNS* **13**, 1–69 (2016).

397. Yan, Y., Dempsey, R. J., Flemmer, A., Forbush, B. & Sun, D. Inhibition of Na+-K+-Cl- cotransporter during focal cerebral ischemia decreases edema and neuronal damage. *Brain Res.* **961**, 22–31 (2003).

398. O'Donnell, M. E., Tran, L., Lam, T. I., Liu, X. B. & Anderson, S. E. Bumetanide inhibition of the blood-brain barrier Na-K-Cl cotransporter reduces edema formation in the rat middle cerebral artery occlusion model of stroke. *J. Cereb. Blood Flow Metab.* **24**, 1046–1056 (2004).

399. Leiserson, W. M., Forbush, B. & Keshishian, H. Drosophila glia use a conserved cotransporter mechanism to regulate extracellular volume. *Glia* **59**, 320–332 (2011).

400. van Vliet, E. A., Aronica, E. & Gorter, J. A. Blood-brain barrier dysfunction, seizures and epilepsy. *Semin. Cell Dev. Biol.* **38**, 26–34 (2015).

401. Dryer, S. E. Na+-activated K+ channels: A new family of large-conductance ion channels. *Trends Neurosci.* **17**, 155–160 (1994).

402. Crossthwaite, A. J. *et al.* The invertebrate pharmacology of insecticides acting at nicotinic acetylcholine receptors. *J. Pestic. Sci.* **42**, 67–83 (2017).

403. Déglise, P., Grünewald, B. & Gauthier, M. Erratum: The insecticide imidacloprid is a partial agonist of the nicotinic receptor of honeybee Kenyon cells. *Neurosci. Lett.* **321**, 13–16 (2002).

404. Brown, L. A., Ihara, M., Buckingham, S. D., Matsuda, K. & Sattelle, D. B. Neonicotinoid insecticides display partial and super agonist actions on native insect nicotinic acetylcholine receptors. *J. Neurochem.* **99**, 608–615 (2006).

405. Ihara, M. *et al.* Loops D, E and G in the Drosophila Dα1 subunit contribute to high neonicotinoid sensitivity of Dα1-chicken β2 nicotinic acetylcholine receptor. *Br. J. Pharmacol.* **175**, 1999–2012 (2018).

406. Palmer, M. J. *et al.* Cholinergic pesticides cause mushroom body neuronal inactivation in honeybees. *Nat. Commun.* **4**, (2013).

407. Watson, G. B. *et al.* A spinosyn-sensitive Drosophila melanogaster nicotinic acetylcholine receptor identified through chemically induced target site resistance, resistance gene identification,

and heterologous expression. *Insect Biochem. Mol. Biol.* **40**, 376–384 (2010).

408. Zimmer, C. T. *et al.* A CRISPR/Cas9 mediated point mutation in the alpha 6 subunit of the nicotinic acetylcholine receptor confers resistance to spinosad in Drosophila melanogaster. *Insect Biochem. Mol. Biol.* **73**, 62–69 (2016).

409. Sun, H., Buchon, N. & Scott, J. G. Mdr65 decreases toxicity of multiple insecticides in Drosophila melanogaster. *Insect Biochem. Mol. Biol.* **89**, 11–16 (2017).

410. Rezával, C., Werbajh, S. & Ceriani, M. F. Neuronal death in Drosophila triggered by GAL4 accumulation. *Eur. J. Neurosci.* **25**, 683–694 (2007).

411. Mabuchi, I. *et al.* Mushroom body signaling is required for locomotor activity rhythms in Drosophila. *Neurosci. Res.* **111**, 25–33 (2016).

412. Sun, J. *et al.* Neural control of startle-induced locomotion by the mushroom bodies and associated neurons in drosophila. *Front. Syst. Neurosci.* **12**, 1–18 (2018).

413. Kondo, S. *et al.* Neurochemical Organization of the Drosophila Brain Visualized by Endogenously Tagged Neurotransmitter Receptors. *Cell Rep.* **30**, 284-297.e5 (2020).

414. Mee, C. J., Pym, E. C. G., Moffat, K. G. & Baines, R. A. Regulation of neuronal excitability through pumilio-dependent control of a sodium channel gene. *J. Neurosci.* **24**, 8695–8703 (2004).

415. Chandrashekaran, S. Mutations at the stm A locus of Drosophila melanogaster confer resistance to the sodium channel neuropoison veratridine. *Curr. Sci.* **65**, 80–82 (1993).

416. Yao Yang, M., Armstrong, J. D., Vilinsky, I., Strausfeld, N. J. & Kaiser, K. Subdivision of the drosophila mushroom bodies by enhancer-trap expression patterns. *Neuron* **15**, 45–54 (1995).

417. Biton, B. *et al.* The antipsychotic drug loxapine is an opener of the sodium-activated potassium channel slack (Slo2.2). *J. Pharmacol. Exp. Ther.* **340**, 706–715 (2012).

418. Alekov, A. K., Masmudur Rahman, M. D., Mitrovic, N., Lehmann-Horn, F. & Lerche, H. Enhanced inactivation and acceleration of activation of the sodium channel associated with epilepsy in man. *Eur. J. Neurosci.* **13**, 2171–2176 (2001).

419. Rhodes, T. H., Lossin, C., Vanoye, C. G., Wang, D. W. & George, A. L. Noninactivating voltage-gated sodium channels in severe myoclonic epilepsy of infancy. *Proc. Natl. Acad. Sci. U. S. A.* **101**, 11147–11152 (2004).

420. Rhodes, T. H. *et al.* Sodium channel dysfunction in intractable childhood epilepsy with generalized tonic-clonic seizures. *J. Physiol.* **569**, 433–445 (2005).

421. Crittenden, J. R., Skoulakis, E. M. C., Han, K. A., Kalderon, D. & Davis, R. L. Tripartite mushroom body architecture revealed by antigenic markers. *Learn. Mem.* **5**, 38–51 (1998).

422. Eberl, D. F. & Kernan, M. J. Recording Sound-Evoked Potentials from the Drosophila Antennal Nerve. *Cold Spring Harb. Protoc.* **2011**, 283–9 (2011).

423. Khurana, S. & Siddiqi, O. Olfactory responses of drosophila larvae. *Chem. Senses* **38**, 315–323 (2013).

424. Sun, Q., Tian, E., Turner, R. J. & Ten Hagen, K. G. Developmental and functional studies of the SLC12 gene family members from Drosophila melanogaster. *Am. J. Physiol. Physiol.* **298**, C26–C37 (2009).

425. DeSalvo, M. K. *et al.* The Drosophila surface glia transcriptome: Evolutionary conserved blood-brain barrier processes. *Front. Neurosci.* **8**, 1–22 (2014).

426. Gamba, G. Molecular physiology and pathophysiology of electroneutral cation-chloride cotransporters. *Physiol. Rev.* **85**, 423–493 (2005).

427. Spéder, P. & Brand, A. H. Gap junction proteins in the blood-brain barrier control nutrient-dependent reactivation of Drosophila neural stem cells. *Dev. Cell* **30**, 309–321 (2014).

428. De Bock, M. *et al.* Endothelial calcium dynamics, connexin channels and blood-brain barrier function. *Prog. Neurobiol.* **108**, 1–20 (2013).

429. Thomson, S. J., Hansen, A. & Sanguinetti, M. C. Identification of the intracellular Na^+ sensor in Slo2.1 potassium channels. *J. Biol. Chem.* **290**, 14528–14535 (2015).

430. Rose, C. R. & Ransom, B. R. Regulation of intracellular sodium in cultured rat hippocampal neurones. *J. Physiol.* **499**, 573–587 (1997).

431. Rose, C. R. & Konnerth, A. NMDA receptor-mediated Na+ signals in spines and dendrites. *J. Neurosci.* **21**, 4207–4214 (2001).

432. Ona-Jodar, T., Gerkau, N. J., Aghvami, S. S., Rose, C. R. & Egger, V. Two-photon Na+ imaging reports somatically evoked action potentials in rat olfactory bulb mitral and granule cell neurites. *Front. Cell. Neurosci.* **11**, 1–12 (2017).

433. Wendt-Gallitelli, M., Voigt, T. & Isenberg, G. Microheterogeneity of Subsarcolemmal Sodium Gradients. Electron Probe Microanalysis in Guinea-Pig Ventricular Myocytes. *J. Physiol.* **472**, 33–44 (1993).

434. Mittmann, T., Linton, S. M., Schwindt, P. & Crill, W. Evidence for persistent Na+ current in apical dendrites of rat neocortical neurons from imaging of Na+-sensitive dye. *J. Neurophysiol.* **78**, 1188–1192 (1997).

435. Fleidervish, I. A., Lasser-Ross, N., Gutnick, M. J. & Ross, W. N. Na+ imaging reveals little difference in action potential-evoked Na+ influx between axon and soma. *Nat. Neurosci.* **13**, 852–860 (2010).

436. Sekar, R. B. & Periasamy, A. Fluorescence resonance energy transfer (FRET) microscopy imaging of live cell protein localizations. *J. Cell Biol.* **160**, 629–633 (2003).

437. Stafstrom, C. E. A persistent little current with a big impact on epileptic firing. *Epilepsy Curr.* **11**, 64–65 (2011).

438. Baskoylu, S. N. *et al.* Single copy/knock-in models of ALS SOD1 in C. elegans suggest loss and gain of function have different contributions to cholinergic and glutamatergic neurodegeneration. *PLoS Genet.* **14**, 1–28 (2018).

439. Şxahin, A. *et al.* Human SOD1 ALS mutations in a Drosophila knock-in model cause severe phenotypes and reveal dosage-sensitive gain- and loss-of-function components. *Genetics* **205**, 707–723 (2017).

440. Han, C. *et al.* Human Nav1.8: Enhanced persistent and ramp currents contribute to distinct firing properties of human DRG neurons. *J. Neurophysiol.* **113**, 3172–3185 (2015).

441. Babcock, D. T., Landry, C. & Galko, M. J. Cytokine Signaling Mediates UV-Induced Nociceptive Sensitization in Drosophila Larvae. *Curr. Biol.* **19**, 799–806 (2009).

442. Boiko, N. *et al.* TrpA1 activation in peripheral sensory neurons underlies the ionic basis of pain hypersensitivity in response to vinca alkaloids. *PLoS One* **12**, 1–21 (2017).

443. Drozd, M., Bardoni, B. & Capovilla, M. Modeling fragile X syndrome in drosophila. *Front. Mol. Neurosci.* **11**, 1–15 (2018).

444. Ju, Y. K., Saint, D. A. & Gage, P. W. Hypoxia increases persistent sodium current in rat ventricular myocytes. *J. Physiol.* **497**, 337–347 (1996).

445. Azad, P., Zhou, D., Russo, E. & Haddad, G. G. Distinct mechanisms underlying tolerance to intermittent and constant hypoxia in Drosophila melanogaster. *PLoS One* **4**, (2009).

446. Bosco, G. *et al.* Effects of oxygen concentration and pressure on drosophila melanogaster: Oxidative stress, mitochondrial activity, and survivorship. *Arch. Insect Biochem. Physiol.* **88**, 222–234 (2015).

447. Babcock, D. T. *et al.* Hedgehog signaling regulates nociceptive sensitization. *Curr. Biol.* **21**, 1525–1533 (2011).

448. Kim, S. E., Coste, B., Chadha, A., Cook, B. & Patapoutian, A. The role of Drosophila Piezo in mechanical nociception. *Nature* **483**, 209–212 (2012).

449. Chin, M. R. & Tracey, W. D. Nociceptive Circuits: Can't Escape Detection. *Curr. Biol.* **27**, R796–R798 (2017).

APPENDIX

A.1 Loss of dSlo2 channels delays thermonociceptive response

Ascending nociceptors, whose cell bodies are in the DRG, detect painful stimuli and transmit the signal to spinal cord neurons in the dorsal horn. Immunostaining has identified $K_{Na}1.1$ and $K_{Na}1.2$ channels in the soma and central terminals of nociceptors of the DRG[278,290,291]. Recent studies found that KO of both *$K_{Na}1.1$* and *$K_{Na}1.2$* is sufficient to increase AP firing rates in cultured small diameter DRG neurons, which was associated with enhanced sensitivity to pruritic stimuli[285]. Another group found that mice with *$K_{Na}1.1$* conditionally knocked out in $Na_V1.8$-sensory neurons displayed enhanced sensitivity to mechanical stimuli[291].

Pain models have been well established using *Drosophila* larvae[343,344,378,447]. There are four classes of tactile primary sensory neurons, of which, Class IV is responsible for sensing noxious mechanical and thermal stimuli[344]. These neurons were shown to specifically express the DEG/ENaC channel *pickpocket* (ppk)[378], and will hereafter be called ppk neurons. ppk neurons have extensive dendritic arborization throughout the body wall, and contain temperature-sensitive TRP channels and mechanically-sensitive DEG/ENaC and piezo channels[343,378,448]. ppk neurons project their axons to the CNS, where two different pathways feed back to the muscle to initiate a rolling response upon exposure to noxious thermal or mechanical stimulation[449]. The rolling response, or nocifensive escape locomotion (NEL), is defined as a 360˚ roll around its body axis, and is specifically initiated by the ppk neurons (Fig. A.1A). Based on expression of dSlo2 channels in ppk neurons (Fig. 3.5B), and localization to the axonal portion (Fig. 3.5C), I tested whether dSlo2 channels may regulate nocifensive responses to noxious thermal stimuli.

To test this, a soldering iron was filed down and connected to a thermocouple, allowing for real-time temperature reading. This soldering iron was plugged into a variac transformer to regulate temperature of the tip. This tip was subsequently held at a specific temperature and applied to the side of freely moving

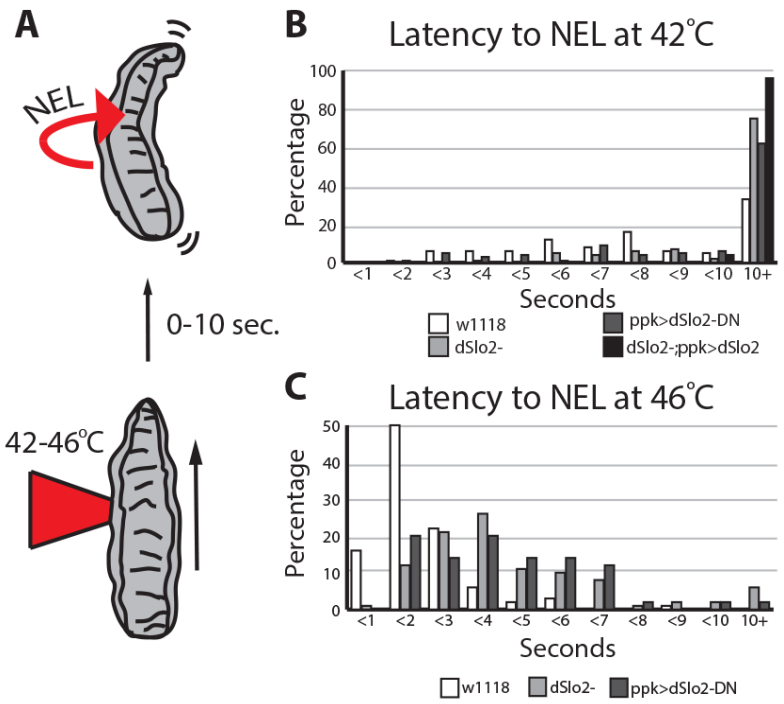

Figure A.1: Altered dSlo2 function in nociceptive neurons delays thermonociceptive response. A) Graphic depiction of thermal stimulation of a freely moving larvae which causes the NEL response. B) The time it took for larvae to exhibit an NEL following 42˚C stimulation onset was measured and binned by seconds. C) The time it took for larvae to exhibit an NEL following 46˚C stimulation onset was measured and binned by seconds.

larvae for a total of 10 seconds, or until the larvae completed an NEL. This was video recorded and blinded to the researcher. Offline analysis of the time to complete an NEL was measured, and binned into seconds following the application of the probe. Surprisingly, at both 42˚C and 46˚C, *dSlo2-* larvae exhibited an increased latency to respond compared to wild-type (Fig. A.1B and A.1C). I next attempted to rescue the *dSlo2-* phenotype by expressing exongenous *dSlo2* in ppk neurons of the *dSlo2* null background. I found that these larvae were less responsive than the *dSlo2-* line. In fact, *dSlo2-; ppk-Gal4>>UAS-dSlo2* larvae rarely exhibited a NEL response to thermal stimulation of 42˚C within 10 sec (Fig. A.1B). This may be due to differing levels of *dSlo2* expression endogenously compared to the driven expression of the exogenous *dSlo2* using the Gal4/UAS system. Expression of *dSlo2-DN* in the ppk neurons, *ppk-Gal4>>UAS-dSlo2-DN*, exhibited altered thermonociceptive phenotype similar to that seen in the *dSlo2-* line at both 42˚C and 46˚C (Fig. A.1B and A.1C). These results suggest the behavioral phenotype is due to loss of dSlo2 conductance specifically in ppk neurons. This is in contrast to the enhanced nociceptive behavioral data in

mice lacking *$K_{Na}1.1$* or *$K_{Na}1.2$*[285,290,291]. One possible explanation is that dSlo2 channels are acting in the axonal compartment to shorten action potential duration, thereby increasing the firing rates of the ppk neurons. Indeed, K_{Na} channels have recently been shown to increase action potential firing by shortening action potential duration[326]. This would need to be further explored to better understand why the absence of dSlo2 decreases thermal sensitivity.